Structure and Function
of Chronically Inflamed Human Airways

Structuur en functie van chronisch ontstoken humane luchtwegen

Harm Tiddens

Structure and Function
of Chronically Inflamed Human Airways

Structuur en functie van chronisch ontstoken humane luchtwegen

PROEFSCHRIFT

ter verkrijging van de graad van Doctor
aan de Erasmus Universiteit Rotterdam
op gezag van de Rector Magnificus Prof. dr P.W.C. Akkermans M.A.
En volgens besluit van de College van Promoties

De openbare verdediging zal plaats vinden op
woensdag 21 januari 1998 om 13.45 uur

door

Harmannus Arnoldus Wilhelmus Maria Tiddens

geboren te Helmond

Promotiecommissie:

Promotor: Prof. dr J.C. de Jongste

Overige leden: Prof. dr J. M. Bogaard
                Prof. dr W.J. Mooi
                Prof. dr P.J. Sterk

*Learn nothing, and the next world
is the same as this one, all the same limitations
and lead weights to overcome.*

To the real Jonathan Seagull who lives within us all

RICHARD BACH, JONATHAN LIVINGSTON SEAGULL, 1972

Voor Rosaria

Table of Contents

Introduction and Aims of Study

Introduction

Chronic airway inflammation, airflow obstruction, and bronchial hyperresponsiveness are important features of asthma, chronic obstructive pulmonary disease (COPD), cystic fibrosis (CF), and bronchopulmonary dysplasia (BPD). The pathophysiology of the chronic inflammation is different for each of these diseases. In asthma allergy to airborne allergens results in an inflammatory reaction of the mucosa. In COPD the chronic inflammation is mainly caused by smoking. In CF mucociliary clearance is impaired due to a genetic defect which results in chronic bacterial infection and airway inflammation[1, 2]. BPD can develop in preterm infants requiring mechanical ventilation at birth[3, 4]. Factors such as barotrauma, oxygen exposure, and infection are thought to trigger inflammation[5-7].

The prevalence of each of these diseases is considerable. The prevalence of asthma is somewhere between 7 and 15 % of the population and is still rising[8-12]. The prevalence of COPD reflects the smoking history of the population[13]. One fifth of all smokers demonstrate an increased susceptibility to tobacco smoke, with a rate of decline in lung function approximately twice that of the mean of all smokers. This is the group that acquires symptoms of COPD in late middle age. The prevalence of COPD in North America is 10% at the age of 55 to 85 years[13]. The prevalence of CF in the Netherlands is 1 in 3600 newborns[14]. BPD develops in one fifth of all preterm infants requiring mechanical ventilation at birth.

Chronic inflammation causes structural as well as functional changes of airway wall components and parenchyma. How these changes lead to airflow obstruction and increased bronchial responsiveness is incompletely understood. Better knowledge of structure-function relationships of chronically inflamed airways can help us to improve treatment. To obtain detailed information on the structure of airway wall components we depend mainly on autopsy or lobectomy specimens. Mucosal biopsies are of limited value for structure-function studies since they contain only small segments of the airway wall and relatively few samples can be taken from large airways. A valid analysis of airway dimensions versus airway size is, therefore, not possible.

In asthma only a few structure-function studies were done with lung tissue obtained

from people who died from asthma or with asthma[15-18]. In the Netherlands it is difficult to do such a study since, fortunately, death due to severe asthma is extremely rare and there is no systematic collection of lung tissue from asthmatic subjects obtained from autopsies. For this thesis we, therefore, did not study structure-function relationships in asthma but focused on COPD, CF, and BPD where lung tissue can be obtained more often. Lung tissue can be obtained from lobectomy or pneumonectomy specimens of smokers operated on for a solitary lung lesion. Routine lung function is done pre-operatively in most patients. These patients are known to have variable degrees of airflow obstruction[19, 20]. In CF, lung tissue can be obtained from recipient lungs of transplanted CF patients, or from autopsies. These patients have pre-operative lung function or routine lung function available. Transplanted CF patients have, without exception, end stage lung disease and severe loss of lung function. Lung tissue from BPD patients can only be obtained from autopsies. Most of these patients have severe BPD. Usually there is no lung function data available of these patients.

Outline and Aims of the Studies

This thesis is focused on the structure of chronically inflamed airways and its relation to airflow obstruction and bronchial hyperresponsiveness. We determined the structure of airways in patients who underwent a thoracotomy because of lung malignancies. These patients were mostly smokers and were classified as "COPD" although one-third had a lung function within the normal range and, therefore, did not strictly fulfil the ATS criteria[43]. Furthermore, we determined the structure of airways in CF and BPD. The relation between airway structure and function was studied in more detail in COPD. The relevance of our findings for the understanding of airflow obstruction and bronchial responsiveness in asthma is discussed in the summary.

In **Chapter 2** the general features of chronic airway inflammation in asthma, COPD, CF, and BPD are described. Furthermore, we describe what is known about structural and functional changes in chronically inflamed airways. Finally, we review how structural changes can relate to maximal airflow limitation and bronchial responsiveness.

Airway wall thickening plays an important role in the pathogenesis of airflow obstruction. It is known that airway wall thickening in membranous airways of patients with COPD correlates with the degree of airflow obstruction[20]. The importance of cartilaginous airway wall dimensions on airflow obstruction have not been systematically studied. We hypothesized that airway wall thickening of cartilaginous airways would contribute to airflow obstruction. The aim of this study was, firstly, to examine the relation between cartilaginous airway wall dimensions and airflow obstruction and, secondly, to study the relation between these cartilaginous airway dimensions and airway resistance in a mathematical lung model. This study was done in the Pulmonary Research Laboratory of the St. Paul's Hospital in Vancouver, Canada where a large number of lung specimens and matching lung function data are available from patients operated on for a peripheral lung tumor. Airway dimensions of cartilaginous airways in lobectomy specimens of patients with COPD were measured. Airway wall dimensions were correlated to pre-operatively measured estimates of airflow obstruction. Airway dimensions were inserted into a computational model[21, 22]. This is described in **Chapter 3**.

Airway cartilage is thought to be an important structure that resists dynamic compression during forced expiration[23]. Loss of airway cartilage due to chronic inflammation could therefore increase airflow limitation. Data on the relation between chronic airway inflammation and the volume of airway cartilage are conflicting[24-28]. Furthermore, it is not known whether the volume of airway cartilage is related to airway collapsibility and hence to airflow obstruction. Airway wall thickness is thought to contribute to airway resistance[15, 29, 30] and could be an important determinant of airway collapsibility[22]. We hypothesized that thickening of the airway wall due to chronic inflammation would make the airway stiffer and, therefore, would reduce airway collapsibility. It has been suggested that the relative contributions of airway conductance and airway collapsibility to airflow obstruction during forced expiration can be estimated from a maximal flow-static recoil (MFSR) curve[31]. The aim of this study was to correlate MFSR estimates of airway conductance and collapsibility and lung compliance to airway wall thickness and cartilage. Airway conductance and collapsibility were calculated from MFSR plots of COPD patients

and correlated to the airway dimensions measured in the lobectomy specimens of these patients. This study is described in **Chapter 4**.

The methodology to study the contractile and dynamic properties of intact airway segments is not well established. The next aim of this work was to develop a device to assess the smooth muscle responses in isolated airway segments under isobaric conditions and a model to study the mechanical properties of isolated airway segments. We developed a micro-plethysmograph that is able to measure small volumes displaced by a constricting or dilating airway segment at any given pre-load. Furthermore, we developed an experimental set-up to measure the dynamic properties of the airway segments. This study is described in **Chapter 5**.

Chronic inflammation of the airway is associated with thickening of the airway wall and deposition of fibrous tissue. This could make the airway less compliant and increase hysteresis and thus contribute to airflow limitation. We hypothesized that airway wall thickness is an important determinant for the mechanical properties of airways and that increased airway wall thickness makes the airways less compliant, less collapsible, and reduces hysteresis. The aim of this study was to investigate the relation between compliance, collapsibility, and hysteresis, on the one hand, and wall dimensions of human peripheral airway segments on the other. Airway segments were dissected out of lung tissue obtained from COPD patients. Dynamical properties were measured in an organ bath and airway wall dimensions were measured morphometrically. This is described in **Chapter 6**.

Lungs of CF patients show extensive inflammation of the bronchial walls, increased volume fraction of the lung occupied by bronchi, and degeneration and sloughing of airway epithelial cells[32-36]. It is not clear how the thickening of the airway wall and the loss of epithelium are distributed along the bronchial tree and how these pathologic findings contribute to the airflow obstruction and increased bronchial responsiveness in these patients. The aim of this study was to measure airway dimensions in CF lungs obtained from lung transplantation and autopsies and to estimate the importance of these dimensions in a computational model for airway resistance. This is described in **Chapter 7**.

Postmortem examination of lungs of infants with BPD show a decreased airway diameter, an increase of smooth muscle area, and loss of epithelium[37-42]. It is not clear whether airways are smaller due to smooth muscle contraction, airway wall thickening, or to small airway size. Furthermore, it is not known how airway wall dimensions are related to airway size. We hypothesized that the average airway size is smaller in BPD than in controls and that the airway wall is thickened and the amount of smooth muscle is increased. The aim of this work was to compare airway wall dimensions of BPD patients to patients who died from sudden infant death syndrome (SIDS). Airway wall dimensions were measured in lung tissue obtained from autopsies of BPD patients and SIDS patients and compared. This is described in **Chapter 8**.

In **Chapter 9** we summarize the studies in this thesis. Next, we discuss how the results of these studies fit in to what is known on the pathogenesis of maximal airflow limitation and bronchial responsiveness in relation to lung structure, and suggest directions for further research.

References

1. Konstan MW, Hilliard KA, Norvell TM, Berger M. Bronchoalveolar lavage findings in cystic fibrosis patients with stable, clinically mild lung disease suggest ongoing infection and inflammation. Am J Respir Crit Care Med 1994;150:448-454.
2. Stern RC. The diagnosis of cystic fibrosis. N Engl J Med 1997;336(7):487-491.
3. Abman SH, Groothius JR. Pathophysiology and treatment of bronchopulmonary dysplasia. Current issues. Pediatr Clin North Am 1994;41(2):277-315.
4. Zimmerman JJ. Bronchoalveolar inflammatory pathophysiology of bronchopulmonary dysplasia. Clin Perinatol 1995;22(2):429-456.
5. Walti H, Tordet C, Gerbaut L, Saugier P, Moriette G, Relier JP. Persistent elastase/proteinase inhibitor imbalance during prolonged ventilation of infants with bronchopulmonary dysplasia: evidence for the role of nosocomial infections. Pediatr Res 1989;26(4):351-355.
6. Coalson JJ, Winter VT, Gerstmann DR, Idell S, King RJ, Delemos RA. Pathophysiologic, morphometric, and biochemical studies of the premature baboon with bronchopulmonary dysplasia. Am Rev Respir Dis 1992;145(4 Pt 1):872-881.
7. Gorenflo M, Vogel M, Herbst L, Bassir C, Kattner E, Obladen M. Influence of clinical and ventilatory parameters on morphology of bronchopulmonary dysplasia. Pediatr Pulmonol 1995;19(4):214-220.
8. von Mutius E, Fritzsch C, Weiland SK, Roll G, Magnussen H. Prevalence of asthma and allergic disorders among children in united Germany: a descriptive comparison. Br Med J 1992;305(6866):1395-1399.
9. Anderson HR, Butland BK, Strachan DP. Trends in prevalence and severity of childhood asthma [see comments]. Br Med J 1994;308(6944):1600-1604.
10. Lewis S, Butland B, Strachan D, Bynner J, Richards D, Butler N, Britton J. Study of the aetiology of wheezing illness at age 16 in two national British birth cohorts. Thorax 1996;51(7):670-676.
11. Martinez FD, Wright AL, Taussig LM, Holberg CJ, Halonen M, Morgan WJ, Associates TGHM. Asthma and wheezing in the first six years of life. N Engl J Med 1995;332(3):133-138.
12. Leung R, Wong G, Lau J, Ho A, Chan JK, Choy D, Douglass C, Lai CK. Prevalence of asthma and allergy in Hong Kong schoolchildren: an ISAAC study. Eur Respir J 1997;10(2):354-360.
13. Anthonisen N. Epidemiology and the lung health study. Eur Respir Rev 1997;7(45):202- 205.
14. Ten Kate L. Cystic fibrosis in the Netherlands. Int J Epidemiology 1977;6(1):23-34.
15. James AL, Paré PD, Hogg JC. The mechanics of airway narrowing in asthma. Am Rev Respir Dis 1989;139(1):242-246.
16. Bai TR. Abnormalities in airway smooth muscle in fatal asthma. Am Rev Respir Dis 1990;141:552-557.
17. Kuwano K, Bosken CH, Paré PD, Bai TR, Wiggs BR, Hogg JC. Small airways dimensions in asthma and chronic obstructive pulmonary disease. Am Rev Respir Dis 1993;148:1220-1225.
18. Carroll NG, Cooke C, James AL. Bronchial blood vessel dimensions in asthma. Am J Respir Crit Care Med 1997;155(2):689-695.
19. Mullen JB, Wiggs BR, Wright JL, Hogg JC, Paré PD. Nonspecific airway reactivity in cigarette smokers. Relationship to airway pathology and baseline lung function. Am Rev Respir Dis 1986;133(1):120-125.
20. Bosken CH, Wiggs BR, Paré PD, Hogg JC. Small airway dimensions in smokers with obstruction to airflow. Am Rev Respir Dis 1990;142(3):563-570.
21. Lambert RK. Role of bronchial basement membrane in airway collapse. J Appl Physiol 1991;71(2):666-673.
22. Lambert RK, Codd SL, Alley MR, Pack RJ. Physical determinants of bronchial mucosal folding. J Appl Physiol 1994;77(3):1206-1216.
23. Olsen CR, Stevens AE, Pride NB, Staub NC. Structural basis for decreased compressibility of constricted trachea and bronchi. J Appl Physiol 1967;23(1):35-39.
24. Tandon MK, Cambell AH. Bronchial cartilage in chronic bronchitis. Thorax 1969;24:607-612.

25. Thurlbeck WM, Pun R, Toth J, Frazer RG. Bronchial cartilage in chronic obstructive lung disease. Am Rev Respir Dis 1974;109:73-80.

26. Nagai A, Thurlbeck WM, Konno K. Responsiveness and variability of airflow obstruction in chronic obstructive pulmonary disease. Am J Respir Crit Care Med 1995;151:635-639.

27. Nagai A, West WW, Paul JL, Thurlbeck WM. The national institutes of health intermittent positive-pressure breathing trial: pathology studies. I. Interrelationship between morphologic lesions. Am Rev Respir Dis 1985;132(5):937-945.

28. Dunnill MS, Massarella GR, Anderson JA. A comparison of the quantitative anatomy of the bronchi in normal subjects, in status asthmaticus, in chronic bronchitis, and in emphysema. Thorax 1969;24:176-179.

29. Freedman BJ. The functional geometry of the bronchi. Bull Physio-path Resp 1972;8:545- 551.

30. Moreno RH, Hogg JC, Paré PD. Mechanics of airway narrowing. Am Rev Respir Dis 1986;133(6):1171-1180.

31. Leaver DG, Tattersfield AE, Pride NB. Contributions of loss of lung recoil and of enhanced airways collapsibility to the airflow obstruction of chronic bronchitis and emphysema. J Clin Invest 1973;52:2117-2128.

32. Bedrossian CWM, Greenberg SD, Singer DB, Hansen JJ, Rosenberg HS. The lung in cystic fibrosis; A quantitative study including prevalence of pathologic findings among different age groups. Hum Pathol 1976;7(2):195-204.

33. Simel DL, Mastin JP, Pratt PC, Wisseman CL, Shelburne JD, Spock A, Ingram P. Scanning electron microscopic study of the airways in normal children and in patients with cystic fibrosis and other lung diseases. Pediatr Pathol 1984;2(1):47-64.

34. Tomashefski JF, Bruce M, Goldberg HI, Dearborn DG. Regional distribution of macroscopic lung disease in cystic fibrosis. Am Rev Respir Dis 1986;133(4):535-540.

35. Sobonya RE, Taussig LM. Quantitative aspects of lung pathology in cystic fibrosis. Am Rev Respir Dis 1986;134(2):290-295.

36. Oppenheimer EH, Esterly JR. Pathology of cystic fibrosis. Review of the literature and comparison with 146 autopsied cases. Prospect Pediatr Pathol 1978;2:241-278.

37. Northway WH, Jr., Rosan RC, Porter DY. Pulmonary disease following respirator therapy of hyaline-membrane disease. Bronchopulmonary dysplasia. N Engl J Med 1967;276(7):357-368.

38. Bonikos DS, Bensch KG, Northway WH, Edwards DK. Bronchopulmonary dysplasia: the pulmonary pathologic sequel of necrotizing bronchiolitis and pulmonary fibrosis. Hum Pathol 1976;7(6):643-666.

39. Stocker JT. Pathologic features of long-standing "healed" bronchopulmonary dysplasia: a study of 28 3- to 40-month-old infants. Hum Pathol 1986;17(9):943-961.

40. Lee RM, H OB. Airway epithelial damage in premature infants with respiratory failure. Am Rev Respir Dis 1988;137(2):450-457.

41. Hislop AA, Haworth SG. Pulmonary vascular damage and the development of cor pulmonale following hyaline membrane disease. Pediatr Pulmonol 1990;9(3):152-161.

42. Margraf LR, Tomashefski JF, Bruce MC, Dahms BB. Morphometric analysis of the lung in bronchopulmonary dysplasia. Am Rev Respir Dis 1991;143:391-400.

43. American Thoracic Society. Standards for the diagnosis and care of patients with chronic obstructive pulmonary disease (COPD) and asthma. Am Rev Respir Dis 1987;136:224-243.

Structure and Function of Chronically Inflamed Human Airways

A Review of the Literature

Introduction

The bronchial tree is a dichotomously branching system of tube-like structures. It goes down from the trachea, with a cross-sectional area of 2.5 cm^2 in adults, to the respiratory bronchioles with a total cross-sectional area of 12.000 cm^2 [1]. The major function of the bronchial tree is to transport air in and out of the lungs in an energy-efficient way. At inspiration ambient air is transported and distributed to the alveoli where gas exchange with the blood takes place. During this transport the air is heated to body temperature, humidified to maximal water saturation, and filtered. Particles and micro-organisms are trapped in the mucus and cleared by the mucociliary clearance in close collaboration with the immune system. In healthy subjects the bronchial tree can fulfill its functions both at rest and during maximal exercise.

In diseases characterized by chronic inflammation of the airways the functions can be substantially altered. Airflow obstruction, and bronchial hyperresponsiveness are important characteristics of diseases such as asthma, chronic obstructive pulmonary disease (COPD), cystic fibrosis (CF), and bronchopulmonary dysplasia (BPD). It is known that chronic inflammation leads to structural and functional changes in airways and parenchyma. However, how these changes relate to airflow obstruction and bronchial responsiveness is complex and incompletely understood. In this review we will first describe general features of airway inflammation for patients with asthma, COPD, CF, and BPD. Next, we describe what is known about structural and functional changes of chronically inflamed airways. Finally, we will discuss how structural changes relate to maximal airflow limitation and bronchial responsiveness.

Chronic Airway Inflammation

Chronic inflammation of the airways is an important feature of asthma[2-6], COPD[7-11], CF[12-17], and BPD[18-22]. The pathophysiology of the chronic inflammation is different for each of these diseases.

ASTHMA. Asthma is characterized by episodic airway obstruction and increased bronchial responsiveness to the inhalation of non-specific irritants[23, 24]. A high percentage of asthmatics is allergic to airborne allergens. Provocation with an allergen

leads to an early and often also a late allergic reaction. The early reaction to allergen results from direct effects of mediators, whereas the late reaction is the consequence of an inflammatory reaction of the bronchial mucosa. Eosinophils, neutrophils, and T- lymphocytes are the predominant cells in the mucosa and alveolar tissue of asthmatic patients[6, 25-30, 300-302], and these play an important role the pathophysiology of asthma[27, 28, 31-33]. The density of the inflammatory infiltrate is highest in airways smaller than 2 mm internal diameter[6].

Asthma is a chronic disease that starts at a very young age[34, 35]. Two-thirds of asthmatic children continue to have symptoms of asthma in adulthood[36]. Of adults with asthma more than half of the patients still have asthma after 25 years[37]. There are indications that airway inflammation is present even in children and adults with stable asthma. Markers of airway inflammation, such as hydrogen peroxide in exhaled air, are elevated in stable asthmatic children compared to healthy controls[38]. This was especially true for children without anti-inflammatory treatment. Furthermore, mucosal biopsies taken from 2 asthmatic children in remission showed peribronchial inflammatory cell infiltration[26]. In mucosal biopsies taken from adult patients with stable allergic asthma a high percentage of the eosinophils within the dense infiltrate were activated[31]. In addition, in mucosal biopsies of patients with severe asthma, who were treated for 10 years with inhaled steroids, inflammatory changes were substantially reduced but not absent compared to the moment of onset of treatment[39]. Furthermore these patients still had increased bronchial responsiveness.

CHRONIC OBSTRUCTIVE PULMONARY DISEASE. The term COPD is used for to describe a collection of conditions which share the feature of chronic obstruction of expiratory flow. Smoking is the major etiological factor in the pathogenesis of COPD as has been shown in many studies[40-43]. For example, it was shown that the number of cigarettes smoked is linearly related to the accelerated rate of loss of lung function among smokers[44]. Furthermore, cigarette consumption is significantly correlated to the severity of inflammation of membranous airways, and to bronchial hyper-responsiveness[40]. The severity of inflammation is correlated to parameters of airflow obstruction[10]. Neutrophils are considered to be the predominant cells in the inflammatory response that occurs in the airspaces of patients with COPD[45].

Firstly, the presence of cigarette smoke in the lungs increases the retention of neutrophils in the lung[46]. Secondly, neutrophil chemotactic activity due to spontaneous secretion of a chemotactic factor by alveolar macrophages from smokers was tenfold higher than in controls[47]. Thirdly, the number of neutrophils correlates significantly to the number of cigarettes smoked[48]. Polymorphonuclear leukocytes can produce tissue damage by the release of mediators, including proteases, oxidants, and toxic peptides such as defensins[49] [50]. An excess of proteases relative to antiproteases degrades extracellular matrix proteins[51]. High concentrations of oxidants in cigarette smoke play a role in the inactivation of antiproteases[52]. These oxidants also have a direct toxicity on many lung structures[52]. There are large differences among smokers in the impact of cigarette smoke on the rate of decline in lung function. Around one fifth of the smokers have a rate of decline in lung function which is almost double that of all smokers[53, 54]. On average, moderate to heavy male smokers roughly have a 15 ml per year large decline in lung function than non-smokers[55]. Airway inflammation in smokers continues as long as smoking continues. Sustained smoking cessation reduces the loss of lung function to a near normal level, whereas in smokers the increased decline in lung function continues.

CYSTIC FIBROSIS. In cystic fibrosis the mucociliary defense mechanism of the lung is severely impaired. Mutations in the CF gene result in defective chloride secretion and increased sodium absorption across the respiratory epithelium. This results in abnormal sputum rheology and impaired clearance of respiratory secretions. As a consequence micro-organisms trapped in the mucus are not efficiently cleared which results in chronic bronchitis. Furthermore, it was shown that the bactericidal function of airway surface fluid in CF was reduced because of the high salt concentration in the mucus[56]. Lung disease in CF is characterized by bacterial infection and chronic airway inflammation which starts at a young age in most children. A bronchoalveolar lavage study done within the first 3 months of life in 45 infants with CF showed that 40% had a culture that was positive for one or more pathogenic microorganisms[16, 17]. Inflammation in airways of CF patients is characterized by an elevated number of neutrophils[14, 28] and a protease-antiprotease imbalance[14, 15]. Proteolytic destruction of lung connective tissue is an ongoing process in the chronically infected CF lung

and contributes to the pathologic changes observed in airways and alveolar parenchyma[57]. Bronchiectasis may be present as early as 2 months of age and was present in many children after 6 months of age[58]. Many patients get colonized with pseudomonas. The location of the pseudomonas is generally endobronchiolar and associated with bronchiolar obliterative changes mainly in small (< 1 mm) airways[59]. Infants with CF, but without respiratory symptoms at diagnosis, start with normal lung function[60, 61] but infants with respiratory symptoms at diagnosis have severe airway obstruction[61]. The latter children were more likely to have impaired lung function at the age of one year[62]. The prognosis of most CF patients is determined by the progression of the lung disease[63]. The median life expectancy of a newborn child with CF treated in a CF center is currently likely to be in the order of 40 years[64].

BRONCHOPULMONARY DYSPLASIA. About one fifth of preterm infants who required mechanical ventilation at birth developes chronic lung disease, which has been termed BPD[65, 66]. The incidence of BPD has increased due to increased survival and other unidentified factors[67]. BPD is clinically characterized by respiratory distress, oxygen dependence, and chest radiograph abnormalities beyond the first month of life[22, 68]. Factors such as barotrauma, oxygen exposure, and infection are thought to trigger inflammation[69-71]. There is mounting evidence that inflammatory lung injury may play a key role in the pathogenesis of BPD[22, 72]. Various inflammatory mediators such as leukotrienes, fibronectins and platelet activating factor are also found in high concentrations in lavage fluid of infants with BPD[18, 21, 73-75]. Furthermore, elevated neutrophil counts and elastase concentration in bronchoalveolar lavage fluid is associated with the development and severity of BPD[19-21, 73]. This elastase is of neutrophilic origin[19]. Its concentration, and that of its inhibitor α_1-antiprotease, is elevated in bronchoalveolar lavage fluid of BPD patients[19-21, 71]. An imbalance between elastase and α_1-antiprotease, which places the infant at risk for proteolytic lung damage, was described in a number of studies[19, 20, 71] but not in others[21]. In fact, there are indications that lung damage due to lung inflammation is increased in BPD. The excretion in urine of degradation products of elastin during the first week of life has been described in infants who subsequently developed BPD[76].

Structure and Function of Chronically Inflamed Airways

The structure of airways in humans can be studied in vivo with radiographic imaging techniques and mucosa biopsies and in vitro in lungs obtained from lobectomies or autopsies using morphometric techniques. The function of the airways can be measured in vivo with lung function measurements, radiographic techniques, and in vitro in whole lung preparations, isolated airway segments, and in bronchial tissue strips. In this section we first describe structure and function relationships of components of normal and diseased airways. Next, we will describe how these airway components interact.

Subdivisions of Bronchial Wall

Airway wall dimensions have been measured in normal lungs, in the lungs of patients with airway disease, and in animal models of airway disease. The terminology for airway wall compartments is somewhat different from that used in the literature related to histology (Figure 1). For this review we use nomenclature which was proposed for quantifying subdivisions of the bronchial wall as seen in histological cross-sections[77] (Figure 2). Basically the airway is divided into two major layers; the inner wall and outer wall. The inner wall consists of the epithelium, basement membrane, lamina propria, and smooth muscle layer. Its borders are the airway lumen and outermost layer of the smooth muscle. The outer wall consists of cartilage and the adventitia. Its borders are the outermost layer of the smooth muscle and the outer border of the adventitia. Alveolar attachments connect the outer wall of intra parenchymal airways to the lung parenchyma. Different pathological processes may result in specific thickening of one of the compartments without influencing the other. For example, an increase of the inner wall area can amplify the effects of a given amount of smooth muscle shortening[78, 79]. An increase of the outer wall area may decrease the elastic load that the surrounding lung parenchyma provides to the smooth muscle and thus facilitate smooth muscle shortening[80, 81].

Inner wall area

EPITHELIUM. The surface area of the airways of the bronchial tree is covered by pseudo-stratified epithelium. The respiratory epithelium forms an active interface between
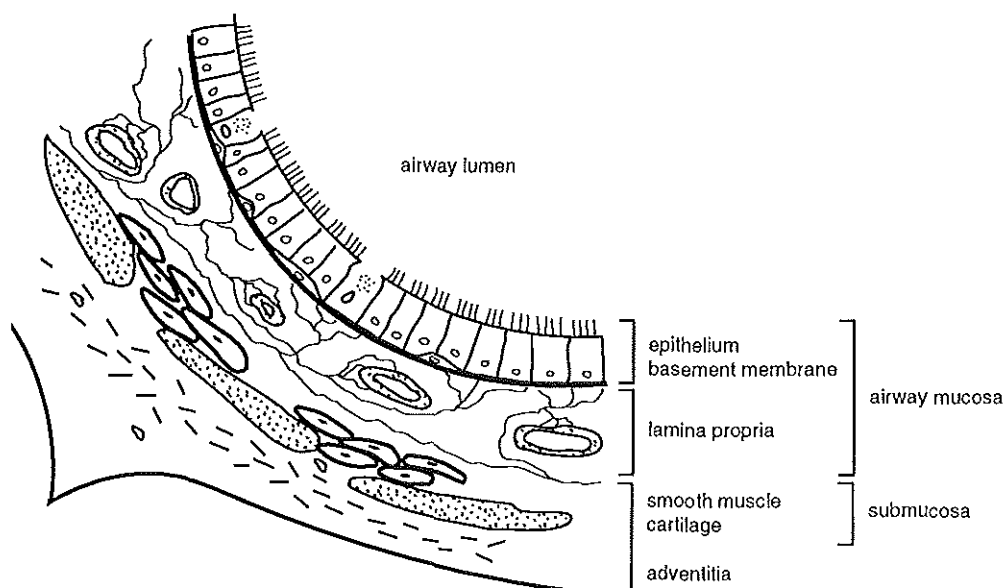
Figure 1. Diagram of airway wall of medium-sized bronchus. The terminology is as used in literature related to airway pathophysiology.
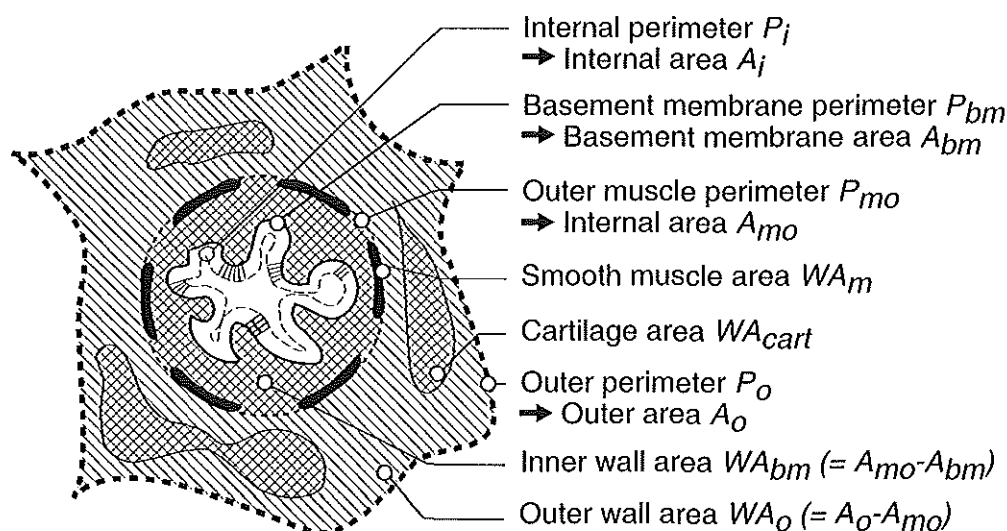

Figure 2. Diagram of airway wall medium-sized bronchus. The terminology is as used in the physiology literature.

the external and the internal environment and has a number of important functions. Firstly, goblet cells within the epithelial layer and submucosal glands produce mucus which is a complex mixture of water, proteins and proteoglycans, lipids and salts. It forms a natural barrier protecting the epithelial cells from invasion and injury by bacteria, viruses, and toxic inhaled molecules. Mucus contains defensins that have bactericidal activity[56].The respiratory mucus entraps inhaled particulate matter and microorganisms deposited within the respiratory tract. The mucus is cleared by ciliary interactions and by airflow. Secondly, the epithelium acts as humidifier of inspired air and prevents excessive fluid loss from the mucosa. Thirdly, it forms a barrier against leakage of solutes into the airways and prevents penetration of particulate matter into the airway interstitium[82, 83]. Fourthly, epithelium modulates smooth muscle tone by production of relaxing factors and by inactivation of bronchoconstricting mediators and neurotransmitters[84-86].

In asthma shedding and damage of airway surface epithelium is prominent and is seen both in fatal asthma and in biopsy specimens of patients with mild asthma[3, 31, 87]. Epithelial tight junctions were found to be either deranged or damaged (or both) in asthma and thereby contributed to the fragility of the epithelial layer[88, 89]. Shedding and damage of airway epithelium seems to be less prominent in COPD than in asthma but is less well described[90, 91]. Loss of respiratory epithelium in CF airways has been described by a number of authors but was never quantified[92, 93]. In infants who died with BPD, loss of the epithelium from up to 50% of the surface area was found in the large airways[94]. In lungs of 9 infants with bronchopulmonary dysplasia, of whom 7 died from respiratory failure, up to 28% of particulary the small airways showed severely damaged epithelium[95]. There is a possibility that this epithelial damage is at least to some extent an artifact due to the delay between the time of death and the time of autopsy.

Extensive loss of epithelium can have the following consequences. Firstly, it can lead to a decreased mucus clearance due to the defect of the ciliary apparatus. Thus mucus can accumulate in the airway tree and lead to colonization and infection of inhaled microorganisms[96, 97]. Airway epithelial injury and repair favor bacterial adherence[97-100]. Secondly, epithelial injury is associated with bronchial hyperrespon-

siveness[3, 27]. Thirdly, desquamated epithelium and mucus can occlude the airway lumen as is reported in patients with a severe acute asthma attack[26, 101]. In patients with COPD the percentage of epithelium occupied by mucus is substantially increased in comparison to control subjects[102]. When the space between folds of the inner wall is filled with fluid, mucus or debris, it compromises the airway lumen and thus contributes to airflow obstruction[103]. Fourthly, exfoliation of epithelium, especially when it takes place in the small airways, will increase the airway lumen. Finally, the loss of epithelium might change the mechanical behavior of the airway wall.

BASEMENT MEMBRANE. The epithelial layer rests on the basement membrane which consists of two layers. The first layer is the basal lamina or "true" basement membrane which can be seen only by electron microscopy. The basal lamina consists of an electron-dense layer of 50 to 250 nm thickness composed principally of type IV collagen, laminin, actin, proteoglycans, and fibronectin[104]. This specialized extra-cellular elastic matrix is considered to provide support for the epithelium[104, 105]. The second layer of the basement membrane, the lamina reticularis, is positioned immediately below the basal lamina. This layer can be seen by light-microscope and consists of a loose array of collagen fibrils that are connected to the smooth muscle and adventitial layer[106, 107]. The width of the lamina reticularis of the basement membrane ranges between 3-17.5 microns, with a median value of 8.5 microns[108]. The mechanical properties of the basement membrane are thought to be an important determinant for the stiffness and folding pattern of the mucosa during smooth muscle shortening[109, 110].

Extensive thickening of the basement membrane has been described in asthma[3, 5, 26, 31, 111-119]. It can even be seen in an early stage of the disease[5, 26, 118]. Thickening of the basement membrane was observed, but not quantitated, in chronic bronchitis[25] and in patients recovering from viral respiratory infections[120]. Whether the basement membrane is thickened in CF or BPD has not been investigated systematically.

Bronchial myofibroblasts are thought to be responsible for the thickening of the basement membrane[115]. The thickness of the lamina reticularis is positively correlated to the number of myofibroblasts immediately beneath the basement membrane. Furthermore, in asthmatic subjects the number of subepithelial cells with a myo-

fibroblast phenotype was increased 24 hr after allergen challenge from 1.6% after diluent to 18% after allergen[121].

The impact of the thickening of the basement membrane on airway mechanics is a matter of speculation. It is likely that this tube-like structure becomes stiffer when it is thickened. Therefore, it was suggested that thickening of the basement membrane in asthma is a protective mechanism that tends to reduce hyperresponsiveness[110].

LAMINA PROPRIA. This is all the tissue between the basement membrane and the loose connective tissue layer underneath the smooth muscle layer. Just below the epithelium a dense microvascular network is embedded in fibrous tissue[122-126]. Blood vessels occupy a volume fraction of 4 to 10% of the inner wall . This network provides nutrients to the epithelium, and plays an important role in the conditioning of the inspired air and the clearance and distribution of inflammatory mediators[127, 128]. It has been suggested that the vascular network plays a role in the way the mucosa folds[129]. The lamina propria further contains a network of elastic fibers that is attached to the basal lamina of the epithelium, to the glands, smooth muscle cells, and cartilage[106].

Increased airway microvascular permeability and plasma exudation are considered to be an important feature of asthma[130-135]. Allergen exposure in sensitized asthmatics causes an acute increase in the permeability of the microvasculature of bronchi[136]. Plasma extravasation may lead to thickening of the inner wall and thus increase airway resistance. In fact, in sensitized dogs that developed a late asthmatic reaction after allergen challenge, vascular permeability and mucosal thickness were increased, especially in small bronchi[137]. There are reasons to believe that increased vascularity with vasodilatation might contribute to airflow obstruction and increased bronchial reactivity in asthma. Bronchial vascular congestion is known to contribute to airway resistance in humans. Furthermore, the absolute number of blood vessels was increased in proportion to the increase in airway wall in autopsy specimen from patients who died from or with asthma[126, 138]. Additionally, the absolute area of the lamina propria occupied by vessels was increased from 10 to 17% in mucosal biopsies taken from the subsegmental carina of allergic asthmatic subjects compared to controls[139]. The number of vessels per mm^2 of lamina propria was 32% higher in asthmatics. It is

unlikely that vascular engorgement or bronchial wall edema could by itself cause sufficient reduction of the airway lumen to have a substantial influence on airway resistance[129, 140]. However, moderate changes of airway wall thickness in combination to smooth muscle shortening can contribute to increased airflow limitation.

AIRWAY SMOOTH MUSCLE. The smooth muscle layer runs down from the trachea to the smallest bronchioles[141]. There are two basic configurations of the airway smooth muscle[142]. The first is found in the trachea, where the muscle is inserted and closely associated, both anatomically and functionally, with the cartilages. The muscle runs transversely and forms a band in the dorsal part of the trachea. The second configuration occurs in the bronchi where the muscle is present internal to the cartilage plates. In cartilaginous bronchi, smooth muscle inserts on the perichondrium and runs in helical strands around the airway circumference. The maximum shortening capacity of the extrapulmonary smooth muscle is thought to be higher than the intrapulmonary smooth muscle[143]. It was suggested that to the extent that airway smooth muscle is arranged in an oblique angle, relative to the transverse axis of the airway, it could contribute to airway closure and thus be an important determinant of airway responsiveness[144]. However, the oblique angle was found to be small in cats, rabbits, and humans[145, 146, 1221] and it is, therefore, doubted whether the angle of the bronchial smooth muscle is an important determinant for airway responsiveness.

Much more research has been done on trachea smooth muscle since it is easily obtained. Smooth muscle makes up 10 to 5% of the bronchial wall volume of small airways with a diameter of 0.3 to 3 mm[138], in large airways this relation was never systematically studied. Only little is known of the normal function of smooth muscle. Firstly, smooth muscle tone contributes to the stability of airways. Smooth muscle tone was shown to be an important determinant of airway collapsibility in isolated large airway segments of humans[147-150] and in airways of rabbits[151] and pigs[152]. In general, collapsibility increases when smooth muscle tone is reduced and decreases when smooth muscle tone is increased. Secondly, smooth muscle tone is a determinant of airway diameter[153], and thus affects airway resistance which is inversely related to at least the fourth power of the airway radius. Thirdly, smooth muscle tone contributes to the elastic recoil of the whole lung[154].

In asthma an increase in the amount of bronchial smooth muscle has been described by a number of authors[79, 111, 112, 138, 155-157]. This increase in muscle can be the result of hypertrophy and hyperplasia of the smooth muscle cells or of an increase of extracellular matrix surrounding the cells. In fact, in airways of patients who died from a severe asthma attack both hypertrophy and hyperplasia of smooth muscle cells was found[157]. Recently, airway muscle stereology in large airways of 5 asthma patients obtained from lobectomies and autopsies was compared to controls[158]. Smooth muscle area, connective tissue area, and extra cellular matrix area were all higher in the asthmatic patients but each of them separately was not significantly different from controls. This study clearly shows that extracellular matrix and connective tissue within smooth muscle bundles contribute substantially to the smooth muscle area. In other words an increase in smooth muscle area as measured with more classical morphometric techniques does not necessarily mean that the volume of the contractile apparatus is increased. However, the increase in connective tissue (and extracellular matrix, maybe) probably contributes to the passive stress in the muscle layer.

In COPD the amount of smooth muscle in small airways of patients with severe airflow obstruction has been shown to be greater than in patients with normal lung function[10, 138, 155]. The amount of smooth muscle in cartilaginous airways has not been well described.

In CF there are a number of studies of lung pathology, however, no studies have been done to quantify the smooth muscle.

The airways of patients with BPD show a substantial increase of the smooth muscle area[65, 159-161]. Margraf and coworkers found that the volume proportion of smooth muscle in central bronchi and the lung was more than twice that of controls. Premature infants with chronic lung disease aged 9 to 29 days had increased muscle in airways with a circumference of 1500 μm or greater compared to age-matched controls[95]. The distribution of the volume of smooth muscle along the bronchial tree in relation to other airway wall dimensions was not clear in these studies.

Increased shortening compared to control of smooth tissue preparations from asthmatic patients has been shown to occur in vitro[162-164]. The degree of airway smooth muscle shortening that occurs in vivo depends on many factors, including force generation,

and the loads against which the smooth muscle contracts. Increased force generation was found in each of the three studies. Whether this was the result of increased smooth muscle mass or of changes of the contractile properties is less clear. It was recently suggested that increased shortening velocity of airway smooth muscle might play a key role in the pathogenesis of airflow obstruction in asthma[165]. Increased shortening due to enhanced contractile properties was found in smooth muscle preparations from tracheae of hyperresponsive guinea pig[166] and mice [167] but not in hyperresponsive greyhounds[168]. Increased shortening as a result of a decreased load provided by the extracellular matrix elements was found in airways obtained from a lobectomy of a patient with asthma[164]. Whether smooth muscle shortening is increased in COPD is not clear. The isometric force generation after stimulation with histamine was increased in bronchial strip preparations from small airways of COPD patients with airflow limitation compared to smokers without airflow limitation[169]. However, there was no difference between both groups after stimulation with methacholine. Isotonic shortening was decreased in the COPD patients compared to the smokers without airflow obstruction[170]. These results might indicate that the load on the contracting smooth muscle is increased in patients with COPD and airflow obstruction. Whether smooth muscle responsiveness in vitro is altered in CF and BPD is unknown.

Outer wall

AIRWAY CARTILAGE. Cartilage is a prominent component of the outer wall and is present from the trachea down to airways with a diameter of around 2 mm. In the trachea and main stem bronchi, cartilage plates are horse-shoe shaped and occupy a large part of the bronchial wall. The more peripheral the airway, the smaller the cartilage plates, until they disappear completely. The cartilage make up 25 to 63% of the total wall in large airways[171] and 4 to 10%[172] in the smaller airways. Its exact volume distribution along the bronchial tree was not investigated. Airway cartilage consists of a fiber-reinforced composite material in which type II collagen fibers entrap a matrix of proteoglycan aggregates[173, 174]. The biochemical composition and biomechanical properties of airway cartilage change with age and may thus contribute to the age-dependent changes in human lung function[173, 174].

Airway cartilage is an important structural contributor to the ability of the airway wall to resist deformation during forced expiration[175]. Softening of tracheal cartilage in rabbits, using papain, increased compliance of the trachea and decreased the ability of the trachea to resist negative pressures[176]. Airway cartilage provides an elastic load on the smooth muscle and is, therefore, a determinant of the degree of airway smooth muscle shortening and the resultant airway narrowing[177-180]. Maximal shortening of bronchial smooth muscle preparations in dogs from which all cartilage had been removed almost doubled compared to intact preparations[178].

Previous studies in patients with COPD have suggested that inflammation reduces cartilage volume and, therefore, contributes to increased airflow obstruction[172, 181-183]. This was not confirmed in other studies[2, 8]. Whether the amount of cartilage is changed in CF is not known. The mean volume proportion of cartilage in central bronchi of BPD patients was not different compared to controls[161]. However, in this study the amount of cartilage was not related to the airway perimeter.

Whether the mechanical properties of airway cartilage are altered due to chronic inflammation in asthma, COPD, and CF is not known. Prematurely born infants have more compliant and more collapsible airways than term infants[184]. Primary tracheo-bronchomalacia which is a rare congenital anomaly in otherwise healthy infants seems to occur more frequently in BPD[185]. Airways become stiffer with age which is related to the water content and to the biochemical composition of cartilage[173, 174]. However, the biochemical composition and biomechanical properties of airway cartilage in BPD were never systematically studied in relation to inflammatory changes within the airways.

ADVENTITIA. The adventitia is the tissue between the cartilage and/or the smooth muscle layer and the parenchyma. It consists of fibrous tissue and blood vessels. The adventitial layer cannot be separated from the parenchyma since these form a continuum. Septa depart from the adventitia into the surrounding parenchyma. Furthermore, it was shown that elastic fibers in intrapulmonary guinea-pig airways connect the adventitia to the lamina reticularis and to the smooth muscle layer[107]. This configuration is compatible with the idea that fibers of the elastic system restrict the folding of the mucosa during bronchoconstriction, and may also provide energy
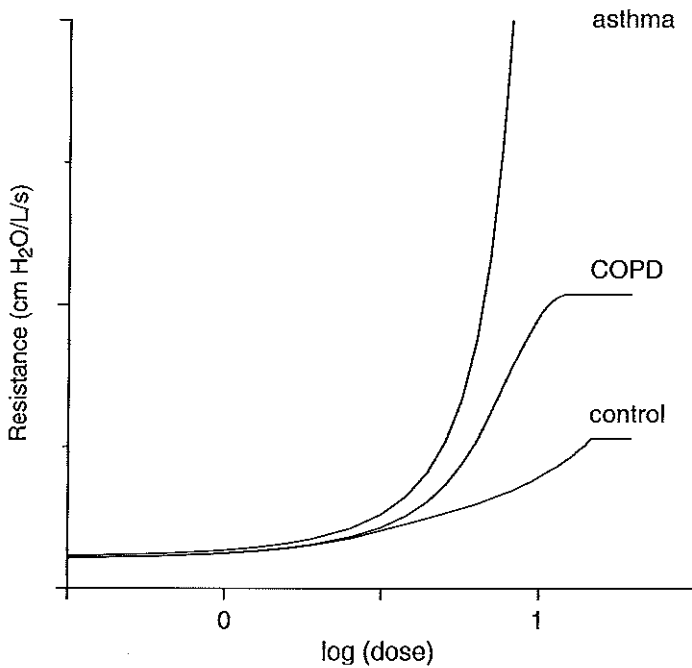
Figure 3. Dose-response curves generated using a computational model for airway dimensions of normal subjects, patients with chronic obstructive pulmonary disease (COPD), and asthma. The only parameter altered in generating these curves was the equation for the inner wall area as a function of airway size. The higher the log(dose) the higher the shortening in the model by the smooth muscle. *This figure was kindly supplied by Dr R.K. Lambert.*

to restore airway configuration to its normal status after contraction. Only little is known on changes in the adventitia in relation to chronic airway inflammation. Probably the adventitia is thickened in severe asthma[138], for COPD this is less clear[10, 138]. For CF and BPD there are no systematic studies available.

Interactions between airway compartments
Since the interactions between airway compartments are so complex computer models have been developed to study the functional significance of altered airway dimensions and physical behavior on outcome parameters such as airway resistance[80, 109, 110, 186-191]. These models are founded on the physics of solid mechanics and fluid dynamics and have integrated data on the geometry and mechanical properties of the

31
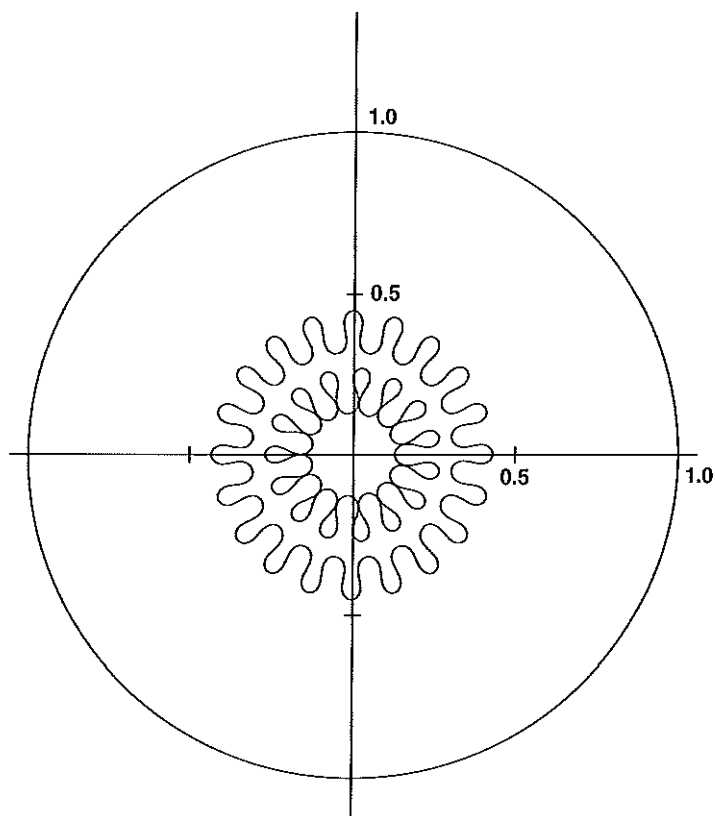
Figure 4. Example of cross sections of airways containing different number of folds at the same transmural pressure difference. The outer cross section has 20 folds, whereas the inner cross section has 15 folds. The ratio between the two lumen areas is 2.83. The scale represents the normalized radius. The fully dilated airway has a radius of 1. The theory behind this graph is described in reference [109]. *This figure was kindly supplied by Dr R.K. Lambert.*

lung. The models are, by definition, a reduction of reality but it helps us to understand the relationship between structural and functional changes, to simulate complex interactions between various airway wall compartments, and to develop new concepts on the pathophysiology of airflow obstruction. In the following paragraphs we will discuss interactions between airway wall compartments and parenchyma.

SMOOTH MUSCLE AND INNER WALL. When the smooth muscle shortens it has to deform the tissue between the smooth muscle layer and the lumen into folds. It is
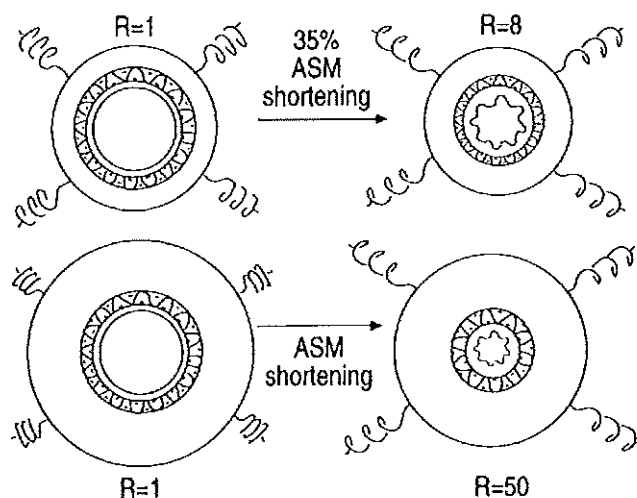
Figure 5. The effect of outer wall thickening. In this example the normal airway has a resistance (R) of 1. When airway smooth muscle (ASM) contraction is stimulated, shortening occurs until the stress in the surrounding parenchyma (represented by the springs) prevents further shortening and narrowing at a resistance of 8. With thickening of the outer wall the stress in the surrounding parenchyma is decreased, and greater smooth muscle shortening is possible before the parenchymal recoil prevents further shortening. *From reference* [299], *with permission.*

predicted in a computational model that thickening of the inner wall increases the airway's ability to resist bronchoconstriction by the smooth muscle[110, 192]. Thickening of the inner airway wall is present in small and large airways of asthma patients[79, 138] and in small airways of COPD patients[10, 138]. For CF[193, 194] and BPD[161, 195, 196] there are indications that the airway wall is thickened but there are no systematic data available relating airway thickness to airway size. Thickening of the inner wall in asthma has only little effect on baseline airway resistance but can enhance the airway narrowing produced by smooth muscle shortening[78, 79, 190] (Figure 3). The folding pattern of the inner wall could influence airway resistance[109, 110]. A low number of folds occludes the airway lumen more than a high number of folds (Figure 4). Whether the smooth muscle is able to shorten depends on the load of the folding inner wall on the shortening smooth muscle. It is predicted that thickening of the structured connective tissue of the airway wall increases the airway's ability to resist broncho-

constriction[110]. In the event of an allergen provocation accompanied by swelling of the inner airway wall by edema it is predicted that airway's stiffness will be reduced. SMOOTH MUSCLE AND OUTER WALL. The outer wall area determines the tethering effect of the parenchyma on the airway and, therefore, the preload and afterload for the bronchial smooth muscle. An increase in outer wall area could theoretically reduce the tethering effect of the parenchyma on the airway and, therefore, reduce the preload and afterload for the bronchial smooth muscle. As a result the smooth muscle could shorten more for a given force generation[81, 110, 197] (Figure 5). The outer wall area might, therefore, play an important role in the pathophysiology of excessive bronchoconstriction[197]. The outer wall is a structure that is difficult to measure in a reliable fashion since it forms a continuum with the parenchyma. In small airways of asthma patients the outer wall is increased compared to control subjects[138]. In COPD patients with airflow obstruction the outer wall area is thicker than in non-obstructed patients only for airways with a diameter between 0.4 and 0.8 mm but not for smaller or larger airways[10]. For CF and BPD there are no data on the outer wall available.

PARENCHYMA-AIRWAY INTERDEPENDENCE. There is a strong functional inter-dependence between lung parenchyma and airways. The alveolar walls attach to the outside of intra- parenchymal airways. They contain elastic fibers which resist deformation and provide radial traction on the airway wall. Alveolar attachments lengthen and airways dilate with lung inflation due to the tethering force of the lung parenchyma on the airways [198]. In excised dog lungs the airway diameter reduced on average by 40% when the transpulmonary pressure was reduced from 30 to 0 cm H_2O[198]. The tethering force is highest at maximal lung inflation when the elastic recoil pressure is maximal. The tethering effect of the parenchyma results in a preload and afterload for the airway smooth muscle when it contracts. When airway smooth muscle contracts and narrows the airway it has to generate force to deform the surrounding lung parenchyma. High lung elastic recoil pressure results in a high load for the smooth muscle. Maximal shortening will therefore be small. In fact, when airways of dogs were maximally contracted with carbachol at transpulmonary pressures of 25, 15, 10, 8, and 6 cm H_2O, lumen area decreased by 7, 62, 78, 32, and 95% compared to baseline, respectively[199]. Lung volume was found to be a major

determinant of the bronchoconstrictor response to methacholine in healthy subjects [200].

Airway Compliance and Parenchyma. Lung elastic recoil has more effect on the airway diameter of peripheral airways than in central airways[201, 202]. In other words, peripheral airways are more compliant than central airways. Airway compliance, therefore, is an important determinant of airway diameter. The increase in diameter from functional residual capacity to total lung capacity was 28 and 5% for airways with a diameter below 1.7 and above 7 mm, respectively[201]. One of the determinants of airway compliance is the smooth muscle tone. The diameter of maximally relaxed airways in dogs was 20 to 30% higher for different lung volumes than in maximal constricted airways[203]. The effect of smooth muscle tone on airway diameter for different recoil pressures is most important for small airways[199, 204, 205]. Smooth muscle tone is not only an important determinant of airway compliance but also influences lung elastic recoil pressure[154]. Contraction of airway smooth muscle with methacholine reduced lung compliance by half and total lung capacity by one third[154]. Compliance of the airway will also depend on the mechanical qualities of the other airway wall components. Only very little is known on this contribution. It is likely that the remodeling of the airway wall as a result of chronic inflammation might substantially alter the compliance of airways and therefore lung compliance.

Smooth Muscle Tone and Interdependence. The forces of interdependence between parenchyma and airways are likely to play an important role in the pathogenesis of airflow obstruction. During tidal breathing the bronchial smooth muscle is stretched regularly due to the forces of interdependence. This depresses the active force generated by the smooth muscle below the force generated during static isometric contraction[206, 208]. A deep inspiration of airways at baseline tone and of bronchoconstricted airways reduces airway tone and, therefore, increases airway diameter in normal subjects for a give transmural pressure[209, 210]. This response is frequently impaired or absent in asthmatics[209, 211-218]. In asthmatic subjects with spontaneous severe airflow obstruction a deep inspiration can even increase obstruction[219]. Intensive treatment diminished the constrictor effect of the deep inspiration[220]. These findings suggest that interdependence is reduced in relation to inflammatory changes within the airways. In COPD interdependence between smooth muscle tone and parenchyma might be

impaired at a local level due to emphysema. There are some arguments to support this. Firstly, small airway disease is related to the destruction of peribronchial alveoli[221, 222], and patients with severe airflow limitation have a reduced density of the lung parenchyma as estimated with computer tomography[223] and a larger distance between alveolar attachments[224]. Secondly, lung elastic recoil is reduced in patients with emphysema[225, 226]. Thirdly, the maximal response to methacholine in patients with α_1- antitrypsin deficiency was positively correlated to the severity of emphysema and negatively to the maximal lung elastic recoil pressure[227]. Fifthly, a deep inspiration did not increase airway conductance, as was the case in normals, but reduced airway conductance in most subjects with COPD[212].

To our knowledge there are no studies on the parenchyma-airway smooth muscle interaction in CF or in BPD. Loss of parenchyma has been described in CF[193] and is a common feature in BPD[228, 229], and airway morphology is substantially altered in both diseases. Therefore, it is likely that parenchyma-airway interaction will be changed. It is unknown how the component of airway compliance that is not related to the smooth muscle interferes in the interdependence between airways and parenchyma.

Forced Expiration and Structural Changes of Airways
Reduction of maximal expiratory flow is an important feature of asthma[23, 35], COPD[10, 11, 54, 138], CF[62, 63, 230, 231], and BPD[232-234].

The forced flow-volume curve requires maximal effort throughout the maneuver. The forced vital capacity (FVC), forced expiratory volume in 1 second (FEV_1), and the ratio between the two (FEV_1 / FVC), as calculated from the flow volume curve, are considered important descriptors of airflow obstruction.

During the maneuver a flow limiting segment is formed in the airways. The places where the flow limiting segment is formed depends on the airway resistance upstream of the flow limiting segment and the lung elastic recoil pressure[235, 236]. The stiffness of the flow limiting segment is an important determinant of the luminal cross sectional area and therefore of the maximal flow[236].

INNER AND OUTER AIRWAY WALL. How can reduced maximal flows be explained from structural changes of the airways? There are only limited data available relating

parameters of forced expiratory flow to airway morphology. The mean FEV_1 of asthma patients who died from a fatal asthma attack, or who had a lobectomy for a solitary lung lesion, was within the normal range[138]. The inner and outer airway wall of these patients was substantially increased compared to smokers without substantial airflow obstruction. However, it is questionable how far the morphologic changes at the time of the lobectomy or death reflect adequately the morphology at the time of lung function testing. Studies using high resolution computed tomography showed that airways of asthmatic subjects with airflow obstruction were significantly thickened compared to normal subjects[303]. Smokers with reduced forced expiratory flows had increased thickness of the airway wall of small airways compared to smokers without airflow obstruction[10, 138]. Thickening of the airway wall could contribute to reduced forced expiratory flows in the following ways: Firstly, thickening of the airway wall will lead to increased airway resistance even in the absence of smooth muscle shortening if it results in decreased lumen area. In fact, upstream resistance is increased in asthma and COPD patients[237, 238]. This can result in a more upstream position of the flow limiting segment which usually leads to reduced maximal flows. In excised lungs of subjects without a history of airflow limitation the position of the flow limiting segment was generally distal of the main stem bronchus [239]. In asthma it was shown that the flow limiting segment was positioned even more peripherally[240]. Peripheral airways are more compliant and more collapsible than central airways[198, 201]. Development of flow limiting segments in more peripheral airways is, therefore, likely to occur at a lower transmural pressure. However, inflammatory thickening of airways might reduce its collapsibility but this was never investigated.

SMOOTH MUSCLE. Airways in asthma, COPD, CF, and BPD probably contain more smooth muscle[79, 111, 112, 138, 155-157] but there is no direct evidence that forced expiratory flow is correlated to the amount of smooth muscle in the airways. Theoretically, increased smooth muscle shortening could increase airway resistance and result in a more peripheral position of the flow limiting segment as explained previously. This is supported by the finding that a more peripheral position was found in lungs of dogs after bronchoconstriction with methacholine[241]. Increased smooth muscle tone reduces the lumen area and airway collapsibility of large airways[147-150].

Therefore, it is a theoretical possibility that the collapsibility of the flow limiting segment is decreased due to increased smooth muscle tone. This was confirmed when it was shown that the compliance of the flow limiting segment was reduced after bronchoconstriction in dogs[241].

CARTILAGE. There are some indications that the amount of cartilage is decreased in COPD in relation to airway inflammation. Loss of cartilage could, theoretically, result in increased collapsibility of airways at the equal pressure point during forced expiration.

When airway cartilage of young rabbits was softened, using papain, their tracheas exhibited a decreased ability to resist negative transmural pressures[176]. Lung function of these animals showed increased airway resistance and decreased maximal expiratory flows[175].

PARENCHYMA. Extensive loss of lung parenchyma, that is emphysema, is a common feature in COPD[242, 243], CF[193] and BPD[228, 229]. Emphysema is found to relate to airflow limitation in a number of studies[223, 224, 226, 242, 244], but not in others[11, 225, 245]. How can emphysema contribute to airflow limitation? Firstly, emphysema can result in a decrease of the lung elastic recoil pressure and therefore of driving pressure to generate maximal airflow[235]. In COPD, the loss of lung elastic recoil pressure correlates with the extent of emphysema[225, 226]. In addition, lung elastic recoil pressure at 90% of total lung capacity correlates significantly to airflow limitation in patients with COPD, asthma, and CF[226, 246]. Secondly, loss of tethering forces on the airways results in a decrease of airway diameter and therefore in an increase of airway resistance[247]. Thirdly, when the flow limiting segment is positioned in airways surrounded by parenchyma, reduced tethering forces can increase the compliance of the flow limiting segment[11].

In conclusion, the many changes in airway structure as previously described can all contribute to the pathophysiology of increased airflow obstruction during a forced expiratory maneuver. However, many pieces of this complex puzzle are still missing.

Airway Hyperresponsiveness and Structural Changes of Airways
Airway hyperresponsiveness refers to an exaggerated response to a bronchoconstrictor

and is indicative of an increased susceptibility of the patient to develop airways obstruction to environmental stimuli[248]. The parameters to monitor the response to a bronchoconstrictor can be derived from a flow-volume curve (peak flow, FEV_1, and FVC) or from measurements of airways resistance or conductance. These parameters are plotted against the concentration or dose of the bronchoconstrictor in dose-response curves. The dose-response curve allows the calculation of the sensitivity to the stimulus as indicated by the position of the curve, as well as measurement of the magnitude of the response with increasing dose as indicated by the slope and maximal response[24, 249].

In the general population there is a high prevalence of hyperresponsiveness to histamine or methacholine in children[250-252] and adults[253]. Atopy and airway caliber, as estimated by FEV_1, are major determinants related to this hyperresponsiveness[250, 251, 253- 256]. Up to two-thirds of all subjects with hyperresponsiveness are asymptomatic[252]. But, these subjects with asymptomatic hyperresponsiveness are at greater risk of developing symptomatic asthma than the general population[256]. The prevalence of hyperresponsiveness is higher in subjects with asthma[230, 257, 258], COPD[259, 260], CF[230, 257, 261-263] and BPD[233, 264 265]. In COPD bronchial responsiveness is related to the number of cigarettes smoked[40].

Bronchial hyperresponsiveness has been related to a wide variety of structural changes of the airways. Reduced airway caliber and secretions alter the deposition pattern of aerosols. Aerosol deposition is inhomogeneous and higher in central airways in patients with asthma[266-268], COPD[269], and in CF[270, 271]. The severity of airflow obstruction is correlated to the abnormality of the distribution pattern[266-268]. The total lung deposition in patients with airflow obstruction is unchanged or even higher than in non-obstructed control subjects[266, 272, 273]. Higher lung deposition of histamine in smokers is associated with an increased bronchoconstrictor response[273]. Furthermore, it was suggested that increased deposition of bronchoconstrictors in central airways at the site of the flow limiting segment might contribute to the bronchial hyperresponsiveness[274].

Airway caliber in the general population is an important determinant of bronchial responsiveness[253, 254]. Airways with a small caliber are expected to be more

hyperreactive than larger airways since airflow through airways depends on at least the fourth power of the radius[275]. Bronchial hyperresponsiveness can, therefore, be the result of abnormal small airways. Whether growth of airways in children is impaired due to chronic airway inflammation is unclear. In children with asthma there is indirect evidence that growth of airways is normal. Lung function estimates of airway size were not different in a cross-sectional study of children with asthma than in matched controls[276]. Reduced airway caliber due to impaired lung growth as a result of prenatal and/or early life exposure to cigarette smoke might play a role in the pathogenesis of COPD[277-279]. Very little is known about airway growth in premature born infants and in patients with BPD. Airway diameter in autopsy lungs of premature infants fixed at a transmural pressure of 30 cm H_2O were of normal size for their postconceptional age, irrespective of artificial ventilation[195]. A drawback of this study is that airway diameter depends on the contractile status of the airway and correlate poorly to the airway internal perimeter[280]. Animal studies show that malnutrition[281, 282] and maternal smoking[283] impair lung growth and development. Patients with severe BPD demonstrate poor weight gain[233, 284]. Impaired growth is also present in many CF infants due to pancreatic insufficiency[285, 286]. Furthermore, the nutritional status of CF patients correlates to survival[287]. Therefore it is possible that impaired lung growth plays a role in the pathophysiology of bronchial responsiveness in BPD and CF. There are, however, no studies on the effects of malnutrition on lung growth in humans[288].

BASEMENT MEMBRANE. The thickness of the lamina reticularis correlates to the severity of bronchial responsiveness of asthmatic patients and to indicators of airflow obstruction[118, 119, 289]. It is difficult to explain how a thicker lamina reticularis would increase bronchial responsiveness. Probably it is more a marker of a disease process than a determinant of bronchial responsiveness.

INNER AND OUTER AIRWAY WALL. Thickening of the inner wall area is theoretically an important determinant of bronchial hyperresponsiveness, since it reduces airway caliber and can enhance airway narrowing when the smooth muscle shortens[79, 190]. As described previously, thickening of the inner airway wall is well documented in asthma and COPD and might play a role in CF and BPD too. COPD patients with

hyperresponsiveness had a thicker inner and outer wall area compared to patients without hyperresponsiveness[304]. Thickening of the airway wall in sheep by 18%, induced by increased bronchial blood flow, did not increase bronchial responsiveness[290]. Chronic hyperoxic exposure of immature rats induces both airway hyperresponsiveness and an increase of the epithelial and smooth muscle layer[291]. It is clear from this study whether or not the smooth muscle force is increased and/or the epithelial layer thickening amplifies the luminal narrowing due to airway muscle shortening.

EPITHELIUM. Epithelial injury is associated with bronchial hyperresponsiveness in asthma[3, 27]. Parameters of epithelial damage correlated to airway responsiveness in 2 studies[3, 27] but not in another[292]. The relation between epithelial injury and bronchial responsiveness has never been systematically investigated in COPD, CF, and BPD. Due to the loss of barrier function, airway permeability may increase and provide easy access of the bronchoconstrictor to the airway smooth muscle. In fact, loss of barrier function is well documented in asthma[293]. Furthermore, airway epithelium is a source of relaxing substances that may act on smooth muscle cells. Damage of the epithelium might therefore increase smooth muscle tone and airway reactivity in vitro[82, 294-298].

SMOOTH MUSCLE. Smooth muscle area was found to be increased in asthma[79, 111, 112, 138, 155-157], COPD[10, 138, 155], and BPD[65, 159-161]. However there are no conclusive studies in humans where the amount of smooth muscle in the airways was correlated to lung function measurements of bronchial responsiveness. Airway hyperresponsiveness in guinea pig, induced with repeated antigen challenge, is associated with both increased force generation and shortening of tracheal smooth muscle, but without increased muscle mass, suggesting enhanced contractile activity[166].

CARTILAGE. The relation between the amount of cartilage and bronchial responsiveness has been investigated in 45 COPD patients. The volume proportion of cartilage was slightly less in airways of patients who had increased responsiveness to a bronchodilator[182]. However, this correlation can be the result of relative decrease, resulting from an increased total wall area, or from a decreased amount of cartilage.

PARENCHYMA. Emphysema can be an important determinant of bronchial hyper-

reactivity. The maximal fall in FEV_1 after provocation with methacholine in patients with α_1-antitrypsin deficiency was significantly higher in patients with a reduced lung density as measured with computer tomography[227]. COPD patients with centrilobular emphysema are more hyperresponsive than patients with panlobular emphysema. Patients with centrilobular emphysema have more diseased airways than patients with panlobular emphysema[245]. The difference in bronchial responsiveness could be the result of the emphysema and / or abnormalities within the airway.

Conclusion

Diseases characterized by chronic inflammation of the airways such as asthma, COPD, CF, and BPD all have substantial structural changes of the airways and parenchyma. Furthermore, many of these patients have airflow limitation and increased bronchial responsiveness. Currently, the pathophysiology of the lung function abnormalities is only partially resolved because of the complex interactions between different components within the airway wall and between the airway wall and the parenchyma. Clearly there is more than smooth muscle alone to obstruct an airway.

References

1. Weibel ER. *Morphometry of the human lung.* Berlin: Springer-Verlag, 1963.
2. Dunnill MS, Massarella GR, Anderson JA. A comparison of the quantitative anatomy of the bronchi in normal subjects, in status asthmaticus, in chronic bronchitis, and in emphysema. Thorax 1969;24:176-179.
3. Jeffery PK, Wardlaw AJ, Nelson FC, Collins JV, Kay AB. Bronchial biopsies in asthma. An ultrastructural, quantitative study and correlation with hyperreactivity. Am Rev Respir Dis 1989;140(6):1745-1753.
4. Djukanovic R, Roche WR, Wilson JW, Beasley CR, Twentyman OP, Howarth RH, Holgate ST. Mucosal inflammation in asthma. Am Rev Respir Dis 1990;142(2):434-457.
5. Laitinen LA, Laitinen A, Altraja A, Virtanen I, Kampe M, Simonsson BG, Karlsson SE, Hakansson L, Venge P, Sillastu H. Bronchial biopsy findings in intermittent or "early" asthma. J Allergy Clin Immunol 1996;98(5 Pt 2):S3-6; discussion S33-40.
6. Hamid Q, Song Y, Kotsimbos TC, Minshell E, Bai TR, Hegele RG, Hogg JC. Inflammation of small airways in asthma. J Allergy Clin Immunol 1997;100:44-51.
7. Cosio M, Ghezzo H, Hogg JC, Corbin R, Loveland M, Dosman J, Macklem PT. The relations between structural changes in small airways and pulmonary- function tests. New Engl J Med 1977;298:1277-1281.
8. Mullen JB, Wright JL, Wiggs BR, Paré PD, Hogg JC. Reassessment of inflammation of airways in chronic bronchitis. Br Med J (Clin Res Ed) 1985;291(6504):1235-1239.
9. Thompson AB, Daughton D, Robbins RA, Ghafouri MA, Oehlerking M, Rennard SI. Intraluminal airway inflammation in chronic bronchitis. Characterization and correlation with clinical parameters. Am Rev Respir Dis 1989;140(6):1527-1537.
10. Bosken CH, Wiggs BR, Paré PD, Hogg JC. Small airway dimensions in smokers with obstruction to airflow. Am Rev Respir Dis 1990;142(3):563-570.
11. Hogg JC, Wright JL, Wiggs BR, Coxson HO, Opazo Saez A. Lung structure and function in cigarette smokers. Thorax 1994;49:473-478.
12. Bedrossian CWM, Greenberg SD, Singer DB, Hansen JJ, Rosenberg HS. The lung in cystic fibrosis; A quantitative study including prevalence of pathologic findings among different age groups. Hum Pathol 1973;7(2):195-204.
13. Tomashefski JF, Jr., Konstan MW, Bruce MC, Abramowsky CR. The pathologic characteristics of interstitial pneumonia cystic fibrosis. A retrospective autopsy study. Am J Clin Pathol 1989;91(5):522-530.
14. Konstan MW, Hilliard KA, Norvell TM, Berger M. Bronchoalveolar lavage findings in cystic fibrosis patients with stable, clinically mild lung disease suggest ongoing infection and inflammation. Am J Respir Crit Care Med 1994;150:448-454.
15. Birrer P, McElvaney NG, Rudeberg A, Wirz Sommer C, Liechti Gallati S, Kraemer R, Hubbard R, Crystal RG. Protease-antiprotease imbalance in the lungs of children with cystic fibrosis. Am J Respir Crit Care Med 1994;150:207-213.
16. Khan TZ, Wagener JS, Bost T, Martinez J, Accurso FJ, Riches DW. Early pulmonary inflammation in infants with cystic fibrosis [see comments]. Am J Respir Crit Care Med 1995;151(4):1075-1082.
17. Armstrong DS, Grimwood K, Gutierrez J, Carzino R, Carlin J, Olinsky A, Phelan P. Lower airway infection and inflammation in infants and young children with Cystic Fibrosis. Am J Respir Crit Care Med 1996;153(4):A777.
18. Bagchi A, Viscardi RM, Taciak V, Ensor JE, McCrea KA, Hasday JD. Increased activity of interleukin-6 but not tumor necrosis factor-alpha in lung lavage of premature infants is associated with the development of bronchopulmonary dysplasia. Pediatr Res 1994;36(2):244-252.
19. Ogden BE, Murphy SA, Saunders GC, Pathak D, Johnson JD. Neonatal lung neutrophils and elastase/proteinase inhibitor imbalance. Am Rev Respir Dis 1984;130(5):817-821.

20. Watterberg KL, Carmichael DF, Gerdes JS, Werner S, Backstrom C, Murphy S. Secretory leukocyte protease inhibitor and lung inflammation in developing bronchopulmonary dysplasia. J Pediatr 1994;125(2):264-269.

21. Groneck P, Gotze-Speer B, Oppermann M, Eiffert H, Speer CP. Association of pulmonary inflammation and increased microvascular permeability during the development of bronchopulmonary dysplasia: a sequential analysis of inflammatory mediators in respiratory fluids of high-risk preterm neonates [see comments]. Pediatrics 1994;93(5):712-718.

22. Zimmerman JJ. Bronchoalveolar inflammatory pathophysiology of bronchopulmonary dysplasia. Clin Perinatol 1995;22(2):429-456.

23. McFadden ER, Kiser R, W.J. de. Acute bronchial asthma. New Engl J Med 1973;288:221-225.

24. Sterk PJ, Bel EH. Bronchial hyperresponsiveness: the need for a distinction between hypersensitivity and excessive airway narrowing. Eur Respir J 1989;2(3):267-274.

25. Salvato G. Some histological changes in chronic bronchitis and asthma. Thorax 1968;23(2):168-172.

26. Cutz E, Levison H, Cooper DM. Ultrastructure of airways in children with asthma. Histopathol 1978;2(6):407-421.

27. Ohashi Y, Motojima S, Fukuda T, Makino S. Airway hyperresponsiveness, increased intracellular spaces of bronchial epithelium, and increased infiltration of eosinophils and lymphocytes in bronchial mucosa in asthma [see comments]. Am Rev Respir Dis 1992;145(6):1469-1476.

28. Azzawi M, Johnston PW, Majumdar S, Kay AB, Jeffery PK. T Lymfocytes and activated eosinophils in airway mucosa in fatal asthma and cystic fibrosis. Am Rev Respir Dis 1992;145:1477-1482.

29. Saetta M. Airway pathology of COPD compared with asthma. Eur Respir Rev 1997;7(45):211-215.

30. Laberge S. Increased expression of interleukin-16 in bronchial mucosa of subjects with atopic asthma. Am J Respir Cell Mol Biol 1997;17:193-202.

31. Beasley R, Roche WR, Roberts JA, Holgate ST. Cellular events in the bronchi in mild asthma and after bronchial provocation. Am Rev Respir Dis 1989;139(3):806-817.

32. Riise GC, Andersson B, Ahlstedt S, Enander I, Soderberg M, Lowhagen O, Larsson S. Bronchial brush biosies for studies of epithelial inflammation in stable asthma and nonobstructive chronic bronchitis. Eur Respir J 1996;9:1665-1671.

33. Faul JL, Tormey VJ, Leonard C, Burke CM, Farmer J, Horne SJ, Poulter LW. Lung immunopathology in cases of sudden asthma death. Eur Respir J 1997;10:301-307.

34. Martinez FD, Wright AL, Taussig LM, Holberg CJ, Halonen M, Morgan WJ, Associates TGHM. Asthma and wheezing in the first six years of life. N Engl J Med 1995;332(3):133-138.

35. Young S, Arnott J, Le Souef PN, Landau LI. Flow limitation during tidal expiration in symptom-free infants and the subsequent development of asthma. J Pediatr 1994;124:681-688.

36. Roorda RJ, Gerritsen J, van Aalderen WM, Schouten JP, Veltman JC, Weiss ST, Knol K. Follow-up of asthma from childhood to adulthood; influence of potential childhood risk factors on the outcome of pulmonary function and bronchial responsiveness in adulthood. J Allergy Clin Immunol 1994;93(3):575-584.

37. Panhuysen CI, Vonk JM, Koeter GH, Schouten JP, van Altena R, Bleecker ER, Postma DS. Adult patients may outgrow their asthma: a 25-year follow-up study. Am J Respir Crit Care Med 1997;155(4):1267-1272.

38. Jöbsis Q, Raatgeep HC, Hermans PWM, de Jongste JC. Hydrogen peroxide in exhaled air is increased in stable asthmatic children. Eur Respir J 1997;10:519-521.

39. Lundgren R, Soderberg M, Horstedt P, Stenling R. Morphological studies of bronchial mucosa from asthmatics before and after ten years of treatment with inhaled steroids. Eur Respir J 1988;1:883-889.

40. Mullen JB, Wiggs BR, Wright JL, Hogg JC, Paré PD. Nonspecific airway reactivity in cigarette smokers. Relationship to airway pathology and baseline lung function. Am Rev Respir Dis 1986;133(1):120-125.

41. Snider GL. Chronic obstructive pulmonary disease: risk factors, pathophysiology and pathogenesis. Annu Rev Med 1989;40:411-429.

42. Peto R, Lopez AD, Boreham J, Thun M, Heath C, Jr. Mortality from tobacco in developed countries: indirect estimation from national vital statistics [see comments]. Lancet 1992;339(8804):1268-1278.

43. Prescott E, Bjerg AM, Andersen PK, Lange P, Vestbo J. Gender difference in smoking effects on lung function and risk of hospitalization for COPD: results from a Danish longitudinal population study. Eur Respir J 1997;10:822-827.

44. Xu X, Dockery DW, Ware JH, Speizer FE, Ferris BG, Jr. Effects of cigarette smoking on rate of loss of pulmonary function in adults: a longitudinal assessment. Am Rev Respir Dis 1992;146(5 Pt 1):1345-1348.

45. MacNee W. Neutrophil traffic and COPD. Eur Respir Rev 1997;43:124-127.

46. MacNee W, Wiggs B, Belzberg AS, Hogg JC. The effect of cigarette smoking on neutrophil kinetics in human lungs [see comments]. N Engl J Med 1989;321(14):924-928.

47. Hunninghake GW, Crystal RG. Cigarette smoking and lung destruction. Accumulation of neutrophils in the lungs of cigarette smokers. Am Rev Respir Dis 1983;128(5):833-838.

48. Bosken CH, Hards J, Gatter K, Hogg JC. Characterization of the inflammatory reaction in the peripheral airways of cigarette smokers using immunocytochemistry. Am Rev Respir Dis 1992;145(4 Pt 1):911-917.

49. Stockley RA. New perspectives on the protease/antiprotease balance. Eur Respir Rev 1997;7(43):128-130.

50. Jorres RA, Magnussen H. Oxidative stress in COPD. Eur Respir Rev 1997;7(43):131-135.

51. Gadek JE, Fells GA, Zimmerman RL, Rennard SI, Crystal RG. Antielastases of the human alveolar structures. Implications for the protease-antiprotease theory of emphysema. J Clin Invest 1981;68(4):889-898.

52. Repine JE, Bast A, Lankhorst I, Group aTOSS. Oxidative stress in chronic obstructive pulmonary disease. Am J Respir Crit Care Med 1997;156:341-357.

53. Anthonisen NR, Connett JE, Kiley JP. Effects of smoking intervention and the use of an inhaled anticholinergic bronchodilator on the rate of decline of FEV1. The lung health study. JAMA 1994;272:1497-1505.

54. Anthonisen N. Epidemiology and the lung health study. Eur Respir Rev 1997;7(45):202-205.

55. Kerstjens HAM, Rijcken B, Schouten JP, Postma DS. Decline of FEV1 by age and smoking status: facts, figures, and fallacies. Thorax 1997;52:820-827.

56. Smith JJ, Travis SM, Greenberg EP, Welsh MJ. Cystic fibrosis airway epithelia fail to kill bacteria because of abnormal airway surface fluid. Cell 1996;85:229- 236.

57. Bruce MC, Poncz L, Klinger JD, Stern RC, Tomashefski JF, Jr., Dearborn DG. Biochemical and pathologic evidence for proteolytic destruction of lung connective tissue in cystic fibrosis. Am Rev Respir Dis 1985;132(3):529-535.

58. Oppenheimer EH, Esterly JR. Pathology of cystic fibrosis. Review of the literature and comparison with 146 autopsied cases. Prospect Pediatr Pathol 1978;2:241- 278.

59. Baltimore R, Christie C, Smith W. Immunohistopathologic localization of Pseudomonas aeruginosa in lungs from patients with cystic fibrosis. Am Rev Respir Dis 1989;140:1650-1661.

60. Godfrey S, Mearns M, Howlett G. Serial lung function studies in cystic fibrosis in the first 5 years of life. Arch Dis Child 1978;53(1):83-85.

61. Tepper RS, Hiatt P, Eigen H, Scott P, Grosfeld J, Cohen M. Infants with cystic fibrosis: pulmonary function at diagnosis. Pediatr Pulmonol 1988;5(1):15-18.

62. Tepper RS, Montgomery GL, Ackerman V, Eigen H. Longitudinal evaluation of pulmonary function in infants and very young children with cystic fibrosis. Pediatr Pulmonol 1993;16(2):96-100.

63. Kerem E, Reisman J, Corey M, Canny GJ, Levison H. Prediction of mortality in patients with cystic fibrosis [see comments]. N Engl J Med 1992;326(18):1187- 1191.

64. Elborn JS, Shale DJ, Britton JR. Cystic fibrosis: current survival and population estimates to the year 2000 [published erratum appears in Thorax 1992 Feb;47(2):139] [see comments]. Thorax 1991;46(12):881-885.

65. Northway WH, Jr., Rosan RC, Porter DY. Pulmonary disease following respirator therapy of hyaline-membrane disease. Bronchopulmonary dysplasia. N Engl J Med 1967;276(7):357-368.
66. Northway WH, Jr. Bronchopulmonary dysplasia: then and now. Arch Dis Child 1990;65(10 Spec No):1076-1081.
67. Parker RA, Lindstrom DP, Cotton RB. Improved survival accounts for most, but not all, of the increase in bronchopulmonary dysplasia. Pediatrics 1992;90(5):663-668.
68. Abman SH, Groothius JR. Pathophysiology and treatment of bronchopulmonary dysplasia. Current issues. Pediatr Clin North Am 1994;41(2):277-315.
69. Gorenflo M, Vogel M, Herbst L, Bassir C, Kattner E, Obladen M. Influence of clinical and ventilatory parameters on morphology of bronchopulmonary dysplasia. Pediatr Pulmonol 1995;19(4):214-220.
70. Coalson JJ, Winter VT, Gerstmann DR, Idell S, King RJ, Delemos RA. Pathophysiologic, morphometric, and biochemical studies of the premature baboon with bronchopulmonary dysplasia. Am Rev Respir Dis 1992;145(4 Pt 1):872-881.
71. Walti H, Tordet C, Gerbaut L, Saugier P, Moriette G, Relier JP. Persistent elastase/proteinase inhibitor imbalance during prolonged ventilation of infants with bronchopulmonary dysplasia: evidence for the role of nosocomial infections. Pediatr Res 1989;26(4):351-355.
72. Bancalari E, Sosenko I. Pathogenesis and prevention of neonatal chronic lung disease: recent developments. Pediatr Pulmonol 1990;8(2):109-116.
73. Mirro R, Armstead W, Leffler C. Increased airway leukotriene levels in infants with severe bronchopulmonary dysplasia. Am J Dis Child 1990;144(2):160-161.
74. Gerdes JS, Yoder MC, Douglas SD, Paul M, Harris MC, Polin RA. Tracheal lavage and plasma fibronectin: relationship to respiratory distress syndrome and development of bronchopulmonary dysplasia. J Pediatr 1986;108(4):601-606.
75. Watts CL, Fanaroff AA, Bruce MC. Elevation of fibronectin levels in lung secretions of infants with respiratory distress syndrome and development of bronchopulmonary dysplasia. J Pediatr 1992;120(4 Pt 1):614-620.
76. Bruce MC, Wedig KE, Jentoft N, Martin RJ, Cheng PW, Boat TF, Fanaroff AA. Altered urinary excretion of elastin cross-links in premature infants who develop bronchopulmonary dysplasia. Am Rev Respir Dis 1985;131(4):568-572.
77. Bai A, Eidelman DH, Hogg JC, James AL, Lambert RK, Ludwig MS, Martin J, McDonald DM, Mitzner WA, Okazawa M, Pack RJ, Paré PD, Schellenberg RR, Tiddens HAWM, Wagner EM, Yager D. Proposed nomenclature for quantifying subdivisions of the bronchial wall. J Appl Physiol 1994;77(2):1011-1014.
78. Moreno RH, Hogg JC, Paré PD. Mechanics of airway narrowing. Am Rev Respir Dis 1986;133(6):1171-1180.
79. James AL, Paré PD, Hogg JC. The mechanics of airway narrowing in asthma. Am Rev Respir Dis 1989;139(1):242-246.
80. Lambert RK, Wiggs BR, Kuwano K. Functional significance of increased airway smooth muscle in asthma and COPD. J Appl Physiol 1993;74:2771-2781.
81. Paré PD, Bai TR. The consequences of chronic allergic inflammation. Thorax 1995;50(4):328-332.
82. Sparrow MP, Mitchell HW. Modulation by the epithelium of the extent of bronchial narrowing produced by substances perfused through the lumen. Br J Pharmacol 1991;103(1):1160-1164.
83. Hulsmann AR, Raatgeep HR, Den Hollander JC, Bakker WH, Saxena PR, De Jongste JC. Permeability of human isolated airways increases after hydrogen peroxide and poly-L-arginine. Am J Respir Crit Care Med 1996;153(2):841-846.
84. Gao Y, Vanhoutte PM. Epithelium acts as a modulator and a diffusion barrier in the responses of canine airway smooth muscle. J Appl Physiol 1994;76(5):1843-1847.
85. Sparrow MP, Omari TI, Mitchell HW. The epithelial barrier and airway responsiveness. Can J Physiol Pharmacol 1995;73:180-190.

86. Hulsmann AR, De Jongste JC. Modulation of airway responsiveness by the airway epithelium in humans, putative mechanisms. Clin Exp Allergy 1996;26:1236-1242.
87. Laitinen LA, Heino M, Laitinen A, Kava T, Haahtela T. Damage of the airway epithelium and bronchial reactivity in patients with asthma. Am Rev Respir Dis 1985;131:505-606.
88. Elia C, Bucca C, Rolla G, Scappaticci E, Cantino D. A freeze-fracture study of human bronchial epithelium in normal, bronchitic and asthmatic subjects. J Submicrosc Cytol Pathol 1988;20(3):509-517.
89. Montefort S, Roberts JA, Beasley R, Holgate ST, Roche WR. The site of disruption of the bronchial epithelium in asthmatic and non-asthmatic subjects. Thorax 1992;47(7):499-503.
90. Chang SC. Microscopic properties of whole mounts and sections of human bronchial epithelium of smokers and nonsmokers. Cancer 1957;10:1246-1262.
91. Ollerenshaw SL, Woolcock AJ. Characteristics of the inflammation in biopsies from large airways of subjects with asthma and subjects with chronic airflow limitation. Am Rev Respir Dis 1992;145(4 Pt 1):922-927.
92. Dovey M, Wisseman CL, Roggli VL, Roomans GM, Shelburne JD, Spock A. Ultrastructural morphology of the lung in cystic fibrosis. J Submicrosc Cytol Pathol 1989;21(3):521-534.
93. Leigh MW, Kylander JE, Yankaskas JR, Boucher TC. Cell proliferation in bronchial epithelium and submucosal glands of cystic fibrosis patients. Am J Respir Cell Biol 1995;12:605-612.
94. Lee RM, H OB. Airway epithelial damage in premature infants with respiratory failure. Am Rev Respir Dis 1988;137(2):450-457.
95. Sward-Comunelli SL, Mabry SM, Truog WE, Thibeault DW. Airway muscle in preterm infants: Changes during development. J Pediatr 1997;130:570-576.
96. Tsang KW, Rutman A, Tanaka E, Lund V, Dewar A, Cole PJ, Wilson R. Interaction of Pseudomonas aeruginosa with human respiratory mucosa in vitro. Eur Respir J 1994;7(10):1746-1753.
97. Puchelle E, Zahm JM, Tournier JM, de Bentzmann S. Airway epithelial injury and repair. Eur Respir Rev 1997;7(43):136-141.
98. Bajolet-Laudinat O, Girod-de Bentzmann S, Tournier JM, Madoulet C, Plotkowski MC, Chippaux C, Puchelle E. Cytotoxicity of Pseudomonas aeruginosa internal lectin PA-I to respiratory epithelial cells in primary culture. Infect Immun 1994;62(10):4481-4487.
99. de Bentzmann S, Roger P, Dupuit F, Bajolet-Laudinat O, Fuchey C, Plotkowski MC, Puchelle E. Pseudomonas aeruginosa adherence to regenerating respiratory epithelial cells. Infect and Immun 1996;in press: 000-000.
100. Plotkowski MC, Tournier JM, Puchelle E. Pseudomonas aeruginosa strains possess specific adhesins for laminin. Inf and Immun 1996;64:600-605.
101. Henke CA, Hertz M, Gustafson P. Combined bronchoscopy and mucolytic therapy for patients with severe refractory status asthmaticus on mechanical ventilation: A Case report and review of the literature. Critical Care Medicine 1994;22(11):1880-1883.
102. Morphometric analysis of intraluminal mucus in airways in chronic obstructive pulmonary disease. Am Rev Respir Dis; 1989.
103. Yager D, Butler JP, Bastacky J, Israel E, Smith G, Drazen JM. Amplification of airway constriction due to liquid filling of airway interstices. J Appl Physiol 1989;66(6):2873-2884.
104. Welling LW, Zupka MT, Welling DJ. Mechanical properties of basement membrane. News Physiol Sc 1995;10:30-35.
105. Cook TA, Salmo NA, Yates PO. The elasticity of the internal lamina. J Pathol 1975;117(4):253-258.
106. Bock P, Stockinger L. Light and electron microscopic identification of elastic, elaunin and oxytalan fibers in human tracheal and bronchial mucosa. Anat Embryol (Berl) 1984;170(2):145-153.
107. Leick-Maldonado EA, Lemos M, Tiberio IFLC, Caldini EG, Montes GS, Martins MA, Saldiva PHN. Differential distribution of elastic system fibers in control and bronchoconstricted intraparenchymatous airways in the guinea-pig lung. Am J Respir Crit Care Med 1997;155:A546.

108. Soderberg M, Hellstrom S, Sandstrom T, Lundgren R, Bergh A. Structural characterization of bronchial mucosal biopsies from healthy volunteers: a light and electron microscopical study. Eur Respir J 1990;3(3):261-266.

109. Lambert RK. Role of bronchial basement membrane in airway collapse. J Appl Physiol 1991;71(2):666-673.

110. Lambert RK, Codd SL, Alley MR, Pack RJ. Physical determinants of bronchial mucosal folding. J Appl Physiol 1994;77(3):1206-1216.

111. Ebina M, Yaegashi H, Chiba R, Takahashi T, Motomiya M, Tanemura M. Hyperreactive site in the airway tree of asthmatic patients revealed by thickening of bronchial muscles. A morphometric study. Am Rev Respir Dis 1990;141(5 Pt 1):1327-1332.

112. Fabbri LM, Danieli D, Crescioli S, Bevilacqua P, Meli S, Saetta M, Mapp CE. Fatal asthma in a subject sensitized to toluene diisocyanate. Am Rev Respir Dis 1988;137(6):1494-1498.

113. Foresi A, Bertorelli G, Pesci A, Chetta A, Olivieri D. Inflammatory markers in bronchoalveolar lavage and in bronchial biopsy in asthma during remission. Chest 1990;98(3):528-535.

114. Roche WR, Beasley R, Williams JH, Holgate ST. Subepithelial fibrosis in the bronchi of asthmatics. Lancet 1989;1(8637):520-524.

115. Brewster CE, Howarth PH, Djukanovic R, Wilson J, Holgate ST, Roche WR. Myofibroblasts and subepithelial fibrosis in bronchial asthma. Am J Respir Cell Mol Biol 1990;3(5):507-511.

116. Wilson JW, Li X. The measurement of reticular basement membrane and submucosal collagen in the asthmatic airway [see comments]. Clin Exp Allergy 1997;27(4):363-371.

117. Saetta M, Maestrelli P, Turato G, Mapp C, Milani G, Pivirotto A, Fabbri L, Di Stefano A. Airway wall remodeling after cessation of exposure to isocyanates in sensitized asthmatic subjects. Am J Respir Crit Care Med 1995;151:489-494.

118. Chetta A, Foresi A, Del Donno M, Bertorelli G, Pesci A, Olivieri D. Airways remodelling is a distinctive feature of asthma and is related to severity of disease. Chest 1997;111:852-857.

119. Boulet L-P, Laviolette M, Turcotte H, Cartier A, Dugas M, Malo J-L, Boutet M. Bronchial subepithelial fibrosis correlates with airway responsiveness to metacholine. Chest 1997;112:45-52.

120. Soderberg M, Hellstrom S, Lundgren R, Bergh A. Bronchial epithelium in humans recently recovering from respiratory infections caused by influenza or mycoplasma. Eur Respir J 1990;3(9):1023-1028.

121. Gizycki MJ, Rogers AV, Adelroth E, O'Byrne PM, Jeffery PK. Ultrastructure of allergen induced myofibroblasts in asthma. Am J Respir Crit Care Med 1997;155:A371.

122. Widdicombe J. Why are the airways so vascular. Thorax 1993;48:290-295.

123. Strek P, Nowogrodzka-Zagorska M, Litwin JA, Miodonski AJ. The lung in closeview: a corrosion casting study on the vascular system of human foetal trachea. Eur Respir J 1994;7(9):1669-1672.

124. Laitinen A, Laitinen LA. Vascular beds in the airways of normal subjects and asthmatics [published erratum appears in Eur Respir J Suppl 1991 Mar;4(3):382, 659S-660S]. Eur Respir J Suppl 1990;12(1s-662s):658s-661s.

125. Persson CGA. Airway epithelium and microcirculation. Eur Respir Rev 1994;4(23):352-362.

126. Carroll NG, Cooke C, James AL. Bronchial blood vessel dimensions in asthma. Am J Respir Crit Care Med 1997;155(2):689-695.

127. Baile EM, Dahlby RW, Wiggs BR, Paré PD. Role of tracheal and bronchial circulation in respiratory heat exchange. J Appl Physiol 1985;58(1):217-222.

128. Deffebach ME, Charan NB, Lakshminarayan S, Butler J. The bronchial circulation. Small, but a vital attribute of the lung. Am Rev Respir Dis 1987;135(2):463-481.

129. Wagner EM, Mitzner W. Effects of bronchial vascular engorgement on airway dimensions. J Appl Physiol 1996;81(1):293-301.

130. Persson CG. Plasma exudation and asthma. Lung 1988;166(1):1-23.

131. Persson CG. Plasma exudation in tracheobronchial and nasal airways: a mucosal defence mechanism becomes pathogenic in asthma and rhinitis. Eur Respir J Suppl 1990;12:652s-656s; discussion 656s-657s.

132. Widdicombe JG. Permeability of the airway mucosa in asthma. Eur Respir J Suppl 1991;13:139s-147s.

133. Chung KF, Rogers DF, Barnes PJ, Evans TW. The role of increased airway microvascular permeability and plasma exudation in asthma. Eur Respir J 1990;3(3):329-337.

134. Barnes PJ, Boschetto P, Rogers DF, Belvisi M, Roberts N, Chung KF, Evans TW. Effects of treatment on airway microvascular leakage. Eur Respir J Suppl 1990;12:663s-670s; discussion 670s-671s.

135. McDonald DM. The ultrastructure and permeability of tracheobronchial blood vessels in health and disease. Eur Respir J Suppl 1990;12:572s-585s.

136. Fick RB, Jr., Metzger WJ, Richerson HB, Zavala DC, Moseley PL, Schoderbek WE, Hunninghake GW. Increased bronchovascular permeability after allergen exposure in sensitive asthmatics. J Appl Physiol 1987;63(3):1147-1155.

137. Ohrui T, Sekizawa K, Aikawa T, Yamauchi K, Sasaki H, Takishima T. Vascular permeability and airway narrowing during late asthmatic response in dogs treated with Metopirone. J Allergy Clin Immunol 1992;89(5):933-943.

138. Kuwano K, Bosken CH, Paré PD, Bai TR, Wiggs BR, Hogg JC. Small airways dimensions in asthma and chronic obstructive pulmonary disease. Am Rev Respir Dis 1993;148:1220-1225.

139. Li X, Wilson JW. Increased vascularity of the bronchial mucosa in mild asthma. American journal of respiratory and critical care medicine 1997;156:229-233.

140. Mitzner W, Wagner E, Brown RH. Is asthma a vascular disorder? Chest 1995;107(3 Suppl):97S-102S.

141. Ebina M, Yaegashi H, Takahashi T, Motomiya M, Tanemura M. Distribution of smooth muscles along the bronchial tree. A morphometric study of ordinary autopsy lungs. Am Rev Respir Dis 1990;141(5 Pt 1):1322-1326.

142. Gabella G. Anatomy of airways smooth muscle. In: Raeburn D, Giembycz MA, editors. *Airways smooth muscle: structure, innervation and neurotransmission*. Basel/Switzerland: Birkhauser, 1994:1-27.

143. Ma X, Li W, Stephens NL. Detection of two clusters of mechanical properties of smooth muscle along the airway tree. J Appl Physiol 1996;80(3):857-861.

144. Bates JH, Martin JG. A theoretical study of the effect of airway smooth muscle orientation on bronchoconstriction. J Appl Physiol 1990;69(3):995-1001.

145. Opazo-Saez A, Okazawa M, Paré PD. Airway smooth muscle orientation and airway stiffness favour airway narrowing rather than airway shortening. Am J Respir Crit Care Med 1994;149(A583).

146. Lei M, Ghezzo H, Chen MF, Eidelman DH. Airway smooth muscle orientation in intraparenchymal airways. J Appl Physiol 1997;82(1):70-77.

147. Fraser RG. Measurements of the calibre of human bronchi in three phases of respiration by cinebronchography. J Canadian Ass Radiol 1961;12:102-112.

148. Olsen CR, Stevens AE, Pride NB, Staub NC. Structural basis for decreased compressibility of constricted trachea and bronchi. J Appl Physiol 1967;23(1):35-39.

149. Olsen CR, Stevens AE, McIlroy MB. Rigidity of trachea and bronchi during muscular constriction. J Appl Physiol 1967;23(1):27-43.

150. Penn RB, Wolfson MR, Shaffer TH. Effect of tracheal smooth muscle tone on collapsibility of immature airways. J Appl Physiol 1988;65(2):863-869.

151. Okazawa M, Paré PD. Pressure area relationship of membranous airways in rabbit. Am J Respir Crit Care Med 1994;149(4):A770.

152. McFawn PK, Mitchell HW. Effect of transmural pressure on preloads and collapse of immature bronchi. Eur Respir J 1997;10(2):322-329.

153. Brown RH, Mitzner W. Effect of lung inflation and airway muscle tone on airway diameter in vivo. J Appl Physiol 1996;80(5):1581-1588.

154. Mitzner W, Blosser S, Yager D, Wagner E. Effect of bronchial smooth muscle contraction on lung compliance. J Appl Physiol 1992;72(1):158-167.

155. Jeffery PK. Morphology of the airway wall in asthma and in chronic obstructive pulmonary disease. Am Rev Respir Dis 1991;143(5 Pt 1):1152-1158; discussion 1161.

156. Carroll N, Elliot J, Morton A, James A. The structure of large and small airways in nonfatal and fatal asthma. Am Rev Respir Dis 1993;147:405-410.
157. Ebina M, Takahashi T, Chiba T, Motomiya M. Cellular hypertrophy and hyperplasia of airway smooth muscles underlying bronchial asthma. A 3-D morphometric study. Am Rev Respir Dis 1993;148(3):720-726.
158. Thomson RJ, Bramley AM, Schellenberg RR. Airway muscle sterology: implications for increased shortening in asthma. Am J Respir Crit Care Med 1996;154:749-757.
159. Bonikos DS, Bensch KG, Northway WH, Edwards DK. Bronchopulmonary dysplasia: the pulmonary pathologic sequel of necrotizing bronchiolitis and pulmonary fibrosis. Hum Pathol 1976;7(6):643-666.
160. Stocker JT. Pathologic features of long-standing "healed" bronchopulmonary dysplasia: a study of 28 3- to 40-month-old infants. Hum Pathol 1986;17(9):943-961.
161. Margraf LR, Tomashefski JF, Bruce MC, Dahms BB. Morphometric analysis of the lung in bronchopulmonary dysplasia. Am Rev Respir Dis 1991;143:391-400.
162. de Jongste JC, Mons H, Bonta IL, Kerrebijn KF. Human asthmatic airways responses in vitro. Eur J Respir Dis 1987;71:23-29.
163. Bai TR. Abnormalities in airway smooth muscle in fatal asthma. Am Rev Respir Dis 1990;141:552-557.
164. Bramley AM, Thomson RJ, Roberts CR, Schellenberg RR. Hypothesis: excessive bronchoconstriction in asthma is due to decreased airway elastance. Eur Respir J 1994;7(2):337-341.
165. Solway J, Fredberg JJ. Perhaps airway smooth muscle dysfunction contributes to asthmatic bronchial hyperresponsiveness after all. Am J Respir Cell Mol Biol 1997;17:144-146.
166. Ishida K, Paré PD, Thomson RJ, Schellenberg RR. Increased in vitro responses of tracheal smooth muscle from hyperresponsive guinea pigs. J Appl Physiol 1990;68(4):1316-1320.
167. Fan T, Yang M, Halayko A, Mohapatra SS, Stephens NL. Airway responsiveness in two inbred strains of mouse disparate in IgE and IL-4 production. Am J Respir Cell Mol Biol 1997;17:156-163.
168. Downes H, Austin DR, Parks CM, Hirsman CA. Comparison of drug responses in vivo and in vitro in airways of dogs with and without airway hyperresponsiveness. J Pharmacol Exp Ther 1986;237(1):214-219.
169. de Jongste JC, Mons H, Block R, Bonta IL, Fredriksz AP, Kerrebijn KF. Increased in vitro histamine responses in human small airway smooth muscle from patients with chronic obstructive pulmonary disease. Am Rev Respir Dis 1987;135:549-553.
170. de Jongste JC, Mons H, Bonta IL, Kerrebijn KF. Relaxation responses of airway smooth muscle from subjects with and without chronic bronchitis and airflow limitation. Pulm Pharmacol 1989;2:75-79.
171. Nagai A, West WW, Paul JL, Thurlbeck WM. The National Institutes of Health Intermittent Positive-Pressure Breathing trial: pathology studies. I. Interrelationship between morphologic lesions. Am Rev Respir Dis 1985;132(5):937-945.
172. Thurlbeck WM, Pun R, Toth J, Frazer RG. Bronchial cartilage in chronic obstructive lung disease. Am Rev Respir Dis 1974;109:73-80.
173. Rains JK, Bert JL, Roberts CR, Paré PD. Mechanical properties of human tracheal cartilage. J Appl Physiol 1992;72(1):219-225.
174. Roberts CR, Paré PD. Composition changes in human tracheal cartilage in growth and aging, including changes in proteoglycan structure. Am J Physiol 1991;261(2 Pt 1):92-101.
175. McCormack GS, Moreno RH, Hogg JC, Paré PD. Lung mechanics in papain-treated rabbits. J Appl Physiol 1986;60(1):242-246.
176. Moreno RH, McCormack GS, Brendan J, Mullen M, Hogg JC, Bert J, Paré PD. Effect of intravenous papain on tracheal pressure-volume curves in rabbits. J Appl Physiol 1986;60(1):247-252.
177. Moreno RH, Paré PD. Intravenous papain-induced cartilage softening decreases preload of tracheal smooth muscle. J Appl Physiol 1989;66(4):1694-1698.
178. Jiang H, Stephens NL. Contractile properties of bronchial smooth muscle with and without cartilage. J Appl Physiol 1990;69(1):120-126.

179. Robinson P, Okazawa M, Bai T, Paré P. In vivo loads on airway smooth muscle: the role of noncontractile airway structures. Can J Physiol Pharmacol 1992;70(4):602-606.

180. Nagase T, Matsui H, Sudo E, Matsuse T, Ludwig MS, Fukuchi Y. Effects of lung volume on airway resistance during induced constriction in papain-treated rabbits. J Appl Physiol 1996;80(6):1872-1879.

181. Maisel JC, Silvers GW, Mitchell RS, Petty TL. Bronchial atrophy and dynamic expiratory collapse. Am Rev Respir Dis 1968;98:988-997.

182. Nagai A, Thurlbeck WM, Konno K. Responsiveness and variability of airflow obstruction in chronic obstructive pulmonary disease. Am J Respir Crit Care Med 1995;151:635-639.

183. Tandon MK, Cambell AH. Bronchial cartilage in chronic bronchitis. Thorax 1969;24:607-612.

184. Burnard ED, Grattan-Smith P, Picton-Warlow CG, Grauaug A. Pulmonary insuffiency in prematurity. Australian Paediatr J 1965;1(12):12-38.

185. McCubbin M, Frey EE, Wagener JS, Tribby R, Smith WL. Large airway collapse in bronchopulmonary dysplasia. J Pediatr 1989;114(2):304-307.

186. Freedman BJ. The functional geometry of the bronchi. Bull Physio-path resp 1972;8:545-551.

187. Lambert RK, Wilson TA, Hyatt RE, Rodarte JR. A computational model for expiratory flow. J Appl Physiol 1982;52(1):44-56.

188. Wiggs BR, Moreno R, Hogg JC, Hilliam C, Paré PD. A model of the mechanics of airway narrowing. J Appl Physiol 1990;69(3):849-860.

189. Lambert RK, Baile EM, Moreno R, Bert J, Paré PD. A method for estimating the Young's modulus of complete tracheal cartilage rings. J Appl Physiol 1991;70(3):1152-1159.

190. Wiggs BR, Bosken C, Paré PD, James A, Hogg JC. A model of airway narrowing in asthma and in chronic obstructive pulmonary disease. Am Rev Respir Dis 1992;145:1251-1258.

191. Lambert RK, Codd SL, Pack RJ, Alley MR. Mucosal folding in sheep bronchi is related to submucosal thickening and to airway narrowing. Eur Respir J 1992;5(suppl 15):255s.

192. Okazawa M, Vedal S, Verburgt L, Lambert RK, Paré PD. Determinants of airway smooth muscle shortening in excised canine lobes. J Appl Physiol 1995;78(2):608-614.

193. Tomashefski JF, Bruce M, Goldberg HI, Dearborn DG. Regional distribution of macroscopic lung disease in cystic fibrosis. Am Rev Respir Dis 1986;133(4):535- 540.

194. Sobonya RE, Taussig LM. Quantitative aspects of lung pathology in cystic fibrosis. Am Rev Respir Dis 1986;134(2):290-295.

195. Hislop AA, Haworth SG. Airway size and structure in the normal fetal and infant lung and the effect of premature delivery and artificial ventilation. Am Rev Respir Dis 1989;140(6):1717-1726.

196. Hislop AA, Haworth SG. Pulmonary vascular damage and the development of cor pulmonale following hyaline membrane disease. Pediatr Pulmonol 1990;9(3):152- 161.

197. Macklem PT. A theoretical analysis of the effect of airway smooth muscle load on airway narrowing. Am J Respir Crit Care Med 1996;153(1):83-89.

198. Hughes JM, Hoppin FG, Jr., Mead J. Effect of lung inflation on bronchial length and diameter in excised lungs. J Appl Physiol 1972;32(1):25-35.

199. McNamara AE, Muller NL, Okazawa M, Arntorp J, Wiggs BR, Paré PD. Airway narrowing in excised canine lungs measured by high-resolution computed tomography. J Appl Physiol 1992;73(1):307-316.

200. Ding DJ, Martin JG, Macklem PT. Effects of lung volume on maximal methacholine-induced bronchoconstriction in normal humans. J Appl Physiol 1987;62(3):1324-1330.

201. Marshall R, Holden WS. Changes in calibre of the smaller airways in man. Thorax 1963;18:54-58.

202. Tisi GM, Minh VD, Friedman PJ. In vivo dimensional response of airways of different size to transpulmonary pressure. J Appl Physiol 1975;39(1):23-29.

203. Clay TP, Hughes JM, Jones HA. Relationship between intrapulmonary airway diameter and smooth muscle tone in excised lungs. J Physiol (Lond) 1977;273(2):355-365.

204. Hahn HL, Graf PD, Nadel JA. Effect of vagal tone on airway diameters and on lung volume in anesthetized dogs. J Appl Physiol 1976;41(4):581-589.

205. Hahn HL, Watson A, Wilson AG, Pride NB. Influence of bronchomotor tone on airway dimensions and resistance in excised dog lungs. J Appl Physiol 1980;49(2):270-278.
206. Fredberg JJ, Jones KA, Nathan M, Raboudi S, Prakash YS, Shore SA, Butler JP, Sieck GC. Friction in airway smooth muscle: mechanism, latch, and implications in asthma. J Appl Physiol 1996;81(6):2703-2712.
207. Inouye DS, Fredberg JJ. Is airway smooth muscle length set by a static force equilibrium. Am J Respir Crit Care Med 1997;155:A544.
208. Shen X, Wu MF, Tepper RS, Gunst SJ. Mechanisms for the mechanical response of airway smooth muscle to length oscillation. J Appl Physiol 1997;83:731-738.
209. Fish JE, Ankin MG, Kelly JF, Peterman VI. Regulation of bronchomotor tone by lung inflation in asthmatic and nonasthmatic subjects. J Appl Physiol 1981;50(5):1079-1086.
210. Skloot G, Permutt S, Togias A. Airway hyperresponsiveness in asthma: a problem of limited smooth muscle relaxation with inspiration. J Clin Invest 1995;96(5):2393-2403.
211. Nadel JA, Tierney DF. Effect of a previous deep inspiration on airway resistance in man. J Appl Physiol 1961;16(4):717-719.
212. Fairshter RD. Airway hysteresis in normal subjects and individuals with chronic airflow obstruction. J Appl Physiol 1985;58(5):1505-1510.
213. Burns CB, Taylor WR, Ingram RH, Jr. Effects of deep inhalation in asthma: relative airway and parenchymal hysteresis. J Appl Physiol 1985;59(5):1590-1596.
214. Ingram RH, Jr. Deep breaths and airway obstruction in asthma. Trans Am Clin Climatol Assoc 1986;98:80-85.
215. Wheatley JR, Paré PD, Engel LA. Reversibility of induced bronchoconstriction by deep inspiration in asthmatic and normal subjects. Eur Respir J 1989;2(4):331-339.
216. Pliss LB, Ingenito EP, Ingram RH, Jr. Responsiveness, inflammation, and effects of deep breaths on obstruction in mild asthma. J Appl Physiol 1989;66(5):2298-2304.
217. Pellegrino R, Wilson O, Jenouri G, Rodarte JR. Lung mechanics during induced bronchoconstriction. J Appl Physiol 1996;81(2):964-975.
218. Brown RH, Croisille P, Permutt S, Diemer F, Mudge B, Togias A. Airway dilation with lung inflation measured by HRCT. Am J Respir Crit Care Med 1997;155:A544.
219. Lim TK, Pride NB, Ingram RH, Jr. Effects of volume history during spontaneous and acutely induced air-flow obstruction in asthma. Am Rev Respir Dis 1987;135(3):591-596.
220. Lim TK, Ang SM, Rossing TH, Ingenito EP, Ingram RH, Jr. The effects of deep inhalation on maximal expiratory flow during intensive treatment of spontaneous asthmatic episodes. Am Rev Respir Dis 1989;140(2):340-343.
221. Willems LNA, Kamps JA, Stijnen T, Sterk PJ, Weening JJ, Dijkman JH. Relation between small airways disease and parenchymal destruction in surgical specimens. Thorax 1990;45:89-94.
222. Saetta M, Kim WD, Izquierdo JL, Ghezzo H, Cosio MG. Extent of centrilobular and panacinar emphysema in smokers' lungs: pathological and mechanical implications. Eur Respir J 1994;7(4):664-671.
223. Gould GA, Redpath AT, Ryan M, Warren PM, Best JJ, Cameron EJ, MacNee W. Parenchymal emphysema measured by CT lung density correlates with lung function in patients with bullous disease. Eur Respir J 1993;6(5):698-704.
224. Lamb D, McLean A, Gillooly M, Warren PM, Gould GA, MacNee W. Relation between distal airspace size, bronchiolar attachments, and lung function [see comments]. Thorax 1993;48(10):1012-1017.
225. Petty TL, Silvers GW, Stanford RE. Mild emphysema is associated with reduced elastic recoil and increased lung size but not with air-flow limitation. Am Rev Respir Dis 1987;136(4):867-871.
226. Gugger M, Gould G, Sudlow MF, Wraith PK, MacNee W. Extent of pulmonary emphysema in man and its relation to the loss of elastic recoil. Clin Sci (Colch) 1991;80(4):353-358.

227. Cheung D, Schot R, Zwinderman AH, Zagers H, Dijkman JH, Sterk PJ. Relationship between loss in parenchymal elastic recoil pressure and maximal airway narrowing in subjects with alpha1-antitrypsin deficiency. Am J Respir Crit Care Med 1997;155(1):135-140.

228. Hislop AA, Wigglesworth JS, Desai R, Aber V. The effects of preterm delivery and mechanical ventilation on human lung growth. Early Hum Dev 1987;15(3):147-164.

229. Erickson AM, de la Monte SM, Moore GW, Hutchins GM. The progression of morphologic changes in bronchopulmonary dysplasia. Am J Pathol 1987;127(3):474-484.

230. Mitchell I, Corey M, Woenne R, Krastins IRB, Levison H. Bronchial hyperreactivity in cystic fibrosis and asthma. J Pediatr 1978;93:744-748.

231. Beardsmore CS, Bar-Yishay E, Maayan C, Yahav Y, Katznelson D, Godfrey S. Lung function in infants with cystic fibrosis. Thorax 1988;43(7):545-551.

232. Tepper RS, Morgan WJ, Cota K, Taussig LM. Expiratory flow limitation in infants with bronchopulmonary dysplasia. J Pediatr 1986;109(6):1040-1046.

233. Mallory GB, Jr., Chaney H, Mutich RL, Motoyama EK. Longitudinal changes in lung function during the first three years of premature infants with moderate to severe bronchopulmonary dysplasia. Pediatr Pulmonol 1991;11(1):8-14.

234. Cano A, Payo F. Lung function and airway responsiveness in children and adolescents after hyaline membrane disease: a matched cohort study. Eur Respir J 1997;10:880-885.

235. Mead J, Turner JM, Macklem PT, Little JB. Significance of the relationship between lung recoil and maximum expiratory flow. J Appl Physiol 1967;22(1):95- 108.

236. Dawson SV, Elliott EA. Wave-speed limitation on expiratory flow-a unifying concept. J Appl Physiol 1977;43(3):498-515.

237. Hogg JC, Macklem PT, Thurlbeck WM, Path MC. Site and nature of airway obstruction in chronic obstructive lung disease. New Engl J Med 1968;278:1355- 1360.

238. Yanai M, Sekizawa K, Ohrui T, Sasaki H, Takishima T. Site of airway obstruction in pulmonary disease: direct measurement of intrabronchial pressure. J Appl Physiol 1992;72(3):1016-1023.

239. Hyatt RE, Wilson TA, Bar-Yishay E. Prediction of maximal expiratory flow in excised human lungs. J Appl Physiol 1980;48(6):991-998.

240. Pedersen OF, Brackel HJL, Bogaard JM, Kerrebijn KF. Flow limitation and airway compliance in central airways of normals and asthmatics during huff-manoeuvres. Am J Respir Crit Care Med 1995;151(4):A118.

241. Mink SN. Mechanism of reduced maximum expiratory flow in methacholine- induced bronchoconstriction in dogs. J Appl Physiol 1983;55(3):897-912.

242. Gelb AF, Schein M, Kuei J, Tashkin DP, Muller NL, Hogg JC, Epstein JD, Zamel N. Limited contribution of emphysema in advanced chronic obstructive pulmonary disease [see comments]. Am Rev Respir Dis 1993;147(5):1157-1161.

243. Gillooly M, Lamb D. Microscopic emphysema in relation to age and smoking habit. Thorax 1993;48(5):491-495.

244. Saetta M, Shiner RJ, Angus GE, Kim WD, Wang NS, King M, Ghezzo H, Cosio MG. Destructive index: a measurement of lung parenchymal destruction in smokers. Am Rev Respir Dis 1985;131(5):764-769.

245. Finkelstein R, Ma HD, Ghezzo H, Whittaker K, Fraser RS, Cosio MG. Morphometry of small airways in smokers and its relationship to emphysema type and hyperresponsiveness. Am J Respir Crit Care Med 1995;152(1):267-276.

246. Zapletal A, Desmond KJ, Demizio D, Coates AL. Lung recoil and the determination of airflow limitation in cystic fibrosis and asthma. Pediatr Pulmonol 1993;15:13-18.

247. Colebatch HJ, Finucane KE, Smith MM. Pulmonary conductance and elastic recoil relationships in asthma and emphysema. J Appl Physiol 1973;34(2):143- 153.

248. Sterk PJ, Fabbri LM, Quanjer PH, Cockroft DW, O'Byrne PM, Anderson SD, Juniper EF, Malo JL. Airway responsiveness. Standardized challenge testing with pharmacological, physical and sensitizing stimuli in adults. Eur Respir J 1993;6(Suppl. 16):53-83.
249. Sterk PJ. The determinants of the severity of acute airway narrowing in asthma and COPD. Respir Med 1992;86:391-396.
250. Peat JK, Salome CM, Woolcock AJ. Factors associated with bronchial hyperresponsiveness in Australian adults and children [see comments]. Eur Respir J 1992;5(8):921-929.
251. Popp W, Bock A, Herkner K, Wagner C, Zwick H, Sertl K. Factors contributing to the occurrence and predictability of bronchial hyperresponsiveness to methacholine in children. J Allergy Clin Immunol 1994;93(4):735-742.
252. Kolnaar BGM, Folgering H, van den Hoogen HJM, van Weel C. Asymptomatic bronchial hyperresponsiveness in adolescents and young adults. Eur Respir J 1997;10:44-50.
253. Britton J, Pavord I, Richards K, Knox A, Wisniewski A, Wahedna I, Kinnear W, Tattersfield A, Weiss S. Factors influencing the occurrence of airway hyperreactivity in the general population: the importance of atopy and airway calibre. Eur Respir J 1994;7(5):881-887.
254. Bourbeau J, Delfino R, Ernst P. Tracheal size is a determinant of the bronchoconstrictive response to inhaled methacholine. Eur Respir J 1993;6(7):991-995.
255. Kanner RE, Connett JE, Altose MD, Buist AS, Lee WW, Tashkin DP, Wise RA. Gender difference in airway hyperresponsiveness in smokers with mild COPD. The Lung Health Study. Am J Respir Crit Care Med 1994;150(4):956-961.
256. Laprise C. Asymptomatic airway hyperresponsiveness: a three-year follow-up. Am J Respir Crit Care Med 1997;156:403-409.
257. Eggleston PA, Rosenstein BJ, Stackhouse CM, Alexander MF. Airway hyperreactivity in cystic fibrosis. Chest 1988;94:360-365.
258. Backer V, Ulrik CS, Hansen KK, Laursen EM, Dirksen A, Bach-Mortensen N. Atopy and bronchial responsiveness in random population sample of 527 children and adolescents. Ann Allergy 1992;69(2):116-122.
259. Bahous J, Cartier A, Ouimet G, Pineau L, Malo JL. Nonallergic bronchial hyperexcitability in chronic bronchitis. Am Rev Respir Dis 1984;129(2):216-220.
260. Yan K, Salome CM, Woolcock AJ. Prevalence and nature of bronchial hyperresponsiveness in subjects with chronic obstructive pulmonary disease. Am Rev Respir Dis 1985;132(1):25-29.
261. Mellis CM, Levison H. Bronchial reactivity in cystic fibrosis. Pediatrics 1978;61:446-450.
262. Tobin MJ, Maguire O, Tempany E, Fitzgerald MX. Atopy and bronchial reactivity in older patients with cystic fibrosis. Thorax 1980;35:807-813.
263. van Asperen P, Mellis CM, South RT, Simpson SJ. Bronchial reactivity in cystic fibrosis with normal pulmonary function. Am J Dis Child 1981;135:815-819.
264. Smyth JA, Tabachnik E, Duncan WJ, Reilly BJ, Levison H. Pulmonary function and bronchial hyperreactivity in long-term survivors of bronchopulmonary dysplasia. Pediatrics 1981;68:336-340.
265. Northway WH, Moss RB, Carlisle KB, Parker BR, Popp RL, Pitlick PT, Eichler I, Lamm R, Brown BW. Late pulmonary sequelea of bronchopulmonary dysplasia. New Engl J Med 1990;323:1793-1798.
266. Chung KF, Jeyasingh K, Snashall PD. Influence of airway calibre on the intrapulmonary dose and distribution of inhaled aerosol in normal and asthmatic subjects. Eur Respir J 1988;1(10):890-895.
267. Backer V, Mortensen J. Distribution of radioactive aerosol in the airways of children and adolescents with bronchial hyper-responsiveness. Clin Physiol 1992;12(5):575-585.
268. O' Riordan T, Walser L, Smaldone GC. Changing patterns of aerosol deposition during methacholine bronchoprovocation. Chest 1993;103(5):1385-1389.
269. Smaldone GC, Messina MS. Flow limitation, cough, and patterns of aerosol deposition in humans. J Appl Physiol 1985;59(2):515-520.

270. Laube BL, Links JM, LaFrance ND, Wagner HN, Jr., Rosenstein BJ. Homogeneity of bronchopulmonary distribution of 99mTc aerosol in normal subjects and in cystic fibrosis patients. Chest 1989;95(4):822-830.
271. Laube BL, Chang DY, Blask AN, Rosenstein BJ. Radioaerosol assessment of lung improvement in cystic fibrosis patients treated for acute pulmonary exacerbations. Chest 1992;101(5):1302-1308.
272. Kim CS, Eldridge MA, Garcia L, Wanner A. Aerosol deposition in the lung with asymmetric airways obstruction: in vivo observation. J Appl Physiol 1989;67(6):2579-2585.
273. Wanner A, Brodnan JM, Perez J, Henke KG, Kim CS. Variability of airway responsiveness to histamine aerosol in normal subjects. Role of deposition. Am Rev Respir Dis 1985;131(1):3-7.
274. Smaldone GC, Messina MS. Enhancement of particle deposition by flow-limiting segments in humans. J Appl Physiol 1985;59(2):509-514.
275. Tattersfield AE. Measurement of bronchial reactivity: a question of interpretation. Thorax 1981;36(8):561-565.
276. Merkus PJ, van Essen-Zandvliet EE, Kouwenberg JM, Duiverman EJ, Van Houwelingen HC, Kerrebijn KF, Quanjer PH. Large lungs after childhood asthma. A case-control study. Am Rev Respir Dis 1993;148(6 Pt 1):1484-1489.
277. Hanrahan JP, Tager IB, Segal MR, Tosteson TD, Castile RG, Van Vunakis H, Weiss ST, Speizer FE. The effect of maternal smoking during pregnancy on early infant lung function. Am Rev Respir Dis 1992;145(5):1129-1135.
278. Wang X, Wypij D, Gold DR, Speizer FE, Ware JH, Ferris BG, Jr., Dockery DW. A longitudinal study of the effects of parental smoking on pulmonary function in children 6-18 years. Am J Respir Crit Care Med 1994;149(6):1420-1425.
279. Corbo GM, Agabiti N, Forastiere F, Dell'Orco V, Pistelli R, Kriebel D, Pacifici R, Zuccaro P, Ciappi G, Perucci CA. Lung function in children and adolescents with occasional exposure to environmental tobacco smoke. Am J Respir Crit Care Med 1996;154(3 Pt 1):695-700.
280. James AL, Hogg JC, Dunn LA, Paré PD. The use of the internal perimeter to compare airway size and to calculate smooth muscle shortening. Am Rev Respir Dis 1988;138(1):136-139.
281. Gaultier C. Malnutrition and lung growth. Pediatr Pulmonol 1991;10(4):278-286.
282. Frank L. Antioxidants, nutrition, and bronchopulmonary dysplasia. Clin Perinatol 1992;19(3):541-562.
283. Collins MH, Moessinger AC, Kleinerman J, Bassi J, Rosso P, Collins AM, James LS, Blanc WA. Fetal lung hypoplasia associated with maternal smoking: a morphometric analysis. Pediatr Res 1985;19(4):408-412.
284. Kurzner SI, Garg M, Bautista DB, Sargent CW, Bowman M, Keens TG. Growth failure in bronchopulmonary dysplasia: elevated metabolic rates and pulmonary mechanics. J Pediatr 1988;112:73-80.
285. Mischler EH, Marcus MS, Sondel SA, Laxova A, Carey P, Langhough R, Farrell PM. Nutritional assessment of infants with cystic fibrosis diagnosed through screening. Pediatr Pulmonol Suppl 1991;7:56-63.
286. Bronstein MN, Sokol RJ, Abman SH, Chatfield BA, Hammond KB, Hambidge KM, Stall CD, Accurso FJ. Pancreatic insufficiency, growth, and nutrition in infants identified by newborn screening as having cystic fibrosis. J Pediatr 1992;120(4 Pt 1):533-540.
287. Corey M, McLaughlin FJ, Williams M, Levison H. A comparison of survival, growth, and pulmonary function in patients with cystic fibrosis in Boston and Toronto. J Clin Epidemiol 1988;41(6):583-591.
288. Merkus PJ, ten Have-Opbroek AA, Quanjer PH. Human lung growth: a review. Pediatr Pulmonol 1996;21(6):383-397.
289. Chetta A, Foresi A, Del Donno M, Consigli GF, Bertorelli G, Pesci A, Barbee RA, Olivieri D. Bronchial responsiveness to distilled water and methacholine and its relationship to inflammation and remodeling of the airways in asthma. Am J Respir Crit Care Med 1996;153(3):910-917.

290. Blosser S, Mitzner W, Wagner EM. Effects of increased bronchial blood flow on airway morphometry, resistance, and reactivity. J Appl Physiol 1994;76(4):1624- 1629.

291. Hershenson MB, Aghili S, Punjabi N, Hernandez C, Ray DW, Garland A, Glagov S, Solway J. Hyperoxia-induced airway hyperresponsiveness and remodeling in immature rats [published erratum appears in Am J Physiol 1993 Aug;265(2 Pt 1):section L following table of contents]. Am J Physiol 1992;262(3 Pt 1):L263-269.

292. Lozewicz S, Wells C, Gomez E, Ferguson H, Richman P, Devalia J, Davies RJ. Morphological integrity of the bronchial epithelium in mild asthma. Thorax 1990;45(1):12-15.

293. Ilowite JS, Bennett WD, Sheetz MS, Groth ML, Nierman DM. Permeability of the bronchial mucosa to 99mTc-DTPA in asthma. Am Rev Respir Dis 1989;139(5):1139-1143.

294. Barrowcliffe MP, Jones JG, Agnew JE, Francis RA, Clarke SW. The relative permeabilities of human conducting and terminal airways to 99mTcDTPA. Eur J Respir Dis 1987;71(Suppl. 153):68-77.

295. Pavlovic D, Fournier M, Aubier M, Pariente R. Epithelial vs. serosal stimulation of tracheal muscle: role of epithelium. J Appl Physiol 1989;67(6):2522-2526.

296. Jongejan R, De Jongste J, Raatgeep R, Stijnen T, Bonta I, Kerrebijn K. Effect of epithelial denudation, inflammatory mediators and mast cell activation on the sensitivity of isolated human airways to methacholine. Eur J Pharmacol 1991;203(2):187-194.

297. Koga Y, Satoh S, Sodeyama N, Hashimoto Y, Yanagisawa T, Hirshman CA. Role of cholinesterase in airway epithelium mediated inhibition of acetylcholine induced contraction of guinea-pig isolated trachea. Eur J Pharmacol 1992;220:141-146.

298. Hulsmann AR, Raatgeep HR, Den Hollander JC, Stijnen T, Saxena PR, Kerrebijn KF, De Jongste JC. Oxidative epithelial damage produces hyperresponsiveness of human peripheral airways. Am J Respir Crit Care Med 1994;149:519-525.

299. Paré PD, Bai TR. Airway remodelling in chronic obstructive pulmonary disease. Eur Respir J 1996;6:259-263.

300. Hamid Q, Song Y, Kotsimbos TC, Minshell E, Bai TR, Hegele RG, Hogg JC. Inflammation of small airways in asthma. J Allergy Clin Immunol 1997;100:44-51.

301. Wenzel SE, Szefler SJ, Donald YM, Sloan SI, Rex MD, Martin RJ. Bronchoscopic evaluation of severe asthma. Am J Respir Crit Care Med 1997;156:737-743.

302. Kraft M, Djukanovic R, Wilson S, Holgate ST, Martin RJ. Alveolar tissue inflammation in asthma. Am J Respir Crit Care Med 1996;154:1505-1510.

303. Okazawa M, Müller N, McNamara AE, Child S, Verburgt J, Paré PD. Human airway narrowing measured using high definition computed tomography. Am J Respir Crit Care Med 1996;154:1557-1562.

304. Riess A, Wiggs B, Verburgt L, Wright JL, Hogg JC, Paré PD. Morphologic determinants of airway responsiveness in chronic smokers. Am J Respir Crit Care Med 1996;154:1444-1449.

Cartilaginous Airway Dimensions and Airflow Obstruction in Human Lungs

Harm A.W.M. Tiddens, Peter D. Paré , Jimm C. Hogg, Wim C.J. Hop, Rodney K. Lambert and Johan C. de Jongste.

Department of Pediatrics, Division Respiratory Medicine and Department of Biostatistics, Erasmus University and University Hospital/Sophia Children's Hospital, Rotterdam, the Netherlands.
Respiratory Health Network of Centres of Excellence, St.Paul's Hospital Pulmonary Research Laboratory, University of British Columbia, Vancouver, Canada.
Department of Physics, Massey University, Palmerston North, New Zealand.

Introduction

Increased airflow obstruction in chronic obstructive pulmonary disease (COPD) is caused by a combination of loss of lung elasticity and increased airway resistance. The mechanism of the increased airway resistance is still unclear. Inflammatory changes in the membranous airways correlate with the degree of airflow obstruction in patients with COPD[1-3]. Both the obstruction and membranous airway inflammation are associated with increased thickness of the airway wall and the smooth muscle layer[4,5]. A similar but more striking increase in airway wall thickness has been reported in the membranous and cartilaginous airways of asthmatic patients and these changes may have a profound effect on the airway narrowing that occurs during airway smooth muscle shortening[6-8]. There have been no systematic studies of lung function in relation to changes in large airway dimensions in patients with COPD. To examine whether such changes have any measurable effect on airflow obstruction, we measured the dimensions of airways from excised lobes of patients with COPD and tested the hypothesis that the thickness of the wall and the amount of bronchial smooth muscle in cartilaginous airways are related to pre-operatively measured estimates of airflow obstruction in these patients. The impact of different airway wall dimensions on airway resistance was checked in a mathematical lung model, and results were compared with lung function measurements.

Methods

Study Population

Lung tissue was obtained from 72 patients who had a lobar resection or pneumonectomy for a solitary peripheral lung lesion. We did not include patients in whom segmental or larger airways were found to be obstructed during bronchoscopy or at pathological examination or patients who showed evidence of obstructive pneumonitis. Furthermore, patients who had a history consistent with a diagnosis of asthma were excluded[9]. Informed consent was obtained in all cases. Sixty-four of the 72 patients proved to have a diagnosis of bronchogenic carcinoma. Carcinoid tumour, hamar-

toma, or granuloma were the final diagnoses in the remaining patients. These patients were mostly smokers and were classified as "COPD" although one-third had a lung function within the normal range and, therefore, did not strictly fulfil the ATS criteria[9].The clinical data for the patients in this study are summarized in Table 1.

Table 1

STUDY POPULATION CHARACTERISTICS

Age, years	61 ± 9.5 (37-83)
Sex, male:female	54:18
Pack years†	54.7 ± 34.5 (0.4-180)
Current smokers, n	45
Life long nonsmokers, n	2
Lung or lobe resected, right side, n	50
Lung or lobe resected, left side, n	22

†Pack years = number of years smoking 1 pack of cigarettes a day; n = number. Age and pack years are expressed as mean ± standard deviation and range.

Lung Function Studies

Lung function tests were done within the week before surgery using a volume displacement pressure-compensated body plethysmograph. Volume was measured with a Krogh spirometer coupled to a linear displacement transducer (Shaevitz Engineering, Pennsauken, N J). Flow was measured with a Fleisch No. 3 pneumotachometer coupled to a Sanborn 270 differential pressure transducer (Sanborn Co., Waltham, MA). Functional residual capacity (FRC) was determined using Boyle's law technique, and residual volume (RV) and total lung volume (TLC) were calculated. Forced expiratory volume in 1s (FEV_1), forced vital capacity (FVC), and maximal flows at 50% ($Vmax_{50}$) and 25% ($Vmax_{25}$) of FVC were calculated from digitized flow and volume signals obtained during forced expiratory manoeuvres. At least 3 expiratory efforts were performed, and the forced expiratory manoeuvre with the largest sum of FEV_1 and FVC was selected. Values were expressed as a percentage of the predicted

values according to the prediction formulae of Morris and coworkers (VC, FVC, FEV_1)[10], Bates and coworkers (FRC)[11], Goldman and coworkers (RV)[12], and Dosman and coworkers ($Vmax_{50}$, $Vmax_{25}$)[13]. As an indicator of the severity of airflow obstruction, we used the FEV_1 expressed as a percentage of FVC. To measure bronchial responsiveness, methacholine challenge was performed in 40 of the 72 subjects using the tidal breathing method of Cockroft and coworkers[14]. PC_{20} was calculated from the dose response curve by linear interpolation, as the concentration of methacholine that caused a 20% fall in FEV_1. A maximal concentration of 16 mg/ml methacholine was used. Reversibility of bronchial obstruction was expressed as the absolute change in FEV_1 as a percentage of the predicted FEV_1 ($DFEV_1$%pred)[15] and as a percentage of the actual pre-bronchodilator FEV_1($DFEV_1$%ini) 15 min after inhalation of 0.2 mg salbutamol.

Morphological Studies

Surgically resected specimens were inflated with either 10% formalin or 2% glutaraldehyde at a pressure of 25 cm H_2O and submerged in fixative for at least 24 h. The fixed specimens were then sliced serially at 1 cm intervals in a sagittal plane. Three to six intrapulmonary cartilaginous airways that were cut in cross section were randomly selected from each specimen for morphometric analysis. Tissue blocks containing cartilaginous airways in cross section were decalcified, embedded in paraffin, transversely cut at 5 micron thickness and stained with haematoxylin and eosin and with Masson's trichrome. Additionally, five lung tissue blocks were obtained in a stratified random fashion from a parasagittal slice for morphologic grading of membranous and respiratory bronchioles. The blocks were embedded in paraffin, and 5 micron sections were cut and stained with haematoxylin and eosin, periodic acid Schiff, and Masson's trichrome.

Measurement of Airway Dimensions

Sections from cartilaginous airways that did not show bifurcation or disruption of the wall were selected for measurement. Airway dimensions were measured on the haematoxylin and eosin stained sections using a microscope fitted with a camera

lucida that superimposed the cursorlight of a digitizing board on the microscope image of the airway. Airways that were too large to be viewed entirely using a microscope were projected with a slide projector, their images were traced onto paper, and the tracings were measured on the digitizing board. The measurements that were made are shown in Figure 1, and including basement membrane perimeter (P_{bm}) and the area of the lumen (and epithelium) contained within the light microscopic image of the basement membrane (A_{bm}); the outer muscle perimeter (P_{mo}), traced at the outer edge of the smooth muscle layer and the enclosed area (A_{mo}); the outer perimeter (P_o); and the outer area (A_o) defined by the outer edge of the adventitial tissue.

Basement membrane perimeter P_{bm}
➡ Basement membrane area A_{bm}

Outer muscle perimeter P_{mo}
➡ Internal area A_{mo}

Outer perimeter P_o
➡ Outer area A_o

Smooth muscle area WA_m

Cartilage area WA_{cart}

Inner wall area WA_i ($= A_{mo}-A_{bm}$)

Total wall area WA_t ($= A_o-A_{bm}$)
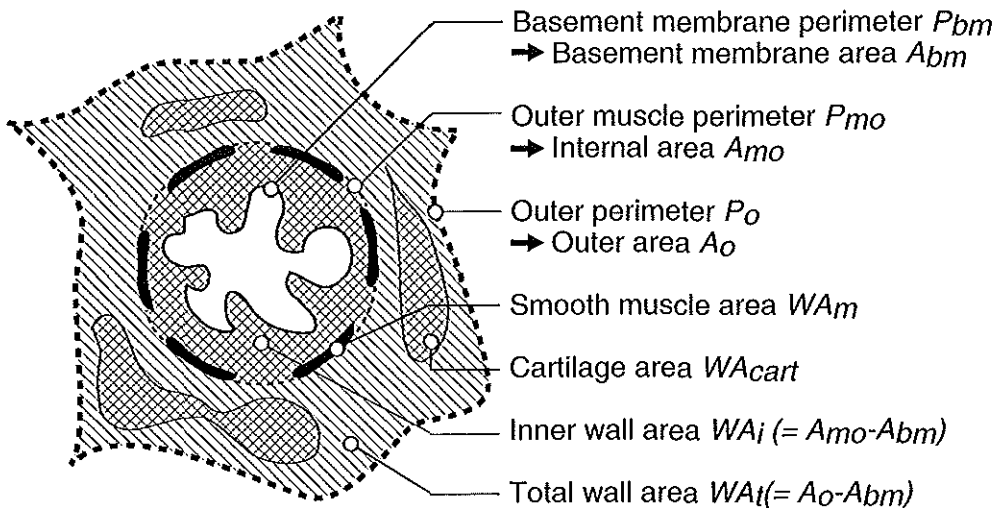
Figure 1. Diagram of measured airway dimensions.

From these measurements we calculated the inner wall area ($WA_i = A_{mo}-A_{bm}$), and the outer wall area ($WA_o = A_o-A_{mo}$). The nomenclature used is according to the recently published communication concerning subdivisions of the bronchial wall[16]. The area occupied by smooth muscle (WA_m) was measured using an automated image analysis system (Bioview, Infrascan, Vancouver, BC, Canada). An area of smooth muscle was selected on a trichrome stained section and colour thresholding was used to calculate automatically the area occupied by muscle. The operator was able to interact with the program to adjust the threshold so that all the muscle and only muscle

was included in the measurement. All measurements of airway dimensions were performed by the same observer (HT). Perimeters (P_{bm}, P_{mo}, P_o) were measured twice; if the difference between the measurements exceeded 10%, they were repeated until the difference between the repeated measurements was below 10%. Intra-observer variability was assessed by remeasurement on 10 randomly selected airways after an interval of 2 months. Inter-observer variability was assessed by remeasurement of 10 randomly selected airways by a second observer.

Measurement of Bronchiolar Inflammatory Changes
For each specimen 5 to 10 membranous and 5 to 10 respiratory bronchioles were graded using a modification of the pictorial grading method of Cosio and coworkers[1, 17]. The following indices were graded in the membranous bronchioles: inflammation, fibrosis, muscle hypertrophy, pigment deposition, goblet cell metaplasia, and squamous cell metaplasia. For each airway these six morphological indices were compared with pictorial reference standards with a score from 0 (normal) to 3 (most abnormal). Next the mean score for each morphological index for each individual specimen was calculated by summing the scores of the airways examined, divided by the number of airways examined. The average score for that variable was expressed as a percentage of maximal possible score. A total membranous airways disease score (MADS) for each specimen was then calculated by summing the mean scores of the six morphological indices (maximal score: 6 x 100 = 600). To calculate the respiratory airways disease score (RADS), a similar procedure was performed. The following indices were graded in the respiratory bronchioles: inflammation, fibrosis, muscle hypertrophy, pigment deposition, and intraluminal macrophages (maximal score: 5 x 100 = 500).

Statistical Analysis
The intra- and inter-observer variability of morphometric measurements were calculated by expressing the difference of the first and second measurement as a percentage of the average of both observations. This percentage difference was plotted against P_{bm} to detect systematic errors dependent on airway size.

Repeated measures analysis of variance (RMANOVA), which allows for differences between and within patients, was used to assess the relationships between airway wall dimensions (WA$_i$, WA$_o$, WA$_m$) and airway size (P$_{bm}$). The previous work of Bosken and coworkers and Kuwano and coworkers found linear relationships between the square root of airway wall dimensions and airway size. Square root transformation of the present data also gave regressions with approximately normal distributions of data around the regression lines. In the analysis the airway size values were centred by subtracting the mean value for P$_{bm}$ 14 mm from all values of P$_{bm}$. In a given patient the intercept of the regression line for a particular airway wall dimension as a function of P$_{bm}$ represents its value at a P$_{bm}$ of 14 mm. The intercept was investigated for its linear relation with various lung function parameters (FEV$_1$, FEV$_1$/FVC, Vmax$_{50}$, Vmax$_{25}$, PC$_{20}$, and DFEV$_1$%pred) and measures of inflammatory changes in membranous and cartilaginous airways (MADS, RADS) using an iterative search for optimal values[18, 19]. RMANOVA analyzes the patients as a continuum.We thus avoided the bias that would result from dividing patients into subgroups. The level of significance was set at $p = 0.05$ (two-sided). Data are expressed as mean ± standard deviation and range, unless indicated otherwise.

Computational Analysis of the Theoretical Significance of Altered Airway Dimensions for Airway Resistance

To predict the effect of airway dimensions on airway resistance, we used a computational model, as described by Wiggs and coworkers[20] and modified by Lambert and coworkers[21]. Briefly, the geometry of the bronchial tree in the model is a dichotomously branching network with 16 generations. The model is designed to examine the relative contributions of thickening of the WA$_i$, WA$_o$ and WA$_m$ to airway responsiveness. The dose-response relationship of airway resistance against an increasing dose of a hypothetical bronchoconstricting agent that causes smooth muscle shortening was calculated. In the model the airway smooth muscle in each generation of the tracheo-bronchial tree contracts in response to the agonist and shortens until the stress generated by the muscle at that length is maximal. The plateau of the dose-response curve is achieved when the muscle stress in all airway generations is maximal.

The model takes account of both the geometry and the mechanics of the airway and parenchymal tissue.

The airway wall dimensions used in the model of Lambert and coworkers[21] were derived from a study by Kuwano and coworkers[5] of membranous airways from patients with and without airflow obstruction, selected from the same data base as used in the present study[5]. To estimate airway wall dimensions of cartilaginous airways extrapolations were made from the data of the membranous airways. For membranous airways (P_{bm} 2-4.7 mm) we used the airway wall dimensions derived from the nonobstructed group of Kuwano and coworkers[5]. For cartilaginous airways (P_{bm} 4.7-58 mm) we used our own data. Since we used airway wall dimensions for membranous airways derived from patients without airflow obstruction and cartilaginous airway dimensions from patients with varying severity of airflow obstruction, we can selectively assess the importance of cartilaginous airway wall dimensions on airway resistance and responsiveness. The regression equations for $\sqrt{WA_i}$, $\sqrt{WA_o}$, and $\sqrt{WA_m}$ used in the computational model are shown in figure 2 (a, b and c). Baseline airway resistance and simulated dose response curves were calculated using the values for the relationship of $\sqrt{WA_i}$ vs P_{bm} as found among the patients in this study. From the simulated dose response curves we calculated the dose of agonist that caused a 10-fold increase in resistance (PD_{10}) as well as the maximal resistance achieved.

Results

Lung Function

Lung function characteristics are shown in Table 2. Twenty-four patients had no significant reduction of maximum expiratory airflow (FEV_1/FVC >75%), 21 patients had a mild reduction of maximum expiratory airflow (FEV_1/FVC 65 to 75%), and 27 patients had a severe reduction of maximum expiratory airflow (FEV_1/FVC < 65% predicted). Increased functional residual capacity (FRC > FRC[pred]+2SD) was present in 21/72 patients, increased residual volume (RV > RV[pred]+2SD) was present in 29/72 patients. Reversibility of bronchial obstruction, defined as $DFEV_1$%pred > 15% and $DFEV_1$%ini >15%, was present in 1 of 58 and five of 58 patients, respectively.

Bronchial hyperresponsiveness to methacholine ($PC_{20} < 16$ mg/ml) was found in 26 of the 40 patients (65%) who had a methacholine challenge.
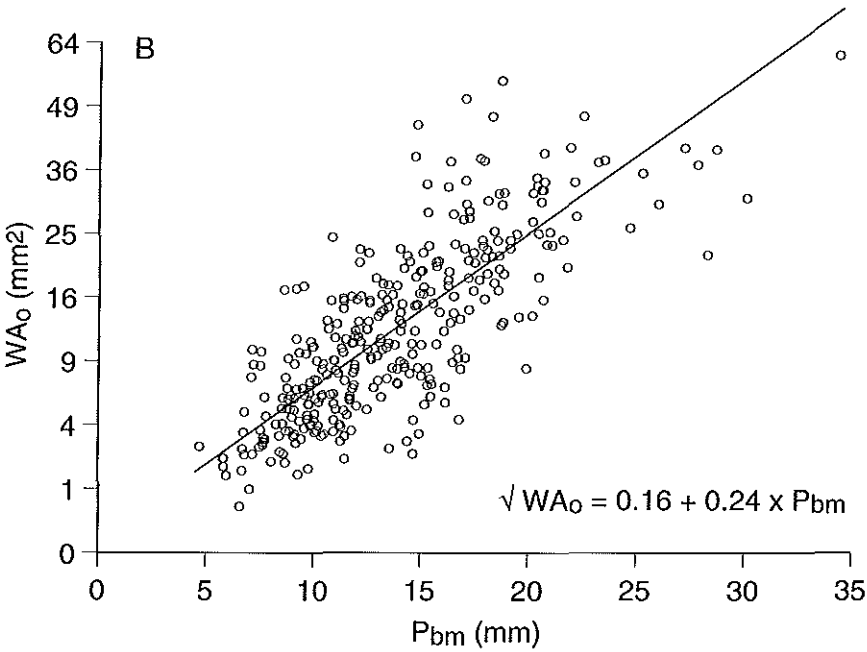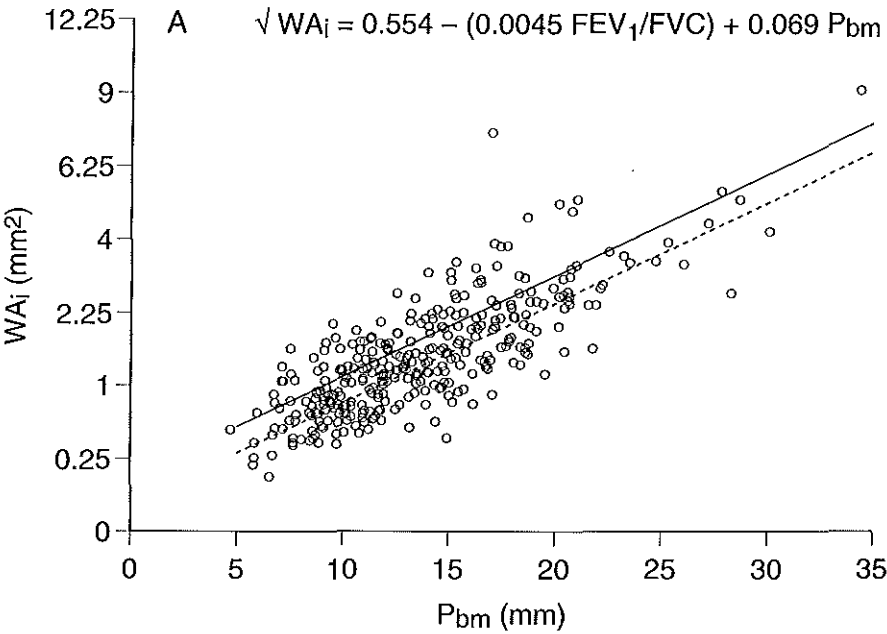
Morphologic Studies

Morphometric measurements were made on 341 cartilaginous airways from 72 patients (mean 4.7, range 3 to 7 airways per patient). The mean value of P_{bm} was 13.8 ± 4.7 (5 to 34) mm (Figure 3). This corresponds to a mean airway diameter of 4.4 ± 1.5 (1.5-10.9) mm, or airway generations 1 to 10 to 12 [22]. The intra-observer variability was $-0.7 \pm 3.4\%$ for P_{bm}, $0.8 \pm 1.7\%$ for P_{mo}, $-4.9 \pm 6.9\%$ for P_o, and $-0.1 \pm 30.1\%$ for WA_m. The inter-observer variability was $0.3 \pm 5.3\%$ for P_{bm}, $1.5 \pm 3.1\%$ for P_{mo}, $-14 \pm 6.6\%$ for P_o, and $24 \pm 44\%$ for WA_m. There was no systematic relationship between airway size (P_{bm}) and the intra- or inter-observer difference for any variable. Highly significant ($p < 0.001$) linear relations were found between airway size (P_{bm}) and airway wall dimensions ($\sqrt{WA_i}$, $\sqrt{WA_o}$, $\sqrt{WA_m}$) (Figure 2a, b, c).

Airway Wall Thickness and Lung Function

The levels and slopes of the regressions of $\sqrt{WA_o}$, and $\sqrt{WA_m}$ on P_{bm} were not related to any measures of lung function (FEV_1, FEV_1/FVC, $Vmax_{50}$, $Vmax_{25}$, PC_{20}, $DFEV_1\%$pred). The level of the $\sqrt{WA_i}$ on P_{bm} regression was significantly related to FEV_1/FVC ($p < 0.05$).

A decrease of 20% in FEV_1/FVC corresponds to a 32% increase in WA_i at a P_{bm} of 6 mm, a 16% increase at a P_{bm} of 15 mm, or a 10% increase at a P_{bm} of 25 mm. There was a trend ($p = 0.06$) towards an increase of the slope of the $\sqrt{WA_i}$ on P_{bm} regression as FEV_1/FVC decreased. Furthermore, the level of the $\sqrt{WA_i}$ on P_{bm} relationship was significantly influenced by $DFEV_1\%$pred ($p < 0.005$) but not by PC_{20}. An increase of 10% in $DFEV_1\%$pred corresponds to a 32% increase in WA_i at a P_{bm} of 6 mm, a 13% increase at a P_{bm} of 15 mm, and a 9% increase at a P_{bm} of 25 mm. Thus patients who showed a thicker inner airway wall area (WA_i) had more severe reduction of maximum expiratory airflow and an increased reversibility of airflow obstruction.
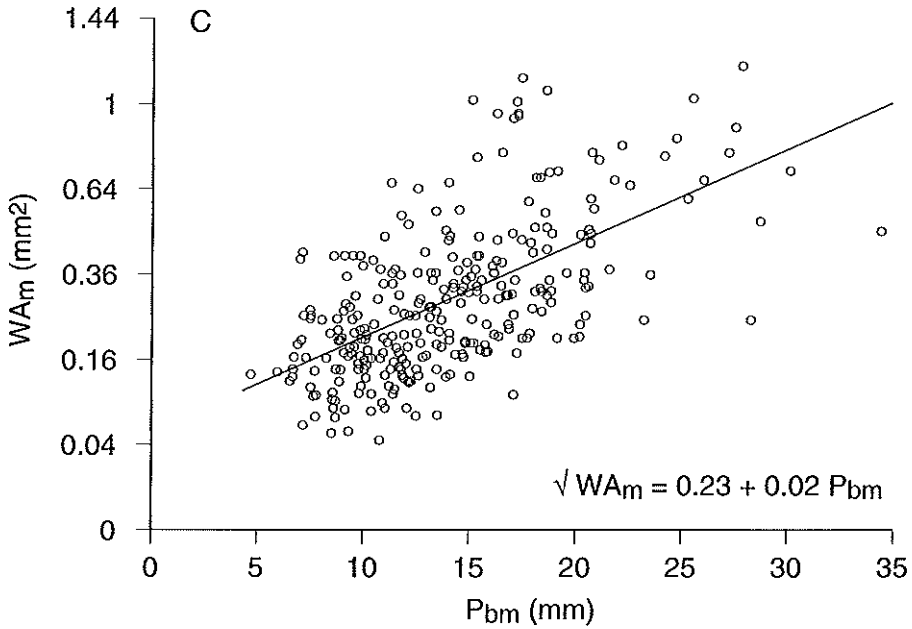
The equation shown on the plot: $\sqrt{WA_m} = 0.23 + 0.02\, P_{bm}$

Axes: $WA_m\ (mm^2)$ vertical; $P_{bm}\ (mm)$ horizontal.

Figure 2. Morphometric airway dimensions versus airway size. There are 341 datapoints from 72 patients plotted in the figure. Due to overlap of data points, some dots appear filled.

(A) WA_i = inner wall area. The dashed regression line represents the relation of WA_i versus P_{bm} for patients with a FEV_1/FVC of 80% and the solid regression line represents this relationship for a FEV_1/FVC of 40%.

(B) WA_o = outer wall area.

(C) WA_m = wall area occupied by smooth muscle. P_{bm} = perimeter basement membrane. Note the square root transformed vertical axes.

Airway Inflammatory Changes and Airway Dimensions

A wide range of values for the inflammatory scores was found in membranous and respiratory airways (Table 3). The mean MADS was 134 ± 47. Among the six parameters evaluated, fibrosis scored highest, followed by inflammation. The mean RADS was 111 ± 52. Scores for inflammation, muscle hypertrophy, pigmentation, and intraluminal macrophages were similar, whereas fibrosis scored much lower.

The levels and slopes of the regressions of $\sqrt{WA_o}$ and $\sqrt{WA_m}$ on P_{bm} were not significantly related to MADS or RADS. The level, but not the slope, of the regression of $\sqrt{WA_i}$ on P_{bm} was significantly related to the MADS (Table 4).

Table 2

LUNG FUNCTION CHARACTERISTICS

	No. Patients	Mean	Range	SD
TLC, % pred	72	109	81-154	15
FRC, % pred	72	123	70-177	24
RV, % pred	72	133	66-219	34
FEV_1, % pred	72	94	58-135	18
FVC, % pred	72	96	64-134	13
FEV_1/FVC, %	72	69	42- 89	9
$Vmax_{50}$, % pred	72	56	6-149	29
$Vmax_{25}$, % pred	72	40	7-108	23
$DFEV_1$ % pred	58	4	-11- 23	5
$DFEV_1$ % ini	58	5	-13- 32	7
Methacholine challenge				
no PC_{20} reached	14/40			
PC_{20}, mg/ml	26/40	2.4*	0.15-12.8	3.6

Definition of abbreviations:
TLC = total lung capacity; FRC = functional residual capacity; RV = residual volume, FEV_1 = forced expiratory volume in 1s; FVC = forced expiratory volume; FEV_1/FVC = forced expiratory volume in 1s as percentage of forced vital capacity; $Vmax_{50}$ = maximal flow at 50% of forced vital capacity; $Vmax_{25}$ = maximal flow at 25% forced vital capacity; $DFEV_1$%pred = change of FEV_1 after bronchodilatation as a percentage of predicted FEV_1; $DFEV_1$%ini = change of FEV_1 after bronchodilatation as a percentage of pre-bronchodilator FEV_1; PC_{20} = concentration of methacholine producing a 20% fall in FEV_1.
* = geometric mean.

Patients who had more severe inflammatory changes in the membranous airways had thicker inner airway walls in the cartilaginous airways. A difference in MADS of 100 corresponds to a 54% difference in WA_i at a P_{bm} of 6 mm, 24% at a P_{bm} of 15 mm, and 15% at a P_{bm} of 25 mm. Of the component scores making up the MADS, squamous

Table 3
MEMBRANOUS AIRWAY DISEASE SCORE (MADS)

Variables:	Mean	SD	Range
Inflammation	30	16	2-85
Fibrosis	35	20	0-82
Muscle hypertrophy	18	13	0-76
Pigment	22	20	0-96
Squamous cell metaplasia	19	13	0-58
Goblet cell metaplasia	10	11	0-57
MADS	134	47	14-296

RESPIRATORY AIRWAY DISEASE SCORE (RADS)

Variables:	Mean	SD	Range
Inflammation	24	149	0-52
Fibrosis	15	13	0-62
Muscle hypertrophy	26	17	0-82
Pigment	26	17	0-82
Intra luminal macrophages	22	17	0-78
RADS	112	55	9-260

Inflammatory changes in membranous and respiratory airways were graded using a pictorial grading method. Each variable in each airway is given a score ranging from 0 (normal) to 3 (highly abnormal). The sum of the scores for each variable in all the airways of each patient is expressed as a percentage of the maximal possible score. The membranous airways disease score (MADS) and the respiratory airways disease score (RADS) are the sum of the 6 or 5 mean scores for each individual. The average score for each variable, as well as the average MADS and RADS, are shown.

Table 4

INNER WALL AREA AS A FUNCTION OF AIRWAY SIZE AND
COVARIABLES

	p-value*
$\sqrt{WA_i} = 0.073*(P_{bm}-14) + (1.17 + (0.0084 * DFEV_1\%pred))$	0.01
$\sqrt{WA_i} = 0.071*(P_{bm}-14) + (1.01 + (0.0014 * MADS))$	0.005
$\sqrt{WA_i} = 0.069*(P_{bm}-14) + (1.52 - (0.0045 * FEV_1/FVC))$	0.05

Definition of abbreviations:
WA_i = inner wall area (mm^2); P_{bm} = perimeter basement membrane (mm); $DFEV_1$ % pred = change of FEV_1 after bronchodilation as a percentage of predicted FEV_1; MADS = membranous airways disease score; FEV_1/FVC = forced expiratory volume in 1s as percentage of forced vital capacity.
* p value for significance effect of covariable.

metaplasia followed by inflammation and fibrosis had the highest correlation with the level of the $\sqrt{WA_i}$ on P_{bm} regression.

Computational Analysis of the Functional Significance of Altered Airway Dimensions
The relationship between Pbm and $\sqrt{WA_i}$, for FEV_1/FVC values of 80%, 60%, and 40% were fed into the computational model of airway resistance.
The increased inner wall area associated with more severe airway obstruction caused a leftward shift and an increase in the maximal plateau resistance on the simulated dose response curves. The position of the dose-response curve was characterized by the PD_{10}, and the maximal plateau by the maximal resistance achieved. When we entered parameters of airway geometry that corresponded with an FEV_1/FVC of 80%, calculated baseline and maximal resistance were 1.02 and 97 cm $H_2O/L/s$, respectively, and PD_{10} was 28.9. With the airway geometry associated with an FEV_1/FVC of 40%, baseline and maximal resistance were 1.11 and 145 cm $H_2O/L/s$, respectively, and the PD_{10} was 25.1.
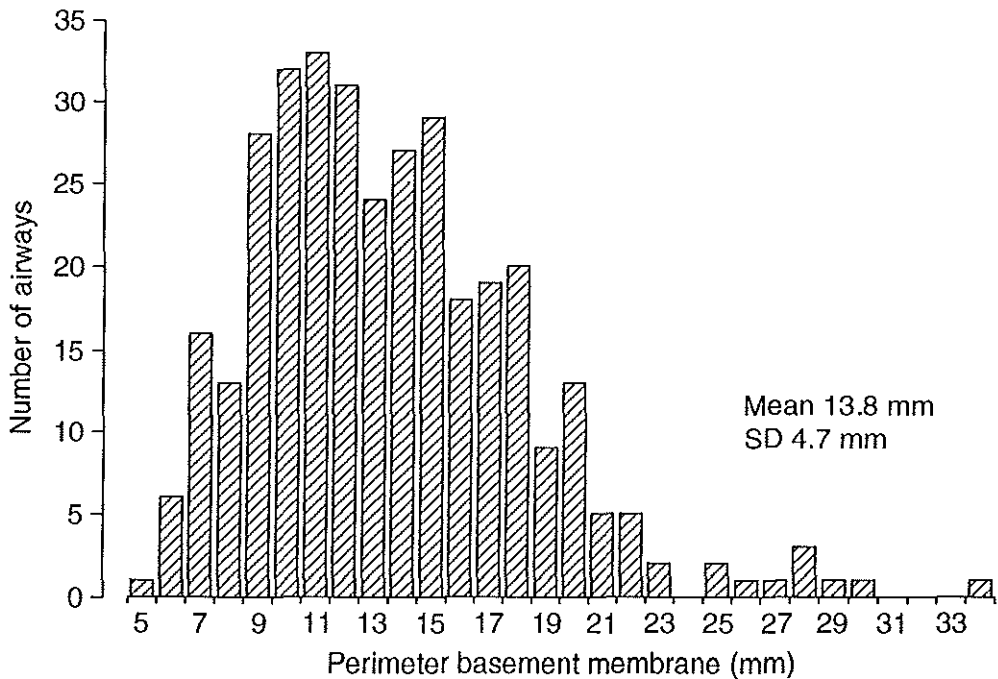
Figure 3. Frequency distribution of cartilaginous airway size (n = 341) measured in 72 patients.

Discussion

The aims of this study were, firstly, to measure airway wall dimensions in cartilaginous airways from patients with COPD to complement the existing morphometric data in the literature. Secondly, we wanted to know whether the dimensions of cartilaginous airways correlated with the degree of airflow obstruction and the severity of airway inflammation. Thirdly, we estimated the effect of different airway dimensions on airway resistance and responsiveness with a computational model. Airway dimensions were related to pre-operatively measured lung function and semi-quantitative grading of peripheral airway inflammation. Our results show that the inner airway wall area but not the outer wall or smooth muscle area of cartilaginous airways is thicker in patients who have more severe airflow obstruction, more reversibility of airflow obstruction, and more severe inflammatory changes in peripheral airways.

Airway Dimensions

To our knowledge this is the first study in which the dimensions of a large number of cartilaginous airways have been measured in a group of patients suffering from varying degrees of airflow obstruction. The inner wall area is thickened over the entire size range of cartilaginous airways and proportionally more in the smaller airways. Thickening of the inner wall area in cartilaginous airways is associated with a reduction in FEV_1/FVC. This finding is in agreement with the hypothesis that increased wall thickness could result in a reduction of maximal expiratory flow[7, 23]. Previous investigators have shown that increased thickness of membranous bronchioles was correlated with increased airflow obstruction in COPD. Bosken and coworkers[4] compared membranous airway inner wall, outer wall, and smooth muscle area in the lungs of 30 smokers with airflow obstruction ($FEV_1/FVC < 65\%$) to the airway dimensions in 30 subjects without airflow obstruction. She found that the inner and outer airway walls of the membranous airways were significantly thicker in the obstructed patients. Though Bosken examined some cartilaginous airways, their number was too small to determine relationships between airway wall dimensions and airway size separately.

The outer wall area is not correlated to the degree of airflow obstruction in the present study. Thickening of the outer wall area could theoretically uncouple the smooth muscle layer from the distending forces provided by the surrounding parenchyma and therefore increase airflow obstruction[23]. We speculate that in large airways the effect of changes in outer wall dimensions on airway smooth muscle behaviour will be reduced by the cartilage plates and, therefore, will be less important than in membranous airways.

Recently Kuwano and coworkers[5] made measurements on the membranous airways of 15 patients with obstructive lung disease and compared these with nonobstructed patients and a group of patients with moderate to severe asthma. In that study only the airway smooth muscle area was significantly increased in the COPD patients as compared with controls. The patients with asthma had substantial increases in all components of the airway wall including the inner, outer, and smooth muscle area. Increased airway smooth muscle could result in more airway narrowing for any degree

of smooth muscle shortening. In the present study we did not find a correlation between the smooth muscle area and airflow limitation. In the large cartilaginous airways smooth muscle is mainly present as small bundles that make accurate and reproducible measurement difficult. Hence, differences in the amount of muscle could have been missed because of the relatively large variability of the smooth muscle area measurement. In an attempt to increase the objectivity and the reproducibility of the measurement, we used an automated image analysis system instead of the more cumbersome and subjective method of tracing individual muscle bundles. Despite this, the variability remained high.

Airway Dimensions and Inflammatory Changes

There is a significant relationship between the inner airway wall area and peripheral airway inflammation. A correlation between peripheral airway inflammation and airway obstruction was originally reported by Cosio and coworkers[1] and has been confirmed by Wright and coworkers[24] and others. More recently Bosken and coworkers[4] showed that peripheral airway inflammation correlates with increased airway wall thickness in membranous airways, and both changes correlated with airflow obstruction. Mullen and coworkers[3] scored inflammatory changes both in membranous and cartilaginous airways using a modified version of the pictorial grading method described by Cosio[1] and coworkers. In this study inflammatory changes were more pronounced in large cartilaginous airways than in smaller cartilaginous airways. These findings suggest that the thickening of the inner wall area that we observed in cartilaginous airways is related to an inflammatory response.

We found no correlation between outer wall area and airflow obstruction or inflammatory changes. The outer wall is much thicker than the inner wall in central airways, whereas in membranous airways they are of similar thickness[4]. This is partly due to the presence of cartilage in the larger airways and, in addition, there is more noncartilaginous connective tissue in the area between the smooth muscle layer and the parenchyma. We speculate that airway cartilage might function as a physical barrier that protects the connective tissue at the parenchymal side of the cartilage against inflammatory processes localised at the mucosal side of the cartilage. Therefore,

inflammatory thickening in the outer airway wall area might be less pronounced than in the inner wall area.

We found no correlation between the smooth muscle area and inflammatory changes in the peripheral airways. As was stated before, we might miss an existing correlation due to the high variability of the smooth muscle measurement.

Airway Dimensions and Airway Resistance

To examine the functional significance of the altered airway dimensions that we measured, we used the computational model of the tracheobronchial tree developed by Lambert and coworkers[21]. In the model it is assumed that large airways have proportionally less smooth muscle than more peripheral airways; therefore, smooth muscle shortening will cease at lower concentrations of a contractile agonist. This assumption is supported by our finding that the central airways contained proportionally two thirds less smooth muscle than peripheral cartilaginous airways. Using the model and the morphologic data of Kuwano and coworkers[5], Lambert and coworkers[21] have shown that the increased outer wall, inner wall, and smooth muscle areas observed in asthmatic patients can explain an increase in baseline resistance and, more importantly, could enhance the airway narrowing produced by smooth muscle shortening. In the present study we used our measured values for cartilaginous airway dimensions in the model rather than extrapolating from the peripheral airway dimensions of Kuwano and coworkers[5]. In addition, we were able to assess theoretically the independent contribution of the altered cartilaginous airway structure on airway resistance.

An important determinant of airway resistance in the model of Lambert and coworkers[21] is the thickness of tissue within the smooth muscle layer or inner airway wall area. In our study the inner wall area for central airways with an airway diameter of 6 to 25mm is increased by 64% to 20% for obstructed patients ($FEV_1/FVC = 40\%$) in comparison to the nonobstructed patients ($FEV_1/FVC = 80\%$). This thickening results in an increase of baseline resistance as calculated by the model of only 8 percent. In addition the hypothetical dose-response curve is shifted to the left by 10%. The effect of smooth muscle shortening on airway resistance can be amplified

by thickening of the airway wall[7]. In fact, in the model the resistance at maximal bronchoconstriction in the obstructed patients was increased by 50%. Maximal resistance therefore seems to be a more sensitive parameter to detect thickening of the airway wall than baseline resistance or the leftward shift of the dose-response curve. This might explain why we did not find a correlation between inner wall thickness and the PC_{20}. The minor shift of the dose-response curve to the left as predicted by the model can easily obscure the possible relation between airway wall thickness and bronchial responsiveness. The plateau resistance or PC_{40} instead of the PC_{20} might have been more adequate to demonstrate the relation between airway wall thickness and bronchial responsiveness.

The major determinant of airway resistance in the model of Lambert and coworkers[21] is the balance between the force generated by the muscle and the load against which the smooth muscle contracts. The force generated by the smooth muscle is assumed to be proportional to the amount of smooth muscle. An increase in the amount of smooth muscle therefore can increase baseline and maximal airway resistance. In asthmatic subjects a marked increase in the amount of smooth muscle in the membranous and cartilaginous airways was found[7]. In COPD the amount of smooth muscle was found to be significantly greater in the smaller airways of patients with airflow obstruction[4, 5]. We did not find such an increase in the amount of smooth muscle in cartilaginous airways of obstructed patients. Table 5 shows a comparison of the prediction equations for airway wall dimensions from the present study and the studies of Bosken and coworkers[4] and Kuwano and coworkers[5].

Implications for Therapy

Increased airflow obstruction in COPD patients is related to thickening of the inner wall area, which is probably the result of inflammatory changes. To the extent that this inflammation is reversible, anti-inflammatory medications such as inhaled corticosteroids could reduce the thickening of the inner wall area and thus reduce airflow obstruction. In fact, it has been shown that maintenance treatment with inhaled or oral corticosteroids substantially reduces airway obstruction and hyper-responsiveness in patients with COPD[25, 26]. However, normal levels for FEV_1 and PC_{20} were not achieved in the majority of patients. It is unlikely that chronic

Table 5

COMPARISON OF PREDICTION EQUATIONS
FOR AIRWAY DIMENSIONS

	$\sqrt{WA_i}$ vs P_{bm} slope (intercept)	$\sqrt{WA_o}$ vs P_{bm} slope (intercept)	$\sqrt{WA_m}$ vs P_{bm} slope (intercept)
Tiddens and coworkers*			
Control (FEV$_1$/FVC = 80%)	0.069 (0.194)	0.240 (0.160)	0.020 (0.23)
COPD (FEV$_1$/FVC = 40%)	0.069 (0.384)	0.240 (0.160)	0.020 (0.23)
Bosken and coworkers[4]			
Control (FEV$_1$/FVC > 75%)	0.096 (0.107)	0.093 (0.099)	0.040 (0.050)
COPD (FEV$_1$/FVC < 65%)	0.101 (0.142)	0.099 (0.148)	0.045 (0.056)
Kuwano and coworkers[5]			
Control (FEV$_1$/FVC = 80%)	0.057 (0.083)	0.079 (0.116)	0.020 (0.056)
Asthma (FEV$_1$/FVC = ?)	0.119 (0.008)	0.137 (0.085)	0.063 (0.001)
COPD (FEV$_1$/FVC = 65%)	0.065 (0.057)	0.086 (0.084)	0.035 (0.016)

Definition of abbreviations:
WA_i = inner wall area (mm^2); WA_o = outer wall area (mm^2); WA_m = smooth muscle area (mm^2); P_{bm} = perimeter basement membrane (mm). *Tiddens = present study.

inflammatory changes in the bronchial wall, such as fibrous tissue deposition, will be entirely reversible with anti-inflammatory treatment. Therefore, we speculate that even long-term anti-inflammatory treatment will not completely return the inner wall area to its normal thickness. Treatment with bronchodilators in patients with obstructive airways disease improves FEV$_1$[27].

The correlation between inner wall area and the reversibility of airflow obstruction after inhaled salbutamol in the present study suggests that therapy with bronchodilators is especially effective in those patients with a thickened inner wall area. Even relaxation of normal smooth muscle tone in combination with a thickened inner wall area could improve airway patency[28].

We conclude that thickening of the inner wall area in cartilaginous airways contributes to airflow limitation and reversibility of bronchial obstruction in patients with COPD, and we speculate that these changes are related to airway inflammation.

Acknowledgements

References:

1. Cosio MG, Ghezzo H, Hogg J, Corbin R, Loveland M, Dosman J, Macklem PT. The relations between structural changes in small airways and pulmonary-function tests. N Engl J Med 1977;298:1277-1281.
2. Cosio MG, Hale KA, Niewoehner DE. Morphologic and morphometric effects of prolonged cigarette smoking on the small airways. Am Rev Respir Dis 1980;122:266-271.
3. Mullen JB, Wright JL, Wiggs BR, Paré PD, Hogg JC. Reassessment of inflammation of airways in chronic bronchitis. B M J (Clin Res Ed) 1985;291(6504):1235-1239.
4. Bosken CH, Wiggs BR, Paré PD, Hogg JC. Small airway dimensions in smokers with obstruction to airflow. Am Rev Respir Dis 1990;142(3):563-570.
5. Kuwano K, Bosken CH, Paré PD, Bai TR, Wiggs BR, Hogg JC. Small airways dimensions in asthma and chronic obstructive pulmonary disease. Am Rev Respir Dis 1993;148:1220-1225.
6. James AL, Hogg JC, Dunn LA, Paré PD. The use of the internal perimeter to compare airway size and to calculate smooth muscle shortening. Am Rev Respir Dis 1988;138(1):136-139.
7. James AL, Paré PD, Hogg JC. The mechanics of airway narrowing in asthma. Am Rev Respir Dis 1989;139(1):242-246.
8. Carroll N, Elliot J, Morton A, James A. The structure of large and small airways in nonfatal and fatal asthma. Am Rev Respir Dis 1993;147:405-410.
9. American Thoracic Society. Standards for the diagnosis and care of patients with chronic obstructive pulmonary disease (COPD) and asthma. Am Rev Respir Dis 1987;136:225-243.
10. Morris JF, Koski A, Johnson LC. Spirometric standards for healthy non-smoking adults. Am Rev Respir Dis 1971;103:57-67.
11. Bates DV, Macklem PT, Christie RV. Respiratory function in disease. (2nd ed.) WB Saunders, Philadelphia 1971
12. Goldman HI, Becklake MR. Respiratory function tests: normal values at medium altitudes and the prediction of normal results. Am Rev Tubercul 1959;79:457-467.
13. Dosman EA. The use of helium-oxygen mixture during expiratory flow to demonstrate obstruction in small airways in smokers. J Clin Invest 1975;55:1090-1099.
14. Cockroft W, Killian DN, Mellon JJA. Bronchial reactivity to inhaled histamine: a method and clinical survey. Clin Allergy 1977;7:235-243.
15. Quanjer PH, Tammeling GJ, Cotes JE, Pedersen OF, Peslin R, Yernault JC. Lung volumes and forced ventilatory flows. Eur J Respir Dis 1993;6:5-40.
16. Bai AB, Eidelman DH, Hogg JC, James AL, Lambert RK, Ludwig MS, Martin J, McDonald DM, Mitzner WA, Okazawa M, Pack RJ, Paré PD, Schellenberg RR, Tiddens HAWM, Wagner EM, and Yager D. Proposed nomenclature for quantifying subdivisions of the bronchial wall. J Appl Physiol 1994; 77(2):1011-1014.
17. Wright JL, Cosio M, Wiggs B, Hogg JC. A morphologic grading scheme for membranous and respiratory bronchioles. Arch Pathol Lab Med 1985;109(2):163-165.
18. Schluchter MD. Module 5V. In: BMDP Statistical software manual, Dixon WJ, ed. Burkely: University of California press, 1990: 1207-1244.
19. Feldman HA. Families of lines: random effects in linear regression analysis. J Appl Physiol 1988; 64(4):1721-1732.
20. Wiggs BR, Moreno R, Hogg JC, Hilliam C, Paré PD. A model of the mechanics of airway narrowing. J Appl Physiol 1990;69(3):849-860.
21. Lambert RK, Wiggs BR, Kuwano K. Functional significance of increased airway smooth muscle in asthma and COPD. J Appl Physiol 1993;74:2771-2781.
22. Hammersley JR, Olson DE. Physical models of the smaller pulmonary airways. J Appl Physiol 1992;72(6):2402-2414.

23. Moreno RH, Hogg JC, Paré PD. Mechanics of airway narrowing. Am Rev Respir Dis 1986;133(6): 1171-1180.
24. Wright JL, Hobson J, Wiggs BR, Paré PD, Hogg JC. Effect of cigarette smoking on structure of the small airways. Lung 1987;165(2):91-100.
25. Kerstjens HAM, Brand PLP, Hughes MD, Robinson NJ, Postma DS, Sluiter HJ, Bleecker ER, Dekhuijzen PN, de Jong PM, Mengelers HJ. A comparison of bronchodilator therapy with or without inhaled corticosteroid therapy for obstructive lung disease. N Engl J Med 1992;327:1413-1419.
26. Weir DC, Burge PS. Effects of high dose inhaled beclomethasone diproprionate, 750 μg and 1500 μg twice daily, and 40 mg per day oral prednisolone on lung function, symptoms, and bronchial hyperresponsiveness in patients with non-asthmatic chronic airflow obstruction. Thorax 1993;48:309-316.
27. Newnham DM, Dhillon DP, Winter JH, Jackson CM, Clark RA, Lipworth BJ. Bronchodilator reversibility to low and high doses of terbutaline and ipratropium bromide in patients with chronic obstructive pulmonary disease. Thorax 1993;48:1151-1155.
28. Paré PD, Wiggs BR, James A, Hogg JC, Bosken C. The comparative mechanics and morphology of airways in asthma and in chronic obstructive pulmonary disease. Am Rev Respir Dis 1991;143:1189-1193.

Physiological and Morphological Determinants of Maximal Expiratory Flow in Chronic Obstructive Lung Disease

Harm A.W.M. Tiddens, Jan M. Bogaard, Johan C. de Jongste, Wim C.J. Hop, Harvey O. Coxson, and Peter D. Paré.

Department of Pediatrics, Division of Respiratory Medicine,
Lung Function Laboratory and Department of Biostatistics,
Erasmus University and University Hospital/Sophia Children's Hospital,
Rotterdam, the Netherlands;
and Respiratory Health Network of Centres of Excellence, St. Paul's Hospital
Pulmonary Research Laboratory, University of British Columbia,
Vancouver, Canada.

Introduction

Reduced maximal expiratory flow is the physiological abnormality which defines chronic obstructive pulmonary disease (COPD) and is used as a measure of its severity. Nevertheless, the exact mechanisms which are responsible for the airflow obstruction in COPD remain incompletely understood. Maximal expiratory flow in COPD could be reduced by three different mechanisms. Firstly, loss of lung elastic recoil can decrease the driving pressure[1, 2]. Secondly, inflammatory thickening and narrowing of airways can decrease the airway conductance upstream of flow-limiting segments. Thirdly, the collapsibility of airways and, therefore, of flow-limiting segments can be increased due to processes such as inflammatory destruction of bronchial cartilage. Decreased cartilage volume in COPD has been described by several author[3-6], but was not found by others[7, 8].

It has been suggested that the relative contributions of decreased lung recoil, decreased airway conductance and increased airway collapsibility to flow obstruction during forced expiration can be estimated from a maximal flow-static recoil (MFSR) curve[9]. MFSR curves can be constructed by plotting maximal flow at specific lung volumes versus the corresponding transpulmonary pressures. These measures are derived from maximal expiratory flow-volume and pressure-volume curves. The slope of the MFSR plot is a measure of airway conductance upstream from the flow-limiting segments. The pressure-axis intercept of the MFSR curve is an index of the collapsibility of the flow-limiting segments.

We hypothesized that decreased upstream conductance would be related to inflammation and thickening of the airway walls, increased collapsibility would be related to decreased airway cartilage volume, and decreased collapsibility to inflammation and thickening of the airway walls.

These questions were addressed by measuring maximal expiratory flow-volume and pressure-volume curves and constructed MFSR plots for 72 patients who had varying degrees of airflow obstruction. Lung function measurements were made in the week before resection of a lung or lobe for a peripheral pulmonary lesion. With these in vivo parameters of lung elastic recoil, MFSR estimates of airway conductance and collapsibility together with morphometric measurements of the airway structure, an

attempt was made to separate the relative importance of decreased recoil, decreased upstream conductance and increased collapsibility of the flow-limiting segments to airflow obstruction in COPD.

Methods

Study Population
Lung tissue was obtained from 72 patients who had a lobar resection or pneumonectomy for a solitary peripheral lung lesion, and who showed no evidence at pathological examination of obstructive pneumonitis. Furthermore, patients who had a history consistent with a diagnosis of asthma were excluded[10]. Informed consent was obtained in all cases. Of the 72 patients, 64 proved to have bronchogenic carcinoma; carcinoid tumour, hamartoma or granuloma were the final diagnosis in the remaining patients. These patients were mostly smokers and were classified as "COPD" although one-third had a lung function within the normal range and, therefore, did not strictly fulfil the ATS criteria[10]. The clinical data for patients in this study are summarized in Table 1.

Pulmonary Function Studies
Pulmonary function tests were performed in the week before surgery using a volume displacement pressure compensated body plethysmograph. Thoracic gas volume was measured with a Krogh spirometer coupled to a linear displacement transducer (Shaevitz Engineering, Pennsauken, NJ, USA). Flow was measured with a Fleisch No. 3 pneumotachometer coupled to a Sanborn 270 differential pressure transducer (Sanborn Co., Waltham, MA, USA). Functional residual capacity (FRC) was determined using the Boyle's law technique, and residual volume (RV) and total lung capacity (TLC) were calculated after the determination of the expiratory reserve volume and inspiratory capacity (IC). Forced expiratory volume in one second (FEV_1) and forced vital capacity (FVC) were calculated from digitized flow and volume signals obtained during forced expiratory manoeuvres. At least 3 expiratory efforts were performed and the forced expiratory manoeuvre with the largest sum of FEV_1

Table 1

STUDY POPULATION CHARACTERISTICS (n=72)

Age, years	61 ± 9.5 (37-83)
Sex, male : female	54:18
Pack years	54.7 ± 34.5 (0.4-180)
Current smokers, n	45
Lifelong nonsmokers, n	2
Lung or lobe resected, right side, n	50
Lung or lobe resected, left side, n	22

Pack years = number of years smoking one pack of cigarettes a day. Age and pack years are expressed as mean ± SD and range; n = number.

and FVC was selected. As an indicator of the severity of flow obstruction, the FEV_1 and FEV_1/FVC were used.

Values were expressed as percentage of the predicted values (% pred) according to the summary equations of the European Coal and Steel Community[11]. Static pressure-volume curves were obtained as described previously[12]. Briefly, transpulmonary pressure (P_L) was measured using a differential pressure transducer (Validyne 45MP $\pm$ 100 cm H_2O; Validyne Co., Northridge, CA, USA), which compared airway opening pressure to oesophageal pressure measured with a balloon catheter. The volume signal was obtained from the body plethysmograph. After 3 vital capacity breaths, the subjects inhaled to TLC and the maximal static recoil pressure (P_L,max) was recorded with the glottis opened. Multiple static pressure-volume points were obtained by occluding the airway every 1-2 s during slow expiration to FRC. At least 3 curves were obtained and a total of not less than 18 pressure-volume points. The pressure-volume data were analysed as described previously[13, 14]. All pressure-volume points between TLC and FRC were used to derive an exponential relationship of the form: $V = A-Be^{-kP}$, where: V = lung volume; A = the lung volume at infinite P_L; B = the lung volume difference between A and the lung volume at a P_L of 0; k = the exponential constant that describes the shape of the pressure-volume curve; and P = transpulmonary
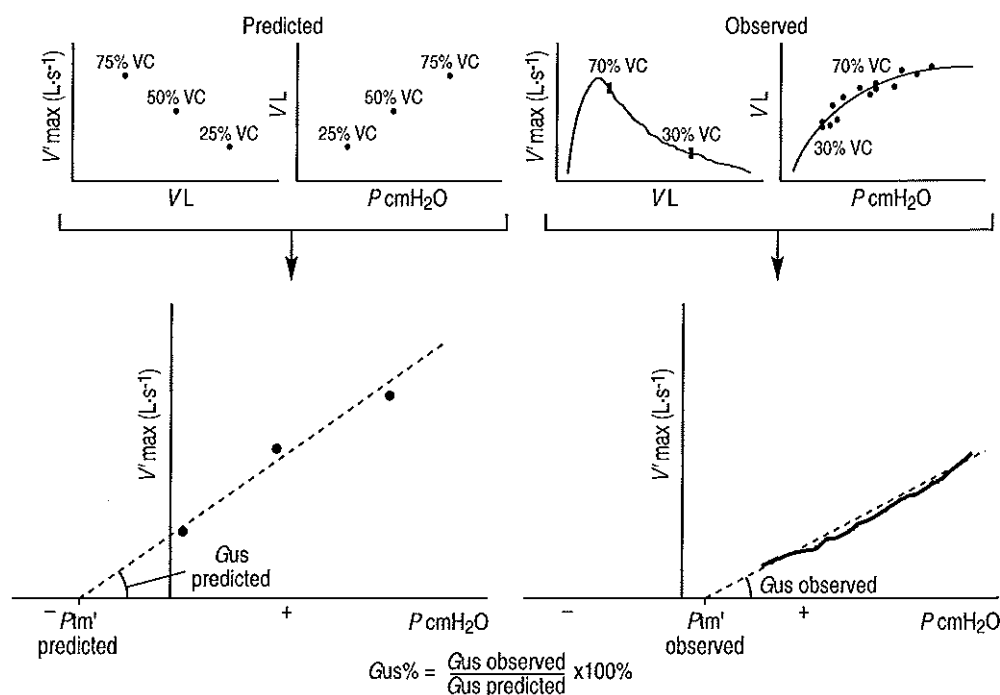
Figure 1. For each patient a maximal flow-static recoil (MFSR) plot is obtained by plotting maximal flow Vmax of the volume-flow curve against the static transpulmonary pressures at the same lung volumes. The slope of the linear part of the MFSR plot between 70% and 30% of vital capacity (VC) is an estimation of upstream airway conductance (G_{us}), the pressure-axis intercept is an estimate of the airway collapsibility of the flow-limiting segments (P_{tm}'). For each patient, a predicted MFSR curve is obtained by plotting predicted V'max at 75, 50, and 25% of VC of the volume-flow curve against the predicted static transpulmonary pressures at the same lung volumes. The slope of the MFSR plot between 75% and 25% VC is G_{us}(pred), the pressure-axis intercept is P_{tm}'(pred). G_{us}% calculated in the figure and $\Delta P_{tm}'$ (= P_{tm}'(pred)-P_{tm}') are used for statistical analysis.

pressure. The recoil pressures at 90 and 60% TLC (P_L90 and P_L60) were calculated using the V = A-Be^{-kP} equation[13, 14].

Construction of Maximal Flow-Static Recoil Curves

A MFSR curve was obtained for each patient by plotting maximal expiratory flow against the static transpulmonary pressures at the same lung volumes (Figure 1). The slope of the relatively linear part of the MFSR plot between 70% and 30% vital

capacity (VC) was calculated to estimate upstream airway conductance during forced expiration (G_{us}:L·s^{-1}·cm H$_2$O^{-1}). For comparison with previous reports on MFSR analysis, G_{us} was also divided by TLC (sG_{us}:cm H$_2$O^{-1}·s^{-1}). The pressure-axis intercept of the extrapolated slope was used to estimate the critical transmural pressure causing airway collapse at the flow limiting segments (P_{tm}':cm H$_2$O), at which flow limiting airways narrow sufficiently to restrict airflow according to the model described by Pride and coworkers[15]. Predicted G_{us} and P_{tm}' (G_{us}(pred) and P_{tm}'(pred)) were predicted for individual patients as follows (Figure 1). Firstly, TLC and FVC(pred) we calculated using the equations of Quanjer and coworkers[11]. Secondly, the absolute lung volumes at 75, 50, and 25% FVC (pred) were calculated by subtracting, respectively, 25, 50 or 75% of FVC(pred) from TLC(pred). Thirdly, the predicted recoil pressures for these 3 lung volumes we calculated as follows: the $V = A-Be^{-kP}$ equation was rearranged to $P = ((\ln A-V)-\ln B)/k$, where V is the lung volume at 75, 50, 25% FVC(pred) and A is the theoretical lung volume at infinite transpulmonary pressure (we used TLC(pred) for A). The k and B were derived from the prediction equations of Colebatch and coworkers[14] for k and B/A%. Fourthly, the maximal expiratory flows at 75, 50, and 25% FVC(pred) were derived from the equations of Quanjer and coworkers[11]. The three predicted flow recoil-pressure points at 75, 50, and 25% FVC(pred) were plotted on a flow-pressure diagram and a regression line was plotted through the 3 flow-pressure points for the 75-25% VC volume intervals. The slope of the regression equation represents G_{us}(pred) and the intercept on the pressure-axis represents P_{tm}'(pred). For statistical analysis, G_{us} was expressed as a percentage of G_{us}(pred)(G_{us}%) and P_{tm}' as the absolute difference of P_{tm}'(pred) - P_{tm}' (ΔP_{tm}') (Figure 1). With increased collapsibility of the flow-limiting segment, P_{tm}' will be more positive and, therefore, ΔP_{tm}' more negative.

Morphological Studies
Surgically resected specimens were inflated with either 10% formalin or 2.5% glutaraldehyde, at a pressure of 25 cm H$_2$O, and submerged in fixative for at least 24 h. The fixed specimens were then sliced serially at 1 cm intervals in a sagittal plane. Three to six intrapulmonary cartilaginous airways, which were cut in cross-

section, were randomly selected from each specimen for morphometric analysis. Tissue blocks containing cartilaginous airways in cross-section were decalcified, embedded in paraffin, transversely cut at 5 μm thickness and stained with haematoxylin and eosin, and with Masson's trichrome. Additionally, five lung tissue blocks were obtained in a stratified random fashion from a parasagittal slice for morphological grading of membranous and respiratory bronchioles and processed in the same way.

Measurement of Airway Dimensions

Sections from cartilaginous airways that did not show bifurcation or disruption of the wall were selected for measurement. Airway dimensions were measured on the haematoxylin and eosin stained sections using a microscope (Nikon) fitted with a camera lucida that superimposed the cursor-light of a digitizing board on the microscopic image of the airway (Bioquant; R&M Biometrics Inc., Nashville TN, USA). Airways that were too large to be viewed entirely using a microscope were projected with a slide projector, and their images were traced onto paper and the tracings were measured on the digitizing board.

The measurements that were made are shown in Figure 2, and include: basement membrane perimeter (P_{bm}); and the area of the lumen (and epithelium) contained within the light microscopic image of the basement membrane (A_{bm}); the outer muscle perimeter (P_{mo}), traced at the outer edge of the smooth muscle layer and the enclosed area (A_{mo}); the outer perimeter (P_o), and the outer area (A_o) defined by the outer edge of the adventitial tissue. From these measurements, total wall area ($WA_t = A_o - A_{bm}$) and inner wall area ($WA_i = A_{mo} - A_{bm}$) we were calculated. The total area of cartilage in the airway wall (WA_{cart}) was calculated by tracing every piece of cartilage separately and calculating the sum of the areas. To measure the area occupied by smooth muscle (WA_m), an automated image analysis system (Bioview, Infrascan, Vancouver, BC, Canada) was used. The smooth muscle was segmented from the airway wall in a trichrome stained section using operator defined colour threshholding. The area of the muscle was calculated automatically. The nomenclature used is according to the special communication concerning subdivisions of the bronchial wall[16]. All measurements of airway dimensions were performed by the same observer
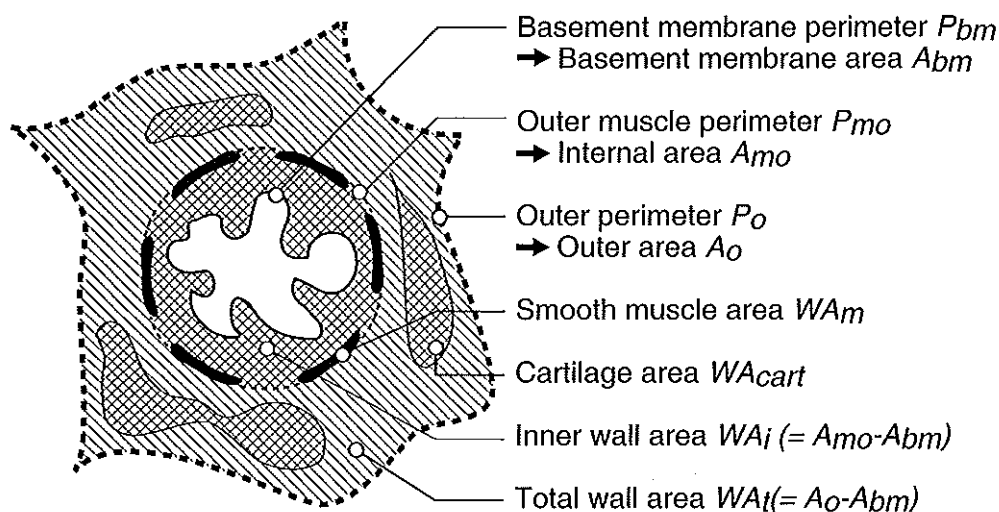
Figure 2. Diagram of measured airway dimensions.

(HT). Perimeters (P_{bm}, P_{mo}, P_o), were measured twice; if the difference between both measurements exceeded 10%, they were repeated. Intra-observer variability was assessed by remeasurement of 10 randomly selected airways with an interval of 2 months. Inter-observer variability was assessed by remeasurement of 10 randomly selected airways by a second observer.

Measurement of Bronchiolar Inflammatory Changes

For each specimen, 5 to 10 membranous airways were graded for the severity of small airways disease using a modification of the pictorial grading method of Cosio and coworkers[17, 18]. The following indices were graded: inflammation; fibrosis; muscle hypertrophy; pigment deposition; goblet cell metaplasia; and squamous cell metaplasia. For each airway, these six morphological indices were compared with pictorial reference standards with a score from 0 (normal) to 3 (most abnormal). Next, the mean score for each morphological index for each individual was calculated by summing the scores of the airways examined and dividing by the number of airways examined. The average score for that variable was expressed as a percentage of maximal possible score. A total membranous airways disease score for each speci-

men was then calculated by summing the mean scores of the six morphological indices (maximal score: 6 x 100 = 600).

Statistical Analysis

Correlation coefficients given are Pearson's. The relationships between airflow obstruction (FEV_1, FEV_1/FVC), on the one hand and various measures of lung recoil ($P_L$max, P_L60, log k), upstream conductance ($G_{us}\%$, sG_{us}), airway collapsibility (P_{tm}', $\Delta P_{tm}'$), and airway dimensions (WA_i, WA_t, WA_{cart}) on the other, were investigated using multiple linear regression analysis.

The intra- and inter observer variability of morphometric measurements were calculated by expressing the difference between the first and second measurement as a percentage of the average of both measurements. This percentage difference was plotted against the average P_{bm} to detect if there were systematic differences dependent on airway size.

Repeated measurement analysis of variance (RMANOVA), which allows for differences between and within patients, was used to asses the relationships between airway wall dimensions (WA_t, WA_{cart}, WA_m) and airway size (P_{bm}). To obtain linear regressions with approximately normal distributions, it was necessary to apply a square root transformation to the airway wall dimensions. In the analysis, the airway size values were centered by subtracting the mean value for P_{bm} of 14 mm from all values of P_{bm}. The intercept of an individual regression line of a particular airway wall dimension as a function of P_{bm}, therefore, denotes its level at a P_{bm} of 14 mm. The intercept and slope of the regression lines were investigated for their linear relationship with $FEV_1(\%pred)$, $FEV_1/FVC(\%pred)$, $\Delta P_{tm}'$, and $G_{us}\%$ using an iterative search for optimal values. RMANOVA analyses the patients as a continuum and, thus, avoids the bias that results from dividing patients into subgroups[19, 20]. The level of significance was set at a p-value equal to 0.05 (two-sided). Data are expressed as mean ± standard deviation and range, unless indicated otherwise.

Results

Lung Function

The mean lung function values of the patients in this study are shown in Table 2. Forty nine patients had no significant airflow obstruction ($FEV_1/FVC > \pm 2SD$ $FEV_1/FVC(pred)$). 12 Patients had mild airflow obstruction (FEV_1/FVC between -2 and -3SD $FEV_1/FVC(pred)$), and 11 patients had severe airflow obstruction (FEV_1/FVC < -3SD $FEV_1/FVC(pred)$). Increased functional residual capacity (FRC > FRC(pred) +2SD) was present in 21 out of 72 patients, and increased residual volume (RV > RV(pred) +2SD) in 29 out of 72 patients. Loss of elastic recoil pressure (k > k(pred) + 2SD) was present in 8 out of 72 patients.

Maximal Flow-Static Recoil Curves

The MFSR curves derived from the patients contained 62 ± 21 (17-125) data points in the 70-30% VC volume interval and were linear within that interval in 59 patients ($R^2 = 0.99 \pm 0.01$ (0.95-0.99)). For 13 patients, the relationship within the 70-30% VC volume interval was clearly not linear at the upper end. The flow-volume curves of these patients showed that the peak expiratory flow was not reached within the first 30% of the expired VC, due to submaximal effort.

A submaximal flow-volume manoeuvre is likely to influence both the slope and the intercept of the linear part of the MFSR curve, and these subjects were, therefore, excluded from further analysis.

Figure 3 shows the values for $G_{us}(pred)$ and $P_{tm}'(pred)$ as a function of age for male and female subjects of the various heights. The relationship between the three predicted flow and pressure points at 75, 50, and 25% VC was adequately described as a linear relationship for all patients ($R^2 = 0.99$ range (0.96-0.99)). Multiple regression analysis showed that $G_{us}(pred)$ and $P_{tm}'(pred)$ were significantly related to age and sex. $G_{us}(pred)$ increased in males and females of 170 cm height for an increase in age of 10 yrs by 0.04 and 0.03 $L \cdot s^{-1} \cdot cm\ H_2O^{-1}$, respectively (p < 0.001). $G_{us}(pred)$ was on average 0.15 $L \cdot s^{-1} \cdot cm\ H_2O^{-1}$ higher in males than in females (p < 0.001). $P_{tm}'(pred)$ increased in males and females of 170 cm height for an increase in age of 10 yrs by 0.25 and 0.6 cm H_2O, respectively. $P_{tm}'(pred)$ was higher in males than in females

Table 2
LUNG FUNCTION CHARACTERISTICS

TLC, % pred	n = 72	109 ± 15	(81-154)
FRC, % pred	n = 72	123 ± 24	(70-177)
RV, % pred	n = 72	133 ± 34	(66-219)
FEV_1, % pred	n = 72	94 ± 18	(58-135)
FVC, % pred	n = 72	96 ± 13	(64-134)
FEV_1/FVC, % pred	n = 72	92 ± 12	(55-114)
$P_L$max, % pred	n = 72	83 ± 28	(28-171)
P_L90, % pred	n = 72	79 ± 21	(40-141)
P_L60, % pred	n = 72	55 ± 46	(10-231)
K, % pred	n = 72	110 ± 51	(17-437)
B/A, % pred	n = 72	81 ± 20	(40-157)
G_{us}% male, % pred	n = 44	108 ± 49	(36-246)
G_{us}% female, % pred	n = 15	143 ± 73	(67-283)
ΔP_{tm}' male, cm H_2O	n = 44	0.15 ± 1.9	(-3.8-4.8)
ΔP_{tm}' female, cm H_2O	n = 15	0.02 ± 1.9	(-2.5-5.3)

Values are presented as mean ± SD, and range in parenthesis. Definition of abbreviations: TLC = total lung capacity; % pred = % of predicted value; FRC = functional residual capacity; RV = residual volume; FEV_1 = forced expiratory volume in 1 second; FVC = forced vital capacity; FEV_1/FVC = forced expiratory volume in 1 second as fraction of forced vital capacity; $P_L$max = transpulmonary pressure at TLC; P_L90 = transpulmonary pressure at 90% TLC; P_L60 = transpulmonary pressure at 60% TLC; k = exponential constant describing shape of the pressure-volume curve; B/A = ratio describing position of the pressure-volume curve in respect to the pressure axis; A = the lung volume at infinite transpleural pressure; B = the lung volume difference between A and the lung volume at a transpleural pressure of 0 cm H_2O; G_{us}% = airway conductance upstream the flow-limiting segment; ΔP_{tm}' = critical transmural pressure at which the flow-limiting segments restrict flow calculated as P_{tm}'(pred) - P_{tm}'; n = number.

(p < 0.001). This difference decreased with increasing age. Figure 4 shows the age dependence of the predicted MFSR curve both for male and female subjects.
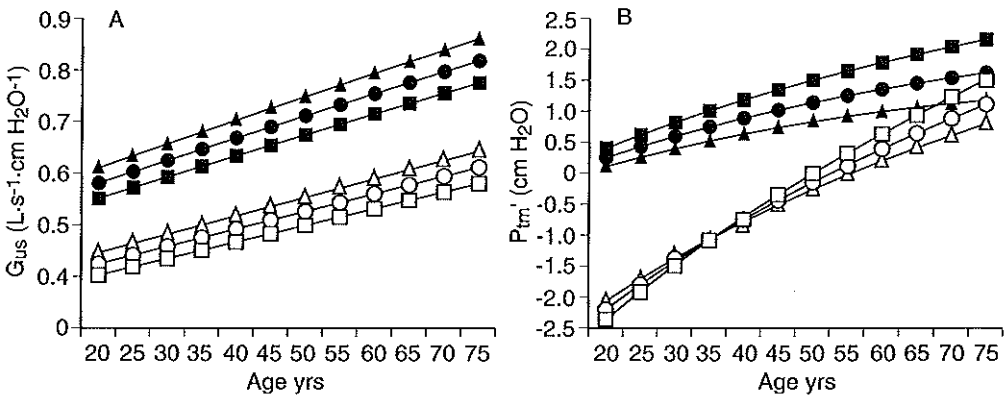
Figure 3. (A) Change of the predicted airway conductance versus age. (B) Collapsibility versus age. Definition of abbreviations: G_{us} = airway conductance upstream the flow-limiting segment; P_{tm}' = critical transmural pressure causing airway collapse at the flow-limiting segment. ■ = male 160 cm; ● = male 170 cm; ▲ = male 180 cm; □ = female 160 cm; O = female 170 cm; Δ = female 180 cm.

Morphologic Studies

Morphometric measurements were made on 341 cartilaginous airways from 72 patients (mean 4.7, range 3 to 7 airways per patient). Mean airway size expressed as the P_{bm} was 13.8 ± 4.7 (5-33) mm. This corresponds to a mean airway diameter of 4.4 ± 1.5 (1.5-10.9) mm, or the fifth branch ± 1[21]. The mean intra-observer variability was -8.3 ± 7.5 % for WA_t and 0.1 ± 3.4 % for WA_{cart}. The mean inter-observer variability was -13.9 ± 11.1 % for WA_t and $2.6 \pm 3.7\%$ for WA_{cart}. The intra- and inter-observer variability for P_{bm}, P_{mo}, P_o, and WA_m has been described previously[22]. There was no systematic relationship between airway size (P_{bm}) and the intra- or inter-observer difference for any variable. Highly significant ($p < 0.001$) linear relationship were found between airway size (P_{bm}) and airway wall dimensions ($\sqrt{WA_t}$, $\sqrt{WA_{cart}}$) (Figure 5). The linear relationships for P_{bm} and WA_i, and WA_m have been described previously[22].

The mean membranous airways disease score (MADS) was 134 ± 47 (14-297). Among the six parameters evaluated, fibrosis followed by inflammation scored highest.

Structure Function Relationships

Table 3 shows pairwise the correlation coefficients for measurements of airflow
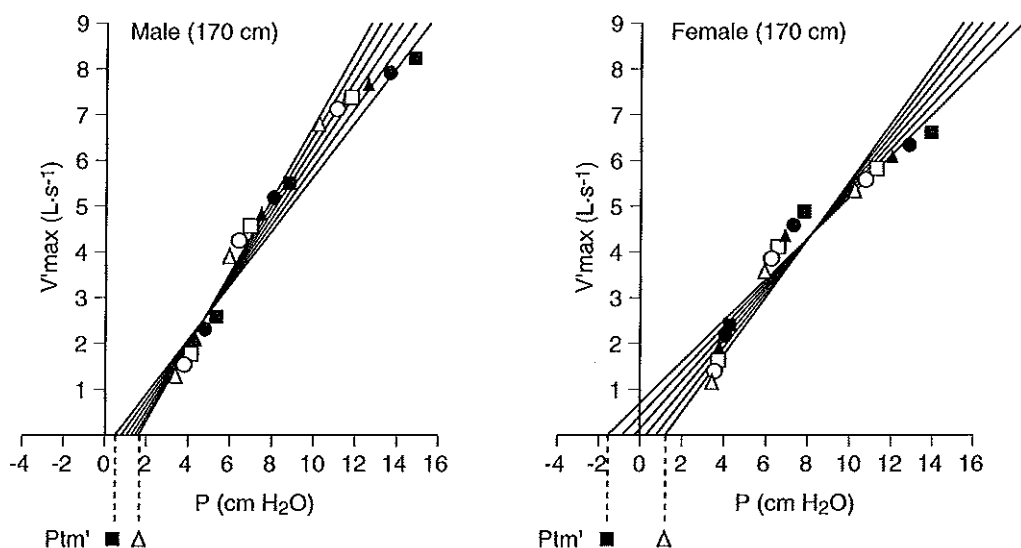
Figure 4. Change of the predicted maximal flow-static recoil (MFSR) plot with age for males and females of 170 cm height. The predicted MFSR plot is the regression line through predicted maximal flow (V'max) and predicted static transpulmonary pressures at 75, 50, and 25% vital capacity. The slope of the MFSR plot becomes steeper and the pressure axis intercept higher with increasing age both for males and females. Definition of abbreviations: Ptm' = critical transmural pressure causing airway collapse at the flow limiting segment; ■ = 20 yrs; ● = 30 yrs; ▲ = 40 yrs; □ 50 = yrs; O = 60 yrs; Δ = 70 yrs.

obstruction (FEV_1(%pred) and FEV_1/FVC(%pred)) and measurements of elastic recoil ($P_L$max(%pred) and P_L60(%pred)), upstream conductance (G_{us}%), airway collapsibility ($\Delta P_{tm}'$), airway wall dimensions (WA_i, WA_{cart}), and airway inflammation. Airflow obstruction increased with lower $P_L$max(%pred), P_L60(%pred), and G_{us}%. In a previous study, we showed that airflow obstruction increased significantly with thickening of WA_i but not with WA_m[22]. In this study, we found no significant correlation of airflow obstruction and WA_t (data not shown) or WA_{cart}. The predictive values of $P_L$max(%pred), P_L60(%pred), WA_i, and WA_{cart} for airflow obstruction were tested using multiple regression analysis. It was found that P_L60(%pred) (p = 0.006) and WA_i (p = 0.01) were both most predictive regarding FEV_1(%pred)(R^2 = 0.22) and FEV_1/FVC(%pred) (R^2 = 0.24). $P_L$max(%pred) and WA_{cart} did not add significantly to the predictive value for either FEV_1(%pred) or FEV_1/FVC(%pred).
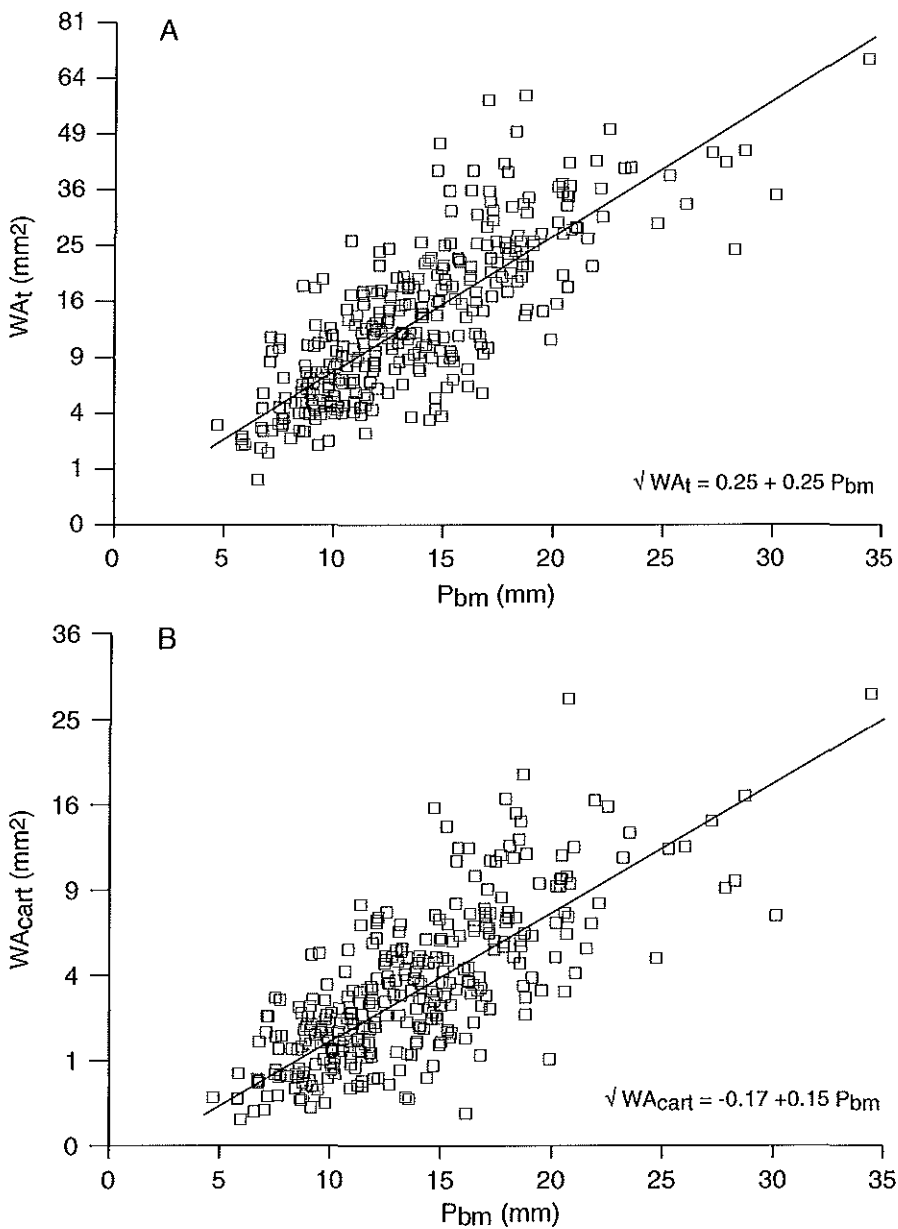
Figure 5. Morphometric airway dimensions versus airway size. There are 341 datapoints from 72 patients plotted in this figure. (A) WA_t = total wall area; P_{bm} = perimeter basement membrane. The regression line represents the relation between WA_t versus P_{bm}. (B) WA_{cart} = cartilage area. The regression line represent the relation between WA_{cart} versus P_{bm}.

G_{us}% decreased as the inner wall area became thicker (R = -0.25, p = 0.03, one sided) or as the MADS increased (R = -0.24, p = 0.04, one sided). G_{us}% did not correlate with any of the other airway dimensions (WA_t, WA_m, WA_{cart}). In addition, the predictive value of WA_i, WA_t, WA_m, WA_{cart} for G_{us} were tested using multiple regression analysis. WA_i was most predictive regarding G_{us}% (p = 0.04), WA_t, WA_m, and WA_{cart} did not add significantly to the predictive value regarding G_{us}%. $\Delta P_{tm}'$ as an estimate of airway collapsibility did not significantly correlate with airflow obstruction (FEV_1(%pred), FEV_1/FVC(%pred)), airway dimensions (WA_t, WA_i, WA_{cart}, WA_m), or to the MADS.

Discussion

In this study, we investigated whether airflow obstruction was related to lung elastic recoil pressure, airway conductance and collapsibility, and whether airway conductance and collapsibility were related to airway inflammation and airway wall dimensions. Airway conductance and collapsibility were calculated from MFSR plots. The results show a significant relationship between airflow obstruction and recoil, airflow obstruction and upstream resistance, and between the inner wall area and upstream conductance. No significant correlation was found for the MFSR plot estimate of airway collapsibility and airflow obstruction or airway wall dimensions or inflammation. The amount of cartilage was not correlated to airway inflammation or to airflow obstruction.

Airflow Obstruction in Relation to Lung Elastic Recoil, Airway Conductance, and Airway Collapsibility
One third of the patients studied suffered from mild-to-severe airflow obstruction. Lung elastic recoil, airway conductance, and airway collapsibility are all important in the pathogenesis of airflow obstruction. Loss of lung elastic recoil pressure results in a reduction of the driving force to generate airflow, and is thought to decrease airway conductance secondary to a loss of the tethering forces that distend the

Table 3

Correlation Coefficients of Structure Function Relationships

	FEV_1	FEV_1/FVC	$G_{us}\%$	$\Delta P_{tm}'$	$P_L max$	$P_L 60$	WA_i	WA_{cart}
FEV_1 %pred	-	0.67§	0.58§	ns	0.30†	0.35‡	-0.33‡	ns
FEV_1/FVC %pred	0.67§	-	0.47§	ns	0.55§	0.40‡	-0.32†	ns
$G_{us}\%$	0.58§	0.47§	-	ns	ns	ns	-0.25*	ns
$\Delta P_{tm}'$	ns	ns	ns	-	ns	-0.31†	ns	ns
$P_L max$ %pred	0.30†	0.55§	ns	ns	-	0.30†	ns	ns
$P_L 60$ %pred	0.35‡	0.40‡	ns	-0.31†	0.30†	-	ns	ns
WA_i	-0.33‡	-0.32†	-0.25*	ns	ns	ns	-	0.31†
WA_{cart}	ns	ns	ns	ns	ns	ns	0.31†	-
MADS	-0.30†	-0.28†	ns	ns	-0.30†	ns	0.4‡	ns

Definition of abbreviations: FEV_1 %pred = forced expiratory volume in 1; FEV_1/FVC %pred = forced expiratory volume in 1 as fraction of the vital capacity; $G_{us}\%$ = conductance upstream the flow limiting segment; $\Delta P_{tm}'$ collapsibility of flow limiting segment; $P_L max$ %pred = transpulmonary pressure at TLC; $P_L 60$ %pred = transpulmonary pressure at 60% TLC; WA_i = inner wall area; WA_{cart} = area of cartilage; MADS = membranous airways disease score. Level of significance: ns = not significant; * p = 0.06; † = p < 0.05; ‡ = p < 0.01; § = p < 0.001.

airways[1, 2, 23]. Airflow obstruction correlated significantly with loss of lung elastic recoil pressure in the group of patients studied.

The peripheral airway conductance has been found to be decreased in COPD. This implies that frictional losses in these airways will be increased[24, 25]. During forced expiration, equal pressure points are formed where lateral pressure losses due to frictional and convective acceleration equal the lung elastic recoil pressure. Flow-limiting segments are formed downstream from these equal pressure points[25]. As a result of increased frictional losses and/or the loss of recoil pressure, the equal pressure point will move upstream, to peripheral airways that are more collapsible than central airways. Therefore, a smaller pressure difference over the airway wall is required to collapse the airway. In the group of patients studied a strong correlation was found between the airway conductance upstream of the flow-limiting segment ($G_{us}\%$) and airflow obstruction (FEV_1, FEV_1/FVC). Airway collapsibility of the flow-limiting segment is thought to be an important determinant of airflow obstruction. In the present study, no significant correlation was found between the collapsibility of the flow-limiting segment as derived from the MFSR plot ($\Delta P_{tm}'$) and airflow obstruction. This could mean that collapsibility might not be an important factor, or that the $\Delta P_{tm}'$ does not adequately represents collapsibility of the flow-limiting segment. We think the latter is true for reasons stated below.

Airway Conductance and Collapsibility versus Structure and Inflammatory Changes.

Reduced airway conductance can result from inflammatory thickening of the airway wall, contraction of airway smooth muscle, loss of tethering forces by the parenchyma which surrounds the airways, and the presence of secretions within the lumen. Cosio and coworkers[17] showed that inflammation of the airways was related to airflow obstruction; this was not confirmed in a more recent study in a large group of patients[2]. Inflammation has been found to be related to the thickness of the airway wall in both cartilaginous and non-cartilaginous airways of patients with COPD[22, 26, 27]. In addition, we and others have previously shown that the thickness of the inner wall area is related to airflow obstruction ($FEV_1/FVC\%$)[22, 26]. In the present study, a significant

correlation was found between the thickness of the inner airway wall area and $G_{us}\%$. No significant relationship was found between $G_{us}\%$ and total airway wall thickness, which is likely to be explained by the more variable measurement of the latter.

During forced expiration, the airways will be compressed at and downstream from the flow-limiting segments and, therefore, maximal airflow is limited[25]. Airway wall structure and diameter are important determinants of the compressibility of the airway at the site of the flow-limiting segments. It is thought that the P_{tm}' as calculated from the MFSR model reflects the compressibility of the airways at the flow-limiting segment. The present study provides a number of observations that argue against the validity of P_{tm}' as a measure of the collapsibility of the flow-limiting segments. Firstly, airway cartilage is considered to be an important structure that resists dynamic compression[28]. We therefore expected a significant correlation between the amount of cartilage and P_{tm}'. In the present study, no such correlation could be demonstrated. Since the mechanical properties of airway cartilage were not investigated, it cannot exclude that these properties would relate to airway collapsibility. In fact, Moreno and coworkers[29] showed that the proteolytic enzyme, papain could weaken airway cartilage, while its histological appearance remained unchanged.

Secondly, it is likely that chronic inflammation affects the collapsibility of the airways at the flow-limiting segment. However, in the present study, no such significant correlation could be detected between airway inflammation parameters and $\Delta P_{tm}'$. Thirdly, increased thickness of the airway wall would be expected to decrease airway collapsibility[30]. Again, no correlation was found between total airway wall thickness, or inner wall thickness and $\Delta P_{tm}'$. Fourthly, airflow obstruction itself did not correlate to $\Delta P_{tm}'$.

Finally, we did not find an increase of P_{tm}' with age, as was predicted by our reference values. The increase in P_{tm}'(pred) is in agreement with the study by Yernault and coworkers[31], who found an increase of P_{tm}' versus age in a group of 74 healthy subjects. But, as was stated by these authors, a number of studies showed that airway compliance decreases with age[32, 33]. The increase of P_{tm}' with age could be explained by a more peripheral position of the flow-limiting segment, since peripheral airways are known to be more compliant than central airways[34].

We did not study whether smooth muscle tone or parenchymal tethering forces were correlated to $\Delta P_{tm}'$. Constriction of smooth muscle is known to decrease airway collapsibility[28, 35]. The importance of the lung parenchyma for airway collapsibility is still a matter of debate. The alveolar walls attach to the outside of the airway and probably provide an elastic load to airway smooth muscle when it shortens or when the airway is compressed[36]. Lamb and co-workers[37] found that loss of these alveolar attachments was associated with airflow obstruction, this was not found by others[2]. Since we found no significant correlations between airway dimensions, inflammation, or airflow obstruction and $\Delta P_{tm}'$, we think it unlikely that P_{tm}' is a valid estimate of the collapsibility of the flow-limiting segment. Calculation of P_{tm}' is determined by extrapolation of the MFSR curve to zero flow. This extrapolation assumes a linear behaviour of the maximal flow versus static recoil relationship below 30% FVC. If the pressure-flow relationship deviates from a linear relationship below 30% FVC, the actual and predicted zero flow intercept could be very different.

Airway Cartilage, Inflammation and Airflow Obstruction.
Previous studies have suggested that chronic inflammation reduces cartilage volume and, therefore, contributes to increased airflow obstruction[3, 6, 38, 39]. This was not confirmed in other studies[7, 8]. In the present study, we could not demonstrate a correlation between inflammatory changes in the airways and the amount of airway cartilage, nor a correlation between the amount of cartilage and the severity of airflow obstruction. The older studies that investigated the relation between inflammation and airway cartilage were handicapped by the fact that the appropriate method to correct for airway size was not yet known[40]. A recent study by Nagai and coworkers[6] expressed cartilage as a volume proportion of the total wall area. Inflammation of the airways results in an increased thickness of the airway wall and, therefore, could result in a reduced volume proportion of airway cartilage[22]. Since we investigated a large number of patients and corrected for airway size, we think that the volume of cartilage is not reduced by inflammation and is not related to airflow obstruction.

Table 4

Maximal Flow-Static Recoil Estimates of Airway Conductance and Collapsibility

First author		n	P_{tm}' cm H_2O		sG_{us} (cm$H_2O^{-1} \cdot s^{-1}$)	
Leaver[9]	Controls	10	-0.8	(3.8-1.7)	0.09	(0.06-0.12)
Zamel[41]	Controls	6	-	(0.5-0.9)	-	(0.08-0.14)
Tiddens	Predicted, all	59	1.05	(-0.95-2.5)	0.11	(0.08-0.15)
	Predicted, male	44	1.24	(0.13-2.54)	0.12	(0.10-0.15)
	Predicted, female	15	0.51	(-0.95-1.97)	-	(0.08-0.14)
Leaver	Patients	17	3.1	(0.6-5.8)	0.05	(0.02-0.08)
Zamel	Emphysema	5	-	(1.1-2.7)	-	(0.08-0.19)
Zamel	Peripheral obstr.	2	-	(1.5-3.3)	-	(0.05-0.09)
Tiddens	Patients, all	59	0.12	(-3.8-5.3)	0.13	(0.03-0.29)
	Male	44	0.15	(-3.8-4.8)	0.12	(0.03-0.29)
	Female	15	0.02	(-2.5-5.3)	0.14	(0.07-0.26)

Definition of abbreviations: n = number; sG_{us} = specific conductance upstream the flow-limiting segment calculated as G_{us} devided by TLC of patient; P_{tm}' = collapsibility of flow-limiting segment; Peripheral obstr. = patients with obstruction of peripheral airways

Predicted Values of Airway Conductance and Airway Collapsibility

To our knowledge no reference values are available for G_{us} and P_{tm}'. In previous studies, G_{us} was corrected for lung volume by dividing G_{us} by the predicted or actual TLC of the subject (Table 4)[9, 41]. In these studies, patients were compared to a limited number of healthy subjects, without matching for age or sex. Yernault and coworkers[31] described an increase in G_{us} with age that was comparable for males and females. G_{us} was higher in males than in females. We calculated predicted values for G_{us} and P_{tm}' (G_{us}(pred) and P_{tm}'(pred)) for each patient using reference values for both elastic recoil pressure and maximal expiratory flows[11, 14]. In agreement with the study of Yernault and coworkers[31], G_{us}(pred) and P_{tm}'(pred) increased with age and were higher for males than for females. An increase in G_{us} with age was described by a

number of authors[31, 42-44]. The decrease of maximal flows at fixed lung volumes, with increasing age, is predominantly related to decreased lung elastic recoil pressure. Our results suggest that the decrease in recoil is greater than the decrease in flow. We speculate that this preservation of flow could be the result of a disproportionately greater loss of elasticity in the airways relative to the loss of recoil in the parenchyma. This could cause airways to be more distended at any lung elastic recoil pressure.

Our predicted values for G_{us} and P_{tm}' were derived from two prediction equations generated in different groups of normal subjects. It can be argued that the increase in predicted G_{us} is an artifact caused by combining the two sources of data. However, we do not believe that this is the case. The mean value for G_{us}, for the 9 normal male subjects of Leaver and coworkers[9] (mean G_{us} = 0.65 L·s^{-1}·cmH$_2$O^{-1}; mean age = 35 yrs) fall within the predicted normal range (Figure 3). In addition, in this study we calculated the mean G_{us} for the 23 male subjects (mean age 63 yrs; height 174 cm) without airflow obstruction (FEV$_1$/VC (pred) > -2 SD) and for the 21 male subjects (mean age 62 yrs; height 173 cm) with airflow obstruction (FEV$_1$ /VC(pred) < -2 SD). For patients without airflow obstruction, G_{us} was 1.04 L·s^{-1}·cmH$_2$O^{-1} (134%pred), for patients with airflow obstruction G_{us} was 0.63 L·s^{-1}·cmH$_2$O^{-1} (80%pred). The increased G_{us} in the patients without airflow obstruction could be explained by the same process we have invoked from the age related increases; a greater loss of airway elasticity than lung elasticity. The decreased G_{us} in the patients with airflow obstruction is likely to be caused by inflammatory thickening of the inner wall area.

Conclusion

In a group of 59 COPD patients strong correlations were found between airflow obstruction on the one hand and lung elastic recoil and airway conductance on the other. No correlation was found between airflow obstruction and measures of airway collapsibility. Airway conductance was correlated to the inner wall thickness. No correlation was found between airflow obstruction and the volume of airway cartilage. Nor was there a significant correlation between the volume of the cartilage and airway inflammation. Therefore, changes in the amount of cartilage are probably not impor-

tant for the pathogenesis of chronic obstructive lung disease. Finally none of the airway dimensions was related to the maximal flow-static recoil plot estimate of airway collapsibility. Therefore, we think that the maximal flow-static recoil model does not adequately estimate the collapsibility of the flow-limiting segment.

Acknowledgements

References

1. Zapletal A, Desmond KJ, Demizio D, Coates AL. Lung recoil and the determination of airflow limitation in cystic fibrosis and asthma. Pediatric Pulmonol 1993;15:13-18.
2. Hogg JC, Wright JL, Wiggs BR, Coxson HO, Opazo Saez A. Lung structure and function in cigarette smokers. Thorax; 1994;49:473-478.
3. Tandon MK, Cambell AH. Bronchial cartilage in chronic bronchitis. Thorax 1969;24:607-612.
4. Thurlbeck W, Dunhill M, Hartung W. A comparison of three methods of measuring emphysema. Hum Pathol 1972;1:215-226.
5. Nagai A, West WW, Paul JL, Thurlbeck WM. The national institutes of health intermittent positive pressure breathing trial: pathology studies. Am Rev Respir Dis 1985;132:937-945.
6. Nagai A, Thurlbeck WM, Konno K. Responsiveness and variability of airflow obstruction in chronic obstructive pulmonary disease. Am J Respir Crit Care Med 1995;151:635-639.
7. Dunhill MS, Massarella GR, Anderson JA. A comparison of the quantitative anatomy of the bronchi in normal subjects, in status asthmaticus, in chronic bronchitis, and in emphysema. Thorax 1969;24:176-179.
8. Mullen JB, Wright JL, Wiggs BR, Paré PD, Hogg JC. Reassessment of inflammation of airways in chronic bronchitis. B M J (Clin Res Ed) 1985;291(6504):1235-1239.
9. Leaver DG, Tattersfield AE, Pride NB. Contributions of loss of lung recoil and of enhanced airways collapsibility to the airflow obstruction of chronic bronchitis and emphysema. J Clin Invest 1973;52:2117-2128.
10. American Thoracic Society. Standards for the diagnosis and care of patients with chronic obstructive pulmonary disease (COPD) and asthma. Am Rev Respir Dis 1987;136:225-243.
11. Quanjer PH, Dalhuijsen A, Zomeren BC. Summary equations of reference values. Bull Eur Physiopathol Respir 1983;19(suppl 5):45-51.
12. Mead J, Whittenberger JL. Physical properties of human lungs measured during spontaneous respiration. J Appl Physiol 1953;5:779-796.
13. Glaister DH, Schroter RC, Sudlow MF, Milic-Emili J. Bulk elastic properties of excised lungs and the effect of a transpulmonary pressure gradient. Respir Physiol 1972;17:347-364.
14. Colebatch HJH, Greaves IA, Ng CKY. Exponential analysis of elastic recoil and aging in healthy males and females. J Appl Physiol 1979;47(7):683-691.
15. Pride NB, Permutt S, Riley RL, Bromberger-Barnea B. Determinants of maximal expiratory flow from the lungs. J Appl Physiol 1967;23:646-662.
16. Bai A, Eidelman DH, Hogg JC, James RK, Ludwig MG, Martin J, McDonald DM, Mitzner WA, Okazawa M, Pack RJ, Paré PD, Schellenberg RR, Tiddens HAWM, Wagner EM, Yager D. Proposed nomenclature for quantifying subdivisions of the bronchial wall. J Appl Physiol 1994;77(2):1011-1014.
17. Cosio M, Ghezzo H, Hogg JC, Corbin R, Loveland M, Dosman J, Macklem PT. The relations between structural changes in small airways and pulmonary-function tests. N Engl J Med 1977;298:1277- 1281.
18. Wright JL, Cosio M, Wiggs B, Hogg JC. A morphologic grading scheme for membranous and respiratory bronchioles. Arch Pathol Lab Med 1985;109(2):163-5.
19. Feldman HA. Families of lines: random effects in linear regression analysis. J Appl Physiol 1988; 64(4):1721-1732.
20. Schluchter MD. Module 5V. In: Dixon WJ, ed. BMDP Statistical Software Manual. Burkely, University of California press, 1990;1207-1244.
21. Hammersley JR, Olson DE. Physical models of the smaller pulmonary airways. J Appl Physiol 1992;72(6):2402-2414.
22. Tiddens HAWM, Paré PD, Hogg JC, Hop WCJ, Lambert R, de Jongste JC. Cartilaginous airway dimensions and airflow obstruction in human lungs. Am J Respir Crit Care Med 1995;152:260-266.

23. Fraser RG. Measurements of the calibre of human bronchi in three phases of respiration by cinebroncho-graphy. J Can Assoc of Radiol 1961;12:102-112.

24. Yanai M, Sekizawa K, Ohrui T, Sasaki H, Takishima T. Site of airway obstruction in pulmonary disease: direct measurement of intrabronchial pressure. J Appl Physiol 1992;72(3):1016-1023.

25. Pedersen OF, Thiessen B, Lyager S. Airway compliance and flow limitation during forced expiration in dogs. J Appl Physiol 1982;52:357-369.

26. Bosken CH, Wiggs BR, Paré PD, Hogg JC. Small airway dimensions in smokers with obstruction to airflow. Am Rev Respir Dis 1990;142(3):563-570.

27. Kuwano K, Bosken CH, Paré PD, Bai TR, Wiggs BR, Hogg JC. Small airways dimensions in asthma and chronic obstructive pulmonary disease. Am Rev Respir Dis 1993;148:1220-1225.

28. Olsen CR, Stevens AE, Pride NB, Staub NC. Structural basis for decreased compressibility of constricted trachea and bronchi. J Appl Physiol 1967;23(1):35-39.

29. Moreno RH, McCormack GS, Brendan J, Mullen M, Hogg JC, Bert J, Paré PD. Effect of intravenous papain on tracheal pressure-volume curves in rabbits. J Appl Physiol 1986;60(1):247-52.

30. Lambert RK, Codd SL, Alley MR, Pack RJ. Physical determinants of bronchial mucosal folding. J Appl Physiol 1994;77(3):1206-1216.

31. Yernault J-C, de Troyer A, Rodenstein D. Sex and age differences in intrathoracic airways mechanics in normal man. J Appl Physiol 1979;46:556-564.

32. Croteau JR, Cook CD. Volume-pressure and length-tension measurements in human tracheal and bronchial segments. J Appl Physiol 1960;16:170-172.

33. Wilson AG, Massarella GR, Pride NP. Elastic properties of airways in human lungs postmortem. Am Rev Respir Dis 1974;110:;716-729.

34. Tisi GM, Minh VD, Friedman PJ. In vivo dimensional response of airways of different size to transpulmonary pressure. J Appl Physiol 1975;39(1):23-29.

35. Okazawa M, Paré PD. Pressure area relationship of membranous airways in rabbit. Am J Respir Crit Care Med 1994;149(4):A770.

36. Paré PD, Bai TR. The consequences of chronic allergic inflammation. Thorax 1995;50:328-332.

37. Lamb D, McLean A, Gillooly M, Warren PM, Gould GA, MacNee W. Relation between distal airspace size, bronchiolar attachments, and lung function. Thorax 1993;48:1012-1017.

38. Maisel JC, Silvers GW, Mitchell RS, Petty TL. Bronchial atrophy and dynamic expiratory collapse. Am Rev Respir Dis 1968;98:988-997.

39. Thurlbeck WM, Pun R, Toth J, Frazer RG. Bronchial cartilage in chronic obstructive lung disease. Am Rev Respir Dis 1974;109:73-80.

40. James AL, Hogg JC, Dunn LA, Paré PD. The use of the internal perimeter to compare airway size and to calculate smooth muscle shortening. Am Rev Respir Dis 1988;138(1):136-139.

41. Zamel J, Hogg J, Gelb A. Mechanisms of maximal expiratory flow limitation in clinically unsuspected emphysema and obstruction of the peripheral airways. Am Rev Respir Dis 1975;113:337-345.

42. Gelb AF, Zamel N. Effect of aging on lung mechanics in healthy nonsmokers. Chest 1975;68:539-541.

43. Mead J, Turner JM, Macklem PT, Little JB. Significance of the relationship between lung recoil and maximum expiratory flow. J Appl Physiol 1967;22(1):95-108.

44. Gibson GJ, Pride NB, O'Cain C, Quagliato R. Sex and age differences in pulmonary mechanics in normal nonsmoking subjects. J Appl Physiol 1967;41:20-25.

The Micro-Plethysmograph: a New Device to Measure Small Volume Displacements by Isolated Human Airway Segments

Harm A.W.M Tiddens, Wim P. Holland, Julius de Vries, and Johan C. de Jongste

Department of Pediatrics, Division of Respiratory Medicine, Central Instrumentation Department, Electronic Data Processing Department of Erasmus University and University Hospital/Sophia Children's Hospital, Rotterdam, The Netherlands

Introduction

The contraction of smooth muscle in isolated airway segments can be measured in several ways. First, as a change in flow or perfusion pressure in perfused airway segments[1-5]. Second, as a change in lumen narrowing with the application of video-imaging[6]. Third, as a change in pressure in a constant volume fluid-filled airway segment (isometric contraction)[7, 8], or as a change of volume in a constant pressure fluid-filled airway segment (isobaric contraction)[7]. Studies have been primarily done on isolated airway segments from animals. For human airways only limited data are available[4, 5, 9-11]. The methodology to study isobaric contraction of airway segments is not well established[7]. The aim of this work was to develop a sensitive device to assess the smooth muscle function in isolated airway segments under isobaric conditions. We developed a micro-plethysmograph that is able to measure small volumes (0.01 to 700 µL) displaced by a constricting or dilating airway segment at any given pre-load or transmural pressure. In addition, this device can be used to measure leak or diffusion at any transmural pressure.

Methods

Experimental set-up

Figure 1 shows the experimental set-up we used to measure the isobaric contraction and relaxation of airway segments, employing a special ultra-sensitive plethysmograph. In addition, this set-up can be used to measure isometric contraction, compliance, hysteresis, and collapsibility as described elsewhere[12]. It consists of a double jacketed organ bath in which an airway segment is mounted on 2 stainless steel cannulas. The organ bath is filled with Krebs-Henseleit buffer (composition in mM: NaCl 118, KCl 4.7, $CaCl_2$ 2.5, $MgSO_4$ 1.2, KH_2PO_4 1.2, $NaHCO_3$ 25, glucose 5.55) at a temperature of 37°C and continuously gassed with carbogen (5% CO_2 in 95% O_2). The airway segment and tubing are filled with buffer. Pressure is measured at both ends of the airway segment (P_{prox} and P_{dist}) using pressure transducers with a low compliance (143PC ± 1psi, Micro Switch, Freeport, Illinois, USA). All connecting tubing has a low compliance.
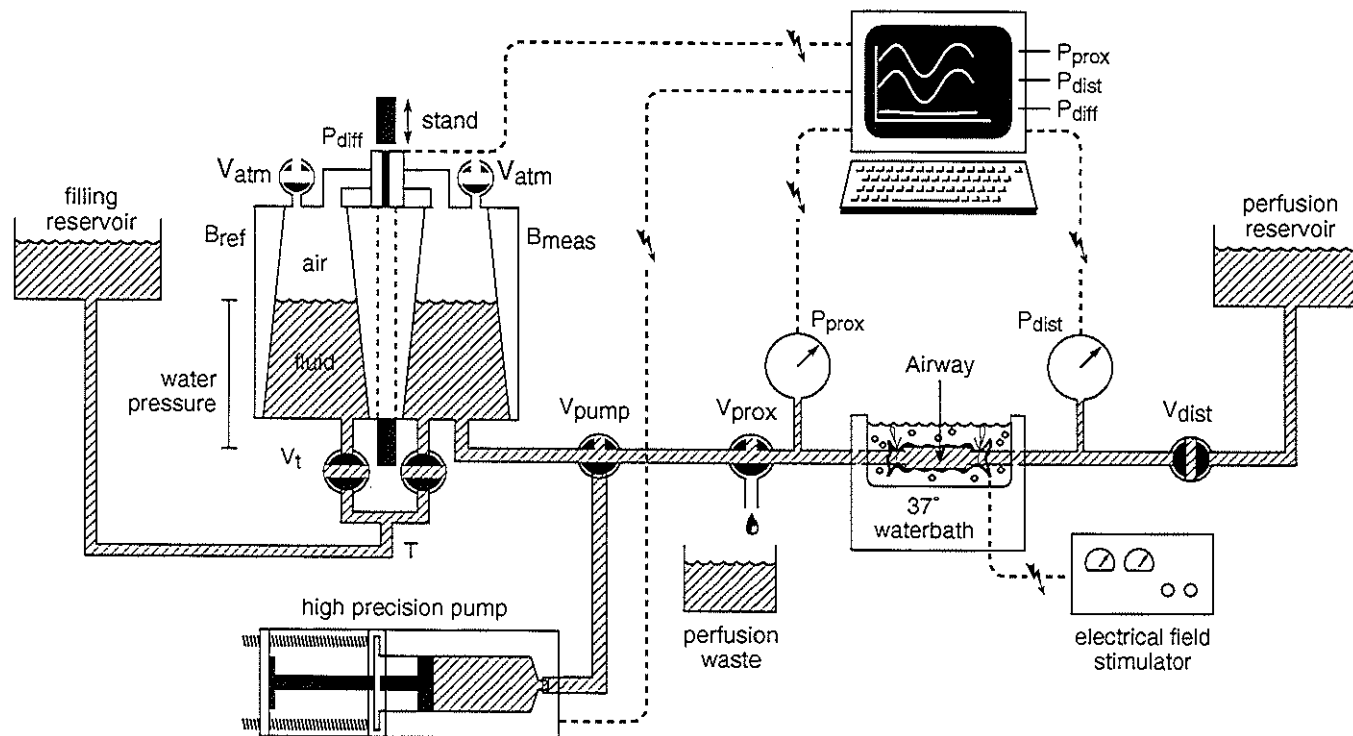
Figure 1. Diagram of the experimental set-up to measure dynamic properties of isolated airway segments. Definition of abbreviations: P_{diff} = differential pressure transducer; V_{atm} = valve to connect air compartment to atmosphere; B_{ref} = reference barrel; B_{meas} = measurement barrel; V_t = valves used for the filling and to obtain identical fluid levels in both barrels; T = large bore tubing; V_{pump} = valve to connect pump to plethysmograph or to airway; V_{prox} and V_{dist} = valves located at the proximal or distal end of the airway; P_{prox} and P_{dist} = pressure transducers to measure the transmural pressure at the proximal and distal end of the airway; The system is servo controlled, which means that the pressure signal from P_{prox} controls the syringe pump.

The compliance of the entire system is 0.03 µL cm H_2O^{-1}. By means of 3-way valves, the airway segment can be connected to a micro-plethysmograph. Furthermore, it can be connected to a reservoir filled with buffer for perfusion. Finally, it can be connected to a gas-tight syringe mounted on a computer controlled high-precision syringe pump (Harvard 22, Harvard Apparatus Inc, South Natick, MA, USA) for inflation and deflation.

Micro-plethysmograph

DESIGN. The micro-plethysmograph (Figure 1) consists of 2 identical water- and air-tight cone-shaped plexiglass barrels each with a maximal filling volume of 350 mL. One is a measurement barrel (B_{meas}) which can be connected to the airway or to the pump, while the other serves as reference barrel (B_{ref}). Both barrels can be filled with buffer to any desired volume by opening a valve located at the bottom of the barrels which connects these to a filling reservoir by means of large bore tubing (T) .

The valves (V_t), located in the large bore tubing, are kept open during the filling process so the barrels communicate and therefore will contain identical fluid levels. After the filling process the valves (V_t) are closed. The air compartments of the barrels are connected by non compliant tubing, located on top of the barrels, to the side-ports of a differential pressure transducer (pressure range 0-2 cm H_2O, LCVR, Celesco, Canoga Park, CA, USA).

Pressure or temperature changes in the environment will affect both barrels simultaneously and therefore will have little if any effect on the differential pressure. The high storage capacity for heat of the buffer used to fill the barrels adds to the temperature stability of this micro-plethysmograph.

To set the differential pressure between the barrels at 0 cm H_2O, valves (V_{atm}) located on top of the micro-plethysmograph can be opened to connect the air compartments of the barrels to the atmosphere. The plethysmograph is in the measurement mode when both top valves (V_{atm}) and bottom valves (V_t) are closed. Any volume change within the measurement barrel (B_{meas}) will result in a change of the differential pressure. The measurement barrel can be connected by means of a 3-way valve to a high-precision syringe pump to calibrate the micro-plethysmograph.

For measurements, the micro-plethysmograph is connected to the cannulated airway in the organ bath.

The plethysmograph is mounted on a stand and its height can be varied in a precise but slow manner by micro screw, or in a gross but quick fashion by unlocking a clamp and sliding the plethysmograph up or down the stand manually.

MEASUREMENT RANGE AND RESOLUTION. The resolution of the micro-plethysmograph depends on the volume of the air compartment in the barrels. This volume can be varied anywhere between 5 and 350 mL by changing the fluid levels within the barrels. In the case of a low fluid level, and therefore a big air volume, the sensitivity of the micro-plethysmograph to volume changes will be low but the range that can be measured will be large. In the case of a high fluid level and therefore a small air volume, the sensitivity to volume changes will be high but the range that can be measured will be small. The resolution and maximal measurement range of the plethysmograph depends also upon the sensitivity of the differential pressure transducer. The differential pressure transducer we used is available for pressure ranges from 0-2 to 0-1000 cm H_2O. For our study we used a pressure range of 0 to 2 cm H_2O.

TRANSMURAL PRESSURE. The transmural pressure is measured at both ends of the airway with pressure transducers (P_{prox} and P_{dist}). These transducers are connected to outlets at the side of the cannulas by tubing of low compliance. Because airway, cannulas, and tubing are all fluid filled, transmural pressure changes of the airway can be readily detected. In order to set the transmural pressure of the airway, its lumen is connected to the micro-plethysmograph while the distal valve (V_{dist}) is closed. The airway is considered patent when the pressures measured at the proximal and distal end of the airway (P_{prox} and P_{dist}) are identical. The transmural pressure in the airway is now the sum of three factors. The first factor is the hydrostatic pressure which depends on the height of the fluid column in the measurement barrel relative to the level of the airway. The second factor is the pressure in the air compartment of the measurement barrel relative to the atmosphere. This pressure is atmospheric when the top valves (V_{atm}) are opened. With the top valves (V_{atm}) closed, volume changes within the air chamber of the measurement compartment will change the pressure

within the air compartment and therefore the transmural pressure. To correct for these pressure changes the height of the micro-plethysmograph can be adjusted to keep the transmural pressure at a constant level. The third factor is the height of the fluid column on top of the airway within the water-bath. In our experiments we keep this factor small by submerging the airway just below the surface of the fluid.

CALIBRATION AND DRIFT. A calibration and drift procedure is done before each measurement because volume changes within the micro-plethysmograph and changes in ambient temperature and pressure could affect its calibration and stability. The micro-plethysmograph is calibrated by a semi-automated procedure as follows (Figure 2). First, the measurement barrel (B_{meas}) is connected to the high-precision pump with valve (V_{pump}). The first differential pressure is set while both top valves (V_{atm}) are opened to the atmosphere. Therefore, this pressure should be 0 cm H_2O (Figure 2). Next, the top valves are simultaneously closed and a preset volume of fluid is automatically infused in one minute by the pump into the measurement barrel (B_{meas}). There should be a perfect linear relation between the infused volume and the differential pressure (cal in Figure 2). Immediately after infusion has been completed, the second differential pressure is automatically recorded by the computer. Next, the computer calibrates the calculated difference between the two pressures into the infused volume. These known pressures and volumes are used for calibration purposes. After infusion of the calibration volume the recording is continued for another minute to record drift (drift 1 in Figure 2). Next, the top valves (V_{atm}) are re-opened to reset the differential pressure at 0 cm H_2O.

Signal processing

The signals from the differential pressure transducer, the transmural pressure transducers (P_{prox} and P_{dist}), and from the high precision pump are processed on-line by a computer (at least 486SX, 25 MHZ). The analog signal generated by the differential pressure transducer (P_{diff}) is first excited and demodulated (LCCD-005, Celesco, Canoga Park, CA, USA). Full scale voltage output is ± 5 V. All signals are converted to digital signals (DAS 1601, Keithley, Taunton, MA, USA). Full scale digital output of this converter is reached at an analogue input of ± 10 V.
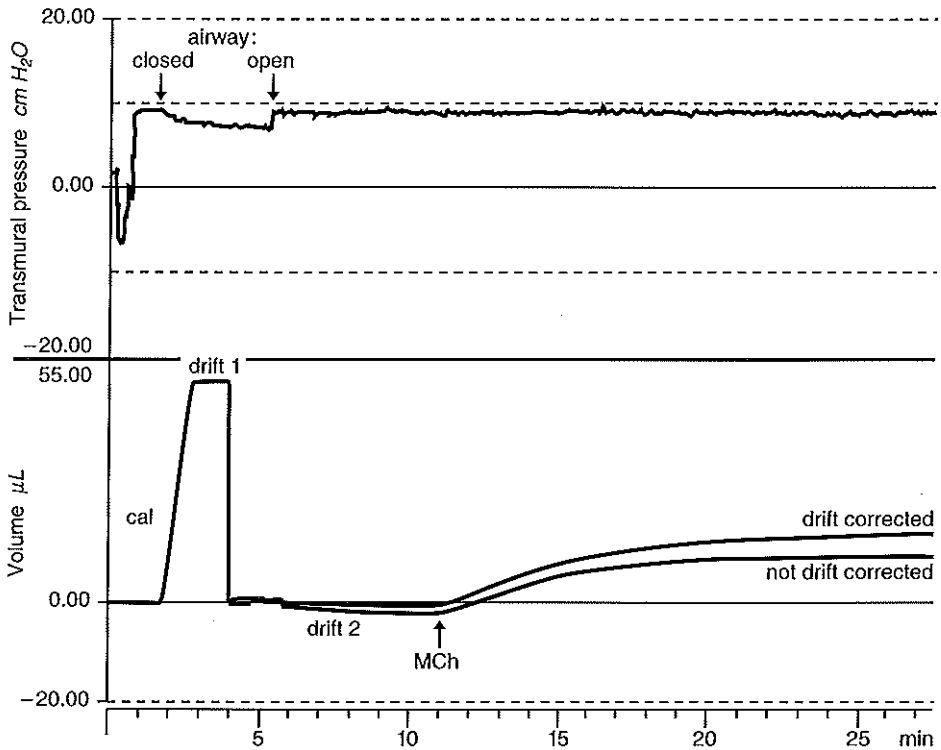
Figure 2. Shows an isobaric contraction after stimulation of the smooth muscle with methacholine. The upper panel shows the transmural pressure measured at the proximal end of the airway. The lower panel shows the volume signal of the plethysmograph. Definition of abbreviations: airway closed = during calibration the airway is closed at both ends; cal = calibration volume is infused into plethysmograph; drift1 = registration of drift of plethysmograph the first minute after infusion of calibration volume; airway open = after calibration and drift have been recorded airway is re-connected to plethysmograph; drift 2 = recording of drift after the plethysmograph is connected to the airway; MCh = moment when methacholine (10^{-4}M) is added to the organ bath. Next fluid is pumped by the airway into the plethysmograph; drift corrected = recording after correction for drift 2.

The absolute accuracy of the converter is 0.01% of the reading + 1, maximal error is 0.03%. All signals are simultaneously displayed on-line on the PC-screen by a multi-channel registration program (MKR system, custom-made software, Erasmus University and University Hospital/Sophia Children's Hospital, Rotterdam, The Netherlands). In our computer setup the sampling rate can be varied between 0.01 and 4000 Hz.
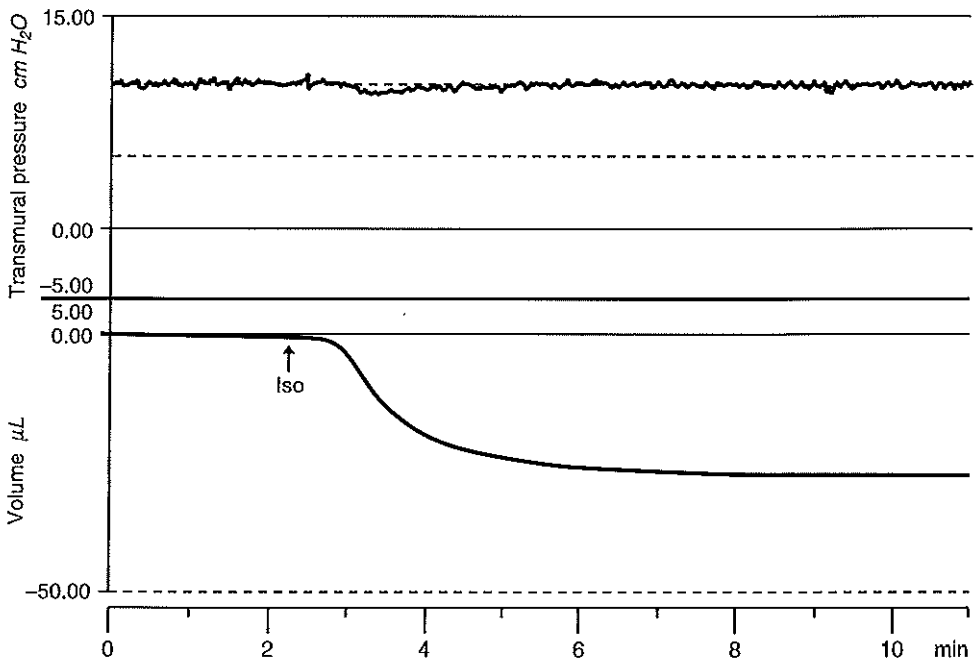
Figure 3. Isobaric relaxation after stimulation of the smooth muscle with isoprenaline (10^{-4} M). The upper panel shows the transmural pressure measured at the proximal end of the airway. The volume signal is corrected for drift as shown in Figure 2. The arrow indicates the moment when isoprenaline (Iso) is added to the organ bath, fluid moves out the plethysmograph into the relaxing airway. Note that the transmural pressure within the airway remains at a constant level during the relaxation.

RESOLUTION OF PLETHYSMOGRAPH. In our setup we use a 12 bit A/D-convertor, the resolution of the digitized signal is therefore maximally 4096 levels. Input sensitivity of the DAS-1601 convertor is software programmable and provides gains of 1, 10, 100, and 500 V. In our setup we used an analog input of ±10 V. The analog input from the differential pressure transducer (P_{diff}) was ± 5 V resulting in a maximal digital output of 2048 levels. When the volume of the air compartments is 5 mL, the estimated measurement range will be ± 10 µL (Table 1). The theoretical resolution at this level will therefore be 20 µL / 2048 or 0.01 µL. With air compartments of 300 mL, the corresponding maximal measurement range will be ± 600 µL. The theoretical resolution will then be 1200 µL /2048, or 0.59 µL. Experiments to define the technical properties of plethysmograph

Table 1

VOLUME OF AIR COMPARTMENT AND RESOLUTION

Volume air compartment (mL)	Volume measurement range (µL)	Theoretical resolution (µL)
5	± 10	0.01
10	± 20	0.019
50	± 100	0.098
100	± 200	0.2
150	± 300	0.29
200	± 400	0.39
250	± 500	0.49
300	± 600	0.59
350	± 700	0.68

Experiments to define the technical properties of plethysmograph

DIFFERENTIAL PRESSURE TRANSDUCER AND STABILITY OF SIGNAL. We evaluated the static common mode rejection of the differential pressure transducer for different pressure levels. To do this, we connected the tubes coming from the 2 side ports of the differential pressure transducer (P_{diff}) to a four-way valve. Next, a gastight syringe (0-100 µL TLL, Hamilton, Reno, Nevada, USA) was connected to another inlet of the valve. The remaining inlet of the valve was connected by tubing of low compliance to a virtually noncompliant pressure transducer (143PC ± 1psi, Micro Switch, Freeport, Illinois, USA). Next, we fluctuated the pressure in this closed system in a cyclic fashion between -5 and 5 cm H_2O by moving the plunger of the syringe.

CALIBRATION, RESOLUTION, AND DRIFT. We measured reproducibility of calibration, resolution, and drift of the micro-plethysmograph at 5 different air volume levels of the air compartment (3, 9, 19, 74, and 290 mL) as follows. The differential pressure

signal was sampled at a rate of 60 Hz. At each air volume level we infused, in one minute, a calibration volume of 50% of the estimated measurement range (5, 10, 20, 75 and 300 μL) into the measurement barrel (B_{meas}) with the automated calibration procedure. Drift was recorded for one minute after infusion, after which the top valves were opened and left open for an equilibration period of five minutes. This period was chosen to reduce possible temperature effects by the calibration procedure on the baseline recording of drift. Next, the top valves were closed again for 30 minutes to record baseline drift. After this drift recording, the top valves were opened again to reset P_{diff} at 0 cm H_2O. Finally, three complete calibration procedures were done one after another. We calculated for each volume level the mean and range of the infused volume and resolution of the calibration procedure. Furthermore, we calculated the drift following calibration and the baseline drift.

TEMPERATURE RELATED DRIFT. To estimate the temperature related drift of the micro-plethysmograph we simultaneously measured the differential pressure (P_{diff}) and the temperature in the laboratory. Temperature was measured using a thermocouple probe (DU-3, Ellab, Copenhagen, DK). The plethysmograph had a volume of the air compartments of 19 mL corresponding to a measurement range of ± 40 μL. For this recording both barrels were connected to the differential pressure transducer (P_{diff}). Recording was started at a differential pressure of 0 cm H_2O. Temperature and pressure were sampled at a rate of 60 Hz. Recording continued for 24 hours. We knew that within this time frame the ambient temperature would change because of automatic changes of the building's climate control settings.

Examples of measurements of isobaric contraction and relaxation
PREPARATION OF AIRWAY SEGMENT. A human peripheral airway was dissected out from a lobectomy specimen. Parenchyma and blood vessels were removed from the airway using a dissection microscope (Stemi 2000, Carl Zeiss, Oberkochen, Germany) and external cold light source (KL1500 electronic, Schott, Wiesbaden, Germany). All side branches were identified and ligated to make the airway watertight. Next, the airway was mounted in the organ bath onto stainless steel cannulas in a watertight fashion (Figure 1). The airway was perfused to test for patency and possible leaks.

BASELINE DRIFT. The plethysmograph was filled with buffer to obtain an appropriate measurement range for the cannulated airway. Next, the plethysmograph was calibrated and its drift recorded. The airway was connected to the plethysmograph while the top valves of the plethysmograph were open. The transmural pressure was set at 10 cm H_2O by adjusting the height of the plethysmograph. Next, V_{atm} were closed and baseline volume displacement out of the plethysmograph recorded for 2 minutes to estimate drift and fluid loss due to leak (drift 2, Figure 2). After this procedure airway smooth muscle was either contracted or relaxed.

ISOBARIC CONTRACTION AND RELAXATION (PHARMACOLOGIC STIMULATION). Sufficient methacholine (or isoprenaline) was added to the organ bath to produce a $10^{-4}M$ solution. The contractile or relaxation response of the airway was recorded until no more fluid was displaced into or out of the plethysmograph.

ISOBARIC CONTRACTION (ELECTRICAL FIELD STIMULATION). The airway was stimulated 10 times with electrical field stimulation via platinum plate electrodes parallel to the tissue (30 sec trains of 30 V, 0.3 msec, 30 Hz square pulses of alternating polarity). During these stimulations, the height of the plethysmograph relative to the airway was adjusted manually to compensate for pressure changes within the air compartment.

Results

Differential pressure transducer and common mode rejection
The differential pressure remained 0.00 ± 0.01 cm H_2O while the pressure at both sides of the transducer was increased.

Calibration, resolution and drift
CALIBRATION. Zero differential pressure did not vary between calibration procedures. However, by closing the top valves the P_{diff} increased by 23 bits at the most sensitive setting of the plethysmograph and by 2 bits at its least sensitive setting. We calculated that the resolution was reduced as a result of this artifact by 1.1 to 0.3 % for its most and least sensitive setting respectively. The time of infusion was 60.59 ± 0.2 (60.28 to 60.7) seconds. The overall variability between the volumes

infused for the calibration procedure was 2.5 and 0.4% for its most and least sensitive setting respectively.

RESOLUTION. Table 2 shows the maximal achieved resolution with the micro-plethysmograph in relation to the volume of the air compartment in the plethysmograph. At its most sensitive setting a volume change of 0.017 µL in the micro-plethysmograph could be detected. At its least sensitive setting, a change of 0.421 µL could be detected.

DRIFT. The absolute drift in the first minute after infusion of the calibration volume was highest when the plethysmograph was in its least sensitive setting (Table 2). When drift was expressed as percentage change of volume infused per minute, it was 2.6 and 1.8 % min^{-1} for its most sensitive and least sensitive settings respectively. Baseline drift 5 minutes after the calibration procedure was 1.7 and 0.2 % min^{-1} of volume infused for its most sensitive and least sensitive settings respectively.

TEMPERATURE-RELATED DRIFT. The temperature varied between 20.5°C at night and 21.73°C during the day. The shift of the temperature from one steady state situation to the next took place over a period of four hours. Drift varied maximally between -0.15 and 0.16 µL min^{-1} or $\pm$ 0.4% of the volume measurement range during the 24 hours recording. Drift was fastest during temperature shifts. At night, temperature remained stable at 20.7°C for 10 hours. Drift remained constant in this period at a level of 0.03 µL min^{-1} or 0.07% min^{-1} of the volume measurement range.

EXAMPLES OF ISOBARIC CONTRACTION AND RELAXATION. The airway that was cannulated for the isobaric contraction after methacholine had an internal radius of 1 mm and length of 12.6 mm. The estimated volume was therefore 40 µL. Figure 2 shows the recording of the isobaric contraction and relaxation. The measurement range of the plethysmograph was set at a full-scale resolution of $\pm$ 100 µL. First, the plethysmograph was calibrated with a volume of 50 µL in 1 minute (Figure 2). Note the straight linear relation between volume and time while the fluid was pumped into the plethysmograph. The drift of the micro-plethysmograph after infusion of 50 µL was 0.18 µL min^{-1}. Drift and leak when the airway was connected to the plethysmograph was 0.34 µL min^{-1}. After the airway was constricted with methacholine, it displaced a volume of 16.7 µL (corrected for baseline drift) in 15 minutes. Note that the transmural pressure remained constant during the contraction since we

Table 2

RESOLUTION AND DRIFT CHARACTERISTICS OF THE MICRO-PLETHYSMOGRAPH

Volume air compartment (mL)	Volume calibration (μL)	Volume infused (μL)	Resolution observed (μL)	Absolute drift first minute (μL min^{-1})	Relative drift first minute (% min^{-1})
3	5	4.7 (4.6 to 4.7)	0.017	-0.1 (-0.08 to -0.17)	2.6
9	10	9.2 (9.1 to 9.3)	0.025	-0.2 (-0.14 to -0.3)	2.2
19	20	19.1 (18.9 to 19.3)	0.046	-0.2 (-0.09 to -0.37)	1.2
74	75	74.5 (74 to 75)	0.103	-0.5 (-0.21 to -1.13)	0.7
290	300	295.8 (295.8 to 299.2)	0.421	-5.2 (-4.14 to -6.7)	1.8

Values of volume infused and absolute drift are presented as means and range in parenthesis. Volume air compartment = volume of air in the barrels which sets the resolution of the plethysmograph; Volume calibration = preset volume used for calibration procedure; Volume infused = pump speed multiplied by actual time of infusion; Resolution observed = volume infused divided by the number of pixels; Absolute drift = drift in first minute directly after infusion of the calibration volume in μL; Relative drift = drift in first minute directly after infusion of the calibration volume in percentage of the volume infused
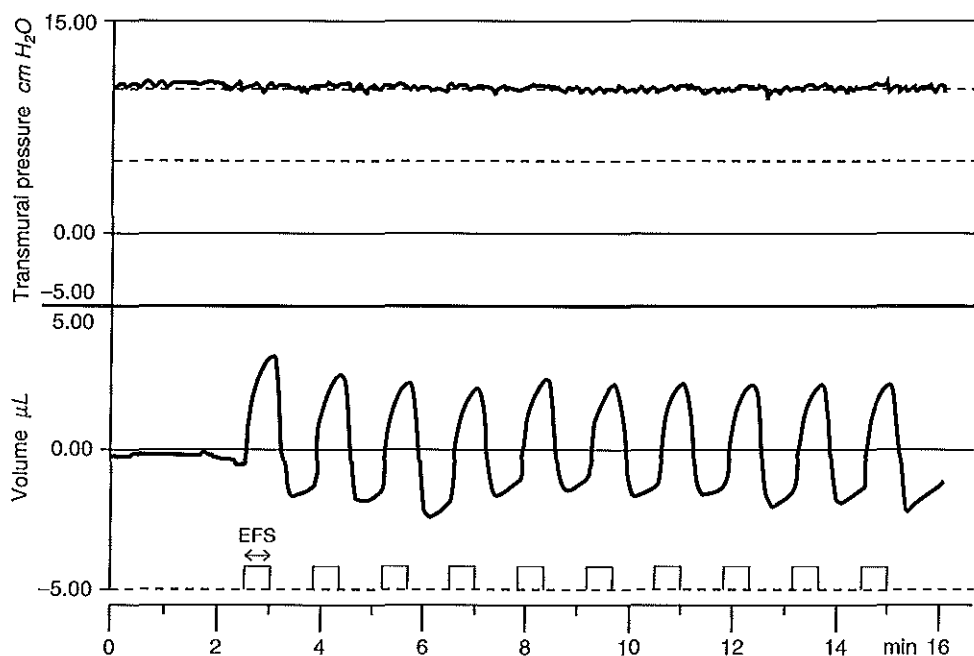
Figure 4. Example of repetitive isobaric contraction of an isolated airway segment. The upper panel shows the transmural pressure measured at the proximal end of the airway. The volume signal is corrected for drift as shown in Figure 2. Arrows indicate the onset and end of the electrical field stimulation (EFS). After onset of a stimulus fluid is pumped by the airway into the plethysmograph. Note that the transmural pressure within the airway remains at a constant level during the contractions.

compensated for the increase in pressure in the air compartment by adjusting the level of the plethysmograph.

Figure 3 shows the same airway as in Figure 2 but after relaxation with isoprenaline. A volume of 26.2 μL moved from the plethysmograph into the airway in 10 minutes. Figure 4 shows the contractile response of a second airway with an internal radius of 1 mm and length of 12.7 mm. The estimated volume was therefore 40 μL. Drift and leak of the airway connected to the plethysmograph was 0.58 μL min^{-1}. The airway was stimulated 10 times with electrical field stimulation (30 sec trains of 30 V, 0.3 msec, 30 Hz). The airway pumped an average volume of 3.73 sem ±0.05 range 3.43 to 4.03 μL.

Discussion

This micro-plethysmograph is, to our knowledge, the first instrument capable of measuring true isobaric contraction or relaxation of airway tube preparations. The micro-plethysmograph is able to measure small volume displacements by a contracting airway at any given pre-load or transmural pressure in a highly sensitive and reproducible way. With the micro-plethysmograph, we are able to measure the contractile properties of airway tube preparations within a diameter range of 1 to 5 mm, a length range of 5 to 20 mm, and a volume range of 3 to 400 μL with high accuracy. The most sensitive setting is used when we measure times airways that can only displace small quantities of fluid. The least sensitive setting is used for larger airways.

Properties of hollow contractile structures can be studied at any physiological transmural pressure. Before the development of this apparatus, studies done in our and other laboratories to measure isobaric contraction on isolated airway segments neglected the increase in pressure induced by the volume displacements[7]. This introduces a substantial error when studying isobaric contraction at low transmural pressures. Our micro-plethysmograph compensates for the pressure changes induced by the volume displacements.

The resolution of the micro-plethysmograph was slightly lower than the theoretically calculated resolution. There are several reasons for this. Firstly, the filling volume is estimated at each level with an accuracy of ± 1 mL. A higher filling volume will increase resolution and decrease measurement range, while a lower volume level will decrease resolution and increase measurement range. Our filling volume may have been higher than used to calculate the theoretical resolution. Secondly, we did not add the volume of air in the tubing going from the barrels to the differential pressure transducer to the volume of the air compartment. We estimate this volume to be 0.8 mL. Therefore we systematically underestimated the volume of the air compartment of the plethysmograph, leading to an overestimation of resolution. Thirdly, drift during the time of infusion of the calibration volumes was in the opposite direction to the pressure rise in the calibration volume. Any reduction of calibration time will reduce the influence of drift on the second calibration pressure and therefore make calibration

more accurate. Fourthly, closure of the top valves of the plethysmograph induced a very small drop in the differential pressure. This artifact can be reduced by using automated electric rotary valves instead of the hand controlled rotary valves we used. We could also set zero calibration pressure after closure of the top valves and reset of the 0 cm H_2O differential pressure after the calibration procedure.

The three-dimensional architecture of a segment of airway or other tissue is an important factor in determining its contractile behavior. Thus intact tissues will give more realistic information on the contractile properties of smooth muscle than tissue strips or rings[8, 13]. The model as displayed in Figure 1 could also be used to study the contractile properties of other watertight and hollow structures such as blood vessels, gut, and ureter. In addition the plethysmograph can be used to measure permeability of a tube at different transmural pressures.

The design of the micro-plethysmograph can be adapted for the situation where the tissues under study require different volume ranges than the ones we used. With large volume displacements, the differential pressure transducer can be exchanged for a less sensitive one. A second possibility is to increase the volume of the barrels. These adaptations will reduce the resolution of the plethysmograph unless the resolution of the measuring system is increased. With small volume displacements the resolution of the plethysmograph could be doubled by amplifying the voltage output of the demodulator to $\pm$ 10 V to profit from the full-scale digital output of the A/D convertor. A match of A/D-convertor input sensitivity to output range of the pressure transducers also results in doubling of the resolution. Furthermore, a 16 bit A/D-convertor would increase resolution 16-fold.

In conclusion, we developed a micro-plethysmograph that can measure small volumes displaced by contractile tube-like structures. The load against which the tube is contracting can be kept constant (i.e. isobaric). In addition this device can be used to measure leak or diffusion at any transmural pressure.

Acknowledgements

References

1. Mitchell HW, Willet KE, Sparrow MP. Perfused bronchial segment and bronchial strip: narrowing vs. isometric force by mediators. J Appl Physiol 1989; 66: 2704- 2709.
2. Mitchell HW, Sparrow MP. Increased responsiveness to cholinergic stimulation of small compared to large diameter cartilaginous bronchi. Eur Respir J 1994; 7: 298-305.
3. Sparrow MP, McFawn PK, Omari TI, Mitchell HW. Activation of smooth muscle in the airway wall, force production, and airway narrowing. Can J Physiol Pharmacol 1992; 70: 607-614.
4. Hulsmann AR, Raatgeep HR, Bonta IL, Stijnen T, De Jongste JC. The perfused human bronchiolar tube: characteristics of a new model. J Pharmacol Toxicol Meth 1992; 28: 28-34.
5. Hulsmann AR, Raatgeep HR, Den Hollander JC, Stijnen T, Saxena PR, Kerrebijn KF, De Jongste JC. Oxidative epithelial damage produces hyperresponsiveness of human peripheral airways. Am J Respir Crit Care Med 1994; 149: 519-525.
6. Mitchell HW, Sparrow MP. Video-imaging of lumen narrowing; muscle shortening and flow responsiveness in isolated bronchial segments of pig. Eur Respir J 1994; 7: 1317-1325.
7. Moreno RH, Hogg JC, McLean TM, Pare PD. Isovolumetric and isobaric rabbit tracheal contraction in vitro. J Appl Physiol 1987; 62: 82-90.
8. Gray PR, Mitchell HW. Effect of diameter on force generation and resonsiveness of bronchial segments and rings. Eur Respir J 1996; 9: 500-505.
9. Baldwin DR, Sivardeen Z, Pavord ID, Knox AJ. Comparison of the effects of salbutamol and adrenaline on airway smooth muscle contractility in vitro and on bronchial reactivity in vivo. Thorax 1994; 49: 1103-1108.
10. McFawn PK, Mitchell HW. Bronchial compliance and wall structure during development of the immature human and pig lung. Eur Respir J 1997; 10: 27-34.
11. Tiddens HAWM, Hop WCJ, de Bruin H, de Jongste JC. What determines compliance of human small airways? Am J Respir Crit Care Med 1996; 155: A545.
12. Tiddens HAWM, Hofhuis W, Bogaard J, Hop WCJ, de Bruin H, Willems LNA, de Jongste JC. Compliance, hysteresis, and collapsibility of human small airways. Submitted 1997.
13. Hulsmann AR, Jongste JC. Studies of human airways in vitro: a review of the methodology. J Pharmacol Toxicol Methods 1993; 30.

Compilance, Hysteresis, and Collapsibility of Human Small Airways

Harm A.W.M. Tiddens, Ward Hofhuis, Jan M. Bogaard, Wim C.J. Hop, Huib de Bruin, Luuk N.A. Willems, and Johan C. de Jongste

Department of Pediatrics, division Respiratory Medicine, Department of Biostatistics and Department of Pathology, Erasmus University and University Hospital/Sophia Children's Hospital, Rotterdam. Department of Pulmonary medicine Leiden University Medical Center, The Netherlands

Introduction

In chronic obstructive pulmonary disease (COPD) airway inflammation is associated with increased airway wall thickness[1]. This thickness is relatively more severe in peripheral airways than in central airways, and is more pronounced in patients with more severe airflow obstruction[1]. Similar findings were obtained in patients who died with or from asthma [2, 3]. Thickening of the airway wall as such has little effect on airway resistance[1]. However, in combination with smooth muscle shortening it causes an important increase of airway resistance[4, 5]. The extent which the smooth muscle in airways of COPD patients shortens will depend on the force it develops and on the load against which the smooth muscle has to contract. The data on abnormal airway smooth muscle force in patients with COPD are conflicting [6, 7]. A decreased load has been suggested as an explanation for increased smooth muscle shortening in asthmatic airways[8, 9]. This is unlikely because chronic inflammation is associated with deposition of fibrous tissue such as collagen and elastin[10-12]. This probably makes airways stiffer (i.e., less compliant) and increases the load against which the smooth muscle contracts. We hypothesize that airway wall thickness is an important determinant of the mechanical properties of airways and that reduced compliance makes the airways less collapsible and decreases their distensibility and hysteresis. This study was undertaken to evaluate the relation between compliance, collapsibility, and hysteresis, on the one hand, and wall dimensions of human peripheral airway segments on the other hand. Therefore, we have developed an experimental model to study compliance, hysteresis, and collapsibility of isolated human small airway segments at baseline tone conditions and after maximal contraction and relaxation of the airway smooth muscle.

Methods

Study Population
Lung tissue was obtained from 31 patients who had a lobar resection or pneumonectomy for a peripheral lung lesion. These patients were mostly smokers and were

classified as "COPD" although one-third had a lung function within the normal range and, therefore, did not strictly fulfil the ATS criteria. Pre-operative routine lung function was obtained from 27 out of 31 patients. Forced expiratory volume in 1 s (FEV_1), forced vital capacity (FVC), maximal flows at 50% ($Vmax_{50}$) and 25% ($Vmax_{25}$) of FVC, functional residual capacity (FRC), total lung capacity (TLC), residual volume (RV), and RV as a fraction of TLC (RV/TLC%pred) are all expressed as percentage predicted[13]. We used FEV_1, expressed as a percentage of FVC (FEV_1/FVC), as an indicator of the severity of airflow obstruction. Reversibility of bronchial obstruction was expressed as the absolute change in FEV_1 as a percentage of the predicted FEV_1 ($DFEV_1$%pred) and as a percentage of the actual pre-bronchodilator FEV_1 ($DFEV_1$%ini).

This protocol was approved by the institutional review board for human studies.

Airway Segments

Lung tissue was collected and transported on ice in carbogenated (5% CO_2, 95% O_2) Krebs-Henseleit buffer (composition in mM: NaCl 118, KCl 4.7, $CaCl_2$ 2.5, $MgSO_4$ 1.2, KH_2PO_4 1.2, $NaHCO_3$ 25, glucose 5.55). Peripheral airways were identified, cannulated with a thin plastic cannula and dissected out with surrounding parenchyma. The airways were stored overnight in carbogenated Krebs-Henseleit buffer at 4°C. Next morning, parenchyma and blood vessels were removed with the help of a dissection microscope (Stemi 2000, Carl Zeiss, Oberkochen, Germany) and all side branches identified and ligated in a water-tight fashion. Airway segments at least 5 mm in length were selected for in vitro measurements. The internal diameters of the endings of the airways were estimated using the microscope by selecting stainless steel cannulas (1, 1.5, 2, 3, or 4 mm) that most closely fitted the diameter of the airway. Next, the airways were mounted in the organ bath on the cannulas in a watertight fashion. The airways were perfused to test for patency and possible leaks. The length of the unstretched airway within the inner borders of the cannula sutures was measured by a digital calipers (precision 0.1 mm). Next, we stretched the airway to 140% of this length, that being the estimated length of an airway close to TLC[14]. At this length the airway remained patent at low transmural pressures and after contraction by methacholine. The volume (in μL) of the airway was estimated by the

formula $\pi r^2 l$, where r is the average of the radius (mm) of the 2 cannulas and l is the length (mm) of the stretched airway.

Description of Experimental Set-up

Figure 1 shows the experimental set-up we used to measure the dynamic properties of the airway segments. It consists of a double jacketed organ bath in which the cannulated airway segment was mounted. The organ bath is filled with Krebs-Henseleit buffer at a temperature of 37°C and continuously gassed with carbogen. Airway segment and tubing are filled with buffer. All connecting tubing has a low compliance. Pressure was measured at both ends of the airway segment (P_{prox} and P_{dist}) using pressure transducers with a low compliance (143PC ± 1psi, Micro Switch, Freeport, Illinois, USA). The compliance of the whole system was 0.03 µL cm H_2O^{-1}. By means of a 3-way valve, the airway segment can be connected to a gas-tight syringe mounted on a computer-controlled high-precision syringe pump (Harvard 22, Harvard Apparatus Inc, South Natick, MA, USA) for cyclic inflation and deflation. Furthermore, the segment can be connected to a micro-plethysmograph that was designed to measure small volume displacements from or to the airway under isobaric conditions. Finally, the segment can be connected to a reservoir filled with buffer for perfusion. The transmural pressure signals (P_{prox} and P_{dist}), the volume signal of the syringe pump, and the volume signal of the micro-plethysmograph (P_{diff}) are all displayed on the PC monitor. The system is servo-controlled, with the pressure signal from P_{prox} being used to control the syringe pump.

Measurement Protocol

The Krebs buffer in the organ bath was replaced every 15 minutes throughout the experiments. Between tests the airway was perfused for 10 minutes. The speed of the pump for inflation and deflation was set at 8 times the estimated volume of the airway segment per minute. From a pilot study, we estimated that this would give a cycling rate between 1 and 4 cycles per minute.

LEAK TEST. To test for a leak the airway was inflated by the pump until a transmural pressure of 15 cm H_2O was obtained. Next, the spontaneous rate of pressure drop of the segment within the first minute of inflation was registered. In case of leakage it

was either impossible to inflate the airway to 15 cm H_2O, or its transmural pressure dropped rapidly to 0 cm H_2O after inflation stopped.

PRESSURE-VOLUME RELATIONSHIP AT BASELINE. Zero pressure of the proximal and distal valves was set by connecting the airway lumen to the atmosphere. The airway was then connected to the pump. Next, the airway was cyclically inflated and deflated between +15 and -15 cm H_2O using the computerized servo-controlled pump (Figure 2). The upper pressure limit of 15 cm H_2O was chosen since it corresponds to a transmural pressure of 30 cm H_2O in an air filled system[15]. This transmural pressure is likely to inflate the airway to a level comparable to TLC. Three complete inflation-deflation cycles were done. After the third cycle, the airway was inflated to 15 cm H_2O at which point the pump automatically stopped. We recorded the spontaneous pressure drop within two minutes to estimate maximal hysteresis and leak.

ISOBARIC CONTRACTILITY AND RELAXATION. To monitor the contractile response to methacholine or relaxation response to isoprenaline the airway was connected to the micro-plethysmograph. The transmural pressure was set at 10 cm H_2O by adjusting the height of the plethysmograph. Baseline volume displacement out of the plethysmograph was registered for 2 minutes before sufficient methacholine or isoprenaline was added to the organ bath to give a final concentration of $10^{-4}M$. The isobaric constriction or relaxation was recorded until no more fluid was displaced into the plethysmograph or until the rate of fluid displacement out of the plethysmograph became constant.

PRESSURE-VOLUME RELATION IN THE PRESENCE OF METHACHOLINE AND ISO-PRENALINE. These were measured as described for baseline tone.

ISOBARIC RELAXATION. To monitor the relaxation response to isoprenaline the airway was connected to the micro-plethysmograph. The transmural pressure was set at 10 cm H_2O by adjusting the height of the plethysmograph. Baseline volume displacement out of the plethysmograph was registered for 2 minutes before isoprenaline ($10^{-4}M$) was added to the organ bath. The isobaric relaxation was recorded until the rate of fluid displacement out of the plethysmograph became constant.

PRESSURE-VOLUME RELATION AFTER ISOPRENALINE. This was measured as described for baseline.
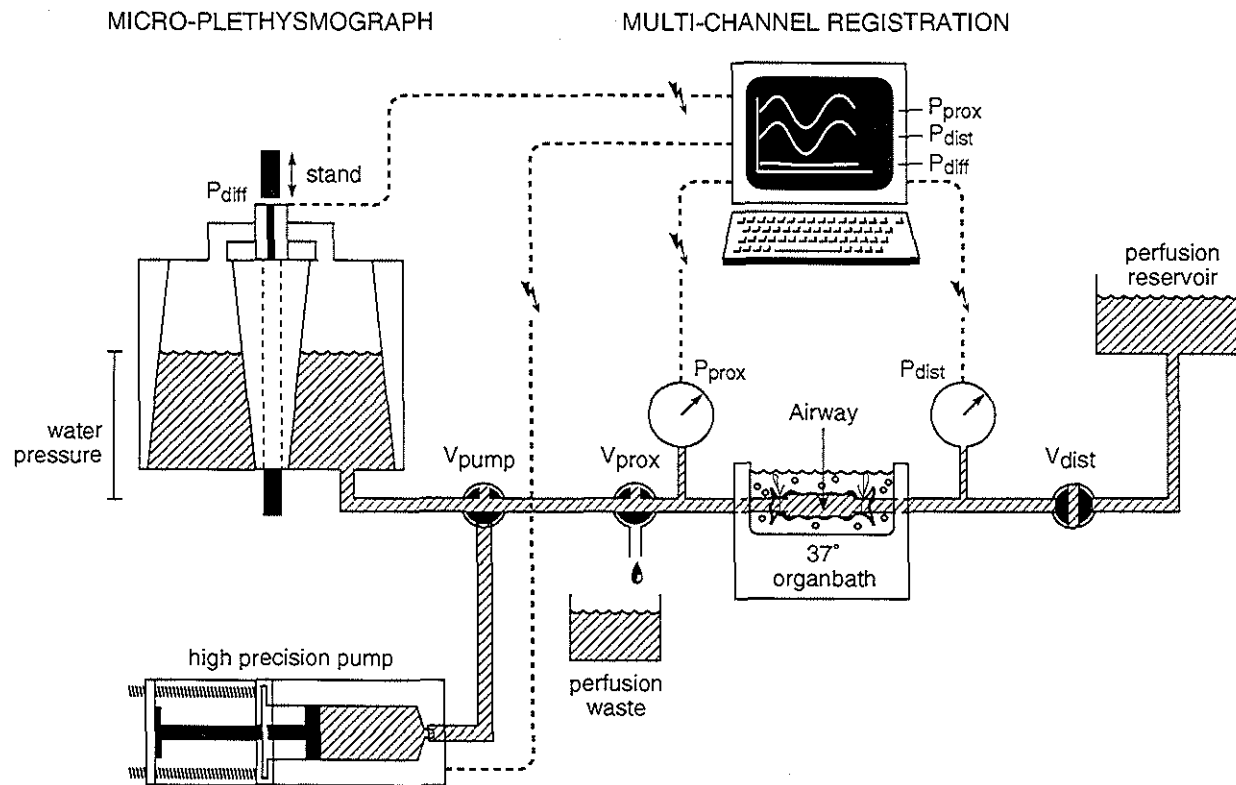
Figure 1. Diagram of the experimental set-up to measure dynamic properties of isolated airway segments. *Definition of abbreviations:* V_{prox} and V_{dist} = valves located at the proximal or distal end of the airway; V_{pump} = valve to connect pump to airway; P_{prox} and P_{dist} = pressure transducers to measure the transmural pressure at the proximal and distal end of the airway; Micro-plethysmograph = device to measure small volume displacements under isobaric conditions; Multi-channel registration = system for processing of pressure and volume signals; high precision pump = pump for cyclic inflation and deflation of airway. The system is servo-controlled, with the pressure signal from P_{prox} controlling the syringe pump.

EXAMPLE OF TRACING   SPECIFIC HYSTERESIS

Figure 2. Example of pressure volume-tracing. The arrow head shows the direction of the loop. Dynamic compliance (Cdyn) is the division of infused volume by 15 cm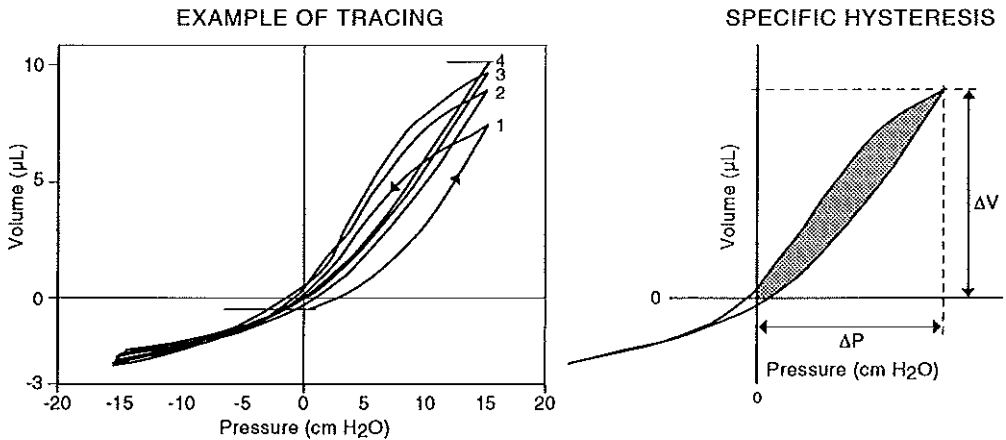 H_2O. Specific hysteresis is the shaded area of the pressure-volume loop above 0 cm H_2O expressed as the percentage of the area of maximal hysteresis.

FIXATION. Finally, the airway was perfused with formalin (10%) from the distal end at a driving pressure of 10 cm H_2O. The valve was closed as soon as formalin came out of the proximal valve and the Krebs buffer in the organ bath was quickly replaced with formalin. After fixation for 12 hours at a transmural pressure of 10 cm H_2O, the airway, including the ligatures at both ends, was gently pushed off the cannulas with forceps and stored in formalin until being processed for histology.

Compliance, Hysteresis, Collapsibility, and Contractility
Compliance (Cdyn, μL (cm $H_2O)^{-1}$) was calculated from the volume infused to inflate the airway from 0 to 15 cm H_2O (Figure 2). The transition point of the pressure-volume curve where inflation changes to deflation was selected as the upper pressure limit for the Cdyn calculation because it is least affected by hysteresis. Furthermore, it results in the Cdyn of the stretched airway close to TLC where collagen is known to be an important mechanical determinant[16]. Therefore, Cdyn should be sensitive to changes in airway collagen content. Hysteresis (η, μL cm H_2O) was calculated as the area of the pressure-volume loop between 0 and 15 cm H_2O. Collapsibility (Pcol, cm H_2O) was defined as the pressure of the deflation limb where the distal pressure did not follow the proximal pressure thus indicating closure of the airway lumen.

Table 1

STUDY POPULATION AND LUNG FUNCTION CHARACTERISTICS

	n Patients	Mean	SD	Range
Age, years	29	61	11	22-73
Sex, male : female	20 : 9			
Lung or lobe resected, right side	14			
Lung or lobe resected, left side	15			
TLC, % pred	18	100	15	67-132
FRC, % pred	9	108	36	74-190
RV, % pred	18	138	59	65-252
FEV_1, % pred	27	80	17	43-106
FVC, % pred	27	99	17	59-135
FEV_1/FVC, %	27	65	12	41-85
FEV_1/FVC%pred	27	84	15	55-115
RV/TLC%pred	18	129	61	72-273
$Vmax_{50}$, % pred	11	42	22	11-77
$Vmax_{25}$, % pred	13	38	22	6-83
$DFEV_1$ % pred	23	1	3	-7-6
$DFEV_1$ % ini	23	1.6	4	-8-7

Definition of abbreviations: TLC = total lung capacity; FRC = functional residual capacity; RV = residual volume; FEV_1 = forced expiratory volume in 1 s; FVC = forced vital capacity; FEV_1/FVC = forced expiratory volume in 1 s as percentage of FVC; FEV_1/FVC%pred = FEV_1 as a fraction of FVC; RV/TLC%pred = RV as a fraction of TLC; $Vmax_{50}$ = maximal flow at 50% of FVC; $Vmax_{25}$, % pred = maximal flow at 25% of FVC; $DFEV_1$ % pred = change of FEV_1 after bronchodilatation as a percentage of predicted FEV_1; $DFEV_1$ % ini = change of FEV_1 after bronchodilatation as a percentage of pre-bronchodilator FEV_1

Cdyn, η, and Pcol were calculated for each cycle. We analyzed Cdyn, η, and Pcol of the first cycle ($Cdyn_1$, η_1, and $Pcol_1$) separately because we observed that these were always substantially different from those of subsequent cycles. The latter were similar

and were therefore taken together (Cdyn, η, and Pcol). The first cycle was excluded for analysis when it did not start exactly from 0 cm H_2O transmural pressure. Volume loops could not be analyzed for hysteresis in 11 airways where we used a high syringe volume and low speed of the pump as this caused artifacts in the PV loops.

To normalize compliance for the volume of the airway segment, $Cdyn_1$ and Cdyn were divided by the volume of the airway segment as calculated by morphometry ($sCdyn_1$, sCdyn). Hysteresis was normalized as a percentage of the area of the maximal possible hysteresis ($s\eta_1$, $s\eta$) which was defined as the product of volume infused and the upper pressure limit (15 cm H_2O). The spontaneous pressure drop within 2 minutes after the last inflation was normalized for the inner surface area of the airway (internal perimeter times length) (specific pressure drop, cm H_2O mm^{-2}).

We calculated the maximal volume displaced by the airway segment after methacholine (V_M), or isoprenaline (V_I). The response was negative when fluid moved out of the contracting segment into the plethysmograph and positive when fluid moved into the relaxing airway segment out of the plethysmograph. The response was corrected for the rate of baseline fluid movement before methacholine or isoprenaline was added. To correct for the volume of the airway segment, V_M and V_I were expressed as the percentage of the volume of the airway segment as calculated from morphometry.

Airway Dimensions

To estimate airway wall dimensions and volume of the lumen, the segment was cut in cross section at both ends just inside the ligatures, decalcified, and embedded in paraffin in such a way that it could be cut in cross-section. A random starting point was selected within the first 0.5 mm at one end of the airway using a randomization table. Sections of 5 μm thickness were cut all the way through the airway with a microtome. Every 100th section (0.5 mm) was selected for morphometric analysis. We estimated that with this procedure we could obtain a reliable estimate of the mean airway wall dimensions. Sections were stained with a combined Gomori trichrome and elastin stain. This stain resulted in a good color contrast between airway wall structures.

The measurements made are shown in Figure 3 and include: inner perimeter (P_i) and area of the lumen bounded by the respiratory epithelium (A_i); basement membrane

perimeter (P_{bm}) and the area enclosed by this perimeter (A_{bm}); the outer muscle perimeter (P_{mo}) and the area enclosed by this perimeter (A_{mo}); the outer perimeter (P_o) and the area enclosed by this perimeter (A_o); the area occupied by smooth muscle (WA_m); and the area occupied by cartilage (WA_{cart}).

Furthermore we measured the height of the respiratory epithelium (H_{epi}) and the fraction of P_{bm} covered by epithelium (F_{epi}). H_{epi} was measured as follows. First, a grid containing parallel sinusoids was superimposed over the computer image of the airway. When respiratory epithelium was present at the point where the sinusoid crossed the basement membrane, we measured the epithelial height by drawing a straight line perpendicular to the membrane and measuring from the membrane to the top of the ciliary border. The length of this line was automatically computed. When respiratory epithelium was absent, a zero was scored for height. Second, H_{epi} was calculated for each airway section by computing the average of at least 15 epithelial height measurements around the lumen. F_{epi} was calculated by dividing the number of intersecting points through the basement membrane covered by respiratory epithelium with the total number of intersecting points, including the intersecting points at sites where the respiratory epithelium was absent. WA_{epi} was calculated by multiplying P_{bm} by H_{epi}.

From these measurements we calculated the inner wall area including epithelium ($WA_i = A_{mo}-A_i$), inner wall area excluding epithelium ($WA_{bm} = A_{mo}-A_{bm}$), outer wall area ($WA_o = A_o-A_{mo}$) and the total wall area ($WA_t = A_o-A_i$). This nomenclature which was proposed for quantifying subdivisions in the bronchial wall[17].

Airway dimensions were measured using an automated image analysis system (KS 400, Kontron Electronic, Eching/Munich, Germany).

Measurements of airway dimensions were performed by 2 observers (WH and HdB). Each observer measured a different set of airway dimensions for all airways. The inter-observer variability was assessed to compare airway dimensions of this study with a previous study where we studied patients with variable degrees of airway wall thickening[1]. This would give us evidence as to whether the patients we included in the present study had airway wall thickening in the same range as in previous studies.

Table 2

MECHANICAL PROPERTIES OF AIRWAY SEGMENTS
FOR THE FIRST AND CONSECUTIVE CYCLES

Condition	n	Cycle 1 Mean ± SD (range)	n	Cycle 2, 3, and 4 Average Mean ± SD (range)
Compliance (Cdyn) μL cm H_2O^{-1}				
Baseline	22	1.45 ± 1.0 (0.2 to 3.8)	35	1.52 ± 1.0 (0.2 to 3.8)
Methacholine	22	1.36 ± 1.1 (0.1 to 3.6)	35	1.42 ± 1.1 (0.1 to 3.9)
Isoprenaline	33	2.43 ± 1.5 (0.1 to 5.7)	35	2.62 ± 1.6 (0.1 to 5.9)
Specific Compliance (sCdyn) cm H_2O^{-1}				
Baseline	22	0.053 ± 0.02 (0.02 to 0.09)	35	0.059 ± 0.03 (0.01 to 0.10)
Methacholine	22	0.049 ± 0.03 (0.01 to 0.09)	35	0.052 ± 0.03 (0.01 to 0.09)
Isoprenaline	33	0.080 ± 0.03 (0.01 to 0.15)	35	0.085 ± 0.03 (0.01-0.15)
Hysteresis (η) μL cm H_2O				
Baseline	18	75.9 ± 71 (4 to 261)	24	55.9 ± 54 (1 to 187)
Methacholine	18	70.1 ± 81 (6 to 267)	24	43.5 ± 45 (3 to 223)
Isoprenaline	25	63.2 ± 88 (4 to 268)	26	48.1 ± 39 (3 to 138)
Specific Hysteresis (sη) %				
Baseline	18	19.8 ± 9 (4 to 34)	24	13.5 ± 7 (1 to 39)
Methacholine	18	18.0 ± 11 (4 to 43)	24	12.9 ± 8 (2 to 35)
Isoprenaline	25	11.2 ± 6 (2 to 28)	26	7.1 ± 4 (1 to 16)
Collapsibility (Pcol) cm H_2O				
Baseline	35	-4.0 ± 5 (-16 to 1)	35	-3.4 ± 5 (-17 to 1)
Methacholine	35	-4.0 ± 5 (-16 to 1)	35	-3.5 ± 4 (-16 to 1)
Isoprenaline	35	-2.1 ± 3 (-11 to 1)	35	-1.9 ± 2.6 (-11 to 1)

Mechanical properties of isolated airway segments at baseline, after contraction with methacholine, and after relaxation with isoprenaline. The mechanical properties examined are compliance *(Cdyn)*, hysteresis *(η)*, and collapsibility *(Pcol)*. Compliance was normalized for airway volume *(sCdyn)* and hysteresis for the maximal possible hysteresis *(sη)*. The values for the first cycle and for the average of the consecutive cycles are shown separately since the mechanical properties of the first cycle were different from subsequent cycles.
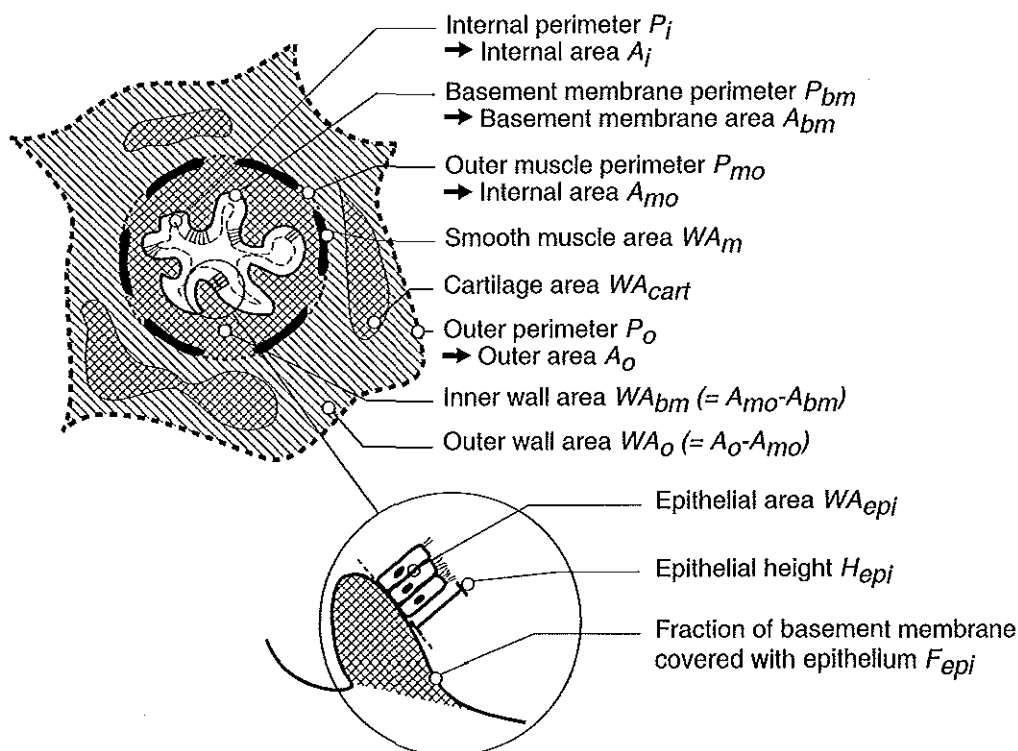
Figure 3. Diagram of measured airway dimensions.

Both observers remeasured 15 randomly selected airways that were measured by the observer (HT) of the previous study. The intra-observer variability was assessed by remeasurement of 10 randomly selected airways after an interval of 2 months. Inflammatory changes of membranous airways were graded using the pictorial grading method of Wright and coworkers[18]. The following indices were graded in the membranous bronchioles: inflammation, fibrosis, muscle hypertrophy, pigment deposition, goblet cell metaplasia, and squamous cell metaplasia. A total membranous airways disease score for each lung specimen was calculated by summing the mean scores of the six morphological indices (maximal score: $6 \times 100 = 600$).

Statistical Analysis

The inter- and intra-observer variability were calculated by expressing the difference of the first and the second measurement as a percentage of the average of both
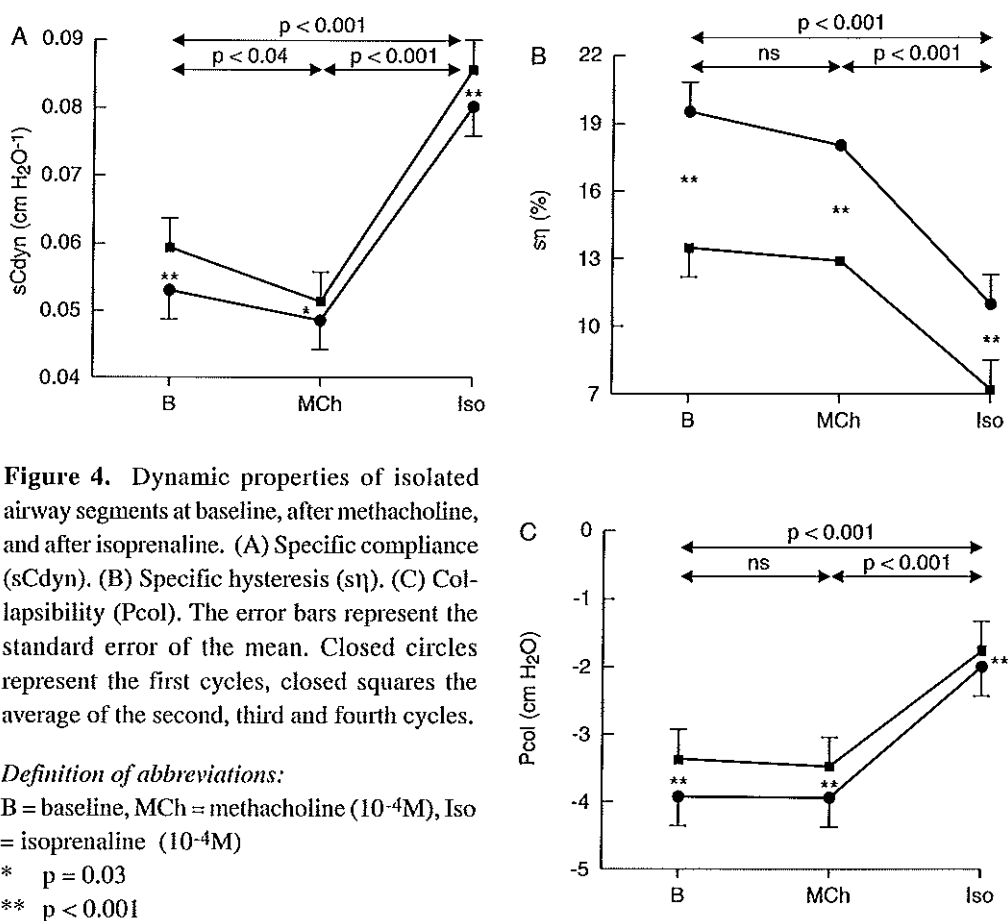
Table 3
DIMENSIONS OF ISOLATED AIRWAY SEGMENTS

Airway dimensions	mean ± SD (range)
Internal perimeter *mm*	6.1 ± 1.2 (4.1-8.4)
Airway wall thickness *mm*	0.3 ± 0.1 (0.11-0.61)
Length of airway segment *mm*	14.2 ± 4.2 (6.7-21.2)

Equations of Airway Dimensions (in mm) as a Function of Airway Size

Wall area basement membrane *(WA_{bm})*	$\sqrt{WA_{bm}} = 0.19 + 0.071\, P_{bm}$
Outer wall area *(WA_o)*	$\sqrt{WA_o} = -0.15 + 0.206\, P_{bm}$
Total wall area *(WA_t)*	$\sqrt{WA_t} = -0.06 + 0.226\, P_{bm}$
Smooth muscle area *(WA_m)*	$\sqrt{WA_m} = 0.04 + 0.034\, P_{bm}$
Cartilage area *(WA_{cart})*	$\sqrt{WA_{cart}} = -0.18 + 0.067\, P_{bm}$
Epithelial area *(WA_{epi})*	$\sqrt{WA_{epi}} = -0.01 + 0.042\, P_{bm}$

observations. This percentage was plotted against P_{bm} to detect systematic errors dependent upon airway size[19].

For each airway and each airway wall dimension, we calculated the average and the standard error of the mean (sem). To estimate the accuracy of our morphometric approach, we calculated for each airway the coefficient of variation of the mean using the formula (100% x sem) / mean. In this formula the sem relates to the variation between sections within a single airway.

The relationships between each airway wall dimension (WA_i, WA_{bm}, WA_o, WA_t, WA_m, WA_{cart}, WA_{epi}, H_{epi}, F_{epi},) and airway size (P_{bm}) were assessed using linear regression analysis. Previous studies found linear relationships between the square root of airway wall areas and airway size[1, 20-23]. We did a square root transformation on the airway areas of this study, again resulting in normal distributions of data.

We calculated the average specific compliance, specific hysteresis, and collapsibility for the first cycle ($sCdyn_1$, $s\eta_1$, $Pcol_1$) and for the average of the second, third, and fourth cycle ($sCdyn$, $s\eta$, $sPcol$) for all airway segments. Furthermore, we calculated

Figure 4. Dynamic properties of isolated airway segments at baseline, after methacholine, and after isoprenaline. (A) Specific compliance (sCdyn). (B) Specific hysteresis ($s\eta$). (C) Collapsibility (Pcol). The error bars represent the standard error of the mean. Closed circles represent the first cycles, closed squares the average of the second, third and fourth cycles.

Definition of abbreviations:
B = baseline, MCh = methacholine (10^{-4}M), Iso = isoprenaline (10^{-4}M)
*   p = 0.03
**   p < 0.001

the average specific pressure drop. This was done for each of the three contractile conditions (baseline, methacholine, and isoprenaline). To compare the mean outcome of two values, the paired t-test was used. We investigated the correlation between the mechanical properties of the second, third, and fourth cycle (sCdyn, $s\eta$, P_{col}) with airway wall dimensions (WA_{bm}, WA_o, WA_t, WA_m, WA_{cart}, WA_{epi}, F_{epi}) using Spearman's correlation coefficient (R). When a mechanical property correlated to various airway wall dimensions in univariate analysis, we studied their simultaneous effects using multiple regression analysis.

The level of significance was set at p = 0.05 (two sided). Data are expressed as mean ± standard deviation and range, unless indicated otherwise.

Results

Study Population and Lung Function

Lung function and patient characteristics of the COPD patients are shown in Table 1. Out of the group of 27 COPD patients with pre-operative lung function test results, 8 patients had no significant reduction of maximal expiratory airflow (FEV_1/FVC >70%), 12 patients had a mild reduction of maximal expiratory airflow (FEV_1/FVC 60 to 70%), and 7 patients had a more severe reduction (FEV_1/FVC <60% predicted). Increased residual volume (RV > RV(pred) + 2SD) was present in 5 of the 18 patients who had body-plethysmography. Reversibility of bronchial obstruction defined as $DFEV_1$%pred > 15% and $DFEV_1$%ini > 15% was not present in any of the 23 patients.

Airway Segments

We successfully completed all measurements of 35 cannulated watertight airway segments. The diameter of the cannulas used was 1.3 ± 0.39 (1 to 2) mm, while the length of the stretched airways was 14.2 ± 4.2 (6.7 to 21.2) mm. The median of the estimated volume of the segments was 30.7 (5.3 to 66.6) µL. Cycling frequency was 3.1 ± 1.9, 5 ± 5.4, and 1.8 ± 0.9 cycles min^{-1} for baseline, methacholine, and isoprenaline respectively. At baseline, methacholine, and isoprenaline, 13, 13, and 2 respectively out of the 35 first cycles started above 0 cm H_2O and were therefore excluded from analysis.

Compliance, Hysteresis, and Collapsibility

The values for compliance and specific compliance (Cdyn and sCdyn), hysteresis and specific hysteresis (η and sη), and collapsibility (Pcol) at baseline, after methacholine, and after isoprenaline are shown in Table 2 and in Figure 4.

On average, the specific compliance of the first cycle (sCdyn$_1$) was 13, 11, and 8% below the mean sCdyn of the subsequent cycles for baseline ($p < 0.001$), methacholine ($p = 0.03$), and isoprenaline ($p < 0.001$) respectively (Figure 4). The mean sCdyn after methacholine was 0.009 cm H_2O^{-1} below that of baseline ($p = 0.04$). sCdyn after isoprenaline was 0.033 cm H_2O^{-1} higher compared to baseline ($p < 0.001$) and 0.042 cm H_2O^{-1} higher compared to methacholine ($p < 0.001$). Expressed as percentages, these differences were 4, 101, and 197%, respectively.
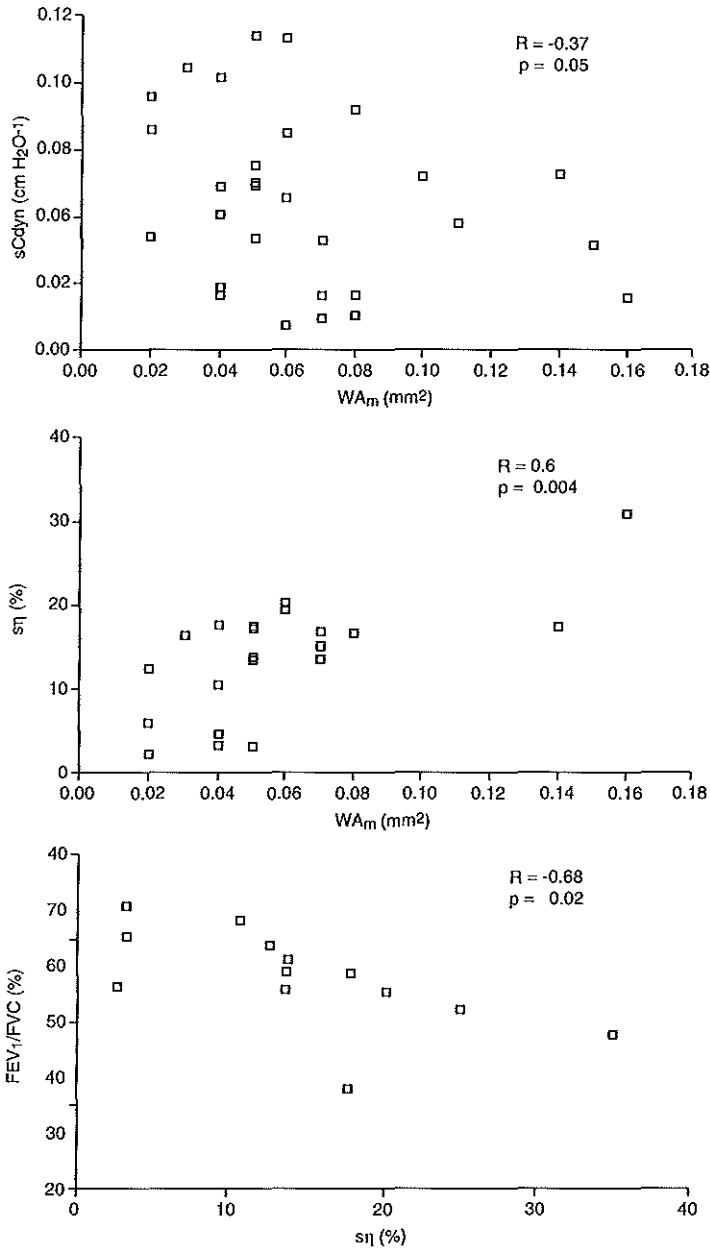
Figure 5. (A) Scatter plot of specific dynamic compliance (sCdyn) versus smooth muscle area (WA_m) after the airway segment was contracted with methacholine.
(B) Scatter plot of specific hysteresis (sη) versus smooth muscle area (WA_m).
(C) Scatter plot of FEV_1 over FVC (FEV_1/FVC) versus specific hysteresis (sη).

The mean specific hysteresis of the first cycle was 34, 30, and 37% higher compared to sη of the subsequent cycles for baseline, methacholine, and isoprenaline respectively (p < 0.001) (Figure 4). The mean sη after methacholine was not significantly different from baseline. sη After isoprenaline was 6.8% lower compared to baseline (p < 0.001) and 7% lower compared to methacholine (p < 0.001). Expressed as percentages, these differences were 9 and 39% respectively.

The mean pressure drop within the two minutes after the last inflation of the compliance measurement was 6.5, 7.1, and 7.2 cm H_2O for baseline, methacholine, and isoprenaline respectively. The mean specific pressure drop for these conditions were 0.009, 0.001, and 0.001 cm H_2O mm^{-2}. The differences between the three conditions were not significant.

The collapsibility of the first cycle was 0.6, 0.5, and 0.2 cm H_2O below Pcol of the next cycles for baseline, methacholine, and isoprenaline respectively (all p < 0.001) (Figure 4). Pcol after isoprenaline was 1.5 and 1.6 cm H_2O above the values at baseline and with methacholine, respectively (both p < 0.001). The collapsibility at baseline and after methacholine were not significantly different. After maximal contraction, there were 5 airways that collapsed at pressures of 0 cm H_2O or higher. After maximal relaxation, this number increased to 9. Pcol and sCdyn after methacholine were significantly correlated (R = 0.54, p = 0.001). In other words, the stiffer the airway after methacholine, the less collapsible it was.

The median fluid volume displaced by methacholine-induced constriction was -9.4 (-41 to 10) μL or -37 (-103 to 119) % of the estimated airway volume. For the relaxing airway after isoprenaline these values were 5.9 (-7 to 46) μL or 31.4 (-14 to 58) %.

Airway Dimensions
The intra- and inter-observer variability were well below 10% and 15% respectively for each of the airway wall dimensions. There was no systematic relationship between airway size (P_{bm}) and the intra- or inter-observer variability for any variable. The mean coefficients of variation of the individual means for the airway dimensions for P_{bm}, WA_{bm}, WA_o, WA_t, WA_m, WA_{cart}, H_{epi}, and F_{epi} were 4, 6, 8, 8, 10, 33, 12, and 13% respectively. Characteristics of the airways are shown in Table 3.

Highly significant ($p < 0.002$) linear relations were found between the square root of all air-way wall areas and P_{bm}. There was a positive correlation between H_{epi} and P_{bm} ($R = 0.43$, $p = 0.02$), and a negative correlation between F_{epi} and P_{bm} ($R = -0.39$, $p = 0.04$). The average H_{epi} was 10.7 ± 6.3 (0.1 to 28.7) μm and F_{epi} was 47 ± 24 (4 to 99) %. The membranous airways disease score was 119 ± 40 (38 to 223).

Lung Function versus Compliance, Hysteresis, and Collapsibility.
Specific hysteresis at baseline correlated to FEV_1/FVC ($R = -0.57$, $p = 0.06$) and RV/TLC%pred ($R = 0.5$, $p = 0.05$). Hysteresis after methacholine correlated to FEV_1/FVC ($R = -0.68$, $p = 0.015$) (figure 5), RV ($R = 0.5$, $p = 0.05$), and RV/TLC%pred ($R = 0.67$, $p = 0.007$). There was no correlation between hysteresis and parameters of reversibility ($DFEV_1$%pred and $DFEV_1$%ini). Specific compliance and collapsibility did not correlate to the parameters as mentioned above.

Airway Dimensions versus Compliance, Hysteresis, and Collapsibility
Specific compliance (sCdyn) at baseline, after methacholine, and after isoprenaline was independent of airway size ($p = 0.2$). Specific compliance at baseline correlated significantly to the total wall area (WA_t) ($R = -0.35$, $p = 0.04$ and outer wall area (WA_o) ($R = -0.39$, $p = 0.02$), but not to other airway wall areas. Since the WA_t components WA_{epi} and WA_{bm} did not correlate to sCdyn, we conclude that WA_o is the most important component for sCdyn at baseline. After methacholine, sCdyn correlated negatively to the amount of smooth muscle (WA_m)($R = -0.37$, $p = 0.05$) (Figure 5) and to the area of epithelium (WA_{epi}) ($R = -0.37$, $p = 0.05$). Due to the strong correlations of WA_m and WA_{epi}, no conclusion about which of the two variables was more predictive for sCdyn could be obtained using multiple regression analysis. Specific compliance after isoprenaline did not correlate to any of the airway dimensions. The difference between sCdyn after isoprenaline and methacholine correlated significantly to WA_m ($R=0.45$, $p=0.02$) but not to WA_{epi}.
The difference between $sCdyn_i$ and sCdyn at baseline, after methacholine, and isoprenaline did not correlate to any airway wall dimension.
Specific hysteresis (sη) at baseline was positively correlated to WA_t ($R = 0.41$, $p = 0.04$) and to WA_m ($R = 0.44$, $p = 0.04$), but not to other airway wall dimensions

$(WA_{bm}, WA_{cart}, WA_{epi})$. Because WA_t and WA_m were significantly correlated, it was not possible to differentiate whether WA_t or WA_m was the most predictive dimension for sh in a multiple regression model. Specific hysteresis after methacholine correlated to WA_t (R = 0.54, p = 0.006), WA_o (R = 0.52, p = 0.01), and WA_m (R = 0.6, p = 0.004), and to WA_{cart} (R = 0.42, p = 0.04). Multiple regression analysis showed that WA_m was the only remaining significant predictive dimension (p = 0.01) (Figure 5). Specific hysteresis after isoprenaline did not correlate to any of the airway dimensions. The difference between $s\eta_1$ and $s\eta$ at baseline, after methacholine, and after isoprenaline did not correlate to any airway wall dimension.

The specific pressure drop after the fourth inflation, indicating hysteresis and leak, was correlated negatively to all airway dimensions for baseline, after methacholine, and after isoprenaline (p < 0.01). Multiple regression analysis showed that at baseline, WA_{epi} was the only remaining significant predictive dimension for the pressure drop. After methacholine, WA_o was the only significant dimension (p = 0.04) determining the pressure drop. After isoprenaline, multiple regression analysis showed that WA_o and WA_{epi} were both predictive. Due to the strong correlations between the two, no conclusion about which variable was most predictive could be obtained. Thus, small airways with thinner epithelium and smaller outer airway wall area had a faster pressure drop after the final inflation.

Collapsibility (Pcol) of the airways at baseline, after methacholine, and after isoprenaline did not correlate to any of the airway wall dimensions $(WA_{bm}, WA_o, WA_t, WA_m, WA_{cart}, WA_{epi})$.

Discussion

Chronic inflammation of the airways results in fibrous tissue deposition and thickening of the airway wall. We thought it likely that this remodeling makes the airway less compliant. This study was undertaken to evaluate the relation between compliance, collapsibility, hysteresis and airway wall dimensions of human peripheral airway segments. This relation was studied for baseline tone, after maximal contraction, and

after maximal relaxation of the smooth muscle. Our results show that the bronchial smooth muscle area, not total wall area, is an important determinant for airway compliance, hysteresis, and collapsibility.

Compliance

In previous studies of airways from patients with COPD it was shown that the inner and outer wall area were positively correlated to inflammatory changes within the airway wall[1, 20]. Furthermore, we know that chronic airway inflammation causes increased elastin and collagen deposition and increased smooth muscle area[10, 21]. Therefore, we expected airway wall areas to be important determinants for airway compliance (sCdyn). Indeed, at baseline tone, sCdyn correlated to the outer airway wall area. After maximal contraction of the airway smooth muscle, sCdyn decreased and smooth muscle area was the most important determinant for sCdyn. After maximal relaxation of the smooth muscle tone we expected the outer and inner wall area to be important determinants for the remaining sCdyn. These results show that smooth muscle area not the outer or inner airway wall area is important for sCdyn. In fact, smooth muscle tone had a substantial influence on sCdyn: compliance doubled when we maximally relaxed the airway. How can we explain that the inner and outer airway wall area did not correlate to sCdyn? First, it could be that the airways we investigated were not thickened by chronic inflammation. We think this is unlikely since the selection criteria for lung tissue for the present study were the same as in a previous study[1] and both the airflow obstruction and the airway dimensions of this study are comparable to those in previous studies[1, 20-23]. Second, we investigated small airways in COPD, where inflammatory changes are known to be most severe[1]. Third, we have studied preparations with a wide variation of sCdyn and airway wall areas. Fourth, inflammation scores were within the same range as in a previous study[1] and these scores correlated positively to the total airway wall area. We think that the lack of correlation between inner and outer wall area versus sCdyn could be explained by assuming that WA_o and WA_{bm} correlate poorly to the presence of structural components such as collagen because of a lack of sensitivity of the measurement to changes in collagen content, which determine sCdyn of airways in the high volume range.

Specific compliance at baseline was two-thirds of sCdyn of the maximally relaxed airway, and this was due to an initially high intrinsic contractile state. This high baseline tone could partly be an artifact related to our tissue preparation. However, we believe that there is also a substantial baseline tone in vivo. The specific compliance we found at baseline was even slightly higher than several of the in vivo studies of human airways suggested, taking into account differences in methodology[24-27]. A high baseline tone of human airway smooth muscle in vivo might explain why such small changes were seen in compliance in asthmatic patients in vivo after inhalation of histamine[28]. It remains puzzling why none of the patients in our study and only one out of 58 patients in a previous study showed reversibility after bronchodilatation[1]. The balance between smooth muscle tone passive wall elasticity and recoil pressure will determine airway diameter in vivo. The volume of the maximally relaxed airway at a pressure of 15 cm H_2O is 50% higher than its volume at maximal contraction. We estimated that the diameter of the maximally relaxed airway was on average 27% higher than the maximally contracted airway. Similar findings were obtained in excised dog lobes by Hahn and co-authors[26]. They found that the mean airway diameter of small airways increased by 31% compared to baseline after a bronchodilator was given at a transpulmonary pressure of 30 cm H_2O. Our findings support the importance of smooth muscle tone for airway diameter.

Hysteresis

Smooth muscle tone is known to be an important contributor to hysteresis[29, 30]. We found a significant decrease of sη with maximal relaxation compared to baseline and to the maximally contracted airways. However, we did not find a difference between sη at baseline and after maximal contraction of the smooth muscle. This can be explained by the smaller increase in volume necessary to inflate a contracted airway to the pressure limit of 15 cm H_2O. Surprisingly, a substantial portion of sη was not contributed by smooth muscle tone. After maximal relaxation, mean sη was still 53% of baseline sη. Hysteresis of lung tissue is related to four different mechanisms; kinetics of cross-bridge attachment-detachment, kinetics related to the surface film, kinetics of fiber-fiber networking within the connective tissue matrix, and the kinetics of

recruitment-derecruitment[31]. Since we studied fluid-filled airway segments, surface tension and recruitment did not play an important role. Therefore it is likely that the remaining sη originates within the connective tissue matrix of the airway wall.

At baseline, sη was correlated both to the smooth muscle area and to total airway wall area. After maximal contraction of the smooth muscle, its area was the most important airway wall dimension determining sη. After maximal relaxation, the total wall area was not correlated to sη. These findings suggest that the total wall area does not reflect changes in fibrous tissue composition which determines sη. We therefore conclude that smooth muscle is the single most important airway dimension for sη. Specific hysteresis at baseline and after methacholine correlated significantly to lung function parameters of airflow obstruction, suggesting that smooth muscle tone plays an important role in airflow obstruction in COPD. Why bronchodilators can reduce hysteresis substantially in vitro but not in vivo is puzzling. We suggest that tethering forces of the lung parenchyma on small airways are reduced or unevenly distributed and therefore insufficient to dilate the entire airway even after relaxation of the bronchial smooth muscle.

The specific pressure drop was best predicted by the thickness of the outer airway wall together with the epithelial area. Since specific pressure drop was independent of the contractile status of the airway, it probably represents pressure loss due to diffusion rather than to hysteresis. Diffusion may depend on the presence of intact epithelium[32]. Indeed there was considerable loss of epithelium, especially in the smaller airways, as a result of the procedure to make the airways watertight. Therefore, we may have overestimated hysteresis and compliance for the smaller airways. However, since hysteresis and compliance after isoprenaline did not correlate with the epithelial area, this epithelial loss is not a likely explanation for differences in hysteresis and compliance between segments.

Collapsibility

To our knowledge, this is the first study on the relation between collapsibility and airway dimensions of human small airways. Airway collapse in vivo depends on transmural pressure, stiffness of the airway wall, and recoil pressure of the parenchyma.

Collapsibility was correlated to smooth muscle tone and not to any of the airway dimensions. Reduction of smooth muscle tone made the airway more compliant and more collapsible. Airways with the biggest change in compliance between the maximally contracted and maximally relaxed state also had the biggest change in collapsibility. The importance of smooth muscle tone for airway collapsibility has been reported for different animal species. Trachea and large airways of lambs, dogs, rabbits, and pigs were less compliant and less collapsible when stimulated with a bronchoconstrictor[33-36].

Many airways collapsed at negative pressures close to 0 cm H_2O or higher. In vivo these airways will depend on parenchymal recoil pressure to remain open. Small airways are more collapsible compared to central airways. Segmental bronchi obtained from infants who died from sudden infant death syndrome collapsed at transmural pressures of -11.4 (-4 to -16) cm H_2O[36]. Central airways are probably less collapsible due to the high percentage of the airway wall made up of cartilage[22]. We conclude that collapsibility of small airways will mainly depend on smooth muscle tone and parenchymal support.

Effects of Volume History

The mechanical characteristics of the first cycle were substantially different from the subsequent cycles. On the first cycle, airways were less compliant, had a greater hysteresis, and were less collapsible compared to subsequent cycles. Similar findings relating to compliance and hysteresis were obtained in bronchi and tracheal strip preparations from dogs[29, 37]. Also, the effect of volume history on compliance and hysteresis has been described for normal subjects, asthmatics, and COPD patients[38-41]. In the general population and in COPD patients a deep inhalation results in broncho-dilatation[38, 41]. In asthmatics deep inhalation can result in broncho-constriction or -dilatation. In COPD, this effect is reduced but still present after inhalation of bronchodilators [41]. In fact, we found that the difference in sCdyn and sη between the first and the consecutive cycles persisted even after maximal relaxation by isoprenaline. We therefore conclude that the effect of volume history on sCdyn and sη is not only related to smooth muscle tone but also to the connective tissue within the airway

wall. We did not find a correlation between the effect of volume history and any of the airway wall areas. Our data suggest that wall areas do not reflect fibrous tissue composition, which probably determine mechanical qualities.

Implications for Therapy, and Conclusions

In this study we showed that smooth muscle area and tone are important determinants for the dynamic properties of human small airways of patients with COPD. Airway compliance is an important predictor of airway diameter and lung compliance[42, 43]. In fact, in this study we showed that maximal bronchodilatation doubled compliance and increased the diameter of the airway segments independently of airway wall thickness. In other words these airways had reversible bronchoconstriction. In vivo we previously found indirect evidence that narrowed airways can still be reversible in spite of wall thickening[1]. Pre-operatively measured reversibility in COPD patients was correlated to airway wall thickness.

Furthermore, we showed that reduction of smooth muscle tone resulted in a decrease of airway hysteresis and therefore has the potential to reduce the work of breathing. Our findings support the use of bronchodilators for COPD patients[44]. But their use could come at a price, because the reduced smooth muscle tone increases airway collapsibility and could therefore facilitate airway closure. In combination with emphysema, dilated airways lacking parenchymal support could collapse at positive transmural pressures and thickening of the airway wall is clearly not protective against airway collapse.

We conclude that smooth muscle area, not the total wall area, and smooth muscle tone are important determinants for airway compliance and hysteresis. In addition, we found that smooth muscle tone is an important determinant for airway collapsibility. Hysteresis of human isolated airway segments is increased in COPD patients with severe airflow obstruction.

Acknowledgement

References

1. Tiddens HAWM, Paré PD, Hogg JC, Hop WCJ, Lambert R, Jongste JC. Cartilaginous airway dimensions and airflow obstruction in human lungs. Am J Respir Crit Care Med 1995;152:260-266.
2. Bai TR. Abnormalities in airway smooth muscle in fatal asthma. Am Rev Respir Dis 1990;141:552-557.
3. Carroll N, Elliot J, Morton A, James A. The structure of large and small airways in nonfatal and fatal asthma. Am Rev Respir Dis 1993;147:405-410.
4. James AL, Paré PD, Hogg JC. The mechanics of airway narrowing in asthma. Am Rev Respir Dis 1989;139(1):242-246.
5. Lambert RK, Wiggs BR, Kuwano K. Functional significance of increased airway smooth muscle in asthma and COPD. J Appl Physiol 1993;74:2771-2781.
6. de Jongste JC, Mons H, Block R, Bonta IL, Fredriksz AP, Kerrebijn KF. Increased in vitro histamine responses in human small airway smooth muscle from patients with chronic obstructive pulmonary disease. Am Rev Respir Dis 1987;135:549-553.
7. Black JL. Pharmacology of airway smooth muscle in chronic obstructive pulmonary disease and in asthma [published erratum appears in Am Rev Respir Dis 1991 Sep;144(3 Pt 1):733]. Am Rev Respir Dis 1991;143(5 Pt 1):1177-1181.
8. Ishida K, Paré PD, Hards J, Schellenberg RR. Mechanical properties of human bronchial smooth muscle in vitro. J Appl Physiol 1992;73(4):1481-1485.
9. Bramley AM, Thomson RJ, Roberts CR, Schellenberg RR. Hypothesis: excessive bronchoconstriction in asthma is due to decreased airway elastance. Eur Respir J 1994;7(2):337-341.
10. Roche WR, Beasley R, Williams JH, Holgate ST. Subepithelial fibrosis in the bronchi of asthmatics. Lancet 1989;1(8637):520-524.
11. Brewster CE, Howarth PH, Djukanovic R, Wilson J, Holgate ST, Roche WR. Myofibroblasts and subepithelial fibrosis in bronchial asthma. Am J Respir Cell Mol Biol 1990;3(5):507-511.
12. Chetta A, Foresi A, Del Donno M, Bertorelli G, Pesci A, Olivieri D. Airways remodelling is a distinctive feature of asthma and is related to severity of disease. Chest 1997;111:852-857.
13. Quanjer PH, Dalhuijsen A, Zomeren BC. Summary equations of reference values. Bull Europ Physiopath Resp 1983;19(suppl 5):45-51.
14. Hughes JM, Hoppin FG, Jr., Mead J. Effect of lung inflation on bronchial length and diameter in excised lungs. J Appl Physiol 1972;32(1):25-35.
15. Hughes JM, Jones HA, Wilson AG. Bronchial hysteresis in excised lungs. J Physiol (Lond) 1975;249(3):435-443.
16. Karlinsky JB, Snider GL, Franzblau C, Stone PJ, Hoppin FG, Jr. In vitro effects of elastase and collagenase on mechanical properties of hamster lungs. Am Rev Respir Dis 1976;113(6):769-777.
17. Bai A, Eidelman DH, Hogg JC, James AL, Lambert RK, Ludwig MS, Martin J, McDonald DM, Mitzner WA, Okazawa M, Pack RJ, Paré PD, Schellenberg RR, Tiddens HAWM, Wagner EM, Yager D. Proposed nomenclature for quantifying subdivisions of the bronchial wall. J Appl Physiol 1994;77(2):1011-1014.
18. Wright JL, Cosio M, Wiggs B, Hogg JC. A morphologic grading scheme for membranous and respiratory bronchioles. Arch Pathol Lab Med 1985;109(2):163-165.
19. Bland JM, Altman DG. Statistical methods for assessing agreement between two methods of clinical measurement. The Lancet 1986;1(8476):307-310.
20. Bosken CH, Wiggs BR, Paré PD, Hogg JC. Small airway dimensions in smokers with obstruction to airflow. Am Rev Respir Dis 1990;142(3):563-570.
21. Kuwano K, Bosken CH, Paré PD, Bai TR, Wiggs BR, Hogg JC. Small airways dimensions in asthma and chronic obstructive pulmonary disease. Am Rev Respir Dis 1993;148:1220-1225.
22. Tiddens HAWM, Boogaard JM, Jongste JC, Hop WCJ, Coxson HO, Paré PD. Physiological and morphological determinants of maximal expiratory flow in chronic obstructive lung disease. Eur Respir J 1996;9:1785-1794.

23. Tiddens HAWM, Koopman LP, Lambert RK, Elliott WM, Hop WCJ, van den Mark TW, de Boer WJ, de Jongste JC. Airway wall dimensions and airway function in cystic fibrosis lungs. Submitted 1997.
24. Tisi GM, Minh VD, Friedman PJ. In vivo dimensional response of airways of different size to transpulmonary pressure. J Appl Physiol 1975;39(1):23-29.
25. Prakash UB, Hyatt RE. Static mechanical properties of bronchi in normal excised human lungs. J Appl Physiol 1978;45(1):45-50.
26. Hahn HL, Watson A, Wilson AG, Pride NB. Influence of bronchomotor tone on airway dimensions and resistance in excised dog lungs. J Appl Physiol 1980;49(2):270-278.
27. Baier H, Zarzecki S, Wanner A. Influence of lung inflation on the cross-sectional area of central airways in normals and in patients with lung disease. Respiration 1981;41(3):145- 154.
28. Gold WM, Kaufman HS, Nadel JA. Elastic recoil of the lungs in chronic asthmatic patients before and after therapy. J Appl Physiol 1967;23(4):433-438.
29. Sasaki H, Hoppin FG, Jr. Hysteresis of contracted airway smooth muscle. J Appl Physiol 1979;47(6):1251-1262.
30. Wang YT, Thompson LM, Ingenito EP, Ingram RH, Jr. Effects of increasing doses of beta-agonists on airway and parenchymal hysteresis. J Appl Physiol 1990;68(1):363-368.
31. Fredberg JJ, Stamenovic D. On the imperfect elasticity of lung tissue. J Appl Physiol 1989;67(6):2408-2419.
32. Hulsmann AR, Raatgeep HR, Den Hollander JC, Bakker WH, Saxena PR, De Jongste JC. Permeability of human isolated airways increases after hydrogen peroxide and poly-L-arginine. Am J Respir Crit Care Med 1996;153(2):841-846.
33. Olsen CR, Stevens AE, McIlroy MB. Rigidity of trachea and bronchi during muscular constriction. J Appl Physiol 1967;23(1):27-43.
34. Penn RB, Wolfson MR, Shaffer TH. Effect of tracheal smooth muscle tone on collapsibility of immature airways. J Appl Physiol 1988;65(2):863-869.
35. Okazawa M, Paré PD. Pressure area relationship of membranous airways in rabbit. Am J Respir Crit Care Med 1994;149(4):A770.
36. McFawn PK, Mitchell HW. Bronchial compliance and wall structure during development of the immature human and pig lung. Eur Respir J 1997;10:27-34.
37. Gunst SJ. Contractile force of canine airway smooth muscle during cyclical length changes. J Appl Physiol 1983;55(3):759-769.
38. Sparrow D, O'Connor GT, Weiss ST, DeMolles D, Ingram RH, Jr. Volume history effects and airway responsiveness in middle-aged and older men: The normative aging study. Am J Respir Crit Care Med 1997;155:888-892.
39. Wheatley JR, Paré PD, Engel LA. Reversibility of induced bronchoconstriction by deep inspiration in asthmatic and normal subjects. Eur Respir J 1989;2(4):331-339.
40. Lim TK, Pride NB, Ingram RH, Jr. Effects of volume history during spontaneous and acutely induced air-flow obstruction in asthma. Am Rev Respir Dis 1987;135(3):591-596.
41. Fairshter RD. Airway hysteresis in normal subjects and individuals with chronic airflow obstruction. J Appl Physiol 1985;58(5):1505-1510.
42. Clay TP, Hughes JM, Jones HA. Relationship between intrapulmonary airway diameter and smooth muscle tone in excised lungs. J Physiol (Lond) 1977;273(2):355-365.
43. Mitzner W, Blosser S, Yager D, Wagner E. Effect of bronchial smooth muscle contraction on lung compliance. J Appl Physiol 1992;72(1):158-167.
44. Jones PW, Bosh TK. Quality of life changes in COPD patients treated with salmeterol. Am J Respir Crit Care Med 1997;155(4):1283-1289.

Airway Wall Dimensions and Airway Function in Cystic Fibrosis Lungs

Harm A.W.M. Tiddens, Laurens P. Koopman, Rodney K. Lambert,
W. Mark Elliott, Wim C.J. Hop, Thomas W. van der Mark, Wim J. de Boer,
and Johan C. de Jongste.

Department of Pediatrics, Division of Respiratory Medicine, and Department of
Biostatistics, Erasmus University and University Hospital/Sophia Children's
Hospital, Rotterdam, the Netherlands. Department of Physics, Massey University,
Palmerston North, New Zealand. Respiratory Health Network of Centers of
Excellence, St. Paul's Hospital Pulmonary Research Laboratory, University of
British Columbia, Vancouver, Canada. Department of Pulmonary Medicine, and
Department of Cardiothoracic Surgery, University Hospital Groningen,
The Netherlands.

Introduction

In most cystic fibrosis (CF) patients, chronic airway inflammation leads to progressive airflow obstruction and increased bronchial responsiveness. The morphological features of CF lungs obtained at autopsy have been described in a number of studies[1-4]. Extensive inflammation of the bronchial walls and an increased volume proportion of the lung occupied by bronchi was found in CF lungs compared to controls[1,3]. It is not clear however, how these pathologic findings relate to the severity of airflow obstruction and increased bronchial responsiveness in CF patients. From a previous study we know that thickening of the airway wall of small cartilaginous airways is an important determinant of airflow obstruction[5]. In addition, another striking finding in CF lungs is the degeneration and sloughing of airway epithelial cells[6]. The respiratory epithelium plays an important role in the modulation of airway responsiveness [7, 8]. How the thickening of the airway wall and the loss of epithelium are distributed along the bronchial tree in CF patients is unknown.

The aim of our study was to measure changes of airway wall dimensions in CF lungs, and to compare these dimensions to those of chronic obstructive pulmonary disease (COPD). CF lungs were obtained from lung transplantation, lobectomy, and autopsy. We measured the airway wall dimensions and epithelial loss in these lungs by means of computerized morphometry. For COPD we used airway wall dimensions from a previous study[5]. Airway dimensions of CF and COPD patients were inserted into a computational model to study their effect on airway resistance and responsiveness.

Methods

Study Population

Lung tissue was obtained from 20 CF patients. In lung tissue of 3 patients we could not identify any intact airways, these patients were therefore excluded from further analysis. Lung tissue of the remaining 17 CF patients was obtained from lung transplantation (n = 12), lobectomy (n = 1), and autopsy (n = 4). All autopsy lungs came from patients who died from respiratory failure. The autopsy was done within

48 hours after death. Airway dimensions of CF patients were compared to those of 72 COPD patients who had a lobar resection or pneumonectomy for a solitary peripheral lung lesion. These COPD patients were previously described[5]. The morphology of the respiratory epithelium could not be measured in these COPD patients. We therefore measured the epithelium in a separate group of 22 COPD patients. COPD patients were excluded when segmental or larger airways were found to be obstructed during bronchoscopy or at pathological examination. Informed consent was obtained in all cases. Clinical data of the CF and COPD patients are summarized in Table 1.

Table 1

STUDY POPULATION CHARACTERISTICS AND LUNG FUNCTION

| | | Cystic Fibrosis | | COPD |
	n	Mean ± SD (range)	n	Mean ± SD (range)
Age, years	17	24.1 ± 9 (7-45)	72	61 ± 9.5 (37-83)
Male/female		10/7		54/18
Pack years		0		54.7 ± 34.5 (0.4-180)
Current smokers		0		45
TLC (% pred)	11	110 ± 17 (80-152)	72	109 ± 15 (81-154)
FRC (% pred)	11	147 ± 33 (104-197)	72	123 ± 24 (70-177)
RV (% pred)	11	284 ± 53 (199-368)	72	133 ± 34 (66-219)
FEV_1 (% pred)	17	27 ± 16 (36-105)	72	94 ± 18 (58-135)
FVC (% pred)	17	41 ± 17 (14-78)	72	96 ± 13 (64-134)
FEV_1/FVC (% pred)	17	56 ± 19 (36-105)	72	92 ± 12 (55-114)

Definition of abbreviations: COPD=chronic obstructive pulmonary disease; SD=standard deviation; Pack years=number of years smoking one pack of cigarettes a day; TLC=Total lung capacity; (% pred)= % of predicted value; FRC=functional residual capacity; RV=residual volume; FEV_1=forced expiratory volume in 1 second; FVC=forced vital capacity; FEV_1/FVC=forced expiratory volume in 1 second as fraction of forced vital capacity.

Lung Function Studies

For CF patients we obtained the most recent lung function tests performed prior to lung transplantation or autopsy. These were done in 3 different lung function laboratories. Dynamic lung volumes could be obtained from all patients. Static lung volumes were present for 11 out of 17 CF patients. Lung function of the group of 72 COPD patients was done within one week prior to surgery in a single laboratory[5].

Values were expressed as a percentage of the predicted values according to the prediction equations of Quanjer[9, 10]. For the four CF patients below the age of 18 years we used the prediction equations of Zapletal[11]. We expressed FEV_1 as the absolute percentage of FVC. Lung function data of the separate group of 22 COPD patients were obtained from 4 different lung function laboratories in a non-standardized way; hence we have not further analyzed these values.

Morphological Studies

The central bronchi of the CF transplant recipients lungs were gently washed to remove sputum, with 0.9% saline, delivered through a fine catheter. The lavage was continued until the return fluid was clear. Next the lung was fixed in 10 % formalin for at least 24 hours. COPD specimens were inflated with 10 % formalin or 2 % glutaraldehyde at a pressure of 25 cm H_2O and submerged in the fixative for at least 24 hours. The fixed specimens were serially sliced at 1 cm intervals in a sagittal plane. Intrapulmonary cartilaginous airways that were cut in cross section were randomly selected from each specimen for morphometric analysis. Tissue blocks containing cartilaginous airways were decalcified, embedded in paraffin, and cut at 5 micron thickness. The CF airways, and the COPD airways used for measurements related to the respiratory epithelium, were stained with a combined Gomori trichrome and Gomori elastin stain. This stain resulted in a good color contrast between airway wall structures and secretions within the lumen. The airways of the group of 72 COPD patients were stained with haematoxylin and eosin and using the Masson's trichrome technique.

Measurement of Airway Dimensions

Sections from cartilaginous airways from CF and COPD patients that were transversely cut and did not show bifurcation or disruption of the wall were selected for
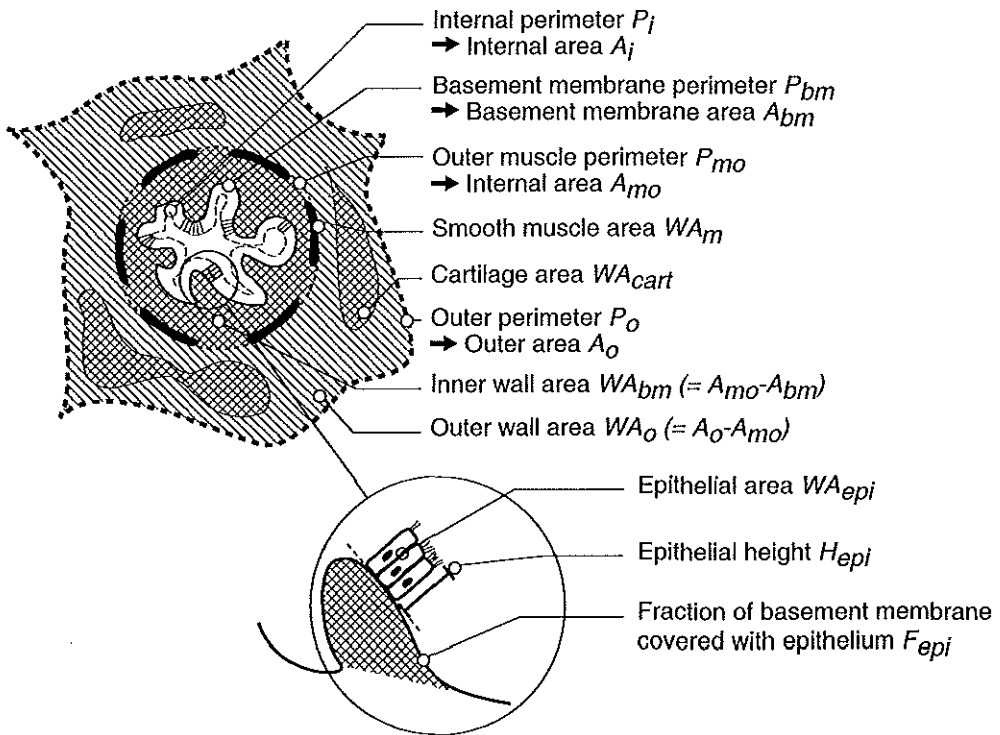
Internal perimeter P_i
→ Internal area A_i

Basement membrane perimeter P_{bm}
→ Basement membrane area A_{bm}

Outer muscle perimeter P_{mo}
→ Internal area A_{mo}

Smooth muscle area WA_m

Cartilage area WA_{cart}

Outer perimeter P_o
→ Outer area A_o

Inner wall area WA_{bm} ($= A_{mo}\text{-}A_{bm}$)

Outer wall area WA_o ($= A_o\text{-}A_{mo}$)

Epithelial area WA_{epi}

Epithelial height H_{epi}

Fraction of basement membrane covered with epithelium F_{epi}

Figure 1. Diagram of measured airway dimensions

measurement. The measurements made are shown in Figure 1 and include: basement membrane perimeter (P_{bm}) and the area of the lumen including respiratory epithelium bound by the basement membrane (A_{bm}); the outer muscle perimeter (P_{mo}) and the area enclosed by this perimeter (A_{mo}); the area occupied by smooth muscle (WA_m); and the area occupied by cartilage (WA_{cart}). From these measurements we calculated the inner wall area ($WA_{bm} = A_{mo}\text{-}A_{bm}$). We used nomenclature which was proposed for quantifying subdivisions in the bronchial wall[12]. Furthermore we measured the height of the respiratory epithelium (H_{epi}) and the fraction of the P_{bm} covered by epithelium (F_{epi}). H_{epi} was measured as follows. First, a grid containing parallel sinusoids was superimposed over the computer image of the airway. The probability of the sinusoidal grid line intersecting with the basement membrane is random and independent of the orientation of the membrane. Second, when respiratory epithelium was present at the point where the sinusoid crossed the basement membrane, we

measured the epithelial height by drawing a straight line perpendicular from the membrane to the top of the ciliary border. The length of this line was automatically computed. When respiratory epithelium was absent a zero was scored for height. Third, H_{epi} was calculated for each airway section by computing the average of at least 15 epithelial height measurements around the lumen. Sites where respiratory epithelium was missing were not included in this average. F_{epi} was calculated by dividing the number of intersecting points through the basement membrane covered by respiratory epithelium by the total number of intersecting points, including the intersecting points at sites where the respiratory epithelium was absent. The wall area covered by epithelium (WA_{epi}) was calculated by multiplying P_{bm} by H_{epi} and F_{epi}. WA_{epi} was expressed as the percentage of the area of the fully relaxed airway lumen (A^*_{bm}) occupied by respiratory epithelium for CF and COPD airways at a P_{bm} of 1 to 35 mm. These calculations were made for $F_{epi} = 1$ in which case, the basement membrane was completely covered by the epithelium and for F_{epi} as found in the airways of CF and COPD patients.

Histological Staining and Image Analysis
Airway dimensions of COPD airways except for WA_m, H_{epi}, and F_{epi} were measured on Hematoxylin and eosin stained sections using a microscope fitted with a camera lucida that superimposed the cursor-light of a digitizing board onto the microscope image of the airway. WA_m was measured on a trichrome stained section using an automated image analysis system (Bioview, Infrascan, Vancouver BC, Canada). An area of smooth muscle was selected by the observer and color thresholding was used to compute the muscle area. The operator was able to interact with the program to adjust the threshold so that all the muscle and only the muscle was included in the measurement. All airway dimensions of the CF patients and H_{epi}, and F_{epi} of the second group of 22 COPD patients were measured using an automated image analysis system (KS 400, Kontron Elektronic, Eching/Munich, Germany). Airways too large to be recorded in one image were recorded in four separate images that were merged to a single image.
Measurements of airway dimensions were performed by 2 observers (HT and LK).

The intra-observer variability was assessed by remeasurement of 10 randomly selected airways with an interval of 2 months. To evaluate the possible influence of different methodologies used in this study we assessed the inter-study variability as follows. We selected randomly 15 hematoxylin and eosin stained airways that were measured previously by observer HT[5]. Recuts were done from the tissue blocks of these airways and sections were stained with a Gomori trichrome and Gomori elastin stain. Next these sections were measured on the KS400 system by another observer (LK). The inter-study variability therefore is the sum of the variability between 2 observers, 2 image analysis systems, 2 different sections, and 2 staining techniques.

Statistical Analysis

The intra-observer and inter-study variability were calculated by expressing the difference of the first and the second measurement as a percentage of the average of both observations[13]. This percentage was plotted against P_{bm} to detect systematic errors dependent on airway size. Furthermore we calculated the mean and the standard error of the mean (sem) of the measurements that were compared.

Repeated measurement analysis of variance (RMANOVA), which allows for differences between and within patients, was used to asses the relationships between airway wall dimensions (WA_{bm}, WA_m, WA_{cart}, H_{epi}, F_{epi}) and airway size (P_{bm})[14, 15]. RMANOVA analyses the patients as a continuum and thus avoids the bias that would result from making subgroups of patients. The previous work of Bosken and coworkers[16], Kuwano and coworkers[17], and Tiddens and coworkers[5] found linear relationships between the square root of airway wall areas and airway size. Square root transformation of the present data (WA_{bm}, WA_m, WA_{cart},) again resulted in normal distributions of data around the linear regression lines. In the analysis the airway size values were centered by subtracting the mean value for P_{bm} of 14mm from all values of P_{bm}. The intercept of the individual regression lines for individual patients of a particular airway wall dimension therefore denotes its level at a P_{bm} of 14mm. The average slope and intercepts of the CF patients were compared to those of the COPD patients. The level of significance was set at $p=0.05$ (two sided). Data are expressed as mean ± standard deviation and range, unless indicated otherwise.

Computational Analysis of Altered Airway Dimensions for Airway Resistance

To predict the effect of airway dimensions on airway resistance we used a computational model, as described by Wiggs et al[18] and modified by Lambert et al[19, 20]. Briefly, the geometry of the bronchial tree in the model is a dichotomously branching network with 16 generations. The model is designed to examine the relative contributions of airway wall dimensions on airway responsiveness. The dose-response relationship of airway resistance against an increasing dose of a hypothetical bronchoconstricting agent that causes smooth muscle shortening was calculated. In the model the airway smooth muscle in each generation of the tracheo-bronchial tree contracts in response to the agonist and shortens until the stress generated by the muscle is maximal. The plateau of the dose-response curve is achieved when the muscle stress in all airway generations is maximal. The model takes account of both the geometry and the mechanics of the airway and parenchymal tissue.

The computational model used the following airway wall dimensions: For COPD patients airway dimensions ($\sqrt{WA_{bm}}$ and $\sqrt{WA_m}$ vs P_{bm}) were derived from a single data base which contains patients with and without airflow obstruction (St. Paul's Hopsital, Pulmonary Research Laboratory, Vancouver, Canada). For membranous airways (P_{bm} 2-4.7 mm) equations were derived from a study by Kuwano et al[17]. For cartilaginous airways (P_{bm} 4.7-58 mm) equations were derived from a study by Tiddens et al[5].

For CF patients, we used the same equations for membranous airways as for the COPD patients[17] since we could not obtain a sufficient number of membranous airways in CF patients to calculate a reliable regression equation for these airways separately. For cartilaginous airways of CF patients we used the equations ($\sqrt{WA_{bm}}$ and $\sqrt{WA_m}$ vs P_{bm}) derived from the present study as shown in Figure 2. Differences in the computed dose response curves of CF and COPD airways are therefore the result of differences in cartilaginous airways dimensions only. For the epithelial area of membranous and cartilaginous airways in CF and COPD patients we used the equation for $\sqrt{WA_{epi}}$ vs P_{bm} of the present study.

In the model we assumed that the area of smooth muscle is correlated with force in a

linear fashion. From the simulated dose response curves we calculated, baseline resistance, the dose of a hypothetical agonist that caused a 10-fold increase in resistance (PD_{10}), and the maximal plateau resistance achieved.

Results

Lung function

Lung function characteristics of the CF and COPD patients are shown in Table 1. All CF patients had severe airflow obstruction (mean FEV_1/FVC 33 ± 3 (29 to 38)%). Out of the group of 72 COPD patients, 24 patients had a maximum expiratory airflow within the normal range(FEV_1/FVC >75%), 21 patients had a mild reduction ($FEV_1/$ FVC 65 to 75%) and 27 patients had a severe reduction (FEV_1/FVC <65% predicted). The inclusion criteria for the second group of 22 COPD patients were the same as for the first group of 72 patients. We assume therefore that the distribution of airflow limitation was similar in both groups.

Morphologic Studies

Morphometric measurements were made on 88 CF airways. The mean number of airways per patient was 4.8 (1 to 11). The range of the P_{bm} was 1.48 to 38 mm, this corresponds to an airway diameter of 0.47 to 12 mm. Airway size ranged from the main stem bronchus to the bronchioles, or airway generations 1 to 16[21]. The range of the P_{bm} of the cartilaginous airways only was 5.9 to 38 mm.

From the group of 72 COPD patients 341 cartilaginous airways were measured, a mean of 4.7 (3 to 7) airways per patient. The range of the P_{bm} was 5 to 34 mm. This corresponds to an airway diameter of 1.5-10.9 mm, or airway generations 1 to 12 [21]. From the second group of 22 COPD patients 63 airways were measured, mean 2.9 (1 to 10) airways per patient. The range of the P_{bm} was 1.5 to 26 mm. This corresponds to an airway diameter of 0.5-8.3 mm, or airway generation 2 to 16 [21].

The intra-observer variability was -1.5 sem $\pm$ 0.85% for P_{bm}, 2.6 sem $\pm$ 2.17% for WA_{bm}, 7.8 sem $\pm$ 11.2% for WA_m, -4.8 sem $\pm$ 3.31 % for WA_{cart}, and 1 sem $\pm$ 4.03
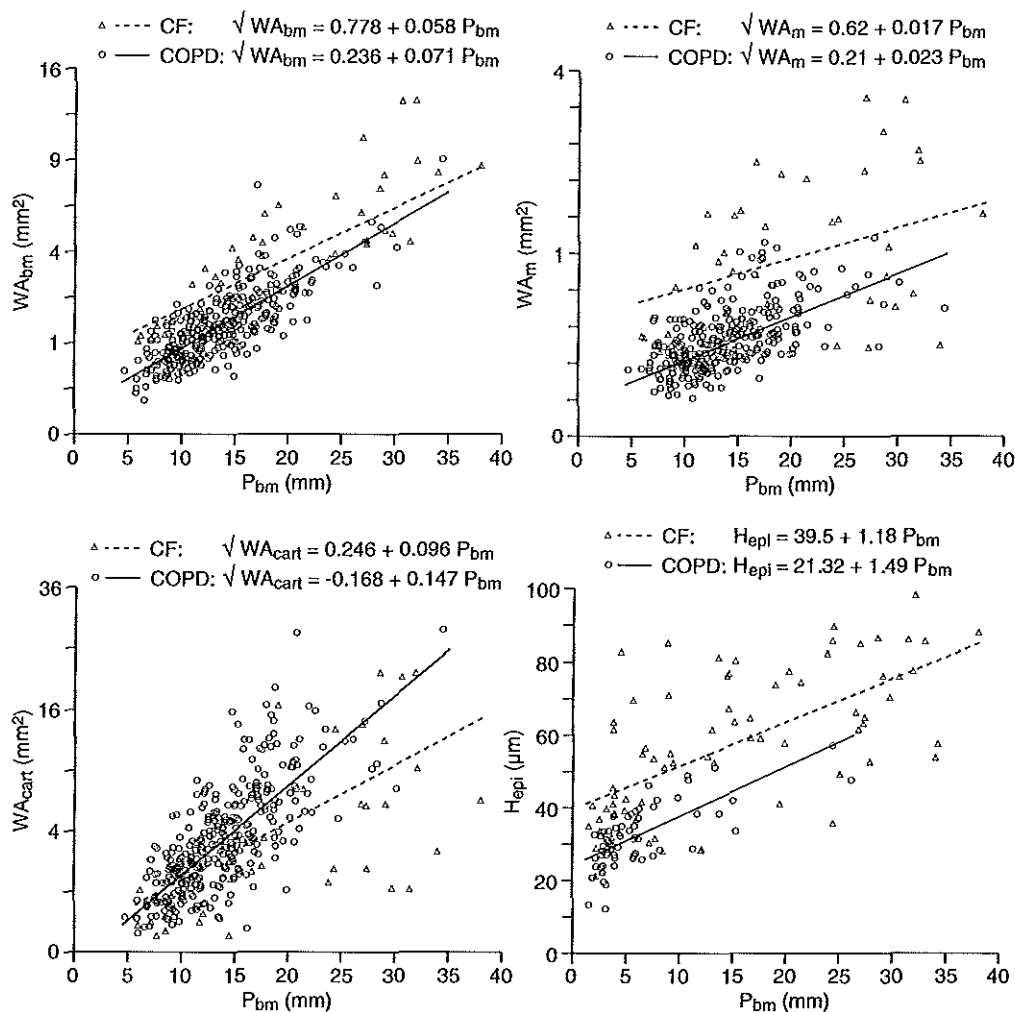
Figure 2. Morphometric airway dimensions versus airway size. The dashed regression line represents the relation of an airway dimension versus perimeter basement membrane (P_{bm}) for CF patients (triangles). The solid line represents the relation of an airway dimension versus P_{bm} for COPD patients (circles). Formulas for the regressions are displayed in the graphs. *(A)* WA_{bm}=inner wall area without epithelial area. *(B)* WA_m=wall area occupied by smooth muscle area. *(C)* WA_{cart}=wall area occupied by cartilage. *(D)* H_{epi}=height of respiratory epithelium. Note the square root transformed vertical axis. There are 88 data points plotted from 17 CF patients in the figures. There are 341 data points from 72 COPD patients plotted in figure (A), (B), and (C), and 63 data points from 22 COPD patients in figure (D). Due to overlap of data points, some circles and triangles appear filled.

% for H_{epi}. The inter-study variability was 4.6 sem $\pm$ 2.6% for P_{bm}, -5.8 sem $\pm$ 7.5 % for WA_{bm} , -3.5 sem $\pm$ 11.8 % for WA_m, -6 sem $\pm$ 20.7% for WA_{cart} . There was no systematic relationship between airway size (P_{bm}) and the intra-observer or inter-study variability for any variable. For CF patients, highly significant (P<0.001) linear relations were found between airway wall dimensions ($\sqrt{WA_{bm}}$, $\sqrt{WA_m}$, $\sqrt{WA_{cart}}$, and H_{epi}) and airway size (P_{bm}) (Figure 2). For COPD patients the linear relations between $\sqrt{WA_{bm}}$, $\sqrt{WA_m}$, and $\sqrt{WA_{cart}}$ and P_{bm} are described elsewhere[5]. The linear relation between epithelial height (H_{epi}) and P_{bm} was highly significant (P<0.001) for COPD patients.

Airway Dimensions
Figure 2 shows airway dimensions ($\sqrt{WA_{bm}}$, $\sqrt{WA_m}$, $\sqrt{WA_{cart}}$, and H_{epi}) versus airway size (P_{bm}) for CF patients and COPD patients. $\sqrt{WA_{bm}}$, $\sqrt{WA_m}$, and H_{epi} versus P_{bm} were at a significantly higher level for CF patients in comparison to COPD patients (p<0.001, <0.01, and <0.01 respectively). $\sqrt{WA_{cart}}$ versus P_{bm} was at a lower level for CF patients than for COPD (P<0.01). Table 2 shows the ratios between the airway dimensions for CF and COPD airways in the P_{bm} range of 5 to 35 mm. F_{epi} was 0.77 for CF and 0.91 for COPD (P<0.01). There was no relation between airway size and F_{epi} for CF and COPD. Figure 3 shows the percentage of the lumen of the fully relaxed airway occupied by respiratory epithelium for CF and COPD airways at a P_{bm} of 1 to 35 mm.

For airway dimensions of CF patients we used airways obtained from transplantation, lobectomy, and autopsy. This could have introduced a bias. The analysis was therefore repeated without the 16 airways obtained from autopsies and lobectomy. This had very little influence on the equations for airway dimensions ($\sqrt{WA_{bm}}$, $\sqrt{WA_m}$, $\sqrt{WA_{cart}}$, and H_{epi}) versus airway size (P_{bm}). The fraction of the P_{bm} covered by epithelium increased from 70 to 77 percent. The differences between the airway dimensions of CF and COPD patients remained highly significant.

Airway Dimensions and Airway Resistance
Figure 4 shows the dose-response relationship of airway resistance against the log
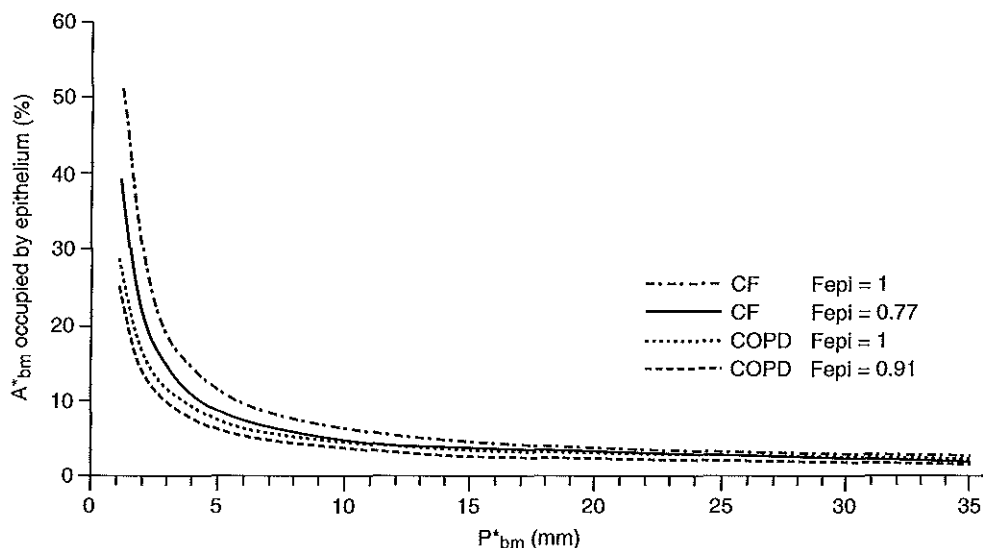
Figure 3. This figure shows the percentage of relaxed airway lumen covered by epithelium versus airway size. This was calcluted for cystic fibrosis (CF), and chronic obstructive pulmonary disease (COPD) patients. The percentage was calculated with and without taking the epithelial loss into account.

Definition of abbreviations: P^*_{bm} = perimeter of basement membrane in the fully relaxed airway; F_{epi} = Fraction of basement membrane covered with epithelium. When F_{epi} = 1 the basement membrane is completely covered by epithelium.

(dose) of a hypothetical bronchoconstricting agent for CF and COPD airways. The curves are shown for CF and COPD when we introduced WA_{bm}, $WA_{epi} \cdot F_{epi}$, and WA_{epi}, in a stepwise fashion into the computational model. Since we found that the area of smooth muscle was increased in CF compared to COPD this would increase the force generated by the smooth muscle for CF in the model. However, we do not know whether in vivo the smooth muscle force is increased in CF. We therefore did the dose-response relationship for CF first with the WA_m equation of COPD. This simulation showed us the effect of WA_{bm}, $WA_{epi} \cdot F_{epi}$, and WA_{epi} on airway resistance without increased smooth muscle force. The simulations with the WA_m equation of CF showed us the effect of WA_{bm}, $WA_{epi} \cdot F_{epi}$, and WA_{epi} on airway resistance with an increased smooth muscle force .

Baseline resistance for CF was 32 to 219% higher than in COPD for the different
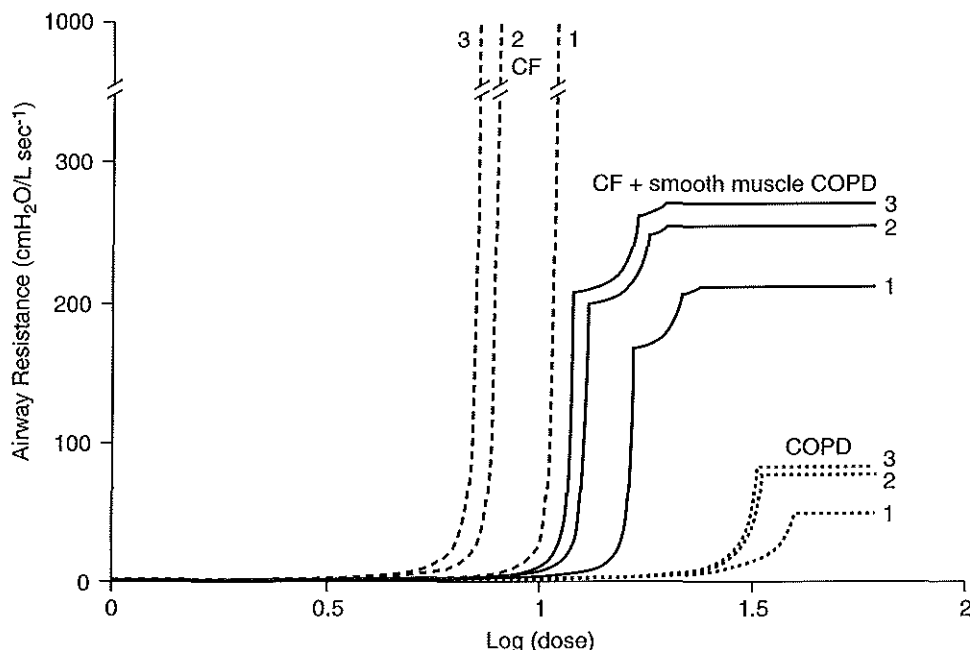
Figure 4. Simulated resistance-dose curves to study the effect of airway dimensions on airway resistance for COPD=chronic obstructive pulmonary disease, and CF=cystic fibrosis. The lines represent the dose-response relationship of airway resistance against an increasing dose of a hypothetical bronchoconstricting agent. Computations were done with airway dimensions of the following 3 groups of patients; COPD (dotted line); CF with the smooth muscle dimensions of COPD patients (solid line); and CF with CF smooth muscle (dashed line). For each of the three groups we did the following simulations; 1=without epithelium; 2=with epithelium but taking epithelial loss into account, 3=with intact epithelium. The humps in the CF with CF smooth muscle lines show the moment when the smooth muscle tension equals the load in a given generation of the bronchial tree. When this is the case in all generations the plateau is obtained.

simulations. The PD_{10} for CF was 0.3 to 0.6 log dose below that of COPD patients. The maximal resistance was 215 cm H_2O / (Ls^{-1}) higher for CF than in COPD when we did the simulation without WA_{epi} and with the WA_m of COPD for both CF and COPD. When we changed for CF the WA_m equation from COPD to CF, and therefore increased the force of the smooth muscle, a maximal plateau resistance was not reached below a resistance of 1000 cm H_2O/Ls^{-1} at which point the calculation was stopped. The maximal resistance in COPD increased from 49 to 83 cm H_2O/Ls^{-1} when we introduced the epithelium into the simulation.

163

Table 2
RATIO BETWEEN CF AND COPD

P_{bm}	WA_{bm}	WA_m	WA_{cart}	H_{epi}
5	3.3	4.7	-	1.6
10	2.1	3.2	0.9	1.4
15	1.7	2.5	0.7	1.3
20	1.4	2.1	0.6	1.2
25	1.2	1.8	0.6	1.2
30	1.1	1.6	0.5	1.1
35	1.1	1.4	0.5	1.1

Definition of abbreviations: CF=cystic fibrosis; COPD=chronic obstructive pulmonary disease; P_{bm}= perimeter basement membrane; WA_{bm}= inner wall area without epithelial area; WA_m= Smooth muscle area; WA_{cart}=cartilage area; H_{epi}=epithelial height.

Discussion

To our knowledge this is the first study in which the dimensions of a large number of airways have been measured in a group of CF patients suffering from end-stage lung disease. The airway dimensions of CF patients were compared to those of COPD patients with varying severity of lung disease. Furthermore we studied the effects of these dimensions on airway resistance and responsiveness in a computational model. Our results show that CF patients have a significant increase in airway wall area and smooth muscle area, taller epithelium, and a decrease in cartilage area compared to COPD patients. In addition we found a high percentage of epithelial loss in these patients. The changes in airway dimensions of CF patients are likely to contribute to the severe airflow obstruction, increased bronchial responsiveness and reversibility as described in these patients.

Airway dimensions
We found a substantial increase of the inner wall area and smooth muscle area of CF patients compared to COPD patients. This increase was larger in peripheral airways than in central airways (Table 2) and would be even more impressive if compared to normal airways for two reasons. First, we did not compare CF patients to healthy controls but to COPD patients in which the inner airway wall is also thickened[5]. Second, it is likely that there was a selection bias towards analysis of the better airways present in the CF lungs. Many airways had to be excluded from morphometric analysis since they were so heavily inflamed that histological structures could not be identified adequately. The inner airway wall area of CF patients of airways with a P_{bm} of 10 mm was increased in comparison to COPD by 210% and is similar to the inner wall area in patients who died from asthma as described by Kuwano and coworkers[17]. The bronchial smooth muscle area of CF patients of airways with a P_{bm} of 10 mm was increased by 320% compared to COPD and is even 33% higher than in patients who died from asthma[17].
For CF and COPD patients we found that the height of the respiratory epithelium increased with increasing size of the airway. The height of the respiratory epithelium in central airways of COPD patients was comparable to that of healthy subjects[22]

The height of the respiratory epithelium of CF patients was increased in comparison to COPD by 60 to 10% for peripheral and central airways respectively. The cause of the taller respiratory epithelium is unknown.

The area occupied by the thickened respiratory epithelium was not increased in our study because of the increased fractional loss of epithelium in CF patients compared to COPD. Inadequate fixation due to mucus impaction or the use of lobectomy or autopsy specimen could account for the increased epithelial loss. However, even when we excluded airways obtained from lobectomy or autopsy specimen the fractional loss in CF remained substantially higher than in COPD.

In a study by Dovey and co-authors[6] the area of ciliated cells in bronchioles of 16 patients who died of CF lung disease was increased when compared to controls. In this study the epithelial area was not related to airway size and therefore no valid size-corrected comparison could be made between CF and controls[23].

A number of authors have suggested a correlation between airway inflammation and the amount of cartilage in COPD patients[24-26]. We and others did not find such a correlation[5, 27, 28]. For CF patients however the area of cartilage in central airways was reduced compared to COPD. Loss of airway cartilage could result in increased airway collapsibility and therefore contribute to the severe expiratory airflow limitation as seen in the end stage lung disease of CF patients. In addition, the mechanical properties of the cartilage might be affected by the chronic inflammatory process.

Airway Dimensions and Bronchial Responsiveness

Increased bronchial responsiveness to bronchoconstricting agents was reported in 29 to 55% of CF patients[29-34] while increased bronchial responsiveness to bronchodilators is present in a similar percentage[31, 34-36]. The origin of this increased bronchial responsiveness is not clear. In CF patients thickening of the inner wall area increased computed baseline resistance up to 66% percent when compared to COPD. When the epithelial area was added to the inner wall area the PD_{10} of the dose-response curve shifted further to the left for CF and COPD airways. The plateau resistance nearly doubled for COPD patients as a result of this, suggesting that the epithelial area contributes substantially to bronchial responsiveness in CF and COPD.

We found an increased smooth muscle area in CF compared to COPD patients.

The increase in smooth muscle area could be the result of hypertrophy or hyperplasia of smooth muscle or an increase in smooth muscle matrix [37-38]. An increase in smooth muscle area does not necessarily imply that the force generated by the smooth muscle is increased. However, there are some indirect arguments that increased smooth muscle force could be present in CF patients. First, many patients have an increased response to directly acting bronchoconstrictors[29-34]. This response to bronchoconstrictors as indicated by PD_{20} and fall in FEV_1 is limited[30, 33]. Yet, it implies that the smooth muscle is able to shorten to some extent despite the load against which its has to shorten. This load is most likely increased due to thickening and stiffening of the heavily inflamed airway wall[39, 40]. Second, a large percentage of CF patients have an increased response to bronchodilators[31, 34-36]. This implies that even under baseline conditions the smooth muscle is shortened to some extent despite of the increased load.

Respiratory Epithelium

Loss of respiratory epithelium in CF airways has been described by a number of authors but was never quantified[6, 41]. We found that one third of the basement membrane in central and peripheral CF airways was not covered by epithelium.This high loss of epithelium might be related to the washing procedure of the large airways after the pneumonectomy. We think this is unlikely since epithelial loss in peripheral airways was as high as in central airways. The respiratory epithelium has a number of important functions and its loss in airways of CF patients can contribute to bacterial colonization, ongoing inflammation, and to impaired lung function. The respiratory epithelium forms a barrier that prevents penetration of substances present in the lumen into the airway wall[8]. Furthermore, normal respiratory epithelium forms a protection against colonization by bacteria. Its loss in airways of CF patients has been associated with the presence of Pseudomonas aeruginosa[42]. Another important function of the respiratory epithelium is modulation of smooth muscle tone by production of relaxing factors and by inactivation of bronchoconstricting mediators and neurotransmitters[43-45]. Loss of epithelial cells could therefore enhance bronchial responsiveness to histamine and methacholine[46]. In fact, in asthma it has been shown that the greater the loss of respiratory epithelium in biopsy specimens the greater the degree of airway

responsiveness[47]. The extensive loss of respiratory epithelium we found in CF could therefore contribute to an increased bronchial responsiveness in these patients.

Altered Airway Dimensions and Therapy

The thickening of the inner airway wall we found in CF airways increases baseline resistance. Airway wall thickness and airflow obstruction in patients with chronic obstructive pulmonary disease are correlated to inflammatory changes[5]. It is likely that the thickening of the airway wall of CF patients is also related to chronic inflammation. Anti-inflammatory therapy might somewhat reduce this thickening and thus improve lung function. In fact, treatment with oral or inhaled steroids, or with ibuprofen improved lung function and slowed the progression of lung disease in CF patients[48-50].

Anti-inflammatory and antibiotic treatment might limit the ongoing damage to the respiratory epithelium and move the balance towards repair of the epithelial layer and restitution of its functions.

Conclusion

CF patients with end-stage lung disease have substantial thickening of their inner wall area and smooth muscle area when compared to patients with COPD. In addition we found a reduction of the cartilage area in the central airways. Finally we found an increased height of the epithelial layer and a high percentage of epithelial loss. These changes in airway dimensions are likely to contribute to the severe airflow obstruction, and to the increased bronchial responsiveness to bronchoconstricting and bronchodilating agents as described in CF patients.

Acknowledgment

References

1. Bedrossian CWM, Greenberg SD, Singer DB, Hansen JJ, Rosenberg HS. The lung in cystic fibrosis; A quantitative study including prevalence of pathologic findings among different age groups. Hum Pathol 1973;7:195-204.
2. Simel DL, Mastin JP, Pratt PC, Wisseman CL, Shelburne JD, Spock A, Ingram P. Scanning electron microscopic study of the airways in normal children and in patients with cystic fibrosis and other lung diseases. Pediatr Pathol 1984;2:47- 64.
3. Tomashefski JF, Bruce M, Goldberg HI, Dearborn DG. Regional distribution of macroscopic lung disease in cystic fibrosis. Am Rev Respir Dis 1986;133:535- 540.
4. Sobonya RE, Taussig LM. Quantitative aspects of lung pathology in cystic fibrosis. Am Rev Respir Dis 1986;134:290-295.
5. Tiddens HAWM, Paré PD, Hogg JC, Hop WCJ, Lambert R, De Jongste JC. Cartilaginous airway dimensions and airflow obstruction in human lungs. Am J Respir Crit Care Med 1995;152:260-266.
6. Dovey M, Wisseman CL, Roggli VL, Roomans GM, Shelburne JD, Spock A. Ultrastructural morphology of the lung in cystic fibrosis. J Submicrosc Cytol Pathol 1989;21:521-534.
7. Sparrow MP, Omari TI, Mitchell HW. The epithelial barrier and airway responsiveness. Can J Physiol Pharmacol 1995;73:180-190.
8. Hulsmann AR, De Jongste JC. Modulation of airway responsiveness by the airway epithelium in humans, putative mechanisms. Clin Exp Allergy 1996;26: 1236-1242.
9. Quanjer PH, Dalhuijsen A, Zomeren BC. Summary Equations of reference values. Bull Europ Physiopath Resp 1983;19:45-51.
10. Quanjer PH, Tammeling GJ, Cotes JE, Pedersen OF, Peslin R, Yernault J-C. Lung volumes and forced ventilatory flows. Eur Respir J 1993;6:5-40.
11. Zapletal A, Samanek M, Paul T. Lung function in children and adolescents. Basel: Karger, In: Herzog H, ed. Progress in respiration research 1987;vol 22.
12. Bai A, Eidelman DH, Hogg JC, James AL, Lambert RK, Ludwig MS, Martin J, McDonald DM, Mitzner WA, Okazawa M, Pack RJ, Paré PD, Schellenberg RR, Tiddens HAWM, Wagner EM, Yager D. Proposed nomenclature for quantifying subdivisions of the bronchial wall. J Appl Physiol 1994;77:1011-1014.
13. Bland JM, Altman DG. Statistical methods for assessing agreement between two methods of clinical measurement. The Lancet 1986;1(8476):307-310.
14. Feldman HA. Families of lines: random effects in linear regression analysis. J Appl Physiol 1988;64:1721-1732.
15. Schluchter MD. Module 5V. In: Dixon WJ, ed. BMDP Statistical software manual. Burkely: University of California press, 1990:1207-1244.
16. Bosken CH, Wiggs BR, Paré PD, Hogg JC. Small airway dimensions in smokers with obstruction to airflow. Am Rev Respir Dis 1990;142:563-570.
17. Kuwano K, Bosken CH, Paré PD, Bai TR, Wiggs BR, Hogg JC. Small airways dimensions in asthma and chronic obstructive pulmonary disease. Am Rev Respir Dis 1993;148:1220-1225.
18. Wiggs BR, Moreno R, Hogg JC, Hilliam C, Paré PD. A model of the mechanics of airway narrowing. J Appl Physiol 1990; 69:849-860.
19. Lambert RK, Wiggs BR, Kuwano K. Functional significance of increased airway smooth muscle in asthma and COPD. J Appl Physiol 1993;74:2771-2781.
20. Okazawa M, Paré PD, Hogg JC, Lambert RK. Mechanical consequences of remodelling of the airway wall. In: Page C, Black J, eds. Airways and vascular remodelling in asthma and cardiovascular disease. London: Academic press, 1994:91-101.
21. Hammersley JR, Olson DE. Physical models of the smaller pulmonary airways. J Appl Physiol 1992;72:2402-2414.

22. Soderberg M, Hellstrom S, Sandstrom T, Lundgren R, Bergh A. Structural characterization of bronchial mucosal biopsies from healthy volunteers: a light and electron microscopical study. Eur Respir J 1990;3:261-266.
23. James AL, Hogg JC, Dunn LA, Paré PD. The use of the internal perimeter to compare airway size and to calculate smooth muscle shortening. Am Rev Respir Dis 1988;138:136-139.
24. Tandon MK, Cambell AH. Bronchial cartilage in chronic bronchitis. Thorax 1969;24:607-612.
25. Thurlbeck WM, Pun R, Toth J, Frazer RG. Bronchial cartilage in chronic obstructive lung disease. Am Rev Respir Dis 1974;109:73-80.
26. Nagai A, Thurlbeck WM, Konno K. Responsiveness and variability of airflow obstruction in chronic obstructive pulmonary disease. Am J Respir Crit Care Med 1995;151:635-639.
27. Dunhill MS, Massarella GR, Anderson JA. A comparison of the quantitative anatomy of the bronchi in normal subjects, in status asthmaticus, in chronic bronchitis, and in emphysema. Thorax 1969;24:176-179.
28. Mullen JB, Wright JL, Wiggs BR, Paré PD, Hogg JC. Reassessment of inflammation of airways in chronic bronchitis. Br Med J (Clin Res Ed) 1985;291:1235-1239.
29. Mellis CM, Levison H. Bronchial reactivity in cystic fibrosis. Pediatrics 1978;61:446-450.
30. Mitchell I, Corey M, Woenne R, Krastins IRB, Levison H. Bronchial hyperreactivity in cystic fibrosis and asthma. J Pediatr 1978;93:744-748.
31. Tobin MJ, Maguire O, Tempany E, Fitzgerald MX. Atopy and bronchial reactivity in older patients with cystic fibrosis. Thorax 1980;35:807-813.
32. van Asperen P, Mellis CM, South RT, Simpson SJ. Bronchial reactivity in cystic fibrosis with normal pulmonary function. Am J Dis Child 1981;135:815-819.
33. Eggleston PA, Rosenstein BJ, Stackhouse CM, Alexander MF. Airway hyperreactivity in cystic fibrosis. Chest 1988;94:360-365.
34. van Haren EHJ, Lammers J-WJ, Festen J, van Herwaarden CLA. Bronchial vagal tone and responsiveness to histamine, exercise and bronchodilators in adult patients with cystic fibrosis. Eur Respir J 1992;5:1083-1088.
35. Larsen G, Barron RJ, Cotton EK, Brooks JG. A comparative study of inhaled atropine sulfate and isoproterenol hydrochloride in cystic fibrosis. Am Rev Respir Dis 1979;119:399-407.
36. Ormerod LP, Thomson RA, Anderson CM, Stableforthe DE. Reversible airway obstruction in cystic fibrosis. Thorax 1980;35:768-772.
37. Bramley AM, Thomson RJ, Roberts CR, Schellenberg RR. Hypothesis: excessive bronchoconstriction in asthma is due to decreased airway elastance. Eur Respir J 1994;7:337-341.
38. Thomson RJ, Bramley AM, Schellenberg RR. Airway muscle sterology: implications for increased shortening in asthma. Am J Respir Crit Care Med 1996;154:749-757.
39. Lambert RK, Codd SL, Alley MR, Pack RJ. Physical determinants of bronchial mucosal folding. J Appl Physiol 1994;77:1206-1216.
40. Wilson JW, Li X, Pain MC. The lack of distensibility of asthmatic airways. Am Rev Respir Dis 1993;148:806-809.
41. Leigh MW, Kylander JE, Yankaskas JR, Boucher TC. Cell proliferation in bronchial epithelium and submucosal glands of cystic fibrosis patients. Am J Respir Cell Biol 1995;12:605-612.
42. Baltimore R, Christie C, Smith W. Immunohistopathologic localization of Pseudomonas aeruginosa in lungs from patients with cystic fibrosis. Am Rev Respir Dis 1989;140:1650-1661.
43. Farmer SG, Hay DWP. Airway epithelial modulation of smooth muscle function: The evidence for epithelium-derived inhibitory factor. In: Farmer SG, Hay DWP, eds. The airway epithelium: physiology, pathofysiology, and pahrmacology. New York: Marcel Dekker, inc., 1991:437-484.
44. Lilly CM, Drazen JM, Shore SA. Peptidase modulation of airway effects of neuropeptides. Proc Soc Exp Bio Med 1993;203:388-404.

45. Koga Y, Satoh S, Sodeyama N, Hashimoto Y, Yanagisawa T, Hirshman CA. Role of cholinesterase in airway epithelium mediated inhibition of acetylcholine induced contraction of guinea-pig isolated trachea. Eur J Pharmacol 1992;220:141-146.
46. Hulsmann AR, Raatgeep HR, Den Hollander JC, Stijnen T, Saxena PR, Kerrebijn KF, De Jongste JC. Oxidative epithelial damage produces hyperresponsiveness of human peripheral airways. Am J Respir Crit Care Med 1994;149:519-525.
47. Jeffery PK, Wardlaw AJ, Nelson FC, Collins JV, Kay AB. Bronchial biopsies in asthma. An ultrastructural, quantitative study and correlation with hyperreactivity. Am Rev Respir Dis 1989;140:1745-1753.
48. Romano L, Antonelli M, Castello M, deCandussio G, Diamanti S, Manzoni P, Minicucci L, Quattrucci S, Serravalle P, Romano C. Mid-term efficacy of inhaled flunisolide associated with albuterol in cystic fibrosis (CF). Ped Pulm suppl 1994;10:289.
49. Eigen H, Rosenstein BJ, FitzSimmons S, Schidlow DV, Group CFFPT. A multicenter study of alternate-day prednisone therapy in patients with cystic fibrosis. J Pediatr 1995;126:515-523.
50. Konstan MW, Byard PJ, Hopel CL, Davis PB. Effect of high-dose ibuprofen in patients with cystic fibrosis. New Engl J Med 1995;332:848-854.

Airway Dimensions in Bronchopulmonary Dysplasia: Implications for Airflow Obstruction

Harm A.W.M. Tiddens, Ward Hofhuis, Anthon R. Hulsmann, Wolter J. Mooi, Wim C.J. Hop, and Johan C. de Jongste

Departments of Pediatrics, Division Respiratory Medicine and Division Neonatology, Pathology, Biostatistics, Erasmus University and University Hospital/Sophia Children's Hospital, Rotterdam.

Introduction

About one fifth of preterm infants who require mechanical ventilation progress to a chronic pulmonary syndrome called bronchopulmonary dysplasia (BPD). BPD is characterized by respiratory distress, oxygen dependence, and chest radiograph abnormalities beyond the first month of life[1, 2]. Pulmonary function tests in patients with BPD show abnormalities of lung volumes, airway resistance, forced expiratory flows, lung compliance, and airway responsiveness in the short as well as in the long term[3-15]. The cause of these lung function abnormalities is incompletely understood. There is mounting evidence that inflammatory lung injury may play a key role in the pathogenesis of BPD[2, 16, 19]. Factors such as barotrauma, oxygen exposure, and infection are thought to trigger inflammation[17-19]. The chronic inflammation in airways and parenchyma can contribute to the lung function abnormalities described above in analogy to asthma[20] and chronic obstructive pulmonary disease (COPD)[20, 21]. Post-mortem examination of the lungs of infants who died with BPD show epithelial injury, inflammatory cell infiltrate, increase of bronchial smooth muscle, interstitial fibrosis, and a decrease of airway diameter[22-26]. In these studies, the thickness of the inner and outer parts of the airway wall, which have shown to be important determinants of airflow obstruction in asthma and COPD, were not measured[20, 21, 27, 28]. Furthermore, there have been no systematic studies of BPD relating airway dimensions to airway size. In asthma and COPD peripheral airways are more thickened compared to central airways and contribute substantially to airflow limitation[20, 21].

Another factor that may contribute to lung function abnormalities in BPD is loss of airway epithelium. The epithelium has bronchodilator activity because it synthesis relaxing substances and protects the underlying airway tissue against broncho-constrictor stimuli[29]. In asthma, loss of epithelium has been shown to correlate with airway responsiveness[30].

The purpose of this study was to investigate whether the smooth muscle area and inner airway wall area are increased in BPD and whether this increase is more severe in peripheral airways compared to more central airways. We, therefore, studied lung tissue of BPD and sudden infant death syndrome patients (SIDS), obtained from

autopsies, and measured airway wall dimensions and epithelial loss in airways in these lungs by means of computerized morphometry.

Methods

Study Population
A list was obtained of all autopsy cases done on infants between 1984 and 1995 from a national pathology registry. From this list infants were selected who were diagnosed as having BPD or SIDS. Copies of the pathology reports were obtained in all cases. For the BPD patients the post-conceptional age was calculated as the sum of gestational and postnatal age. Next, we selected all BPD patients who received mechanical ventilation, who died from respiratory failure, and with a post-conceptional age of 30 weeks or older. The control population was selected from those cases in the registry labeled as SIDS, without a history of chronic pulmonary disease and selected for the best possible match for sex and age. A copy of the autopsy report and all available paraffin blocks containing lung tissue were obtained for each case.

Morphological Studies
Paraffin blocks were cut at 5 μm thickness and stained with a combined Gomori trichrome and elastin stain. This stain resulted in a good color contrast between airway wall structures. In each tissue block all airways cut in cross section that did not show bifurcation or disruption of the wall were selected for further morphometric analysis. Airway dimensions were measured using an automated image analysis system (KS 400, Kontron Electronic, Eching/Munich, Germany). Measurements of airway dimensions were performed by 2 observers (WH and HdB). Each observer measured a different set of airway dimensions for all airways. The measurements made (Figure 1) include: basement membrane perimeter (P_{bm}) and the area enclosed by this perimeter (A_{bm}); the outer muscle perimeter (P_{mo}) and the area enclosed by this perimeter (A_{mo}); the outer perimeter (P_o) and the area enclosed by this perimeter (A_o); the area occupied by smooth muscle (WA_m); and the area occupied by cartilage (WA_{cart}).
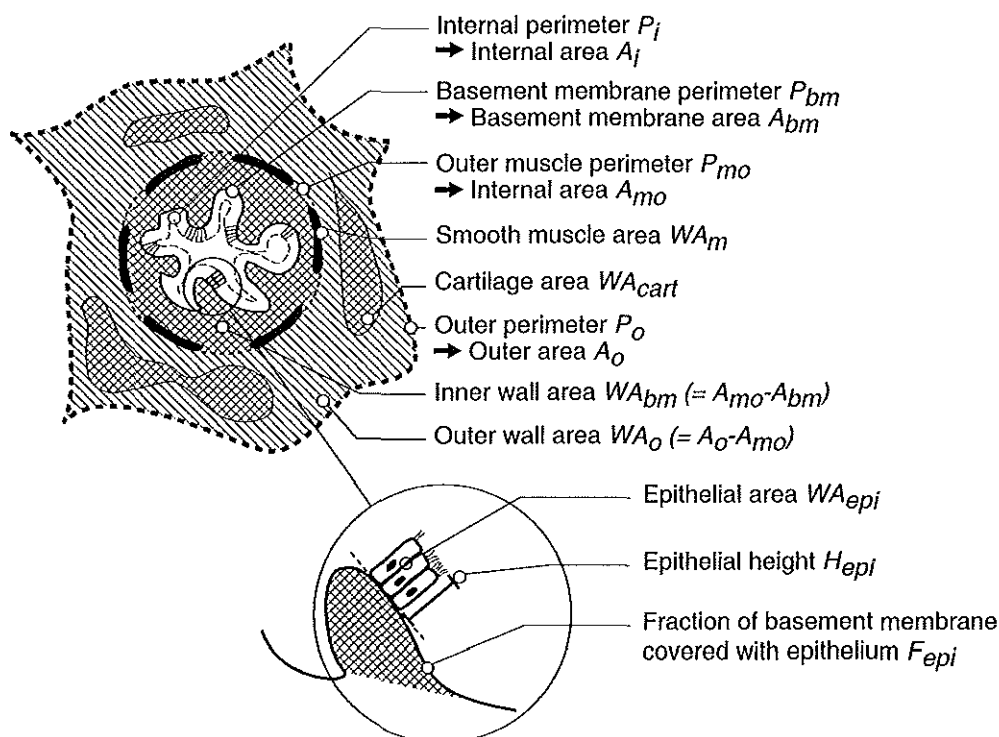
Figure 1. Diagram of measured airway dimensions.

We also measured the average height of the respiratory epithelium (H_{epi}) and the fraction of the P_{bm} covered with epithelium (F_{epi}). H_{epi} was measured as follows. First, a grid containing parallel sinusoids was superimposed over the computer image of the airway. When respiratory epithelium was present at the point where the sinusoid crossed the basement membrane, the epithelial height was measured by drawing a straight line perpendicular to the membrane and measuring from the membrane to the top of the ciliary border. The length of this line was automatically computed. When respiratory epithelium was absent, a zero was scored for height. H_{epi} was calculated for each airway section by computing the average of at least 15 epithelial height measurements around the lumen. F_{epi} was calculated by dividing the number of intersecting points through the basement membrane where respiratory epithelium was present with the total number of intersecting points.

From the above measurements we calculated the area within the basement membrane

of the fully dilated airway ($A^*_{bm} = P_{bm}^2 \, 4\pi$), the inner wall area excluding epithelium ($WA_{bm} = A_{mo} - A_{bm}$), outer wall area ($WA_o = A_o - A_{mo}$), the total wall area excluding epithelium ($WA_t = A_o - A_{bm}$), the wall area occupied by epithelium ($WA_{epi} = P_{bm} \cdot H_{epi.}$). We have used the nomenclature for quantifying subdivisions in the bronchial wall as proposed by Bai and coauthors[31]. To estimate the importance of the effect of the epithelial area on the lumen area WA_{epi} was expressed as a percentage of A^*_{bm} (WA_{epi} / A^*_{bm} %). The contractile status of the airway was examined by comparing A_{bm} versus airway size (P_{bm}) of BPD and SIDS patients.

The BPD and SIDS cases were measured in random order. The observers had no knowledge of the clinical history. The intra- and inter-observer variability was assessed by remeasurement of 10 randomly selected airways after an interval of 2 months.

Statistical Analysis

Repeated measures analysis of variance (RMANOVA), which allows for differences between and within patients, was used to assess the relationships between airway wall dimensions (WA_{bm}, WA_o, WA_t, WA_m, WA_{cart}, WA_{epi}, H_{epi}, F_{epi}) and airway size (P_{bm}). Previous studies found linear relationships between the square root of airway wall areas and airway size[20, 21, 28, 32-34]. We did a square root transformation on the airway areas of this study, again resulting in normal distributions of data. To obtain a linear relationship between WA_{epi} / A^*_{bm} % versus airway size (P_{bm}) both variables were log transformed. Next, for each of the airway dimensions versus airway size the mean slope and intercept was calculated, for the BPD and SIDS groups separately, using an iterative search for optimal values[35, 36]. The intercept and slope were investigated for their linear relation with age and gender for BPD and SIDS patients combined and for each group separately.

The distribution of airway size was plotted after logarithmic transformation for the BPD and SIDS patients and compared using nested analysis of variance. The level of significance was set at $p = 0.05$ (two sided). Data were expressed as mean ± standard deviation and range, unless indicated otherwise. The intra- and inter-observer variability of morphometric measurements was calculated by expressing the difference of the first and second measurement as a percentage of the average of both

observations[37]. This percentage difference was plotted against P_{bm} to detect systematic errors dependent on airway size.

Results

Study population
The characteristics of the study population are shown in Table 1. The median post-conceptional age at birth was 175 days for the 5 BPD patients. No data were available on the post-conceptional age of the SIDS patients which was therefore set for all patients at 38 weeks or 266 days. The median post-conceptional age at time of death was 299 and 372 days for BPD and SIDS patients, respectively.

Airway Wall Dimensions
Morphometric measurements were made on 75 airways from 5 BPD patients with a mean of 15 ± 3.4 (10 to 18) airways per patient and 176 airways from 11 SIDS patients with a mean of 16 ± 10.8 (4 to 39) airways. The intra- and inter-observer variability, for each of the airway wall dimensions, were always less than 10% and 15%, respectively. There was no systematic relationship between airway size (P_{bm}) and the intra- or inter-observer variability for any variable.

Analysis of variance of P_{bm} showed no significant difference between the two groups. The median values for P_{bm} were 0.82 and 0.81 for BPD and SIDS patients, respectively. This corresponds to a median dilated airway diameter of 0.26 mm. The frequency distribution of P_{bm} was not significantly different between the two groups. The linear relations between the square root of airway dimensions ($\sqrt{A_{bm}}$, $\sqrt{WA_{bm}}$, $\sqrt{WA_o}$, $\sqrt{WA_t}$, $\sqrt{WA_m}$, $\sqrt{WA_{epi}}$) and airway size (P_{bm}), and between $\log (WA_{epi}/A^*_{bm} \%)$ and $\log (P_{bm})$ were all highly significant ($p < 0.001$) for BPD and SIDS patients (Table 2 and Figure 2). There was no significant correlation between F_{epi} and P_{bm} for either group. The median F_{epi} was 0.986 (0.9 to 1) and 0.85 (0.52 to 1) for BPD and SIDS patients respectively ($p = 0.02$). When we excluded all airways with an F_{epi} below 0.85. WA_{epi} for BPD patients was 0.17 mm^2 higher than of SIDS patients ($p < 0.001$) (Figure 2). The linear relation between the square root of $\sqrt{H_{epi}}$ and P_{bm} for BPD patients was on average 0.85 µm higher than the SIDS patients ($p < 0.001$) (Figure 2). WA_{epi} expressed
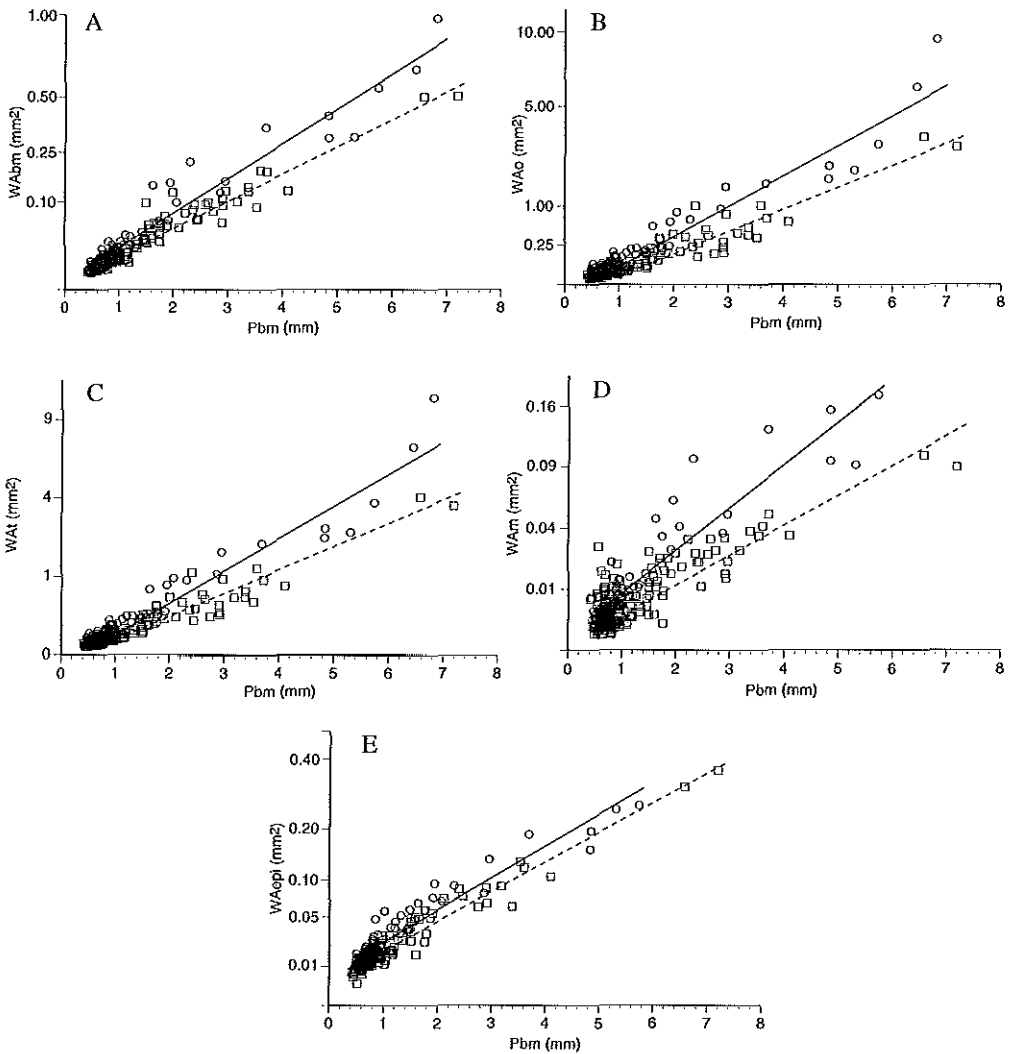
Figure 2. Morphometric airway wall dimensions versus airway size. The solid regression line represents the relation of an airway wall dimension versus basement membrane perimeter (P_{bm}) for BPD patients (circles). The dashed line represents the relation of an airway dimension versus P_{bm} for SIDS patients (squares). *(A)* WA_{bm} = inner wall area exclusive of the epithelium *(B)* WA_{o} = outer wall area. *(C)* WA_{t} = total wall area exclusive of epithelium *(D)* WA_{m} = smooth muscle area. *(E)* WA_{epi} = area of epithelium. Note the square root transformed vertical axis. There are 74 data points plotted from 5 BPD patients and 175 data points from 11 SIDS patients in figure A, B, C, and D. For Figure E, there are 68 and 136 data points from the BPD and the SIDS patients respectively. Due to overlap of data points, some circles appear filled.

as a percentage of A^*_{bm} was 48% greater for BPD than for SIDS patients ($p < 0.001$) (Figure 3). The cross sectional lumen area of all airways ($\sqrt{A_{bm}}$ versus P_{bm}) was not significantly different between both groups.
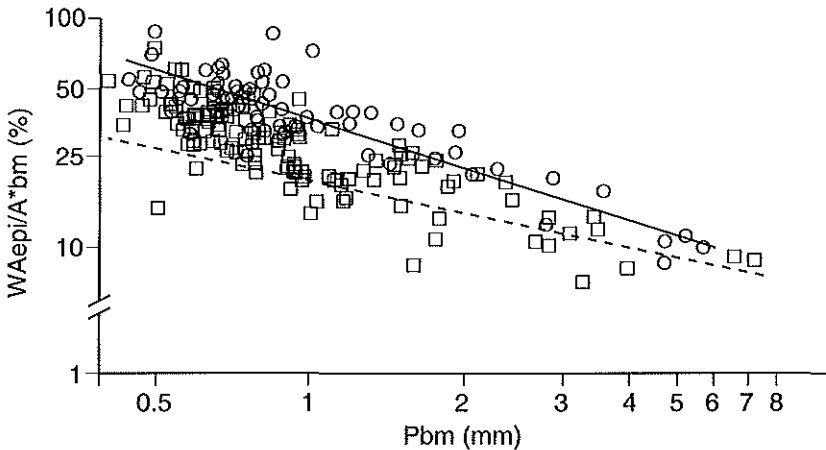

Figure 3. Percentage of surface area of relaxed airway lumen occupied by epithelium as a function of airway size. Definition of abbreviations: P_{bm} = perimeter basement membrane; WA_{epi} / A^*_{bm} (%) = wall area occupied by epithelium expressed as a percentage of the relaxed lumen area. The solid regression line represents the BPD patients, and the dashed regression line the SIDS patients.

The slopes of the regressions ($\sqrt{WA_{bm}}$, $\sqrt{WA_o}$, $\sqrt{WA_m}$) versus airway size (P_{bm}) were all steeper for BPD than for SIDS patients ($P < 0.001$) (Figure 2). The intercepts, but not the slopes, of the $\sqrt{WA_t}$ and $\sqrt{WA_{epi}}$ versus P_{bm} regressions were significantly higher for BPD than for SIDS patients ($P < 0.001$) (Table 2 and Figure 2). Table 3 shows the ratios between the airway dimensions for BPD and SIDS airways at a P_{bm} between 0.5 and 8 mm. Gender did not influence the slope or intercept of any airway wall dimension versus airway size regression. Age had a very small effect on the slope of the $\sqrt{WA_{bm}}$ versus P_{bm} regression for both groups ($P < 0.001$). WA_{bm} increased by 6.4×10^{-5} mm^2 for an increase in age of 100 days. The SIDS patients were 71 days older than the BPD. Correction for this age difference increases the difference in WA_{bm} between the groups by 4.5×10^{-5} mm^2 which is negligable. Age did not influence the slope or intercept of any other airway dimension versus airway size regression. For the BPD patients 16 out of 75 airways (21%) contained cartilage, and for the

Table 1

STUDY POPULATION CHARACTERISTICS

Bronchopulmonary Dysplasia

Patient No.	Sex M/F	Post-conceptional age (at time of birth) days	Post-conceptional age (at time of death) days	Other diagnosis in lungs at autopsy
1	M	167	216	-
2	F	243	251	-
3	M	175	299	pneumonia
4	F	184	390	infarction lower lobe
5	F	172	613	-
Median (range)		*175 (167-243)*	*299 (216-613)*	

Control Subjects (SIDS)

Patient No.	Sex M/F	Post-conceptional age (at time of birth) days	Post-conceptional age (at time of death) days	Other diagnosis in lungs at autopsy
6	F	266	288	-
7	F	266	293	-
8	M	266	315	-
9	F	266	316	-
10	F	266	351	some infiltrate
11	M	266	372	-
12	M	266	390	mucus in airways
13	M	266	440	-
14	F	266	560	-
15	F	266	623	-
16	M	266	646	-
Median (range)		*266 (-)*	*372 (288-646)*	

Table 2

EQUATIONS FOR AIRWAY WALL DIMENSIONS AS A FUNCTION
OF AIRWAY SIZE

Wall dimension	Bronchopulm. Dysplasia		Control Subjects (SIDS)		p-value slope
	slope $\cdot P_{bm}$	intercept	slope $\cdot P_{bm}$	intercept	
$\sqrt{WA_{bm}} =$	0.126	0.0275	0.101	0.0276	<0.001
$\sqrt{WA_o} =$	0.363	-0.055	0.257	-0.052	<0.001
$\sqrt{WA_t} =$	0.363	-0.008	0.282	-0.027	<0.001
$\sqrt{WA_m} =$	0.07	0.025	0.045	0.026	<0.001
$\sqrt{WA_{epi}} =$	0.082	0.082	0.078	0.059	0.4
$\sqrt{H_{epi}} =$	0.35	5.06	0.48	3.93	0.4

Definition of abbreviations: P_{bm} = basement membrane perimeter; WA_{bm} = inner wall area exclusive of the epithelium; WA_o = outer wall area; WA_m = smooth muscle area; WA_{epi} = area of epithelium; H_{epi} = height of epithelium; p value = level of significance.

SIDS patients 29 out of 176 airways (16%). This number of airways was too small to make a meaningful comparison for $\sqrt{WA_{cart}}$ versus P_{bm} between the groups using RMANOVA.

Table 3

RATIO FOR AIRWAY WALL DIMENSIONS

BETWEEN BPD AND CONTROL SUBJECTS (SIDS)

P_{bm} (mm)	WA_{bm}	WA_o	WA_t	WA_m	WA_{epi}
0.5	1.35	2.73	1.60	1.53	1.58
1	1.43	2.26	1.35	1.79	1.43
2	1.49	2.11	1.25	2.02	1.31
4	1.52	2.05	1.20	2.19	1.22
8	1.55	2.02	1.18	2.30	1.17

Definition of abbreviations: BPD = bronchopulmonary dysplasia; SIDS =sudden infant death syndrome; P_{bm} = perimeter basement membrane; WA_{bm} = inner wall area excluding epithelium; WA_o = outer wall area; WA_t = total wall area; WA_m = smooth muscle area; WA_{epi} = wall area occupied by epithelium.

Discussion

Among the possible mechanisms underlying airflow obstruction in BPD are thickening of the airway wall, increased smooth muscle mass, and epithelial loss. To our knowledge this is the first study in which wall dimensions of a large number of airways have been measured in relation to airway size in patients with BPD. The aim of this study was to compare airway wall dimensions of BPD patients with those of infants without chronic airways disease. We tested the hypotheses that the inner airway wall area, smooth muscle area and epithelial loss in BPD is increased, and that the increase in areas is more severe in peripheral airways compared to more central airways. Lungs of BPD and SIDS patients, who served as controls, were obtained from stored autopsy material. We measured the airway wall dimensions and epithelial loss in these lungs by means of computerized morphometry. Our results show that there are important differences between BPD and SIDS patients, with substantial thickening of all airway wall dimensions in BPD.

Airway Dimensions

In previous studies structures of interest were expressed as a proportion of lung volume[24, 38]. This introduced an important bias. Since the compliance of the lungs of BPD patients is decreased[9] fixation of the lung at a given pressure results in a lower lung volume than that of controls with normal lung compliance. The volume proportion of the lung occupied by airway wall will, therefore, be relatively higher in lungs of low compliance than in lungs of normal compliance. Furthermore, airway diameter was used as a measurement for airway size in these studies. Airway diameter depends on the contractile status of the bronchial smooth muscle and on the tethering forces by the parenchyma and is, therefore, not suitable as an estimate of airway size. The perimeter of the basement membrane as used in our study has been shown to be independent of parenchymal and muscle state and is, therefore, used as the gold standard of airway size[39].

For the present study we were able to calculate the relation between airway dimensions and airway size in a highly reliable fashion since we measured a large number of airways for each patient at different generations of the bronchial tree. All BPD airway wall dimensions were increased over the entire size range of airways we measured when compared with the SIDS patients. The total wall area was proportionally greater in the smaller airways. A comparable distribution of airway wall thickening has been found in other diseases characterized by chronic inflammation of the airways such as asthma[20, 27], COPD[21], and CF[28].

The amount of smooth muscle was substantially increased in BPD and proportionally more so in central airways than in peripheral airways. The smooth muscle area in airways with perimeters of 1 and 4 mm (diameters 0.3 and 1.3 mm) was increased by 79 and 119 %, respectively. In a study similar to ours, smooth muscle area in 9 preterm infants (mean post- conceptional age 27.3 weeks) with chronic lung disease was compared to that in 46 preterm infants who died within 72 hours of birth[26]. Bronchial smooth muscle was significantly higher in the children with chronic lung disease in airways with a diameter of 3.1 mm or higher, but not in the smaller airways.

That we did find significantly more smooth muscle in small airways in BPD patients may be related to the sensitive statistical method we used, and to the different selection of control tissue.

Abnormalities in the volume or mechanical qualities of airway cartilage might contribute to the pathophysiology of airflow limitation in BPD. Chronic airway inflammation has been related to loss of cartilage in other diseases characterized by chronic inflammation of the airways such as COPD[40] and cystic fibrosis[28]. The question as to whether the amount of airway cartilage is decreased in BPD remains unanswered by the present study. Airway cartilage is a highly variable structure in more peripheral airways. Therefore, a larger number of cartilaginous airways has to be sampled to estimate its relation to airway size in a reliable fashion.

To our knowledge, this study is the first to show that the lumen area occupied by epithelium was increased in BPD compared to SIDS patients. This difference was still present and significant after we excluded airways with a high loss of epithelium and could not be explained by differences in the contractile status of the airways as estimated by the cross sectional lumen area. The increased epithelial area in BPD substantially reduces the airway lumen, especially in the small airways.

The loss of epithelium was minimal in the BPD patients and, surprisingly, extensive in some of the SIDS patients. Extensive loss of epithelium was found previously in central airways of BPD patients who had assisted ventilation[41]. This damage was less severe in segmental bronchi. In the study by Sward-Comunelli and coworkers 28% of the airways showed extensive loss of epithelium and were, therefore, excluded from analysis[26]. The loss of epithelium in some of the SIDS patients might have been caused by necrosis of the tissue before tissue fixation which can result in detachment of the epithelium from the underlying basement membrane. Whether this will occur will depend on both the time delay between death, cooled storage, and autopsy[42]. We think it likely that especially time delay between the moment of death and moment of storage was shorter for the BPD than for some of the SIDS patients since the first all died in hospital. Furthermore, loss of epithelium might be the result of an infection of the lower airways since such infection of the airways might damage the epithelium directly or reduce the time between the moment of death and moment of necrosis. We note that SIDS patients 10 and 12 showed signs of infection and had a high epithelial loss of 13 and 48%, respectively.

Lung Function and Airway Dimensions

Altered airway dimensions can have a substantial effect on lung function[43]. In BPD, lung function abnormalities such as increased airway resistance[5, 9, 11], reduced forced expiratory flows[6, 8, 11, 12], and increased bronchial responsiveness[12] have been described. Thickening of the inner and outer airway wall area are likely to contribute to these lung function abnormalities. Thickening of the inner wall in the absence of smooth muscle shortening has relatively little effect on airway resistance but, in combination with smooth muscle shortening, it increases airway resistance drastically[27]. Furthermore, thickening of the inner wall increases upstream airway resistance which results in reduced maximal expiratory flows during forced expiration[44, 45]. Thickening of the outer airway wall partly uncouples the smooth muscle layer from the tethering forces of the parenchyma[46, 47]. The bronchial smooth muscle can, therefore, shorten more at a given force development. Thus thickening of the inner and outer wall area can both contribute to the lung function abnormalities as described in BPD.

Airways of BPD patients contain substantially more smooth muscle than airways from SIDS patients. In asthma increased smooth muscle mass is associated with increased maximal force generation and, therefore, increased smooth muscle shortening[48]. To our knowledge there are no in vitro data to support the hypothesis that a similar relation is present in BPD. There are, however, some indirect arguments that the smooth muscle tone plays a role in airflow obstruction in BPD. Firstly, increased responsiveness to bronchodilators is common in BPD[3-5, 11, 12, 49] suggesting that smooth muscle shortening explains part of the airway narrowing. Secondly, lung compliance is decreased in BPD[9] and increases after nebulization of bronchodilators[5]. Increased smooth muscle tone could contribute to this increased lung compliance[50]. Thirdly, the parenchyma of BPD patients is highly abnormal[23, 24]. This is likely to interfere with the tidal volume stretching of bronchial smooth muscle that seems necessary to reduce smooth muscle tone[51, 52]. Abnormal parenchyma-airway interaction might, therefore, contribute to increased smooth muscle shortening in BPD.

Implications for Therapy

Both the inner and outer airway walls are thickened in BPD, and this is probably related to chronic inflammation. Anti-inflammatory medications such as inhaled corticosteroids seems a rational choice to reduce thickening of airway wall and thus improve lung function. Indeed, maintenance treatment with nebulized beclomethasone improved lung function in infants with BPD[53]. It is unknown whether the changes in the architecture of the bronchial wall, such as fibrous tissue deposition, are entirely reversible with anti-inflammatory treatment. Though these lung function abnormalities decrease with age they can still be found in adolescents and young adults[9, 11]. Regarding the increased smooth muscle area in combination with airway wall thickening and abnormal lung parenchyma, use of bronchodilators seems a rational choice to limit airflow obstruction[1]. It has been shown that bronchodilators reduce airway resistance and increase lung compliance in BPD[4, 5, 54]. Their efficacy should be evaluated for each individual patient because reduced smooth muscle tone can also increase airway collapsibility and, therefore, facilitate airway closure[34].

We conclude that airways of BPD patients, at the severe end of the disease spectrum, show extensive thickening of the inner and outer airway wall areas, epithelial area, and smooth muscle area when compared to airways of SIDS patients. Differences in the ante- or postmortem conditions might have reduced or increased differences in airway wall dimensions between both groups. However, when the altered airway dimensions in BPD patients are representative for the in vivo situation they explain much of the pathophysiology of airflow limitation and reversibility of bronchial obstruction. Based on these findings, maintenance treatment with inhaled steroids and beta-agonists seems a rational choice to improve lung function in these patients.

References

1. Abman SH, Groothius JR. Pathophysiology and treatment of bronchopulmonary dysplasia. Current issues. Pediatr Clin North Am 1994;41(2):277-315.
2. Zimmerman JJ. Bronchoalveolar inflammatory pathophysiology of bronchopulmonary dysplasia. Clin Perinatol 1995;22(2):429-456.
3. Smyth JA, Tabachnik E, Duncan WJ, Reilly BJ, Levison H. Pulmonary function and bronchial hyperreactivity in long-term survivors of bronchopulmonary dysplasia. Pediatrics 1981;68:336-340.
4. Kao LC, Warburton D, Platzker ACG, Keens TG. Effect of isoproterenol inhalation on airway resistance in chronic bronchopulmonary dysplasia. Pediatrics 1984;73:509-514.
5. Gomez-del Rio M, Gerhardt T, Hehre D, Feller R, Bancalari E. Effect of a beta agonist nebulization on lung function in neonates with increased pulmonary resistance. Pediatr Pulmonol 1986;2:287-291.
6. Tepper RS, Morgan WJ, Cota K, Taussig LM. Expiratory flow limitation in infants with bronchopulmonary dysplasia. J Pediatr 1986;109(6):1040-1046.
7. Berman W, Jr., Katz R, Yabek SM, Dillon T, Fripp RR, Papile LA. Long-term follow-up of bronchopulmonary dysplasia. J Pediatr 1986;109(1):45-50.
8. Bader D, Ramos AD, Lew CD, Platzker ACG, Stabile MW, Keens TG. Childhood sequelae of infant lung disease: Exercise and pulmonary function abnormalities after bronchopulmonary dysplasia. J Pediatr 1987;110:448-456.
9. Gerhardt T, Hehre D, Feller R, Reifenberg L, Bancalari E. Serial determination of pulmonary function in infants with chronic lung disease. J Pediatr 1987;110(3):448- 456.
10. Duiverman EJ, Den Boer JA, Roorda RJ, Rooyackers CM, Valstar M, Kerrebijn KF. Lung function and bronchial responsiveness measured by forced oscillometry after bronchopulmonary dysplasia. Arch Dis Child 1988;63(7 Spec No):727-732.
11. Northway WH, Moss RB, Carlisle KB, Parker BR, Popp RL, Pitlick PT, Eichler I, Lamm R, Brown BW. Late pulmonary sequelea of bronchopulmonary dysplasia. New Engl J Med 1990;323:1793-1798.
12. Mallory GB, Jr., Chaney H, Mutich RL, Motoyama EK. Longitudinal changes in lung function during the first three years of premature infants with moderate to severe bronchopulmonary dysplasia. Pediatr Pulmonol 1991;11(1):8-14.
13. Tarnow-Mordi WO, Wilkie RA, Reid E. Static respiratory compliance in the newborn. I: A clinical and prognostic index for mechanically ventilated infants. Arch Dis Child Fetal Neonatal Ed 1994;70(1):F11-15.
14. Santuz P, Baraldi E, Zaramella P, Filippone M, Zacchello F. Factors limiting exercise performance in long-term survivors of bronchopulmonary dysplasia. Am J Respir Crit Care Med 1995;152(4 Pt 1):1284-1289.
15. Cano A, Payo F. Lung function and airway responsiveness in children and adolescents after hyaline membrane disease: a matched cohort study. Eur Respir J 1997;10:880-885.
16. Bancalari E, Sosenko I. Pathogenesis and prevention of neonatal chronic lung disease: recent developments. Pediatr Pulmonol 1990;8(2):109-116.
17. Gorenflo M, Vogel M, Herbst L, Bassir C, Kattner E, Obladen M. Influence of clinical and ventilatory parameters on morphology of bronchopulmonary dysplasia. Pediatr Pulmonol 1995;19(4):214-220.
18. Coalson JJ, Winter VT, Gerstmann DR, Idell S, King RJ, Delemos RA. Pathophysiologic, morphometric, and biochemical studies of the premature baboon with bronchopulmonary dysplasia. Am Rev Respir Dis 1992;145(4 Pt 1):872-881.
19. Walti H, Tordet C, Gerbaut L, Saugier P, Moriette G, Relier JP. Persistent elastase/proteinase inhibitor imbalance during prolonged ventilation of infants with bronchopulmonary dysplasia: evidence for the role of nosocomial infections. Pediatr Res 1989;26(4):351-355.
20. Kuwano K, Bosken CH, Pare PD, Bai TR, Wiggs BR, Hogg JC. Small airways dimensions in asthma and chronic obstructive pulmonary disease. Am Rev Respir Dis 1993;148:1220-1225.

21. Tiddens HAWM, Pare PD, Hogg JC, Hop WCJ, Lambert R, Jongste JC. Cartilaginous airway dimensions and airflow obstruction in human lungs. Am J Respir Crit Care Med 1995;152:260-266.
22. Bonikos DS, Bensch KG, Northway WH, Edwards DK. Bronchopulmonary dysplasia: the pulmonary pathologic sequel of necrotizing bronchiolitis and pulmonary fibrosis. Hum Pathol 1976;7(6):643-666.
23. Stocker JT. Pathologic features of long-standing "healed" bronchopulmonary dysplasia: a study of 28 3- to 40-month-old infants. Hum Pathol 1986;17(9):943- 961.
24. Margraf LR, Tomashefski JF, Bruce MC, Dahms BB. Morphometric analysis of the lung in bronchopulmonary dysplasia. Am Rev Respir Dis 1991;143:391-400.
25. Hislop AA, Haworth SG. Pulmonary vascular damage and the development of cor pulmonale following hyaline membrane disease. Pediatr Pulmonol 1990;9(3):152- 161.
26. Sward-Comunelli SL, Mabry SM, Truog WE, Thibeault DW. Airway muscle in preterm infants: Changes during development. J Pediatr 1997;130:570-576.
27. James AL, Pare PD, Hogg JC. The mechanics of airway narrowing in asthma. Am Rev Respir Dis 1989;139(1):242-246.
28. Tiddens HAWM, Koopman LP, Lambert RK, Elliott WM, Hop WCJ, van den Mark TW, de Boer WJ, de Jongste JC. Airway wall dimensions and bronchial responsiveness in cystic fibrosis lungs. Submitted 1997.
29. Hulsmann AR, De Jongste JC. Modulation of airway responsiveness by the airway epithelium in humans, putative mechanisms. Clin Exp Allergy 1996;26:1236-1242.
30. Jeffery PK, Wardlaw AJ, Nelson FC, Collins JV, Kay AB. Bronchial biopsies in asthma. An ultrastructural, quantitative study and correlation with hyperreactivity. Am Rev Respir Dis 1989;140(6):1745-1753.
31. Bai A, Eidelman DH, Hogg JC, James AL, Lambert RK, Ludwig MS, Martin J, McDonald DM, Mitzner WA, Okazawa M, Pack RJ, Pare PD, Schellenberg RR, Tiddens HAWM, Wagner EM, Yager D. Proposed nomenclature for quantifying subdivisions of the bronchial wall. J Appl Physiol 1994;77(2):1011-1014.
32. Bosken CH, Wiggs BR, Pare PD, Hogg JC. Small airway dimensions in smokers with obstruction to airflow. Am Rev Respir Dis 1990;142(3):563-570.
33. Tiddens HAWM, Boogaard JM, Jongste JC, Hop WCJ, Coxson HO, Pare PD. Physiological and morphological determinants of maximal expiratory flow in chronic obstructive lung disease. Eur Respir J 1996;9:1785-1794.
34. Tiddens HAWM, Hofhuis W, Bogaard J, Hop WCJ, de Bruin H, Willems LNA, de Jongste JC. Compliance, hysteresis, and collapsibility of human small airways. Submitted 1997.
35. Schluchter MD. Module 5V. In: Dixon WJ, editor. BMDP Statistical software manual. Burkely: University of California press, 1990:1207-1244.
36. Feldman HA. Families of lines: random effects in linear regression analysis. J Appl Physiol 1988;64(4):1721-1732.
37. Bland JM, Altman DG. Statistical methods for assessing agreement between two methods of clinical measurement. The Lancet 1986;1(8476):307-310.
38. Sobonya RE, Logvinoff MM, Taussig LM, Theriault A. Morphometric analysis of the lung in prolonged bronchopulmonary dysplasia. Pediatr Res 1982;16:969- 972.
39. James AL, Hogg JC, Dunn LA, Pare PD. The use of the internal perimeter to compare airway size and to calculate smooth muscle shortening. Am Rev Respir Dis 1988;138(1):136-139.
40. Nagai A, Thurlbeck WM, Konno K. Responsiveness and variability of airflow obstruction in chronic obstructive pulmonary disease. Am J Respir Crit Care Med 1995;151:635-639.
41. Lee RMKW, O'Brodovich H. Airway epithelial damage in premature infants with respiratory failure. Am Rev Respir Dis 1988;137(2):450-457.
42. Lee RMKW, Rossman CM, O'Brodovich H. Assessment of postmortem respiratory ciliary motility and ultrastructure. Am Rev Respir Dis 1987;136:445-447.
43. Moreno RH, Hogg JC, Pare PD. Mechanics of airway narrowing. Am Rev Respir Dis 1986;133(6):1171-1180.

44. Mead J, Turner JM, Macklem PT, Little JB. Significance of the relationship between lung recoil and maximum expiratory flow. J Appl Physiol 1967;22(1):95- 108.
45. Dawson SV, Elliott EA. Wave-speed limitation on expiratory flow-a unifying concept. J Appl Physiol 1977;43(3):498-515.
46. Macklem PT. A theoretical analysis of the effect of airway smooth muscle load on airway narrowing. Am J Respir Crit Care Med 1996;153(1):83-89.
47. Lambert RKP, P.D. Lung parenchymal shear modulus, airway wall remodeling, and bronchial hyperresponsiveness. J Appl Physiol 1997;83(1):140-147.
48. de Jongste JC, Mons H, Bonta IL, Kerrebijn KF. Human asthmatic airways responses in vitro. Eur J Respir Dis 1987;71:23-29.
49. de Kleine MJ, Roos CM, Voorn WJ, Jansen HM, Koppe JG. Lung function 8-18 years after intermittent positive pressure ventilation for hyaline membrane disease [see comments]. Thorax 1990;45(12):941-946.
50. Mitzner W, Blosser S, Yager D, Wagner E. Effect of bronchial smooth muscle contraction on lung compliance. J Appl Physiol 1992;72(1):158-167.
51. Fredberg JJ, Jones KA, Nathan M, Raboudi S, Prakash YS, Shore SA, Butler JP, Sieck GC. Friction in airway smooth muscle: mechanism, latch, and implications in asthma. J Appl Physiol 1996;81(6):2703-2712.
52. Shen X, Wu MF, Tepper RS, Gunst SJ. Mechanisms for the mechanical response of airway smooth muscle to length oscillation. J Appl Physiol 1997;83:731-738.
53. LaForce WR, Brudno DS. Controlled trial of beclomethasone diproprionate by nebulization in oxygen- and ventilator-dependent infants. J Pediatr 1993;122:285- 288.
54. Kao LC, Durand DJ, Nickerson BG. Effects of inhaled metaproterenol and atropine on the pulmonary mechanics of infants with bronchopulmonary dysplasia. Pediatr Pulmonol 1989;6:74-80.

Summary, General Discussion, and Future Research

Summary

Airway inflammation, airflow obstruction and bronchial hyperresponsiveness are well known features of asthma, chronic obstructive pulmonary disease (COPD), cystic fibrosis (CF), and bronchopulmonary dysplasia (BPD). Chronic inflammation of airways is associated with structural and functional changes of the airway wall and parenchyma. However, how these changes are related to airflow obstruction and bronchial responsiveness is complex and not completely understood. Understanding the relationship between structure and function in chronically inflamed airways and parenchyma is needed to improve therapy.

This thesis contains investigations of airway structure and function in COPD, CF, and BPD.

Chapter 1 contains a general introduction to the thesis and the aims of the study.

In **Chapter 2,** the pathology of airway inflammation and the structure-function relationships of components of normal and diseased airways for patients with asthma, COPD, CF, and BPD are reviewed.

In **Chapter 3** structure-function relationships in airways from COPD patients are described. The question as to whether airflow obstruction and peripheral airway inflammation correlated with airway wall thickness and the amount of bronchial smooth muscle in cartilaginous airways was addressed. In addition, the theoretical relationship between airway dimensions and airway resistance was studied with a computational model. Lung tissue was obtained from 72 patients, mostly smokers, with different degrees of obstructive pulmonary disease who were operated on for a solitary peripheral lung lesion. In 341 transversely cut cartilaginous airway sections airway size and airway wall dimensions were measured. Inflammation scores for non-cartilaginous airways from the same lungs were evaluated. Pre-operatively measured maximal expiratory flows and the response to a bronchodilator were correlated with airway wall dimensions. Maximal expiratory flow, the reversibility of airflow obstruction, and peripheral airway inflammation were found to be significantly related to the inner airway wall area but not to the smooth muscle area.

It was concluded that airflow obstruction and its reversibility in COPD is in part caused by thickening of the cartilaginous airway wall, and is related to inflammatory changes.

In **Chapter 4** the relationship between upstream conductance, as estimated from the maximal flow-static recoil (MFSR) curve, and inflammation and thickening of the airway walls was investigated. In addition, the relationship between the collapsibility of airways and the amount of airway cartilage and the thickness of the airway walls was investigated.

Maximal expiratory flow can be reduced by three different mechanisms; loss of lung elastic recoil, decreased airway conductance upstream of flow limiting segments, and increased collapsibility of airways. It has been suggested that the relative contributions of lung recoil, airway conductance, and airway collapsibility to airflow obstruction during forced expiration can be estimated from an MFSR curve. Lung tissue was obtained from 72 patients with different degrees of airflow obstruction who were operated on for a solitary peripheral lung lesion. Maximal flow-static recoil curves to estimate upstream resistance and airway collapsibility were derived in 59 patients from pre-operatively measured maximal expiratory flow-volume and pressure-volume curves. In 341 transversely cut airway sections airway size, airway wall dimensions and inflammatory changes were measured. Airflow obstruction correlated with lung elastic recoil and the MFSR estimate of airway conductance but not to airway collapsibility or to the amount of airway cartilage. The upstream conductance decreased as the inner wall became thicker. Airway collapsibility did not correlate with the amount of airway cartilage, inflammation, or airway wall thickness. The MFSR model does not adequately reflect the collapsibility of the flow limiting segment.

In **Chapter 5** we describe a micro-plethysmograph developed in our laboratory to assess smooth muscle responses in isolated airway segments under isobaric conditions and an experimental set-up to measure the dynamic properties of airway segments. For the study of airway responsiveness in vitro, airway segments have important advances over strip or spiral preparations. However, the method for studying isobaric contraction of segments is not well established. For this reason we developed the

micro-plethysmograph which has a volume measurement range of 10 to 700 µL, a resolution of 0.02 to 0.4 µL, and a drift of 2.6 to 0.7 % of measurement range min^{-1} for its most and least sensitive setting, respectively. The plethysmograph is able to compensate for the pressure changes induced by the volume changes, thus enabling true isobaric measurements. We show examples of the isobaric contraction and relaxation of isolated human airway segments after stimulation of an airway segment by methacholine, isoprenaline, and by electrical field stimulation. Apart from studying airway responses, the micro-plethysmograph is potentially useful for studying the contractile properties of watertight and hollow structures such as blood vessels, gut, and ureter. In addition, this device can be used to measure leak or diffusion through the wall at any transmural pressure.

In **Chapter 6** the relationship between compliance, collapsibility, and hysteresis of isolated human small airway segments, on the one hand, and airway wall dimensions on the other hand are described. Airway wall dimensions are important determinants for the mechanical properties of airways. Chronic airway inflammation is likely to change these mechanical properties. Lung tissue was obtained from 31 patients with different degrees of airflow obstruction who were operated on for a solitary lung lesion. Segments of 35 small airways were mounted on cannulas in an organ bath and inflated and deflated cyclically between +15 and -15 cm H_2O. For each airway this was done at baseline, after methacholine, and after isoprenaline. Specific compliance (sCdyn), specific hysteresis (sη), and pressure at which the airways collapsed (Pcol) were calculated from each recording. Airway wall dimensions were measured morphometrically. Lung function parameters of airflow obstruction were correlated to sCdyn, sη, and Pcol. At baseline, after methacholine, and after isoprenaline sCdyn was 0.059, 0.052, and 0.085 cm H_2O^{-1}, sη was 13.5, 12.9, and 7.1%, and Pcol was -3.4, -3.5, and -1.9 cm H_2O respectively. Differences between sCdyn, sη and Pcol after methacholine and after isoprenaline were highly significant ($p < 0.001$). Smooth muscle area, but not total wall area, was an important determinant for sCdyn and for sη after methacholine. Specific hysteresis at baseline correlated with RV/TLC ($R = 0.5$, $p = 0.05$) and after methacholine with FEV_1/FVC ($R = -0.68$, $p = 0.02$) and RV/TLC ($R = 0.5$, $p = 0.05$). From these results we conclude that smooth muscle area and

smooth muscle tone, but not total wall area, are important determinants for airway compliance, hysteresis, and collapsibility. Hysteresis seems to be an important determinant for chronic airflow obstruction

In **Chapter 7** airway dimensions of CF patients were measured and compared to those of COPD patients. The importance of these dimensions for airway resistance were estimated in a computational model. In most CF patients, chronic airway inflammation leads to progressive airflow obstruction and increased bronchial responsiveness. It is not clear how the airway pathology relates to the severity of airflow obstruction and increased bronchial responsiveness in these patients. Airway dimensions were measured in lungs obtained from CF patients who underwent lung transplantation (12), lobectomy (1), or autopsy (4). These dimensions were compared to those of airways from lobectomies of 72 patients with COPD. Airway dimensions of CF and COPD patients were introduced into a computational model to study their effect on airway resistance. The inner wall area and smooth muscle area of peripheral CF airways were increased 3.3- and 4.3-fold respectively compared to those of COPD airways. The epithelium was 53% higher in peripheral CF airways. The sensitivity and maximal plateau resistance of the computed dose-response curve were substantially increased in the CF patients compared to COPD. The changes in airway dimensions of CF patients are likely to contribute to the severe airflow obstruction, and increased bronchial responsiveness to bronchoconstricting and bronchodilating agents as described in these patients.

In **Chapter 8** airway dimensions of BPD patients were measured and compared to those of control subjects. Whether airway wall dimensions contribute to lung function abnormalities in BPD is unknown. Lung tissue of patients with BPD was obtained at autopsy and lung tissue from children who died from sudden infant death syndrome (SIDS) patients served as control group. Airway wall dimensions and epithelial loss were measured in 75 airways from 5 BPD patients and 176 airways from 11 SIDS. Repeated measures analysis of variance was used to assess the relationships between airway wall dimensions and airway size for BPD and SIDS patients. Little epithelial loss was present in the BPD patients while extensive loss was observed in some of the SIDS patients. The inner wall area, outer wall area, epithelial area, and smooth

muscle area were all substantially thicker (all $p < 0.001$) in the BPD than in SIDS patients. It is likely that the increased thickness of the airway wall components contributes to airflow obstruction and its reversibility in BPD patients.

General discussion
Airways in COPD, CF, and BPD have showed a number of features in common that are relevant for the understanding of the pathophysiology of airflow obstruction and bronchial hyperresponsiveness. From the study of isolated airway segments we have gained important information on structure-function relationships of chronically inflamed airways. In this section we discuss, for different airway wall components, how the results of our studies fit into the pathophysiology of airflow limitation and bronchial hyperresponsiveness.

EPITHELIUM. The epithelium in the airways showed substantial loss of epithelium in CF and only little loss in COPD and BPD. Much higher epithelial loss, of half the basement membrane area, was found previously in biopsies of COPD patients[1]. This might have been an artifact caused by increased fragility of the epithelium[2, 3]. Extensive loss of respiratory epithelium in CF airways has been described previously but was never quantified[4, 5]. It is likely that some of the observed damage to the epithelium is related to improper fixation. However, epithelial loss in CF patients was substantial even when we excluded tissues obtained at autopsy. The higher epithelial loss previously described in BPD is probably an artifact related to the delay between the time of death and time of autopsy. Damage of airway epithelium is a common finding in patients with asthma. As is discussed in chapter 2, loss of epithelium impairs mucociliary clearance resulting in mucus retention which can contribute to airflow obstruction and, perhaps, to closure[6]. Furthermore, it can contribute to bronchial hyperresponsiveness[7]. We therefore believe that increased fragility and loss of epithelium is a true feature common to chronically inflamed airways.

INNER AIRWAY WALL. Thickening of the inner airway wall area was present in COPD, CF, and BPD. The thickening was more prominent in CF than in COPD. In fact, the

thickening was comparable to that described in patients who died from a severe asthma attack. Airway wall thickening was relatively more pronounced in smaller cartilaginous airways than in more central airways. This has important implications for treatment. In patients with chronic airway inflammation, aerosol deposition is inhomogeneous and more in central than in peripheral airways[8-10]. Thus, it seems important to develop methods that deliver drugs more effectively to abnormal peripheral airways.

Airway wall thickening increases airway resistance even in the absence of smooth muscle shortening and thus can contribute to airflow limitation. In fact, in COPD we found a strong correlation between maximal airflow and upstream conductance. It is possible that the decreased airway conductance results in a more peripheral position of the flow limiting segment and that this contributes to the airflow limitation. Thickening of the inner airway wall can amplify the effect of smooth muscle shortening drastically as we have shown with the computational model. Whether this plays an important role in vivo is doubtful for reasons discussed in the next paragraph.

SMOOTH MUSCLE. The amount of smooth muscle in cartilaginous airways in patients with COPD was not related to airflow limitation. We cannot conclude from this study, however, that the amount of smooth muscle is normal in COPD. We measured airways of smokers operated on for a lung tumor and variable degrees of airflow obstruction. Even smokers with lung function within the normal range might have altered airway dimensions compared to healthy non-smokers. In airways from CF and BPD patients we did find a substantial increase in the amount of smooth muscle. This increase in smooth muscle mass could result in an increase in constricting force generation and, hence, more severe airway narrowing. Whether or not smooth muscle shortening is increased depends not only on the force but also on the load on the smooth muscle. We did not measure this load but we have some indirect arguments that this load is normal: Airway wall thickness in COPD was not related to the compliance of airways suggesting that even in thickened and inflamed airways the dynamic properties are not substantially altered. However, we do not know whether compressibility of thickened airways is normal. Theoretically, compressibility of thickened airways could be decreased reducing dynamic compression during forced expiration at the site of

the flow limiting segments. Baseline tone was high and close to maximal tone in isolated airways and was substantially reduced with a bronchodilator. If this reflects the in vivo situation then the question arises as to why bronchodilators have so little effect in many COPD patients? We think this is due to defective airway-parenchyma dependence. We found that the first inflation of the airway segment increased compliance. This confirms earlier studies where a relationship was found between stretching of a smooth muscle preparation and the compliance of the preparation. In vivo, the airway is stretched by the parenchyma during inflation of the lung. Loss of alveolar attachments to the airway wall results in decreased stretching of the airway and thus airway compliance remains low and the diameter small for a given transmural pressure. However, many studies have failed to relate measurements of emphysema to airflow obstruction[11, 12]. We believe that loss of alveolar attachments, of even small parts of an airway segment, are probably sufficient to reduce airway diameter, distort airway configuration, and thus increase airway resistance. Three dimensional reconstructions of peripheral airways in emphysematous lungs could, therefore, provide us with relevant information on the impact of loss of alveolar attachments on the airway structure[13]. In BPD and CF, abnormalities of the parenchyma have been described and the same mechanism as that described above might play a role. In conclusion, we believe that increased smooth muscle shortening is present in COPD due to abnormal parenchyma-airway interactions and, perhaps, to an increase in smooth muscle force. It is unlikely that the load on the bronchial smooth muscle is increased.

CARTILAGE. Observing a large number of airways microscopically made it clear that airway cartilage is well integrated within the connective tissue and smooth muscle network of airways. Alterations of airway cartilage are therefore likely to influence airway mechanics. We did not find a difference in cartilage between COPD patients with and without airflow limitation. Cartilage is a very irregular structure and is therefore difficult to measure morphometrically in a reliable fashion. Therefore, we might have missed small differences in cartilage volume. However, in CF airways there was substantially less cartilage than in COPD airways. Loss of cartilage is likely to make airways more collapsible and might therefore contribute to airflow limitation

in CF. We did not investigate the mechanical properties of the airway cartilage. These mechanical properties could be altered due to chronic inflammation[14] and thus influence the load for the bronchial smooth muscle and the collapsibility of the airways. The amount of cartilage might be reduced in severe chronic airway inflammation [15] but whether this contributes to airflow limitation is unknown.

Outer wall area. The outer wall was difficult to measure in large cartilaginous airways using our morphometric approach since there is no clear boundary between the outer airway wall and the lung parenchyma. As a result, the variability of the measurement was high. In small airways it was much easier to distinguish the outer wall area from the parenchyma and here the variability was low. It has been suggested that thickening of the outer wall area could uncouple the smooth muscle from the tethering forces of the parenchyma. As discussed previously in this chapter we support the idea that the parenchyma-smooth muscle interaction is an important determinant for airway compliance. Thickening of the outer airway wall could therefore contribute to airflow obstruction.

Directions for Future Research

Smooth muscle. The exact role of the bronchial smooth muscle in the pathophysiology of airflow obstruction and bronchial responsiveness in asthma and COPD is still incompletely understood. It is not clear whether smooth muscle shortening in asthma is increased due to increased smooth muscle shortening capacity or increased force generation, to a decreased load, or to a combination of these three.

The relationship between smooth muscle shortening and the load imposed on the smooth muscle by the inner wall area can be studied more adequately in isolated airway segments than in strip preparations. The importance of parenchyma-airway interactions on smooth muscle mechanics are probably underestimated. It is now recognized that cyclic expansion of the airway by tidal volume breathing and/or deep inspirations are important to reduce smooth muscle tone[16-18]. Abnormalities in parenchyma-airway interactions might therefore play a key role in the pathogenesis of chronic airflow obstruction. Animal models of emphysema could be used to study

these interactions in more detail. Furthermore, preparations of isolated airway segments with intact parenchyma could be developed.

EMPHYSEMA. The impact of loss of alveolar attachments on the three dimensional airway geometry in vivo should be studied in more detail. Studies of this kind will provide insight on how emphysema can lead to airflow obstruction. We hypothesize that peripheral airways of patients with emphysema are distorted and show narrowed sections due to loss of parenchyma-airway interdependence. A "distorted airway index" should be developed to test this "distorted airway theory" (Figure 1).

Distorted Airway Theory
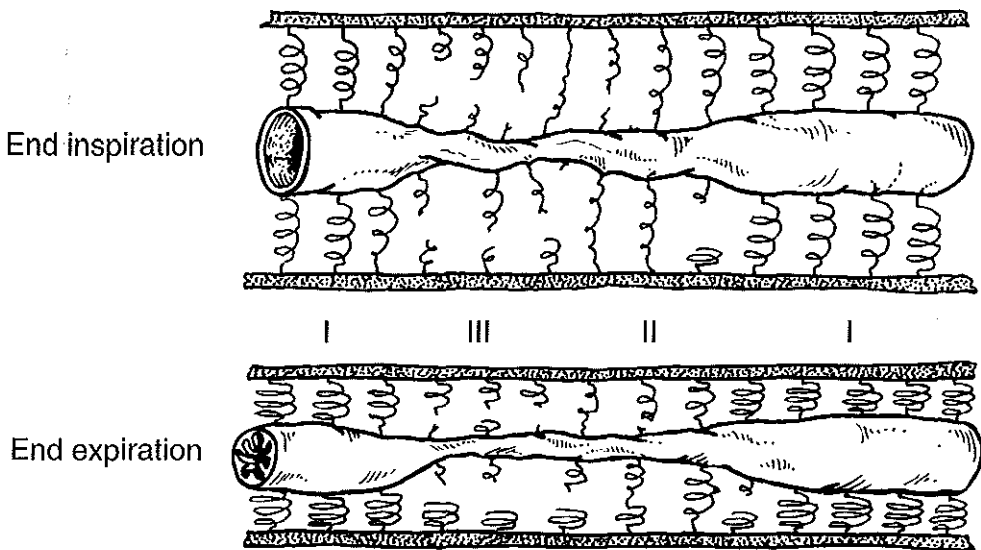
Figure 1. Schematic view of interaction between peripheral airway and parenchyma at end inspiration and at end expiration. I = section of airway with normal alveolar attachments and, therefore, maximally increased cross sectional area at end inspiration. II = section of airway with "moderate emphysema". Compliance is reduced due to impaired parenchyma-airway interaction. At end inspiration this section is somewhat distorted and its cross sectional area reduced. III = section of airway with "severe emphysema". The airway is stiff due to absent parenchyma-airway interaction. At end inspiration this section is very distorted and its cross sectional area substantially reduced.

AIRWAY WALL THICKNESS AND TREATMENT. Airway wall thickening is more severe in peripheral airways than in central airways in asthma, COPD, CF and BPD. Aerosol deposition of drugs used in the treatment of these diseases is inhomogeneous and in central airways preferentially. How chronic airway disease influences the pattern of aerosol deposition in lungs of children is largely unknown and should be investigated. Drugs should be developed that can more effectively target peripheral airways even in the presence of chronic airway inflammation.

COMPUTATIONAL MODELS OF AIRWAY RESISTANCE. Airway mechanics are complex due to the large number of variables involved. Computational models have been developed to organize available knowledge on airway mechanics. The importance of these models is underestimated. In fact, worldwide, only a few groups work on the improvement of such models. Models are, by definition, a simplification of reality but they enable us to study complex interactions between variables. Furthermore, they highlight the gaps in our knowledge. Such models have helped us to understand the importance of airway wall thickness for airway resistance. A more systematic worldwide approach is needed to improve available models and to direct research to fill in missing components. Furthermore, a computational model of airway resistance in infants and children should be developed for our understanding of airway pathophysiology in children which is probably dramatically different from that in adults.

COMPUTATIONAL MODEL AND MOLECULAR BIOLOGY. Knowledge of the molecular biology of the airway has expanded enormously over the last decades. However, few researchers within that field seem to see the whole picture. We think the time has come to develop a computational model of airway molecular biology in parallel to airway physiology. This will force molecular biologists to integrate knowledge and to define outcome measurements relevant for disease activity. Some molecular biologists say that there are too many interactions and reality is too complex for a computational model. We state the opposite: since there are so many interactions and reality is so complex - start modeling!

CAST STUDIES OF INFANT LUNGS. Detailed knowledge of airway geometry at different ages is required for the development of adequate computational models of airway function in children. However, to date, the airway geometry of children has not been investigated systematically. Airway geometry can be measured from casts of lungs, obtained from autopsies of children.

References

1. Ollerenshaw SL, Woolcock AJ. Characteristics of the inflammation in biopsies from large airways of subjects with asthma and subjects with chronic airflow limitation. Am Rev Respir Dis 1992;145(4 Pt 1):922-927.

2. Jeffery PK. Morphology of the airway wall in asthma and in chronic obstructive pulmonary disease. Am Rev Respir Dis 1991;143(5 Pt 1):1152-1158; discussion 1161.

3. Elia C, Bucca C, Rolla G, Scappaticci E, Cantino D. A freeze-fracture study of human bronchial epithelium in normal, bronchitic and asthmatic subjects. J Submicrosc Cytol Pathol 1988;20(3):509-517.

4. Dovey M, Wisseman CL, Roggli VL, Roomans GM, Shelburne JD, Spock A. Ultrastructural morphology of the lung in cystic fibrosis. J Submicrosc Cytol Pathol 1989;21(3):521-534.

5. Leigh MW, Kylander JE, Yankaskas JR, Boucher TC. Cell proliferation in bronchial epithelium and submucosal glands of cystic fibrosis patients. Am J Respir Cell Biol 1995;12:605-612.

6. Hill MJ, Wilson TA, Lambert RK. Effects of surface tension and intraluminal fluid on mechanics of small airways. J Appl Physiol 1997;82(1):233-239.

7. Hulsmann AR, De Jongste JC. Modulation of airway responsiveness by the airway epithelium in humans, putative mechanisms. Clin Exp Allergy 1996;26:1236-1242.

8. O' Riordan T, Walser L, Smaldone GC. Changing patterns of aerosol deposition during methacholine bronchoprovocation. Chest 1993;103(5):1385-1389.

9. Smaldone GC, Messina MS. Flow limitation, cough, and patterns of aerosol deposition in humans. J Appl Physiol 1985;59(2):515-520.

10. Laube BL, Links JM, LaFrance ND, Wagner HN, Jr., Rosenstein BJ. Homogeneity of bronchopulmonary distribution of 99mTc aerosol in normal subjects and in cystic fibrosis patients. Chest 1989;95(4):822-830.

11. Petty TL, Silvers GW, Stanford RE. Mild emphysema is associated with reduced elastic recoil and increased lung size but not with air-flow limitation. Am Rev Respir Dis 1987;136(4):867-871.

12. Hogg JC, Wright JL, Wiggs BR, Coxson HO, Opazo Saez A. Lung structure and function in cigarette smokers. Thorax 1994;49:473-478.

13. Verbeken EK, Cauberghs M, van de Woestijne KP. Membranous bronchioles and connective tissue network of normal and emphysematous lungs. J Appl Physiol 1996;81(6):2468-2480.

14. Lambert RKP, P.D. Lung parenchymal shear modulus, airway wall remodeling, and bronchial hyperresponsiveness. J Appl Physiol 1997;83(1):140-147.

15. Nagai A, Thurlbeck WM, Konno K. Responsiveness and variability of airflow obstruction in chronic obstructive pulmonary disease. Am J Respir Crit Care Med 1995;151:635-639.

16. Pellegrino R, Wilson O, Jenouri G, Rodarte JR. Lung mechanics during induced bronchoconstriction. J Appl Physiol 1996;81(2):964-975.

17. Fredberg JJ, Jones KA, Nathan M, Raboudi S, Prakash YS, Shore SA, Butler JP, Sieck GC. Friction in airway smooth muscle: mechanism, latch, and implications in asthma. J Appl Physiol 1996;81(6):2703-2712.

18. Shen X, Wu MF, Tepper RS, Gunst SJ. Mechanisms for the mechanical response of airway smooth muscle to length oscillation. J Appl Physiol 1997;83:731-738.

Samenvatting

Ontsteking van de luchtwegen, luchtwegobstructie en bronchiale hyperreactiviteit zijn belangrijke kenmerken van astma, chronisch obstructief longlijden (COPD), cystic fibrosis (CF) en bronchopulmonale dysplasie (BPD). Chronische ontsteking van luchtwegen is geassocieerd met functionele veranderingen van de luchtwegwand en van het longparenchym. Hoe deze veranderingen gerelateerd zijn aan luchtwegobstructie en bronchiale hyperreactiviteit is complex en onduidelijk. Een beter inzicht in de relatie tussen structuur en functie van chronisch ontstoken luchtwegen en parenchym is noodzakelijk, het zou kunnen leiden to betere therapie.

Dit proefschrift bevat de resultaten van een aantal studies naar de structuur en functie van luchtwegen afkomstig van patiënten met COPD, CF en BPD.

Hoofstuk 1 geeft een algemene introductie van het proefschrift en de doelen van de studies.

Hoofdstuk 2 geeft een overzicht van de pathofysiologie van luchtwegontsteking en de structuur-functierelaties van componenten van normale en zieke luchtwegen bij patiënten met astma, COPD, CF en BPD.

In **hoofstuk 3** worden de structuur-functierelaties van luchtwegen afkomstig van COPD- patiënten beschreven. De vraag wordt beantwoord of luchtwegobstructie en ontsteking in perifere luchtwegen correleert met de dikte van de wand van kraakbeenhoudende luchtwegen en de hoeveelheid glad spierweefsel in die wand. Verder wordt de theoretische relatie tussen luchtwegwanddimensies en luchtwegweerstand bestudeerd in een rekenkundig computermodel. Longweefsel werd verkregen van 72 patiënten met verschillende mate van chronisch obstructief longlijden die geopereerd werden aan een solitaire perifere longafwijking. Bij 341 transversaal aangesneden secties van kraakbeenhoudende luchtwegen werden zowel de grootte van de luchtweg als verschillende dimensies van de wand gemeten. Verder werd een ontstekings-score bepaald in het longweefsel bij niet-kraakbeenhoudende luchtwegen. De pre-operatief gemeten maximale uitademingssnelheid en de reactie op een bronchusverwijder werden gecorreleerd met de luchtwegwanddimensies.

De maximale uitademingssnelheid, de reversibiliteit van luchtwegobstructie en de

ontstekingsscore van perifere luchtwegen waren alle significant gecorreleerd met het volume van de binnenwand maar niet met het volume van het bronchiaal spierweefsel. De conclusie van dit hoofdstuk is dat bij patiënten met COPD luchtwegobstructie en de reversibiliteit hiervan ten dele veroorzaakt wordt door ontstekingsgerelateerde verdikking van de wand van kraakbeenhoudende luchtwegen.

In **hoofdstuk 4** wordt de relatie onderzocht tussen de stroomopwaartse conductantie, zoals geschat met de "maximal flow-static recoil" (MFSR)-curve, en de ontsteking en verdikking van de luchtwegen. Verder werd de relatie onderzocht tussen de collapsibiliteit van luchtwegen, de hoeveelheid kraakbeen in de wand en de dikte van de luchtwegwand.

De maximale uitademingssnelheid kan verminderd zijn door drie mechanismen; verlies van de elastische retractiekracht van de long, verminderde luchtwegconductantie stroomopwaarts van de flow-limiterende segmenten en toegenomen collapsibiliteit van de luchtwegen. Het is gesuggereerd dat het relatieve aandeel van de elastische retractiekracht van de long, conductantie van de luchtwegen en luchtwegcollapsibiliteit voor luchtwegobstructie kan worden geschat met een MFSR-curve. Longweefsel werd verkregen van 72 patiënten met luchtwegobstructie in verschillende ernst, die geopereerd werden aan een solitaire perifere longafwijking. Om de conductantie en collapsibiliteit van luchtwegen te schatten werden MFSR curves samengesteld uit pre-operatief gemeten flow-volume en druk-volume curves bij 59 patiënten. Bij 341 transversale secties van kraakbeenhoudende luchtwegen werden de grootte van de luchtweg en de wanddimensies gemeten. De mate van luchtwegobstructie correleerde met de elastische retractiekracht van de long en met de luchtwegconductantie als geschat met de MFSR curves, maar niet met de luchtwegcollapsibiliteit en de hoeveelheid kraakbeen. De luchtwegconductantie verminderde met het dikker worden van de binnenwand. Collapsibiliteit van de luchtweg correleerde niet met de dikte van de luchtwegwand of met de hoeveelheid kraakbeen of ontsteking in de luchtwegwand. De conclusie van dit hoofdstuk is dat het MFSR-model niet de collapsibiliteit van het flow-limiterend segment voorspelt.

In **hoofdstuk 5** beschrijven we een micro-plethysmograaf die ontwikkeld werd om de respons te meten van glad spierweefsel in geïsoleerde luchtwegen onder isobare

omstandigheden. Tevens beschrijven we een experimentele opstelling die ontwikkeld werd om de mechanische eigenschappen te meten van luchtwegsegmenten. Het in-vitro meten van een contractie- of relaxatierespons bij geïsoleerde luchtwegsegmenten heeft belangrijke voordelen boven het meten aan strip- of spiraalpreparaten. Echter, er was geen goede methode om de isobare respons van luchtwegsegmenten te meten. Daarvoor ontwikkelden wij een micro-plethysmograaf met een volumemeetbereik van 10 tot 700 µL, een resolutie van 0.02 tot 0.4 µL, en een drift van 2.6 tot 0.7% van het meetbereik per minuut voor respectievelijk de meest en minst gevoelige instelling. De plethysmograaf is in staat de druk die ontstaan is door volumeveranderingen te compenseren. We laten voorbeelden zien van stimulatie van geïsoleerde humane luchtwegsegmenten onder isobare omstandigheden met methacholine, isoprenaline of met een electrisch veld. Behalve bij luchtwegen kan de microplethysmograaf ook gebruikt worden om de contractiele eigenschappen te bestuderen van andere waterdichte en holle structuren zoals bloedvaten, darm en ureter. Verder kan de plethysmograaf gebruikt worden om lek of diffusie door de wand van een holle structuur te meten bij elke willekeurige transmurale druk.

In **hoofdstuk 6** wordt de relatie beschreven tussen compliantie, collapsibiliteit en hysterese van geïsoleerde humane kleine luchtwegsegmenten enerzijds en luchtwegwanddimensies anderzijds. Luchtwegwanddimensies zijn belangrijk als determinant voor de mechanische eigenschappen van luchtwegen. Chronische ontsteking verandert naar alle waarschijnljkheid deze mechanische eigenschappen. Longweefsel werd verkregen van 31 patiënten met luchtwegobstructie van verschillende ernst die geopereerd werden aan een geïsoleerde solitaire longafwijking. Segmenten van 35 kleine luchtwegen werden waterdicht gemonteerd op canules in een orgaanbad en cyclisch opgepompt en leeggezogen tussen +15 and -15 cm H_2O. Dit werd voor elke luchtweg gedaan voor de uitgangs situatie, na methacholine, en na isoprenaline. Specifieke compliantie (sCdyn), specifieke hysterese (sη), en de druk waarbij de luchtwegcollabeerde (Pcol) werden berekend voor elke registratie. Luchtwegwanddimensies werden morfometrisch gemeten. Longfunctieparameters van luchtwegobstructie werden gecorreleerd met sCdyn, sη, en Pcol. sCdyn na isoprenaline was significant hoger en sη en Pcol significant lager dan na metacholine. Het oppervlak

van het glad spierweefsel, maar niet van de totale luchtwegwand, was een belang-
rijke determinant voor sCdyn en voor sη na methacholine. Specifieke hysterese voor
baseline correleerde met RV/TLC en na methacholine met FEV_1/FVC en RV/TLC.
Uit deze resultaten kunnen we concluderen dat het oppervlak en de tonus van het
glad spierweefsel, maar niet het oppervlak van de totale wand, belangrijke determi-
nanten zijn voor de luchtwegcompliantie, hysterese, en collapsibiliteit. Hysterese lijkt
een belangrijke determinant voor chronische luchtwegobstructie.

In **hoofdstuk 7** worden luchtwegwanddimensies van CF-patiënten vergeleken met
die van COPD-patiënten. Verder wordt de theoretische relatie tussen deze luchtweg-
wanddimensies en luchtwegweerstand bestudeerd in een rekenkundig computermodel.
Chronische ontsteking van luchtwegen leidt bij de meeste CF-patiënten tot progres-
sieve luchtwegobstructie en tot een toename van de bronchiale hyperreactiviteit. Het
is niet duidelijk hoe luchtwegpathologie bij deze patiënten gerelateerd is aan de ernst
van de luchtwegobstructie en de toegenomen bronchiale reactiviteit. Luchtweg-
dimensies werden gemeten in longen van CF-patiënten afkomstig van long-
transplantatie (12), lobectomie (1) of autopsie (4). Deze dimensies werden vergele-
ken met die van luchtwegen afkomstig van lobectomieën van 72 patiënten met COPD.
De luchtwegdimensies van CF- en COPD-patiënten werden ingevoerd in een reken-
kundig computermodel om het effect op de luchtwegweerstand te bestuderen. Het
volume van de binnenwand en van het glad spierweefsel van perifere CF-luchtwegen
was met een factor 3.3- tot 4.3 toegenomen in vergelijking met die van COPD- lucht-
wegen. Het epitheel was 53% hoger in perifere CF-luchtwegen. De sensitiviteit en de
maximale plateauweerstand van de met het computer model berekende dosis-respons-
curve waren substantieel toegenomen in CF-patiënten vergeleken met COPD. De
veranderingen in luchtwegdimensies van CF-patiënten dragen naar alle waarschijn-
lijkheid bij aan de ernstige luchtwegobstructie en aan de bronchiale hyperreactiviteit
zoals beschreven bij CF-patiënten.

Of luchtwegwanddimensies bijdragen aan longfunctieafwijkingen zoals beschreven
voor BPD patiënten is onbekend.

In **hoofdstuk 8** worden luchtwegdimensies van BPD-patiënten vergeleken met die
van controles. Longweefsel werd verkregen van obducties van patiënten met BPD en

van overleden patiënten met de diagnose wiegedood (SIDS) welke dienden als controlegroep. Luchtwegdimensies en epitheelverlies werden gemeten bij 75 luchtwegen afkomstig van 5 BPD-patiënten en bij 176 luchtwegen van 11 SIDS-patiënten. De relatie tussen luchtwegwanddimensies en luchtweggrootte van BPD- en SIDS-patiënten werd berekend met een variantie analyse (RMANOVA). Het epitheelverlies was gering in de BPD-patiënten terwijl een uitgebreid epitheelverlies werd waargenomen in sommige SIDS-patiënten. Het volume van de binnenwand, buitenwand en van het glad spierweefsel was substantieel groter bij de BPD-patiënten in vergelijking met de SIDS-patiënten. Het is waarschijnlijk dat bij BPD-patiënten de toegenomen luchtwegwanddimensies bijdragen aan de luchtwegobstructie en de reversibiliteit van die obstructie.

In de **Algemene Discussie** wordt besproken hoe veranderingen van de luchtwegwand kunnen bijdragen aan de pathofysiologie van luchtwegobstructie en bronchiale hyperreactiviteit. De epitheliale laag van chronisch ontstoken luchtwegen is waarschijnlijk beschadigd door toegenomen fragiliteit. Dit heeft een gestoorde mucociliaire klaring tot gevolg en kan bijdragen aan verhoogde tonus van het bronchiaal glad spierweefsel.

Evenals bij astma is bij COPD, CF en BPD de dikte van de binnenwand toegenomen. Dit heeft een verhoogde luchtwegweerstand tot gevolg en versterkt het effect van verkorting van het bronchiaal glad spierweefsel. De hoeveelheid bronchiaal glad spierweefsel is verhoogd bij patiënten met CF en BPD maar niet bij rokers met luchtwegobstructie. In-vivo hebben bronchusverwijders weinig effect op de luchtwegdoorgankelijkheid bij COPD. In-vitro zijn de mechanische eigenschappen van luchtwegen van patiënten met COPD sterk afhankelijk van de tonus en van de hoeveelheid bronchiaal glad spierweefsel. De beperkte reversibiliteit van luchtwegobstructie bij COPD wordt waarschijnlijk veroorzaakt door factoren gelegen buiten de luchtwegwand zoals een gestoorde parenchym-luchtweginteractie.

De hoeveelheid kraakbeen in de luchtwegwand is niet verminderd bij COPD maar wel bij CF. Het is onduidelijk of het volume van het luchtwegkraakbeen een rol speelt bij de pathofysiologie van luchtwegobstructie.

De dikte van de buitenwand van kraakbeenhoudende luchtwegen was niet betrouwbaar te meten bij luchtwegen van patiënten met CF en COPD. De buitenwand van kleinere luchtwegen bij BPD waren sterk verdikt ten opzichte van controles. Verdikking van de buitenwand ontkoppelt naar alle waarschijnlijkheid het glad spierweefsel van het parenchym en kan aldus bijdragen aan luchtwegobstructie.

Chronische luchtwegontsteking veroorzaakt verdikking van de luchtwegwand maar verandert de mechanische eigenschappen van de wand niet in belangrijke mate. Luchtwegobstructie bij chronische luchtwegontsteking kan het gevolg zijn van een gestoorde luchtweg-parenchyminteractie in combinatie met verdikking van luchtwegwand.

**Een promotieonderzoek is een beetje als "De Toverberg"
van Thomas Mann;**

- *je krijgt het werk als "cadeau" van "vrienden"*
- *zonder innerlijke rust kun je er niet in doordringen*
- *je moet niet gestoord worden door je zoemer als je er mee bezig bent*
- *het kost je veel tijd*
- *je legt het niet weg want mensen die je respecteert hebben het ook uitgelezen*
- *het geeft je een voldaan gevoel als je er mee klaar bent*
- *en ..... je wordt er wijzer van.*

Dit proefschrift was nooit tot stand gekomen zonder de enthousiaste medewerking van velen. Een aantal van hen wil ik speciaal bedanken.

Rosaria, mijn allochtoontje, jouw moederschap, creativiteit, kookkunst en vakmanschap maken de Mahatma Gandhistraat nummer 12 een bijzonder, levendig en vrolijk huis. Door jou vergeet ik het vaderschap niet en kan ik inmiddels woeste katten prikken. De zomer van "de tomaat" zal ik met warmte koesteren. Ik zal het koken weer oppikken ondanks dat Elena en Chiara weigeren te eten als iemand anders dan mama kookt.
Mijn "power girls" Elena en Chiara doen mij dagelijks beseffen dat kinderen bij het leven horen.

Mijn ouders wil ik speciaal bedanken voor het Tiddens-nest (volgens sommigen de Tiddens-mafia). Iedereen uit ons nest doet veel met de veelzijdige bagage die we hebben meegekregen. Ik heb er nu dit proefschrift mee gemaakt.

Prof. dr J.C. de Jongste, beste Johan, leermeester en promotor, je hebt vele talenten. Voor mij is het belangrijkste dat je meer lid bent van het "SKZ-pulmoteam" dan baas. Bedankt voor je vertrouwen, de ruimte die je me geeft, je collegialiteit en je snelle correcties van mijn schrijfsels.

Prof. dr P.D. Paré, dear Peter, you make clear that someone with true qualities doesn't have to show off. Your only bad thing is your "é". Thank you for your hospitality in Vancouver and love from all the women in the Tiddens house.

Dr W.C.J. Hop, beste Wim, jouw werkkamer ..... heeft een professorabel uitzicht. Jij hebt alleen geen tijd om naar buiten te kijken, te druk om iedereen van dienst te zijn. Je hebt veel werk gehad aan het "mixed model" zonder dat was dit proefschrift er niet!

Dr R.K. Lambert, dear Rod. Thank you for your trans-global collaboration, friendship, Apfelstrudel, and being our guest. See you in New-Zealand in 2001!

Prof. dr J.M. Bogaard, beste Jan, van jouw enthousiasme voor het vak word ik altijd vrolijk. Je geniet van het fitten van een curve en van het uitwerken van een fysisch probleem in zwarte inkt en met een regelmatig handschrift.

Prof. dr W.J. Mooi, beste Wolter, als co-assistent heb ik gezien hoe jij elders als assistent een afdeling pathologie in roerige tijden overeind hield. In Rotterdam sta je nu vol enthousiasme aan het roer van de afdeling pathologie. Hoofdstuk 8 uit dit proefschift beschouw ik als het begin van onze samenwerking, met veel humor!

Prof. dr P.J. Sterk, beste Peter, jij kunt je internationaal meten met de andere grote Peters. Ik ben je dankbaar voor je goede ideeën waarvan er een aantal in dit proef-schrift terug te vinden zijn. Met genoegen kijk ik uit naar de verdere samenwerking.

Huib de Bruin. Beste Huib, je hebt voor de uitdaging gekozen om als research analist op het project te gaan werken. Je bent gegroeid in je baan en je hebt ook onder de werkdruk van het afgelopen jaar je goede humeur weten te behouden. Aan mij de taak om een nieuw project gefinancierd te krijgen zodat jouw expertise niet verloren gaat.

Prof. dr K.F. Kerrebijn, beste Karel, dank je voor het zeer aparte sollicitatiegesprek waarin je me direct na het handen schudden hebt aangenomen om vervolgens ter zake te komen over het onderzoek dat de basis vormde voor dit proefschrift.

Mijn vrienden Berent Prakken, Maarten Noyons, Marc van de Vijver, Pieter Meyers, Lieke Schellens-Sanders en Bernard Prins. Zonder jullie zou het leven een stuk schraler zijn.

De repetitieavonden met de mannen van de IM band Eddie, Mark, Marc C en Tim waren in de laatste jaren extra belangrijk als uitlaatklep en voor de innerlijke balans. Als ik geen tijd meer heb voor de band zoek ik een ander vak! Wie heeft er nog een band nodig voor een swingend feest?

Curriculum vitae

Harm Tiddens was born in Helmond, The Netherlands, on 1 December 1956. He passed his secondary school exam (VWO) at the 'Stedelijk Lyceum' in Maastricht in 1977. In 1977 he started his medical training at the Medical Faculty of the University of Amsterdam. As a student he did research in the field of molecular biology at the National Institute for Medical Research, Mill Hill London, England and at Biogen Research Corporation, Cambridge, Massachusetts, USA (head: Prof. dr R.A. Flavell) in 1981 and 1983. In 1985 he obtained his medical degree and started his specialist training in paediatrics first in the Elisabeth Hospital, Tilburg (head: Drs. J.A. Rammeloo) and later in the Wilhelmina Children's Hospital, Utrecht (head: Prof. dr J.W. Stoop). Together with his colleague and friend Berent Prakken he initiated a fund-raising campaign to set up home-care for patients with cystic fibrosis in the last year of his specialization. He was registered as paediatrician in March 1991. From June 1991 to June 1994 he followed a clinical and research fellowship at the department of Paediatric Respiratory Medicine (head: Prof. dr J.C. de Jongste) of the Sophia Children's Hospital, under auspices of the Netherlands Asthma Foundation. He worked as a research fellow at the Pulmonary Research Laboratory, St. Paul's Hospital, University of British Columbia, Vancouver, Canada (head: Prof. dr P.D. Paré) in 1992 and 1994. During this period the research bundled in this thesis was performed at the Departments of Pediatrics, Pathology, and Pharmacology of the Erasmus Medical Center (heads: Prof. dr H.A. Büller, Prof. dr W.J. Mooi, Prof. dr P.R. Saxena). He is a staff paediatric pulmonologist at the Sophia Children's Hospital.

He is married to Rosaria Macrí, veterinarian, and they have two children: Elena, and Chiara. He has one daughter from a former marriage: Giulia. With Rosaria he built a house and small animal clinic (Dierenkliniek Prinsenland) from 1994 tot 1996. He plays bass guitar in the rock-pop band 'IM'.

List of publications

1. Weiss EH, Golden L, Fahrner K, Mellor AL, Devlin JJ, Bullman H, Tiddens HA, Bud H, Flavell RA. Organisation and evolution of the class-I gene family in the major histocompatibility complex of the C57BL/10 mouse. Nature 1984;310:650-655.

2. Hiemstra I, Sanders EA, Tiddens HA. Juvenile dermatomyositis, systemic lupus erythematosus, and mixed connective tissue disease. Tijdschr Kindergeneeskd 1991;59:185-189.

3. Tiddens HA, van der Net JJ, de Graeff-Meeder ER, Fiselier TJ, de Rooij DJ, van Luijk WHJ, Herzberger R, van Suijlekom LWA, Venrooij WJ, Zegers BJM, Kuis W. Juvenile- onset mixed connective tissue disease: Longitudinal follow-up. J Pediatr 1993;122:191- 197.

4. Bai A, Eidelman DH, Hogg JC, James AL, Lambert RK, Ludwig MS, Martin J, McDonald DM, Mitzner WA, Okazawa M, Pack RJ, Paré PD, Schellenberg RR, Tiddens HAWM, Wagner EM, Yager D. Proposed nomenclature for quantifying subdivisions of the bronchial wall. J Appl Physiol 1994;77:1011-1014.

5. Haraldson A, Tiddens HAWM, Fiselier T, Bakkeren JAJM, Weemaes CMR. Altered immunoglobulin concentrations and light chain ratios in juvenile onset mixed connective tissue disease. Clinical Rheumatology 1995;14:51-54.

6. Joosten KFM, Hazelzet JA, Tiddens HAWM, Hazebroek FWJ, Dzoljic-Danilovic G, Neijens HJ, de Groot R. Staphylococcal intervention in childhood: will early surgical intervention lower mortality. Pediatr Pulmonol 1995;20:83-88.

7. Tiddens HAWM, Paré PD, Hogg JC, Hop WCJ, Lambert R, de Jongste JC. Cartilaginous airway dimensions and airflow obstruction in human lungs. Am J Respir Crit Care Med 1995;152:260-266.

8. Struycken VHJ, Tiddens HAWM, van den Broek ET, Dzoljic-Danilovic G, van der Velden AJCM, de Jongste JC. Problemen met gebruik, reiniging en onderhoud van vernevelapparatuur in de thuissituatie. Ned Tijdschr Geneeskd 1996;140:654-658.

9. Stam H, van den Beek A, Grunberg K, Stijnen T, Tiddens HA, Versprille A. Pulmonary diffusing capacity at reduced alveolar volumes in children. Pediatr Pulmonol 1996;21:84- 89.

10. Tiddens HAWM, Boogaard JM, de Jongste JC, Hop WCJ, Coxson HO, Paré PD. Physiological and morphological determinants of maximal expiratory flow in chronic obstructive lung disease. Eur Respir J 1996;9:1785-1794.

11. Tiddens HAWM, de Jongste JC. Airflow obstruction in asthma: There is more than smooth muscle. In: Tibboel D, van der Voort E, editors. Intensive care in childhood. Berlin, Heidelberg, New York: Springer-Verlag, 1996:337-343.

12. Borsje P, Tiddens HAWM, Mouton JW, de Jongste JC. Aerosol therapy in cystic fibrosis; a survey among 54 CF-centres. Pediatr Pulmonol 1997;submitted.

13. Tiddens HAWM, Koopman LP, Lambert RK, Elliott WM, Hop WCJ, van den Mark TW, de Boer WJ, de Jongste JC. Airway wall dimensions and bronchial responsiveness in cystic fibrosis lungs. Submitted 1997.

14. Tiddens HAWM, Hofhuis W, Hulsmann AR, Mooi WJ, Hop WCJ, de Jongste JC. Airway dimensions and mechanisms of airflow obstruction of patients with bronchopulmonary dysplasia. Submitted 1997.

15. Janssens HM, Devadason SG, Hop WCJ, LeSouëff PN, de Jongste JC, Tiddens HAWM. Variability of aerosol delivery via spacer devices in young asthmatic children in daily life. Submitted 1997.

List of Abbreviations

A	lung volume at infinite transmural pressure
A_{bm}	basement membrane area
A^*_{bm}	area of the fully relaxed airway lumen
A/D	analog to digital converter
A_i	internal area
A_{mo}	outer muscle area
A_o	outer area
B	the lung volume difference between lung volume at infinite transmural pressure and at a pressure of 0 cm H_2O
B_{meas}	measurement barrel
BPD	bronchopulmonary dysplasia
B_{ref}	reference barrel
Cdyn	average dynamic compliance of pressure-volume loops
$Cdyn_1$	dynamic compliance of first pressure-volume loop
CF	cystic fibrosis
COPD	chronic obstructive pulmonary disease
$DFEV_1\%ini$	absolute change in FEV_1 as a percentage of the pre-bronchodilator FEV_1
$DFEV_1\%pred$	absolute change in FEV_1 as a percentage of the predicted FEV_1
$\Delta P_{tm}'$	absolute difference of $P_{tm}'(pred) - P_{tm}'$
F_{epi}	fraction of basement membrane covered with respiratory epithelium
FEV_1	forced expiratory volume in 1 second
FEV_1/FVC	ratio between forced expiratory volume in 1 second and forced vital capacity
FRC	functional residual capacity
FVC	forced vital capacity
G_{us}	airway conductance upstream from flow limiting segment during forced expiration
$G_{us}\%$	G_{us} expressed as percentage of $G_{us}(pred)$

217

H_{epi}	Height of respiratory epithelium
IC	inspiratory capacity
Iso	isoprenaline
k	the exponential constant that describes the shape of the pressure-volume curve
MADS	membranous airways disease score
MCh	methacholine
MFSR	maximal flow-static recoil
n	number
η	average hysteresis of the subsequent pressure-volume loops
η_1	hysteresis of first pressure-volume loop
p	level of significance
P_{bm}	basement membrane perimeter
PC_{20}	concentration of bronchoconstricting agent that causes a 20% fall in FEV_1
Pcol	pressure of airway closure of subsequent pressure-volume loops
$Pcol_1$	pressure of airway closure of first pressure-volume loop
PD_{10}	dose that causes a 10 fold increase in baseline resistance of simulated dose-response curve
P_{diff}	differential pressure transducer
P_{dist}	transducer to measure transmural pressure at distal end of airway
P_i	internal perimeter
P_L	transpulmonary pressure
P_L60	transpulmonary pressure at 60% of total lung capacity
P_L90	transpulmonary pressure at 90% of total lung capacity
P_{mo}	outer muscle perimeter
P_o	outer perimeter
P_{prox}	transducer to measure transmural pressure at proximal end of airway
pred	predicted
P_{tm}'	transmural pressure causing airway collapse at the flow limiting segment

R	Spearman's correlation coefficient
RADS	respiratory airways disease score
RMANOVA	repeated measures analysis of variance
RV	residual volume
sCdyn	specific average dynamic compliance of pressure-volume loops
$sCdyn_1$	specific dynamic compliance of first-pressure volume loop
SD	standard deviation
sem	standard error of the mean
sG_{us}	airway conductance upstream from flow limiting segment during forced expiration divided by total lung capacity
SIDS	sudden infant death syndrome
$s\eta$	average hysteresis of subsequent pressure-volume loops normalized as a percentage of the maximal possible hysteresis
$s\eta_1$	hysteresis of first pressure-volume loop normalized as a percentage of the maximal possible hysteresis
T	large bore tubing
TLC	total lung capacity
V	volume
V_{atm}	valve to connect air compartment to atmosphere
VC	vital capacity
V_{dist}	valve at distal end of the airway
V_I	volume displaced by airway segment after relaxation by isoprenaline. expressed as percentage of volume of segment.
V_M	volume displaced by airway segment after contraction with methacholine expressed as percentage of volume of segment
$Vmax_{25}$	maximal flows at 25% of forced vital capacity
$Vmax_{50}$	maximal flows at 50% of forced vital capacity
V_{prox}	valve at proximal end of the airway
V_{pump}	valve to connect pump to micro-plethysmograph or to airway
V_t	valves used for the filling and to obtain identical fluid levels in barrels
WA_{bm}	inner wall area, exclusive epithelium

WA_{cart}	cartilage area
WA_{epi}	wall area covered by epithelium
WA_i	inner wall area, inclusive epithelium
WA_m	smooth muscle area
WA_o	outer wall area
WA_t	total wall area